AD

FA-TR-76011

A CRITICAL ASSESSMENT OF THE ALUMINUM CARTRIDGE CASE FAILURE MECHANISM

March 1976

Approved for public release; distribution unlimited.

Munitions Development and Engineering Directorate

U.S. ARMY ARMAMENT COMMAND
FRANKFORD ARSENAL
PHILADELPHIA, PENNSYLVANIA 19137

DISPOSITION

Destroy this report when it is no longer needed. Do not return it to the originator.

Citation of manufacturers' names in this report does not constitute an official indorsement of the use of such commercial hardware or software.

The findings in this report are not to be construed as an official Department of the Army position, unless so designated by other authorized documents.

UNCLASSIFIED

SECURITY CLASSIFICATION OF THIS PAGE (When Data Entered)

REPORT DOCUMENTATION PAGE

READ INSTRUCTIONS BEFORE COMPLETING FORM

1. REPORT NUMBER: FA-TR-76011	2. GOVT ACCESSION NO.
3. RECIPIENT'S CATALOG NUMBER	
4. TITLE (and Subtitle): A CRITICAL ASSESSMENT OF THE ALUMINUM CARTRIDGE CASE FAILURE MECHANISM	5. TYPE OF REPORT & PERIOD COVERED: Technical rsch report
	6. PERFORMING ORG. REPORT NUMBER
7. AUTHOR(s): WALTER H. SQUIRE REED E. DONNARD	8. CONTRACT OR GRANT NUMBER(s)
9. PERFORMING ORGANIZATION NAME AND ADDRESS: Frankford Arsenal ATTN: SARFA-MDS-S Philadelphia, PA 19137	10. PROGRAM ELEMENT, PROJECT, TASK AREA & WORK UNIT NUMBERS
11. CONTROLLING OFFICE NAME AND ADDRESS: Small Arms Systems Agency Aberdeen Proving Ground MD 21005	12. REPORT DATE: March 1976 13. NUMBER OF PAGES: 202
14. MONITORING AGENCY NAME & ADDRESS (if different from Controlling Office)	15. SECURITY CLASS. (of this report): Unclassified 15a. DECLASSIFICATION/DOWNGRADING SCHEDULE: N/A

16. DISTRIBUTION STATEMENT (of this Report)

Approved for public release; distribution unlimited .

17. DISTRIBUTION STATEMENT (of the abstract entered in Block 20, if different from Report)

18. SUPPLEMENTARY NOTES The authors would like to recognize the contributions provided to this study by the following firms: Texas Instruments, Inc. -- Supplied clad metal laminates; TRW, Inc. -- Emission spectroscopy, holographic interferometry; Princeton University -- Erosion test fixture work;

19. KEY WORDS (Continue on reverse side if necessary and identify by block number)

Aluminum alloys
Aluminum alloy cartridge case
Gas path
Vapor-phase reaction
Burn-through
High performance small & medium caliber ammo
Erosion of metals

20. ABSTRACT (Continue on reverse side if necessary and identify by block number)

This report summarizes the basic physical processes that occur before and during the catastrophic failure of aluminum alloy cartridge cases. These processes include: (1) the presence of a gas path such as that presented by a sidewall split wherein propellant gas can flow through the path and out of the weapon; (2) the presence of a highly energetic propellant gas which interacts with the aluminum in the gas path surface; (3) a primary vapor-phase reaction principally of CO_2 and

DD FORM 1 JAN 73 1473 EDITION OF 1 NOV 65 IS OBSOLETE

UNCLASSIFIED

SECURITY CLASSIFICATION OF THIS PAGE (When Data Entered)

18. SUPPLEMENTARY NOTES- Cont'd

Thiokol Chemical Corporation -- Supplied HMX propellants; Reynolds Metals Company -- Metallographical examination of eroded aluminum surfaces; Aluminum Company of America -- Metallographical examination of eroded weapon parts.

20. ABSTRACT- Cont'd

H_2O (some of the propellant combustion products) with aluminum vapor from the gas path; and (4) a secondary oxidation of aluminum to aluminum oxide external to the gas path. Understandings gained by various experimental and theoretical programs have formed the basis for both developed and other possible engineering solutions to the burn-through problem.

TABLE OF CONTENTS

List of Tables

List of Figures

List of Figures (Cont.)

List of Figures (Cont.)

List of Figures (Cont.)

List of Figures (Cont.)

List of Figures (Cont.)

List of Figures (Cont.)

List of Figures (Cont.)

List of Figures (Cont.)

CHAPTER 1. INTRODUCTION

This report is one in a series of reports that present the technical achievements of an exploratory development program at Frankford Arsenal. The program was initiated to determine the engineering parameters required for successful utilization of aluminum alloys in high pressure, small caliber cartridge cases. The report describes the experiments conducted to develop an understanding of the basic technical barrier, referred to as "burn-through", which occurs with use of aluminum-cased ammunition. An understanding of this phenomenon was essential for development of practical solutions to the problems encountered in this application of aluminum alloys.

For many reasons, aluminum alloys are attractive materials for use in the manufacture of such cartridge cases. Besides being a less expensive material than conventional brass, aluminum is not anticipated to be constricted by supply shortages during an emergency, whereas the future availability of copper indicates that demand could out-strip supply. Its major advantage, however, is its inherent light weight. Aluminum cartridge cases, weighing one-third that of brass cases, are ideal for improving the combat load effectiveness of an infantryman, a combat vehicle or a gunship.

To enable application of the pertinent engineering parameters to any future lightweight weapon/ammunition system, the scope of an exploratory development program on aluminum cartridge cases is, of necessity, very broad. However, due to its present logistic position, the 5.56mm system -- using the M16A1 rifle -- was selected as a test vehicle. The broad structure of this program would therefore enable application of empirical information to any future system, provided this application is within the boundary conditions used in this study.

Successful development and acceptance of aluminum alloy cartridge cases in the logistic system is dependent upon the solution of two related problems.[1] The first concerns cartridge case integrity. The cartridge case must provide a high degree of strength, toughness, elasticity, and durability for highly reliable function in the weapon for which the ammunition is intended. This requirement was addressed in the overall program by:

1. The use of new case design procedures whereby stress analysis is used in conjunction with optimization routines for the establishment of the desired case geometry.

---

[1]Donnard, R.E. and McCaughey, J.M., "Proposal to Improve Combat Load Effectiveness of Weapon/Ammunition Systems by Demonstrating Feasibility of Lightweight Aluminum Alloy Cartridge Cases in the 5.56mm Weapon", Frankford Arsenal Proposal, December 1969.

2. The development of improved aluminum alloys that will significantly reduce case mechanical failures by their substantially increased toughness.

3. The development of new processing techniques for case fabrication.

The second problem concerns the consequences of the failure of an aluminum cartridge case during firing. This exploratory development program was not the first attempt to investigate the feasibility of aluminum cartridge cases. The archives, dating back to the 1890's, describe many attempts to use aluminum alloys.[2,3] A significant fact which has precluded the acceptance of aluminum cartridge case in the logistic system is the nature of the failure process -- heretofore identified as "burn-through."[4] When a brass cartridge case fails during firing in the field, the rifleman is often unaware that the case has split or has had a leaking primer. However, when certain types of mechanical failures are experienced with aluminum cases, the event can be spectacular. The failure of an aluminum cartridge case is characterized by a large efflux of very luminous gases at the breech of the weapon, the serious erosion of the cartridge case, and often, the inability of the weapon to function properly thereafter as a result of severe chamber and bolt erosion. Thus, a failure may result in serious harm to the rifleman and damage to the weapon.[5]

Unlike the brass cartridge case, the aluminum case is vulnerable to this failure mechanism when a major sidewall split is encountered along the case wall -- particularly when this split either progresses to or initiates from a point just in front of the extractor groove. Another site in the aluminum cartridge case where this phenomenon can occur is at the interface between the primer and case surface in the primer-pocket area.

---

[2]Lewis, L.D., "Calibre .30 Cartridge Cases Made from Aluminum Alloys", Technical Report No. R-16, Frankford Arsenal, Phila., Pa., 25 February 1926.

[3]Proceeding of Symposium on Aluminum Cartridge Case Development, Frankford Arsenal, Phila., Pa., 17 January 1956.

[4]Miller, S., "Design, Development and Fabrication of 100,000 Cartridges, Ball, Caliber .50, M33 Type Assembled with Case, Cartridge Aluminum Caliber .50, FAT 39", Frankford Arsenal Report R-1265, June 1956.

[5]Squire, W.H., and Donnard, R.E., "Analysis of Local Temperature Profiles Encountered in the Aluminum Cartridge Case Drilled Hole Experiment", Frankford Arsenal Technical Note TN-1163, August 1971.

In order to demonstrate the feasibility of aluminum cartridge cases by showing their insensitivity to "burn-through", a broad spectrum of concepts, including case designs and case/weapon interface designs, were investigated as possible solutions.[6,36] In addition to this activity, theoretical and experimental studies to investigate, identify, and understand this failure phenomenon have been undertaken. These studies serve as the basis for the concepts and designs that were and are being investigated for use in aluminum cases as practical means to eliminate the "burn-through" result in the use of such cartridge cases.

---

[6] Donnard, R.E. and Squire, W.H., "The Aluminum Cartridge Case Exlporatory Development Program Status Report", Frankford Arsenal Report M72-6-1, April 1972.

[36] Donnard, R.E. and Hennessy, T.J., "Aluminum Cartridge Case Feasibility Study using the M16A1 Rifle with the 5.56mm Ball Ammunition as the Test Vehicle", Technical Report R-2065, November 1972, Frankford Arsenal, Phila., PA

CHAPTER 2. WHAT IS "BURN-THROUGH"?

The term "burn-through" has been used during past aluminum cartridge case programs to describe the entire, unique failure process associated with high performance, high pressure aluminum cartridge cases.[4] As this document will explain, the catastrophic failure of an aluminum cartridge case does not result from any part of the interior surface of the cartridge case "burning-through". The term "burn-through", therefore, is a misnomer. Nevertheless, because of its widespread use and acceptability, the term "burn-through" will be used throughout this document as a synonym for the aluminum cartridge case failure process.

The results of an aluminum cartridge case "burn-through" are observed in three different ways. During the firing of an aluminum cartridge case in which a major sidewall split or leaking primer is developing, a characteristic bright plume is observed exterior to the weapon. As will be discussed more fully in Chapters 3 and 4, a sidewall split or leaking primer are precursors to "burn-through".

When a cartridge undergoes a "burn-through" in firing, and after the cartridge is removed from the chamber (automatic weapon ejection is often prevented), the head region of the case is observed to be seriously eroded. A photograph of a "burned-through" 7.62mm aluminum cartridge case is shown in Figure 1. This cartridge case was fabricated from aluminum alloy 7475 and resulted during burst fire in a minigun. There is a crack along the case's longitudinal axis and erosion in the head region; the eroded pathways suggest that portions of the cartridge case's head at one point in time were molten. The molten case surface recorded the trajectory of the propellant gases.

The third observation that a "burn-through" has occurred may be seen by examining the chamber of the weapon in which the "burn-through" took place. Those parts of the weapon that were exposed to the "burn-through" plume also become severely eroded, badly scarred, and deeply pitted. Other vulnerable parts in addition to the chamber, include the bolt and the firing pin.

Figure 2b shows a sectioned M16A1 chamber and barrel that has experienced a "burn-through". The cartridge case which caused the chamber damage is shown in Figure 2a; the other half of the sectioned chamber and barrel, which was unaffected by the "burn-through" plume, is seen in Figure 2c. A magnification of the chamber erosion is shown in Figure 3. Observe the eroded pathways and pitting in the chamber.

---

[4]Miller, S., "Design, Development and Fabrication of 100,000 Cartridges, Ball, Caliber .50, M33 Type Assembled with Case, Cartridge Aluminum Caliber .50, FAT 39", Frankford Arsenal Report R-1265, June 1956.

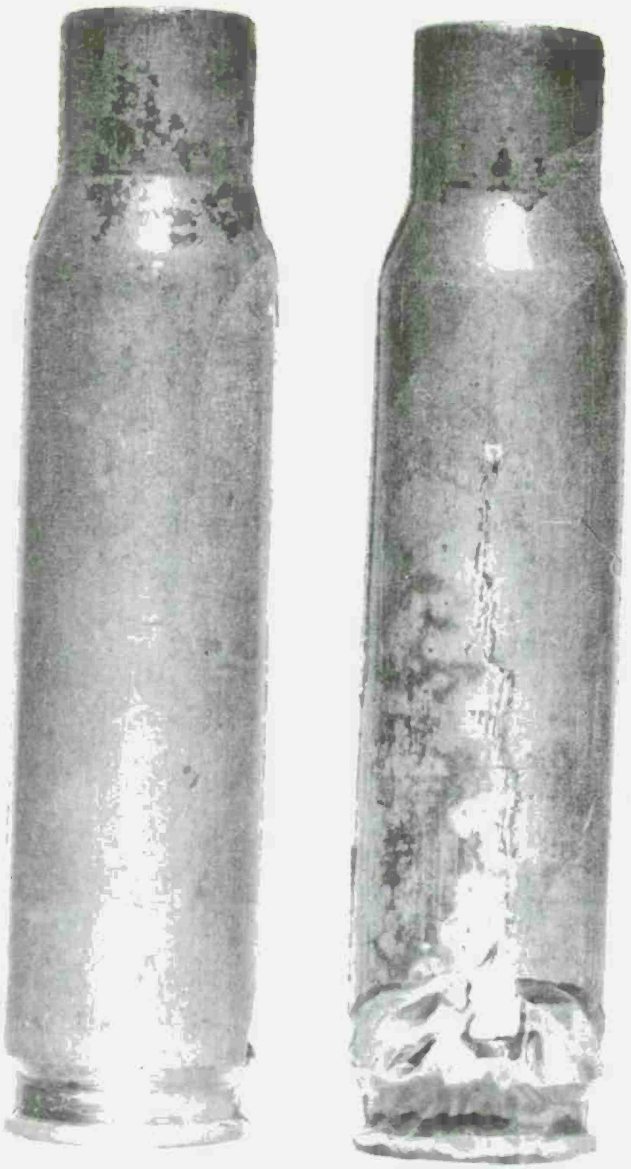

Figure 1. 7.62 mm Aluminum Cartridge Case Evidencing "Burn-Through"

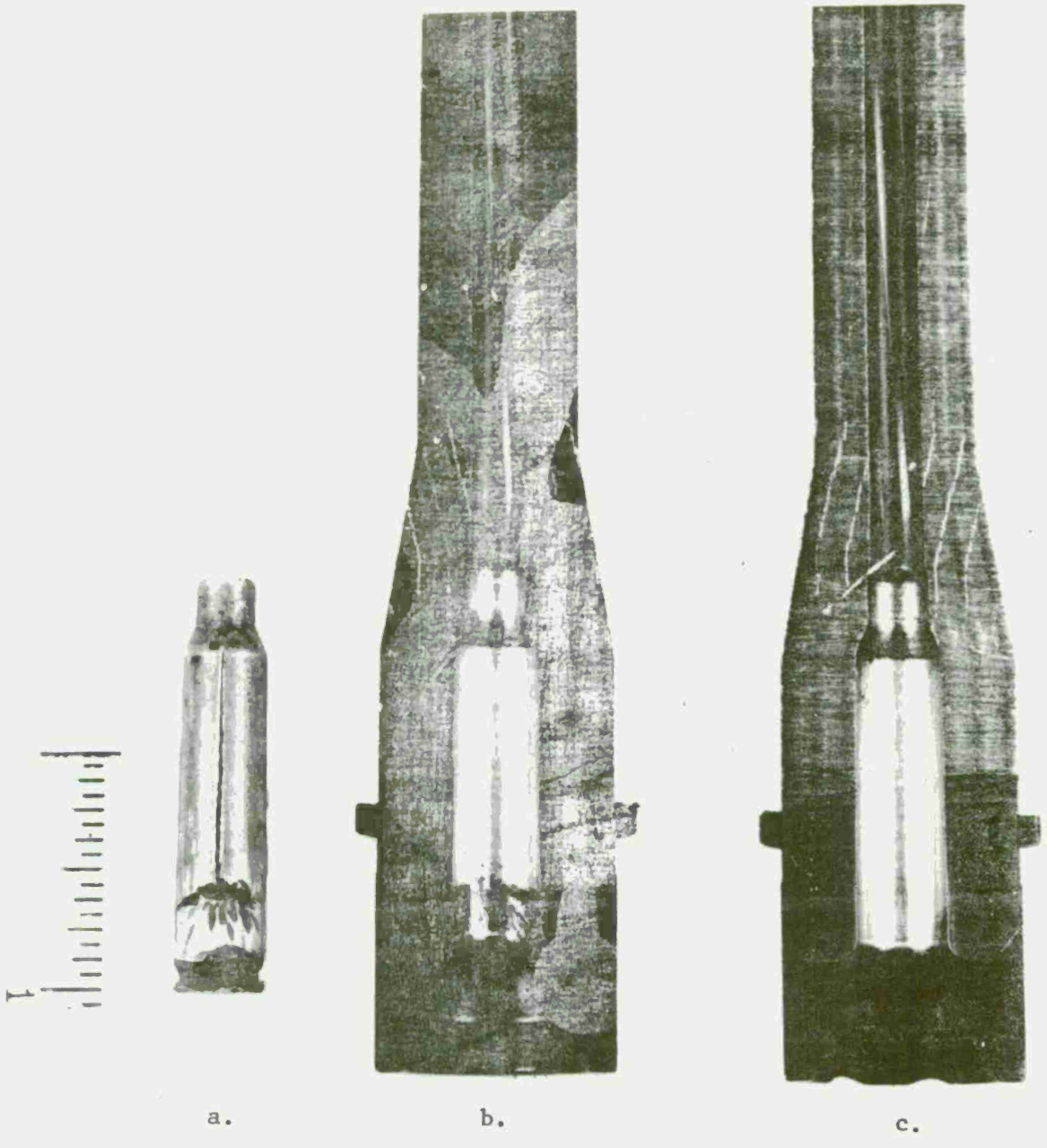

Figure 2. Results of 5.56 mm Aluminum Cartridge Case "Burn-Through"

a. Cartridge Case, b. Sectioned M16A1 Chamber and Barrel Showing Erosion, c. Sectioned M16A1 Chamber and Barrel Showing Unaffected Areas

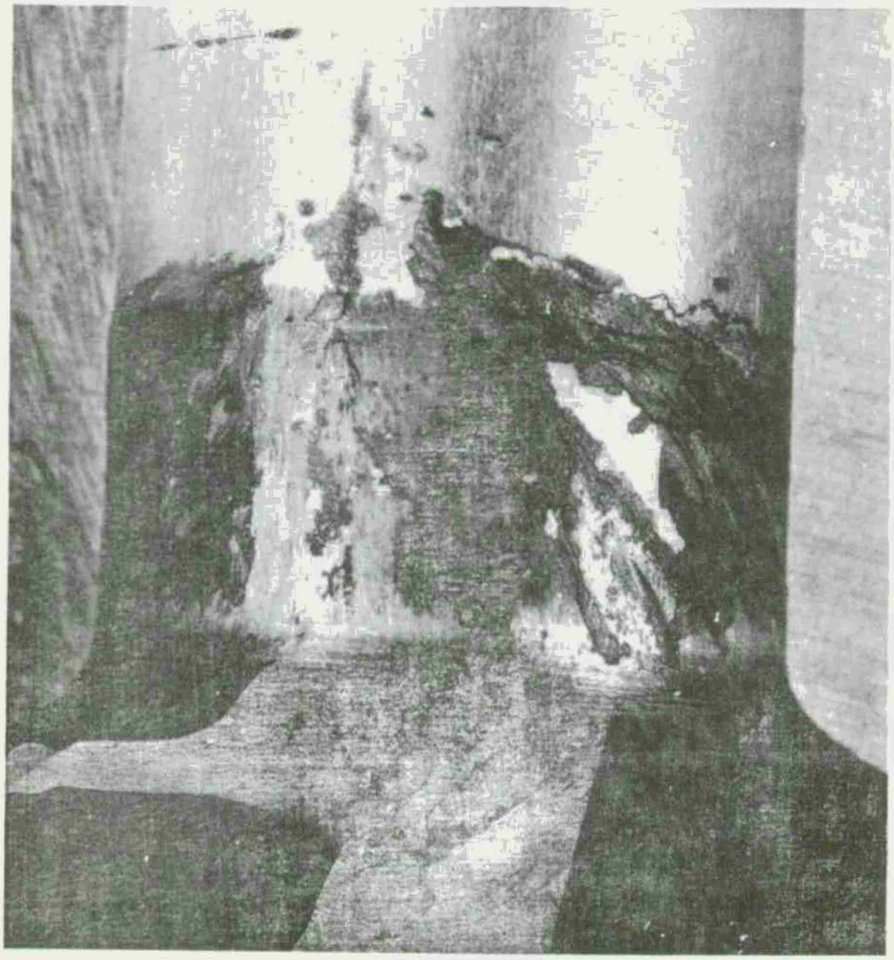

Figure 3. Magnification of Figure 2b Showing Severe Erosion and Pitting

These three observations form natural divisions for more extensive discussions on "burn-through". The characteristic bright flash, discussed in Chapter 5, is described by: (1) high speed motion pictures taken of the plume and the case surface during "burn-through"; (2) a series of still photographs; (3) a high speed motion picture study taken of the plume discharging into an inert atmosphere; (4) a rapid scan emission spectra; and (5) a family of holographic interferograms. The damage sustained by the cartridge case -- Chapter 6 -- is explained in greater depth by: (1) studies using erosion test fixtures; (2) a parametric study wherein initial gas path size, peak chamber pressure, and propellant flow time are correlated with damage; (3) a standard slit experiment; (4) a determination of the heat flux to the cartridge case surface; (5) a metallurgical postmortem examination of the eroded areas; and (6) a discussion of the aluminum surface during "burn-through". Chapter 7 discusses a metallurgical postmortem of a weapon chamber that was exposed to the "burn-through" plume. Finally, Chapter 8 deals with other topics peculiar to the "burn-through" such as: (1) the nature of the vapor-phase reaction; (2) the effect of leading edges and sharp corners; and (3) a study using "cool" burning propellants.

CHAPTER 3. WHY "BURN-THROUGH"?

Prior to the program which was undertaken to investigate, identify, and understand "burn-through", the underlying causes of this phenomenon were subject to speculation. Observations of aluminum cartridge cases which have undergone "burn-through" provide some insight into possible causes. It is possible to generalize that "burn-through", as observed on the cartridge case, results in damage at either of two locations. Erosion may be seen at the juncture between the primer and primer pocket (at the base of the cartridge case) as is seen in Figure 4, and/or along the case body (in the vicinity of the extractor groove) in the head region as shown in Figure 1. These two locations allow a separation of the hypotheses identifying possible causes of the phenomenon into two categories -- possible causes for "burn-through" at the primer and possible causes for "burn-through" along the body.[7]

For the primer region, the following hypotheses were formulated:

1. As a result of the interior ballistic processes, heat transfer to the head of the cartridge case occurs at an excessive rate. The head-end of the cartridge case becomes overheated and fails mechanically either because the yield strength or allowed elongation is exceeded. This action loosens the primer and allows propellant gases to escape through the vacant primer pocket. The propellant gas flow causes an aggravated increase in the heat transfer rate to the primer pocket and thus accounts for the damage or triggers additional heat sources in the form of chemical reactions. In this case, the removal of the primer from the pocket is a prequisite for "burn-through",

2. The gas pressure causes the initially tight, press-fit seal between the brass primer cup and the aluminum pocket to open and thereby allows the flow of propellant gas through the newly created opening. In this case, "burn-through" may result without initial removal of the primer.

3. Thermal expansion causes the initially tight, press fit seal between the brass primer cup and the aluminum pocket to open and thereby allows the flow of propellant gas through the newly created opening. Thus, "burn-through" may result also without initial removal of the primer.

---

[7] Summerfield, M., Letter to Reed E. Donnard, Subject: "Cartridge Burn-Through Problem", Princeton University, Guggenheim Aerospace Propulsion Laboratory, Princeton, N.J., September 1969.

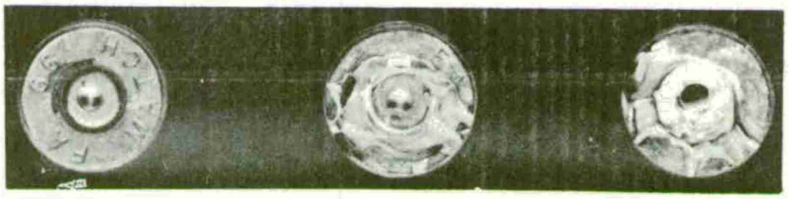

Figure 4. Base Regions of Aluminum Cartridge Cases Evidencing "Burn-Through" (Case on left shows no effect and serves as a comparison. Middle and right cases show severe erosion.)

4. The aluminum alloys used to fabricate the cartridge cases are expecially vulnerable to the reactive gases generated during propellant combusion.

5. Initially, there is a microscopic gap at the juncture between the primer and primer pocket through which propellant gas flows as soon as a pressure differential is established.

For the case body, the following hypotheses were constructed:

1. As the propellant gas pressure increases, excessive heating of the case wall can cause rupture.

2. If a discrete failure site is present, such as a localized mechanical defect, a crack can occur in the case body resulting from the pressurization -- even though the strain may be well within the allowable elongation.

3. "Burn-through" may occur as a result of over-pressurization of the cartridge case.

4. "Burn-through" may occur as a result of an anomalous increase in the propellant gas flame temperature much above the normal limit.

5. A burr on the inside surface of the cartridge case may present a possible site for aluminum particle combustion and thereby support the notion that the case wall can "burn-through".

6. A structural flow may be present in the case's sidewall at the time of firing. As the gas pressure is increased, this structural flaw results in the formation of a crack. The ensuing gas flow through this crack increases the net heat flux to the crack surface and is either solely responsible for the observed damage or leads to exothermic chemical reactions which, in concert with the heat flux from the gas flow, produce the observed damage. This structural flaw may be a metallurgical defect or void, an occlusion, or an internal or external scratch stemming from rough handling or improper processing.

7. An unsupported region of the aluminum body, either due to prior gradual chamber wear or severe chamber erosion resulting from a previous "burn-through", may cause a crack or split to occur.

Undoubtedly, many additional hypotheses concerning possible caused for "burn-through" can be enumerated. Those presented in the preceeding paragraphs were voiced at a meeting held in-house at the beginning of the program. These thoughts are formally documented in reference 7 and are presented here to serve as a basis for more detailed discussions on the exact cause of "burn-through". Nevertheless, the myriad hypotheses indicate the widespread uncertainty about the possible cause or causes of the aluminum cartridge case "burn-through" phenomenon. As

will be explained more fully in Chapter 4, it is possible, however, to confirm some of the hypotheses through successful simulations of the failure in aluminum cartridge cases.

Although the attempt was made to separate possible causes of "burn-through" into two classes according to location, there are definite similarities between each category. For example, primer region hypotheses 1, 2, 3, and 4 for "burn-through" are predicated on the fact that there must be an opening between the primer and primer pocket to permit propellant gas flow from the cartridge case. The only difference between these hypotheses is the manner in which the opening was created.

Likewise, case body hypotheses 2, 6, and 7 for "burn-through" are based on the fact that there must be a crack or split in the case's sidewall prior to or during firing. Again, the nature of crack formation is different for each hypothesis. The commonality of both sets of hypotheses is the fact that "burn-through" is the result of propellant gas flow through an opening in the cartridge case. Thus, with these hypotheses, the existence of a gas path as a precursor for "burn-through" is paramount.

The occurance of "burn-through" under normal firing conditions in standard field weapons is very rare. Statistics, available at Frankford Arsenal from firing programs conducted during recent MUCOM and U.S. Air Force sponsored 7.62mm aluminum cartridge case programs, indicate that the "burn-through" rate experienced was one cartridge per sample of 25,000 fired.[8] This rate is cited only to indicate that the conditions initiating "burn-through" are relatively rare; it does not occur frequently in an otherwise sound case. It may be added that under optimized conditions of case design, material and processing, this rate is expected to be very much smaller than the one in 25,000 failure noted above. However, this rate suggests that the phenomenon is not the result of a deficiency in the basic cartridge design, but rather the result of something that escapes the quality controls in the manufacturing process. If the basic cartridge design or material were at fault, "burn-through" would be experienced in every cartridge that was fired, assuming that each cartridge in the test sample was identical. It is possible to extend this argument to include the fact that perhaps some aspect of the cartridge design may be marginal; this in turn would allow small variations in the manufacturing process (small enough to escape quality controls or inspection) to produce the conditions (gas path, burr, etc.) which result in "burn-through".

---

[8] Rosenbaum, M., Hennessy, T., Marziano, S.J., and Donnard, R.E., "Design and Development of a 7.62mm Aluminum Alloy Cartridge Case", Technical Report R-2062, Frankford Arsenal, Phila., Pa., January 1973.

Therefore, in this light it is difficult to accept hypotheses which predict greater rates of "burn-through" than have been observed in actual cartridge firings. How can one argue that thermal expansion, chamber pressure, or aluminum vulnerability cause "burn-through" and then defend the fact that these possibilities do not cause "burn-through" everytime a cartridge is fired? Solely on the basis of the low "burn-through" rate and the previous hypothetical argument, the hypothesis for "burn-through" originating at the primer, which has the most credence, is the one based on gas flow through a microscopic gap between the primer and primer pocket, which develops as the result of excessive case head deflection during firing of the cartridge. Additionally, it is very conceivable that during the standard assenbly operations, the primer may be incorrectly inserted or aligned in the primer pocket. Therefore, it is possible that once or twice during fabrication of a large production quantity, a small gap between the primer and primer pocket may result.

Similar arguments can be applied to isolate the most plausible hypotheses for "burn-through" originating along the case. If excessive heating, over-pressurization, or crack generation of a sound cartridge case from the interior ballistics were the cause, the expected rate would be much higher than that experienced. Not eliminated on the basis of statistics are the possibilities that "burn-through" may result from an increase in the propellant gas flame temperature, a burr on the inside surface of the cartridge case, crack formation originating from a structural or metallurgical flaw, or crack formation stemming from an unsupported region of the cartridge body. It is not difficult to conduct a series of diagnostic tests to confirm which of these hypotheses is correct and in addition ascertain the validity of whether or not "burn-through" can be simulated by producing a small opening between the primer and primer pocket. These tests are discussed in Chapter 4.

CHAPTER 4. SIMULATION OF "BURN-THROUGH"

As the natural occurrence of an aluminum cartridge case "burn-through" is very rare, it is necessary to have at our disposal certain techniques to induce or simulate this phenomenon. A successful simulation would enable isolation of the possible cause or causes of "burn-through". Once possible causes of this phenomenon were identified, systematic investigation of the failure dynamics could be undertaken to provide a basis for determining a solution or solutions to the problem. Thus, the following diagnostic tests were conducted to further our understanding of the phenomenon that has hindered the acceptance of aluminum cartridge cases into the logistic system.

Very early in the experimental program it was found that a small hole drilled in the head region of an aluminum cartridge case, or a four to five thousandth inch deep longitudinal scratch would, upon firing, lead to the "burn-through". Figure 5 shows the results of firing brass and aluminum cartridge cases with a 0.0135 inch (diameter) hole in the head region of each case. The two brass cases seem unaffected after firing. However, the two aluminum cartridge cases show the typical erosion in the head region; the unfired aluminum cartridge case can be used to compare the damage after firing with its initial, drilled condition. Figure 6 shows sectioned aluminum alloy and brass cartridge cases before and after firing. As indicated in the photograph, the small fissure in the brass case undergoes only a slight alteration. On the other hand, the increase in the hole's diameter of the aluminum alloy cartridge case is obvious. Although attempts have been made to induce "burn-through" by drilling small holes in the case body, no evidence of "burn-through" resulted. Figure 7 shows typical cases after such an experiment. Even though the diameter of the hole is the same as that which produced the damage to the aluminum cartridge cases in the previous two figures with similar ballistics, no "burn-through" is observed. This is indeed surprising until one realizes that the sidewall of the case expands, as a result of high gas pressures, to the point where it is constrained by the weapon's chamber. Once the sidewall physically touches the chamber, obturation occurs and the propellant gas flow is prevented. As discussed in reference 5, the high speed propellant gas flow is a precursor for "burn-through". The drilled hole experiment has been introduced in reference 5 and is discussed more fully in Section 6.1 of this document. Suffice it to say, the drilling of a small hole in the head region of an aluminum cartridge case -- thereby providing a path for the high energy propellant gas -- has been shown to duplicate the damage sustained by the cartridge case under normal "burn-through" conditions.

Brass

Aluminum

Unfired
Aluminum

Figure 5. Drilled Hole Experiment

Before After
Aluminum

Before After
Brass

Figure 6. Sectioned Aluminum Alloy and Brass Cartridge Cases Before and After Firing

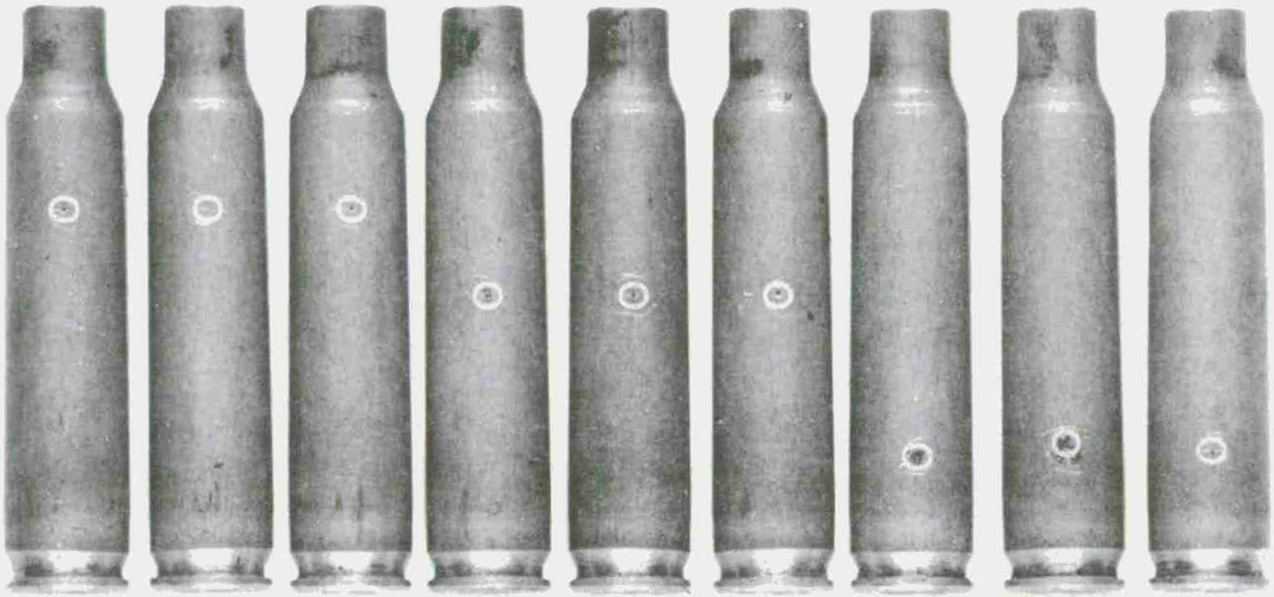

Figure 7. 5.56 mm Aluminum Cartridge Cases with Holes Along Case Body Providing Gas Path to Simulate "Burn-Through" (Observe lack of erosion along case body.)

The other technique of simulating "burn-through" -- the slitting or scratching of the case body -- is treated in reference 9. A photograph showing the resultant damage to 5.56mm aluminum cartridges, which were scratched according to the procedure set forth in reference 9, is provided as Figure 8. Observe the similarity between the "burn-through" simulated in these cases and the one which occurred naturally, shown in Figure 1. Again, the point is to be made that a gas path must be provided for the propellant gases. In this experiment, a slit -- not even completely through the case sidewall -- produced the gas path once the case sidewall began to expand. It is to be noted that where the case obturated in the chamber (along the body) there is no evidence of "burn-through".

Another experiment involving slit or scratched aluminum cartridge cases bears mentioning. Reference 10 discusses an experiment wherein propellant gas flow through an induced path in the case was reduced to almost nil be the use of a special weapon bolt/chamber design. The novel design involved a modification to the bolt of an M16A1 rifle such that an extension or collet was provided which completely surrounded and supported the head of the slit cartridge case. There was no damage to the case or weapon test fixture even though a gas path existed in the case wall at a location where typical case and weapon damage would have otherwise occurred. Stopping or, at least, drastically reducing propellant gas flow through the path in this case eliminated the damage.[10]

Other techniques used to induce a "burn-through" were unsuccessful. Small silvers of aluminum -- to simulate a burr -- were raised on the interior surface of the cartridge case. These silvers, which presented possible sites for aluminum particle combustion, yielded no evidence of "burn-through". The adiabatic flame temperature of the propellant gases was increased by homogeneously mixing varying amounts of fine aluminum powder with the propellant charge. When aluminum cases loaded with these special mixtures of propellant and aluminum powder were fired, no "burn-through" was observed. The overpressurizing of the cartridge case was accomplished by increasing the standard charge of WC 846 propellant from 27.4 grains to 28.3 grains. Again, no evidence of "burn-through" was recorded from firing cartridges with

---

[9]Donnard, R.E., and Skochko, L., "Induced-Failure Test Procedure for Aluminum Alloy Cartridge Cases", Report #6019, Frankford Arsenal, June 1971.

[10]Unpublished data, "The Aluminum Cartridge Case "Burn-Through" Problem - Characteristics, Isolation, and Means of Elimination", Frankford Arsenal, Phila., Pa.

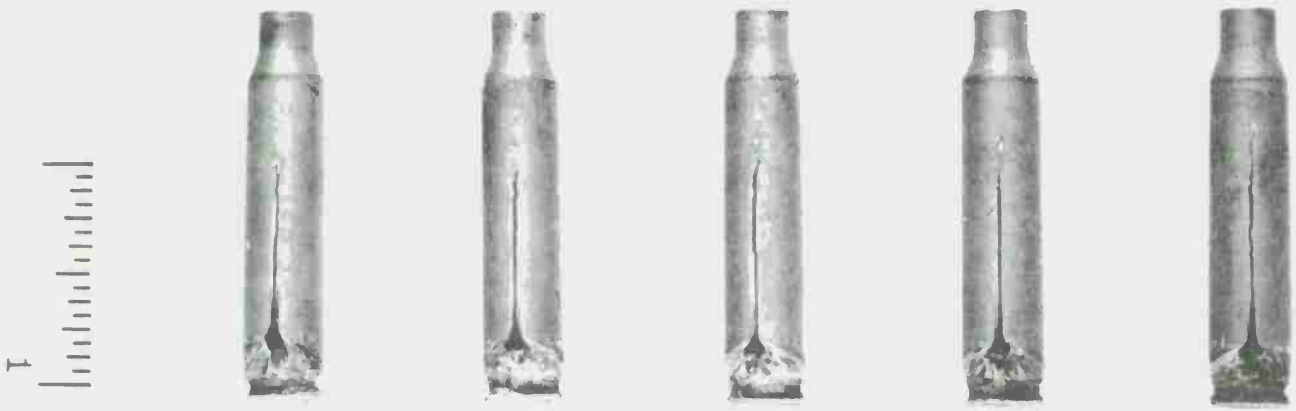

Figure 8. Examples of 5.56 mm Aluminum Alloy Cartridge Cases in Which "Burn-Through" has been Simulated by Scratching the Exterior Surface

increased charges. From this work it was concluded that a gas path must be available for the unrestricted flow of propellant gases. Coupling the successful simulation of "burn-through" resulting from drilling a small hole in an unsupported region of the case, or by slitting or scratching the cartridge body and the fact that the natural occurrence is very rare, it is easy to single out those hypotheses which indicate the underlying causes.

Aluminum cartridge case "burn-through" at the primer region is caused by the flow of propellant gases through a microscopic gap at the juncture between the primer and primer pocket. Along the case body "burn-through" occurs when the flow of propellant gas from the interior of the cartridge takes place during firing. In both instances, structural integrity of the case is usually responsible for the "burn-through". Also, if an appreciable part of the chamber has been eroded, the cartridge upon expanding to meet the chamber may split or crack. The manifestation of the gas path will result in "burn-through". In summation, it is to be stressed that the presence of a gas path through or past the aluminum surface will result in "burn-through".

The problems involving microscopic gaps at the primer/primer pocket interface, structural flaws in the case body, or splitting cases during firing are not unique with aluminum cases. These same problems occur in brass cartridge cases. However, the post-break-through damage is unusually severe with aluminum cartridge cases. The question is then raised as to what is peculiar about the passage of propellant gases through a fissure -- either occurring naturally or induced -- in aluminum cartridge cases. The remainder of this document is concerned with answers to this question.

CHAPTER 5. STUDIES OF THE PLUME INITIATED WITH INDUCED CASE FAILURES

This section of the report is devoted to an analysis of the plume that arises from the failure site of an aluminum case during firing. Not all case failures lead to "burn-through". It occurs only where propellant gas combustion products are free to flow through the case wall or primer/primer pocket juncture during the internal ballistic cycle. It was thought that clues to the "burn-through" phenomenon could be found by an appropriate analysis of this plume. Induced failure techniques, wherein the entire case failure cycle was created on demand, were used to initiate "burn-through". The experiments conducted to produce data for this analysis are discussed below.

SECTION 5.1. M16A1/UNIVERSAL RECEIVER MOTION PICTURE ANALYSIS

The body of this report is introduced with a series of excerpts printed from a high speed movie of the "burn-through" phenomenon. This is perhaps the best way to present the phenomenon, define the problem, and provide a suitable introduction for the remainder of the report. The use of high speed motion picture technology has been employed and referenced on other occasions throughout this program; therefore, the excerpts which follow serve as introductory data.

As mentioned earlier, the aluminum cartridge case failure process differs drastically from its brass counterpart. There are three serious consequences resulting from this failure process. First, there is a large, luminous plume of hot gases exiting the breech of the weapon. This gaseous cloud could cause serious harm to the rifleman. Second, the failure also affects weapon performance by making it either inoperable or unsafe to operate. Third, there is the damage sustained by the cartridge case itself.

Failures were introduced in 5.56mm aluminum cartridge cases according to the procedure as outlined by Donnard and Skochko.[9] An M16A1 rifle, fired in the semiautomatic mode, was used as the test weapon; the prescratched cartridge cases were clipped into the standard magazine. A Fastex, 16 millimeter camera, with the framing rate set at 500 frames/second (the time interval between each frame when the camera is at full speed is 2.0 milliseconds), was used to take the motion pictures.

Frame 1 (Figure 9) shows a full shot of the M16A1 rifle and the ten prescratched, 5.56mm aluminum cartridges used in this test. After the camera was started and allowed to accelerate to maximum speed, the lanyard to the trigger was pulled.

Frame 2 is a closeup of the M16A1's receiver. The remainder of the film sequence is taken with the camera/object distance and camera settings as shown in this frame.

The first evidence of the "burn-through" is seen in Frame 3 (Figure 9) in the emergence of light at the bolt/chamber interface and at the bottom of the magazine.

Frame 4, taken 2.0 milliseconds after the previous frame, shows a bright, luminous cloud exiting the bolt of the M16A1. This cloud

---

[9] Donnard, R.E., and Skochko, L.W., "Induced-Failure Test Procedure for Aluminum Alloy Cartridge Cases", Report #6019, Frankford Arsenal, June 1971.

Frame 1 Test Weapon

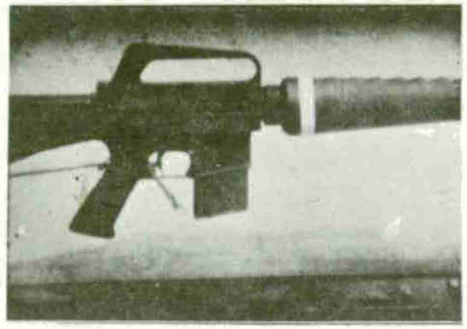

Frame 2 Close-Up

Frame 3 t = 0.000 msec

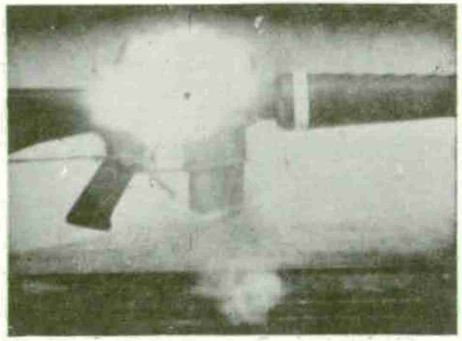

Frame 4 t = 2.000 msec

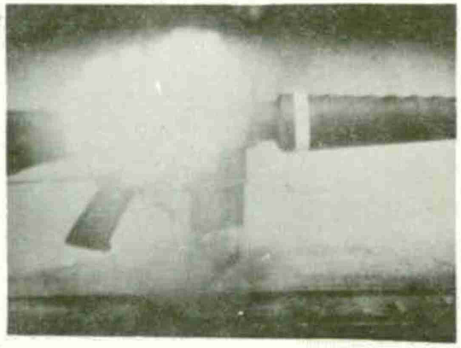

Frame 5 t = 4.000 msec

Framing Rate: 500 Frames/Sec Semi-Automatic Firing Mode

Figure 9. High Speed Motion Picture Sequence of Aluminum Cartridge Case "Burn-Through" in M16A1 Rifle (Up to 4.0 milliseconds.)

is different from the gaseous discharge which exits the muzzle of the weapon. It is, therefore, concluded that the "burn-through" is governed by processes different from the expansion and cooling characteristic of the muzzle blast.

Frames 5 (Figure 9) and 6 (Figure 10) -- representing a total elapse time of 4.0 milliseconds -- show that the luminous plume is propagating rearward -- toward the rifleman. This plume is generally characterized by the white center and the orange periphery.

The plume is observed to be separated from the weapon in Frame 7, and to be of such a configuration as to obscure the M16A1's receiver and stock. The cloud is definitely emitting energy even though it is separated from its point of origin. There is also evidence of a small, localized, luminous region at the bolt/chamber interface.

The luminous cloud seems to have propagated out of the field of view in Frame 8 (Figure 10). There is also evidence of solid particles (probably propellant grains) in the bolt cavity of the weapon. The initial blast, observed at the bottom of the magazine, has sufficient force to destroy the magazine; the spring can be seen ejecting from the magazine's body.

Frame 9 was taken approximately 60.0 milliseconds after "burn-through" was first observed. The plume is no longer visible but its consequences can still be observed as the bottom, spring, and follower leave the magazine.

Frame 10 shows the results of "burn-through". Although all ten cartridges were prescratched, only the first round in the magazine was fired. The blast, channeled throughout the magazine, terminated the test after one round. The "burn-through" which was induced in the aluminum cartridge case is a fair representation of the natural failure as shown in Figure 1.

The use of an M16A1 rifle as the test weapon precluded focusing the camera on the surface of the cartridge case and making a close examination of the "burn-through" dynamics. To accomplish this, a universal test fixture and velocity barrel were modified to allow exposure of the failure area. Care had to be exercised in modifying the test barrel which provided support to the case. If too much metal were removed from the test barrel, the case would be unable to withstand the pressure buildup and rupture before the "burn-through" occurred. For this reason the viewing area was limited to that portion of the case which could function without chamber support. As the schematic, Figure 11, shows, the head portion of the case is in view at the bottom of the viewing slot.

The cartridge case is fired by remotely initiating a goose control unit. The unit starts the 16 millimeter Fastex camera, and a built-in

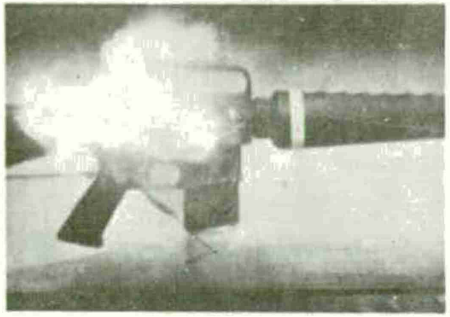

Frame 6 t = 6.000 msec

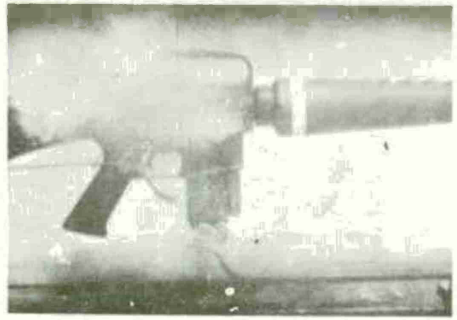

Frame 7 t = 10.000 msec

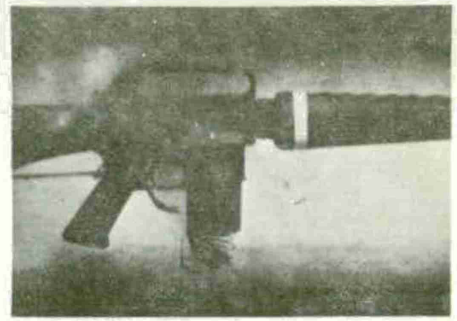

Frame 8 t = 14.000 msec

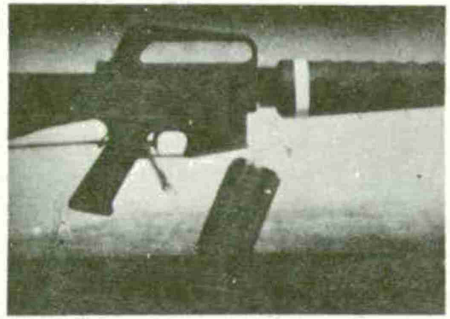

Frame 9 t = 60.000 msec

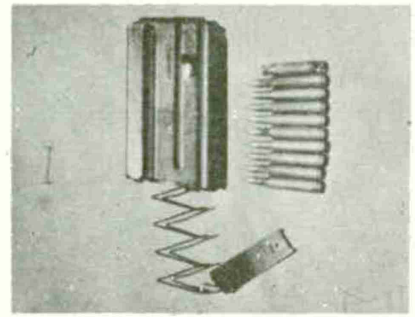

Frame 10 Results

Framing Rate: 500 Frames/Sec Semi-Automatic Firing Mode

Figure 10. High Speed Motion Picture Sequence of Aluminum Cartridge Case "Burn-Through" in M16A1 Rifle (From 6.0 milliseconds to 60 milliseconds.)

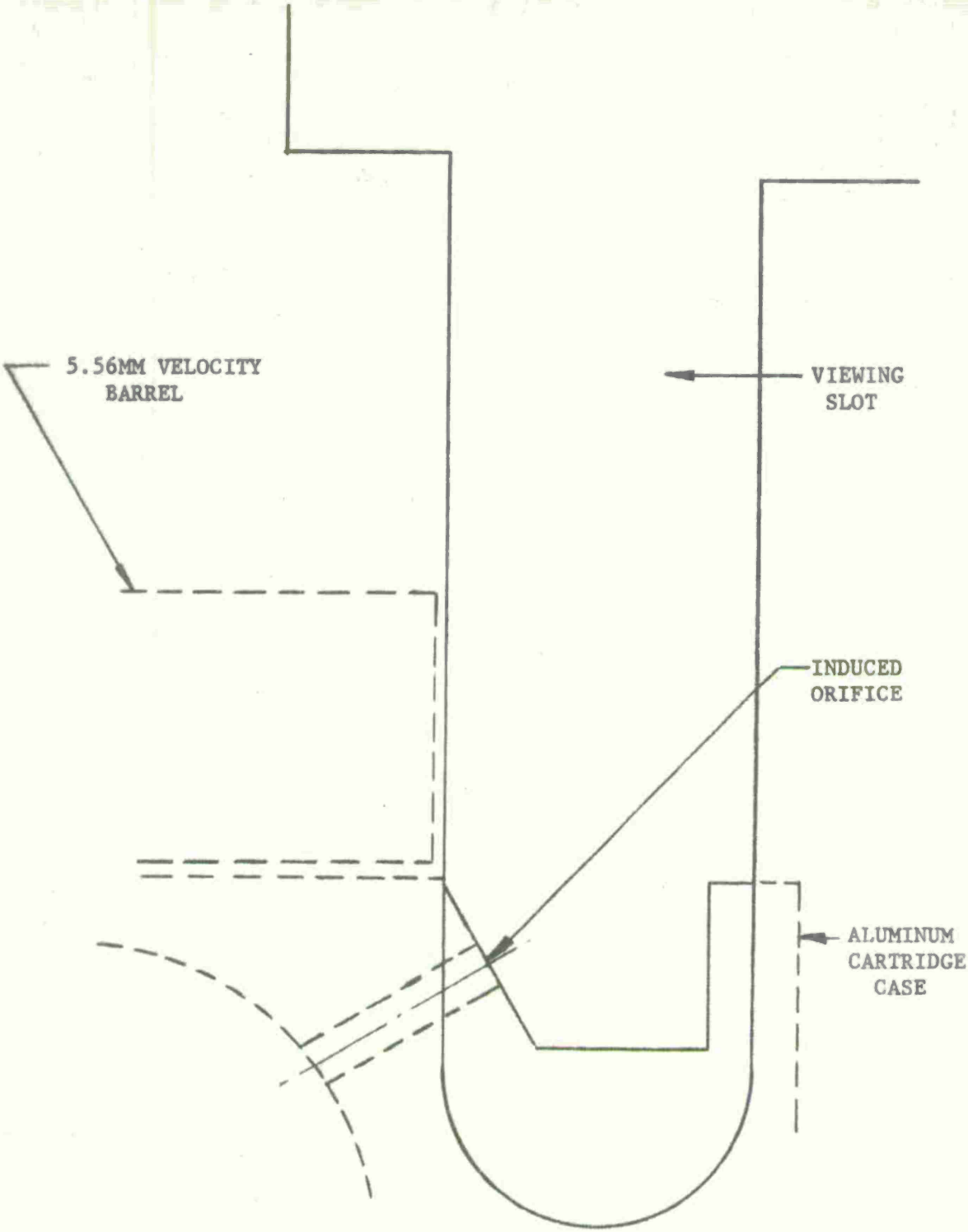

Figure 11. Location of Aluminum Cartridge Case in Viewing Slot (Note location of drilled hole in extractor groove.)

delay unit activates the firing mechanism of the universal receiver after the camera achieves maximum framing rate; the usual delay time is 0.6 millisecond.

In the first pictures of this series the camera, equipped with a 12.5 millimeter lens, is positioned fifty-six inches from the viewing slot. With this setup it was possible to determine the extent and duration of the gaseous plume characteristic of the "burn-through". Care should be exercised in attempting to compare the results obtained with the experimental setup and pictures taken of the plume using the M16A1 as the test weapon. Major differences include the facts that this series of pictures was taken using a test weapon which does not restrict the gaseous discharge (the modified universal receiver and test barrel do not have a bolt/locking mechanism), and artifical lighting was used to illuminate the subject (three or more flood lights). In addition, the camera's framing rate was much greater in this experiment (12,000 frames per second compared to 500 frames per second). Figures 12, 14 and 15 are photographs of selected frames from three different high speed framings. The times which accompany the individual frame identifications in Figure 12, 14 and 15 do not refer to the interior ballistic cycle. Each interval represents time elapsed after the initial exposure. Since pressure-time curves were not taken in this experiment, comparison of each frame with corresponding events in the interior ballistic cycle is precluded.

Frame 1 (Figure 12) shows the viewing slot in the universal receiver. The universal receiver and test barrel were positioned in the usual horizontal arrangement during the test. However, both the universal receiver and the film clip are coincidentally positioned in the report for proper viewing with Figure 13.

Frame 2 (Figure 12) taken 0.083 millisecond later, shows the viewing slot completely filled with the luminous gaseous discharge. Since the length of the viewing slot is 1.30 inches and since the time interval for this discharge to occur is at least 0.083 millisecond, the average velocity for this plume to propagate (in Frame 2) is 1.25×10^3 feet per second.

In Frame 3, the viewing slot is still filled with the characteristic white light, but the plume is now beginning to propagate externally to the universal receiver. Frame 3 is recorded 0.083 millisecond after Frame 2.

Frames 4, 5, and 6 show clearly the formation of the plume. Since this experiment was performed in a darkened range, with flood lights used to illuminate the subject, the plume appears to be brighter when compared with the pictures taken out-of-doors using the M16A1 as the test weapon.

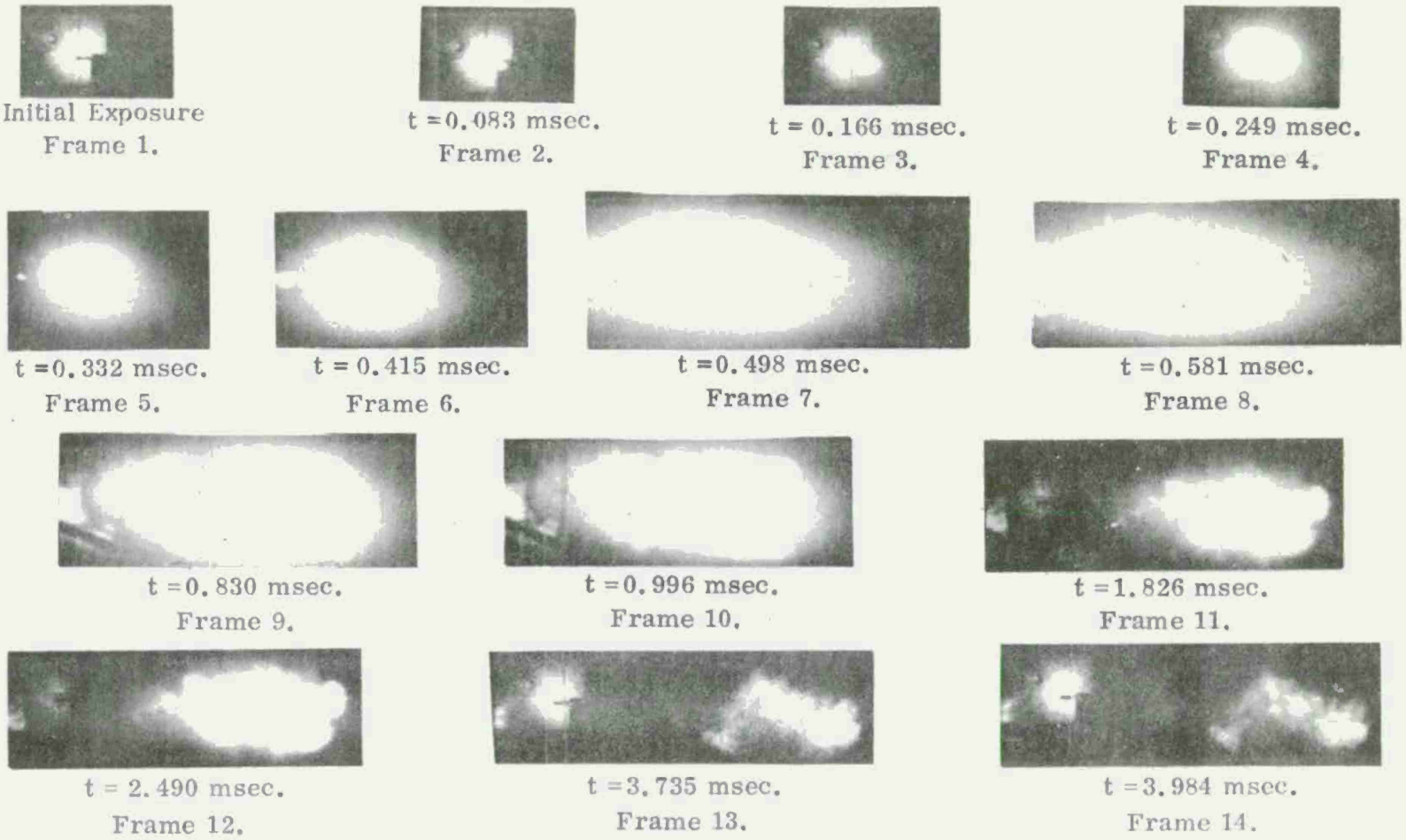

5.56mm ALUMINUM CARTRIDGE CASE VIEWING SLOT EXPERIMENT

Framing Rate: 12,000 Frames/sec. Camera/Object Distance: 56 inches
Atmosphere: Air Slit Cartridge Case
Propellant Charge: 27.4 grains

Figure 12. High Speed Motion Picture Study of Aluminum Cartridge Case "Burn-Through" Plume (12.5 mm lens)

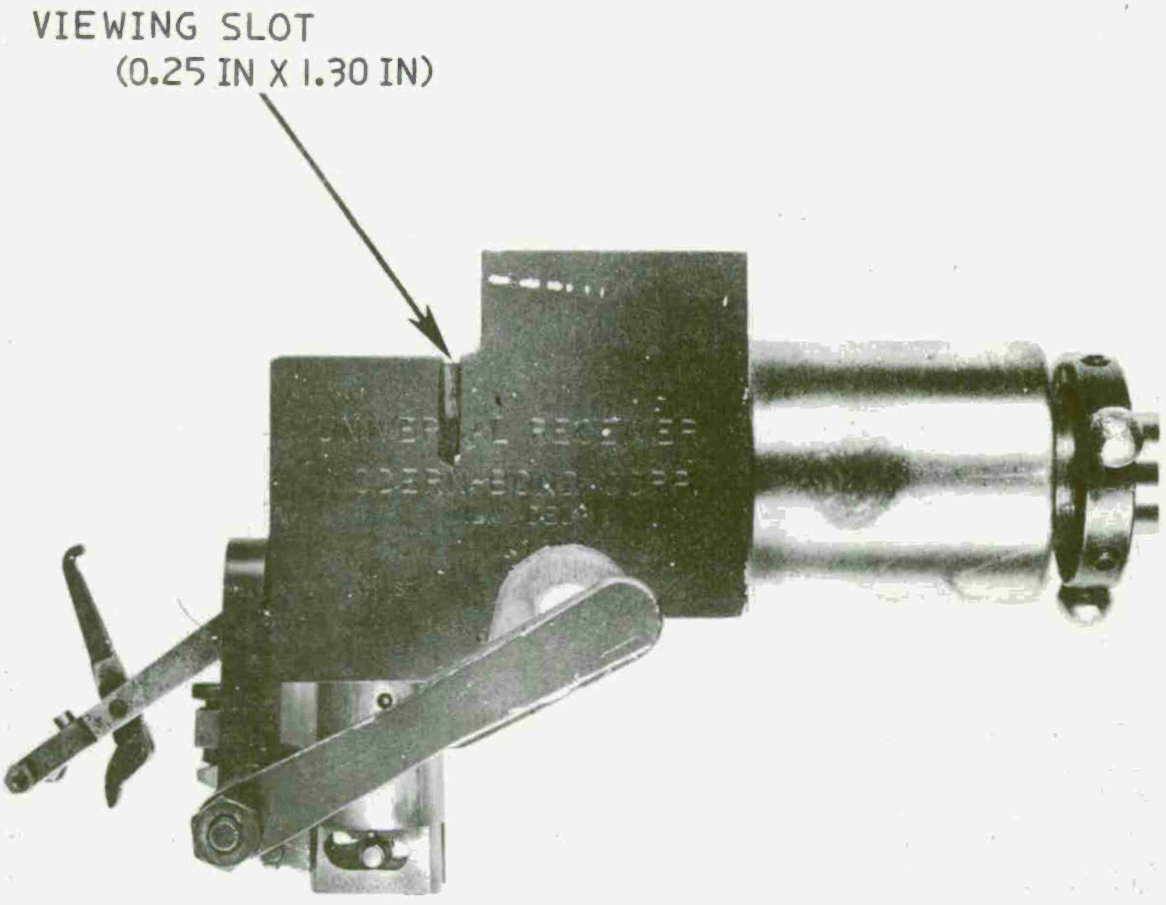

Figure 13. Universal Receiver (with Viewing Slot) Used in High Speed Motion Picture Study.

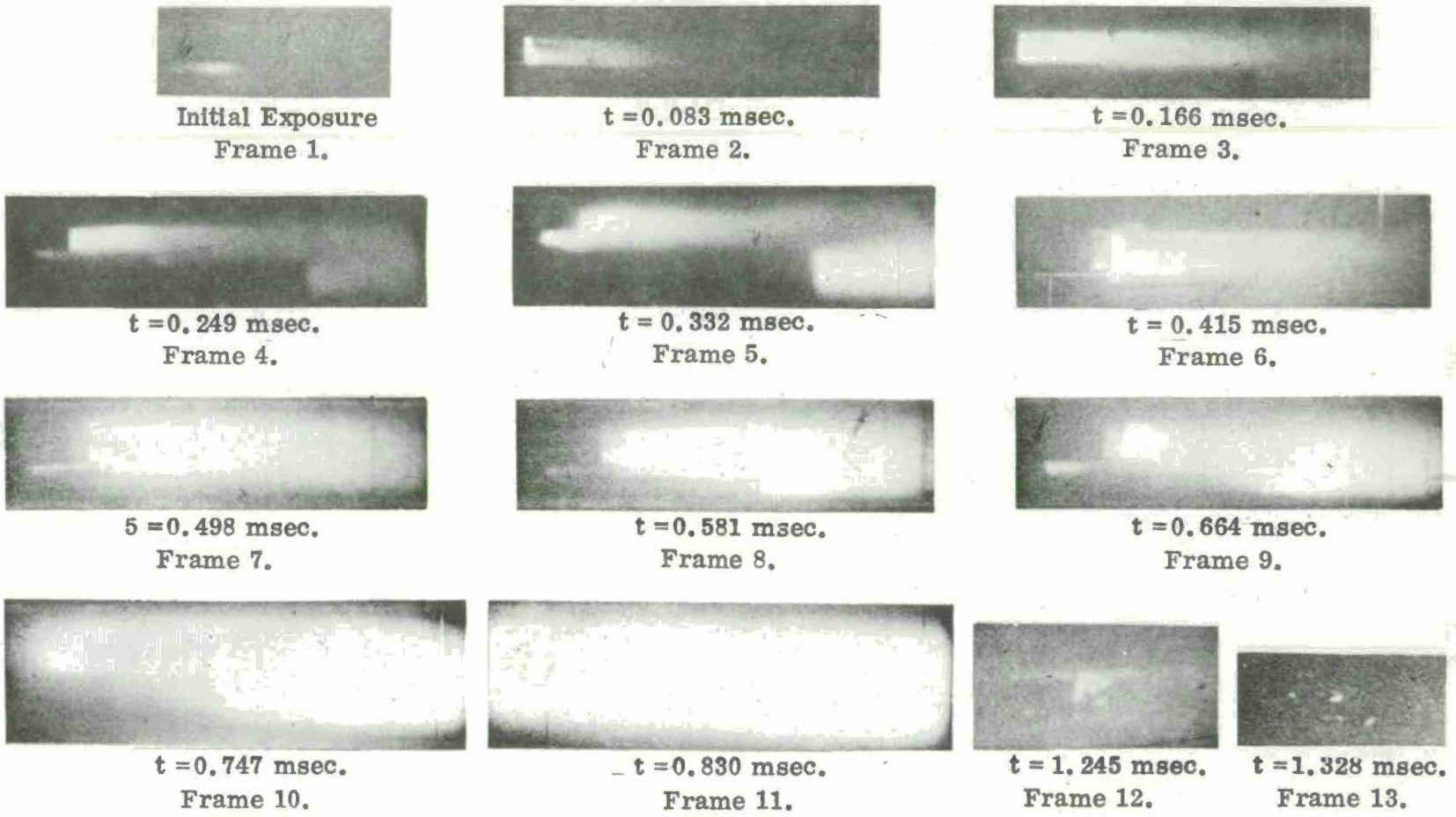

5.56mm ALUMNIUM CARTRIDGE CASE VIEWING SLOT EXPERIMENT

Framing Rate: 12,000 Frames/sec. Camera/Object Distance: 32 inches
Atmosphere: Air Slit Cartridge Case
Propellant Charge: 27.4 grains

Figure 14. High Speed Motion Picture of Aluminum Cartridge Case "Burn-Through" Plumes (2-inch lens)

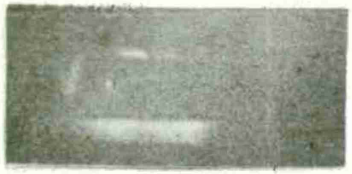

Frame 1. Initial Exposure

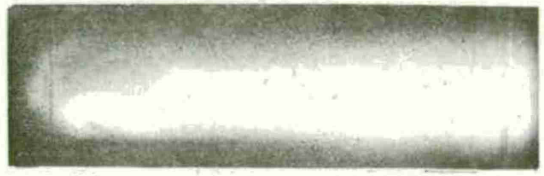

Frame 2. t = 0.166 msec.

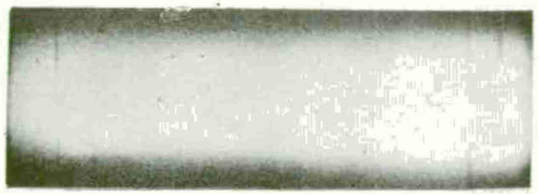

Frame 3. t = 0.332 msec.

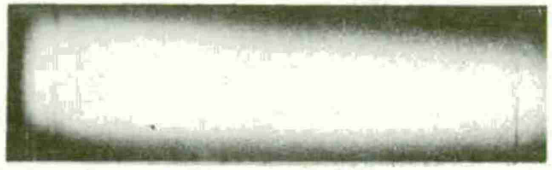

Frame 4. t = 0.415 msec.

Frame 5. t = 0.498 msec.

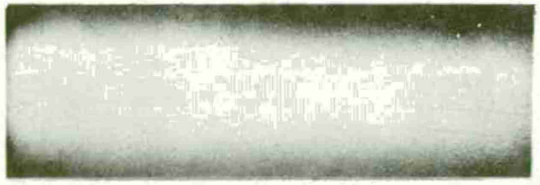

Frame 6. t = 0.581 msec.

Frame 7. t = 0.830 msec.

Frame 8. t = 1.079 msec.

Frame 10. t = 1.328 msec.

Frame 9. t = 1.245 msec.

5.56mm ALUMNIUM CARTRIDGE CASE VIEWING SLOT EXPERIMENT

Framing Rate: 12,000 Frames/sec.
Atmosphere: Air
Propellant Charge: 27.4 grains
Camera/Object Distance: 23 inches
Slit Cartridge Case

Figure 15. High Speed Motion Picture of Aluminum Cartridge Case "Burn-Through" Plumes (4-inch lens)

Moving ahead to 0.083 millisecond, Frame 9 provides a good representation of the size of the gaseous plume. Comparison of the cloud shown in Frame 9 with that of Frame 2 indicates that the plume has propagated about twenty inches.

Frame 11, taken 1.826 milliseconds after Frame 1, shows that the plume is still growing but, as evidenced by the dull region between it and the receiver, the plume has separated from its point of origin. Since at this time the cloud is relatively bright but separated from its point of origin, it may be concluded that there are chemical reactions occurring within the cloud and producing the light energy.

After 3.735 milliseconds, as is shown in Frame 13, the cloud is still observed although somewhat diffused. Events observed before and during Frame 13 can be related to the interior ballistic cycle by considering that it takes only 1.2 milliseconds for the projectile to exit the barrel and approximately 2.0 to 3.0 milliseconds for the pressure to return to atmospheric level in the cartridge case. Therefore, the information conveyed in Frame 13 is occurring during the depressurization of the cartridge case.

Frame 14, taken 3.984 milliseconds after Frame 1, shows that the cloud is clearly in the field of view although its intensity has diminished considerably. Analyses of these and pictures of similar setups provide the generalization that the plume resulting from the "burn-through" (when the experiment is performed in the modified universal receiver) is approximately cylindrically shaped, thirty-six to forty inches in height, twelve inches in diameter, and exists for 4.4 to 4.6 milliseconds. In addition, since the gaseous plume is still emitting light energy, after being separated from its origin, chemical reactions are definitely occurring. This plume has been analyzed by state-of-the-art techniques and will be discussed later in this document.

The next series of film excerpts were taken with a two inch lens maintained at a camera/object distance of thirty-two inches. With this setup it was possible to obtain a closer examination of the case surface.

The first evidence that the "burn-through" was occurring is seen in Frame 2 of Figure 14. Frame 3 taken 0.083 millisecond later shows the development of a localized region of bright light. This light appears to be originating from the surface of the cartridge case. An orange hue seems to be propagating throughout the viewing slot.

Frames 4 and 5 (Figure 14) taken 0.249 and 0.332 millisecond respectively after the initial frame, indicate that the localized region of bright light is spreading throughout the viewing slot.

The entire viewing slot is filled with the orange hue in Frame 6.

There is, however, a small region of the characteristic bright (white) light at the extreme left of the frame.

The most dramatic change occurs in Frame 7, in which the complete viewing slot is masked by the bright, white light. The frame was taken 0.498 millisecond after the initial observation. This condition in the viewing slot lasted for approximately 0.665 millisecond. Events are then resumed with Frame 9, taken 0.664 millisecond after Frame 1, and an orange region in the viewing slot amidst the bright, white light can be observed.

The bright light in the viewing slot disappears after approximately 1.163 milliseconds. In the first series of pictures taken with the universal test fixture the region of bright illuminosity existed in the test fixture for 4.4 to 4.6 milliseconds. It is possible, therefore, that due to the limited field of view (the entire viewing slot) the bright light has propagated out of camera range.

Frame 12 shows a large area of orange light. Since the characteristic white light has disappeared, a source for this orange cloud must be postulated. After these experiments were performed, observation of the chamber/receiver interface showed deposits of metallic residue. The hypothesis is presented that this depositing of the metallic residue is being recorded during this frame. This material has been carefully scraped from the receiver and analyzed, another section of this report will discuss this analysis.

From this film series, it is possible to conclude that the plume associated with "burn-through" occurs in two distinct regions. First, there is a localized region of white light occurring at or near the surface of the cartridge case. This zone is observed to last for approximately 1.500 milliseconds. Then, as observed in the first series taken of the "burn-through" in the universal receiver, there is a second reaction zone, occurring external to and separated from the test weapon and cartridge case.

The third and final series of high speed motion pictures was taken using a 4-inch lens with a camera/object distance of twenty-three inches. This experimental setup allows the closest observation of the viewing slot (the cartridge case surface is also visible) such that the entire slot fills most of the field of view. However, the secondary plume -- that which occurs external to the test weapon -- is not visible.

The "burn-through" is first observed in Frame 1 of Figure 15 as an orange light at the surface of the cartridge case. The aluminum cartridge case is clearly seen at the left of the frame.

Frame 2, taken 0.166 millisecond later, shows the existence of a white region at the surface of the case. In Frame 2, the bright luminous light appears to fill the entire viewing slot. Frame 3,

taken 0.415 millisecond after the initial observation, shows that the intensity of the bright light has diminished considerably, as a noticeable dull region appears in the middle of the viewing slot. There is, however, a region of light at the cartridge case surface.

Action 0.498 millisecond after Frame 1, as seen in Frame 4, shows the existence of the characteristic bright cloud completely filling the viewing slot. At the surface of the cartridge in Frame 5, the existence of a white region can be clearly seen. Frame 6 shows the same effect as Frame 5, but as the intensity of the white light in the viewing slot is reduced, this region is more clearly visible. Frame 9, taken 1.245 milliseconds after the first frame, shows the glowing residue which was also observed in the second series of pictures taken in the universal receiver.

SECTION 5.2. "STILL" PHOTOGRAPHIC OBSERVATIONS

A series of special test fixtures were designed and fabricated to investigate the erosivity of materials which can be used to manufacture small arms cartridge cases. Three such test fixtures were available during various phases of the program: (1) A low-pressure, venting vessel (tested statically to 15 kpsi); (2) A high-pressure, venting vessel (tested statically to 60 kpsi); (3) and a conventional test barrel modified to allow propellant gas impingement on selected metal targets.

Although the low-pressure venting vessel shown schematically in Figure 16 (a complete discussion of this device is given in Section 6.1) is used primarily to study the erosivity of various materials as a function of peak chamber pressure, initial hole size, material thickness, and propellant gas flow time, it is possible to adapt this fixture to study another aspect of "burn-through". Since the gaseous discharge exiting the fixture is not restrained by any part of the vessel, this presents another excellent opportunity to study the formation of the plume.

Figure 17 is a photograph obtained by leaving the shutter of a "still" camera open during the gaseous discharge. The photograph then represents the maximum extent and intensity of the "burn-through". Figure 18 is the discharge which results from propellant gases flowing through a brass (70-30) test specimen; the peak pressure was approximately 15 kpsi. Note that there is no characteristic bright flash. The only observables are the streaks of orange light. Due to the relative thickness of these streaks, their orange color, the fact that they are relatively "short-lived" and the observation that there was negligible erosion sustained by the test disc, it is concluded that they were produced by burning propellant grains ejected from the orifice in the test specimen.

When the brass disc is replaced with an aluminum test specimen and the experiments performed again (15 kpsi, peak chamber pressure), the results are quite different. As seen in Figure 19, the characteristic bright flash is observed in the "still" photograph. Coupling this information with the high speed camera study, the hypothesis that the "burn-through" occurs in two phases is clearly substantiated. There is a primary reaction zone which occurs close to the surface of the test specimen. The characteristic secondary reaction zone, which has been observed external to the test weapon, is also seen. Note that this secondary plume is separated from the primary zone by a dull region. Although the primary zone is much smaller than the extensive secondary plume, the relative intensitives of each zone are comparable. In addition to the obvious "burn-through" flash, the "tracks" left by the burning propellant grains are also visible.

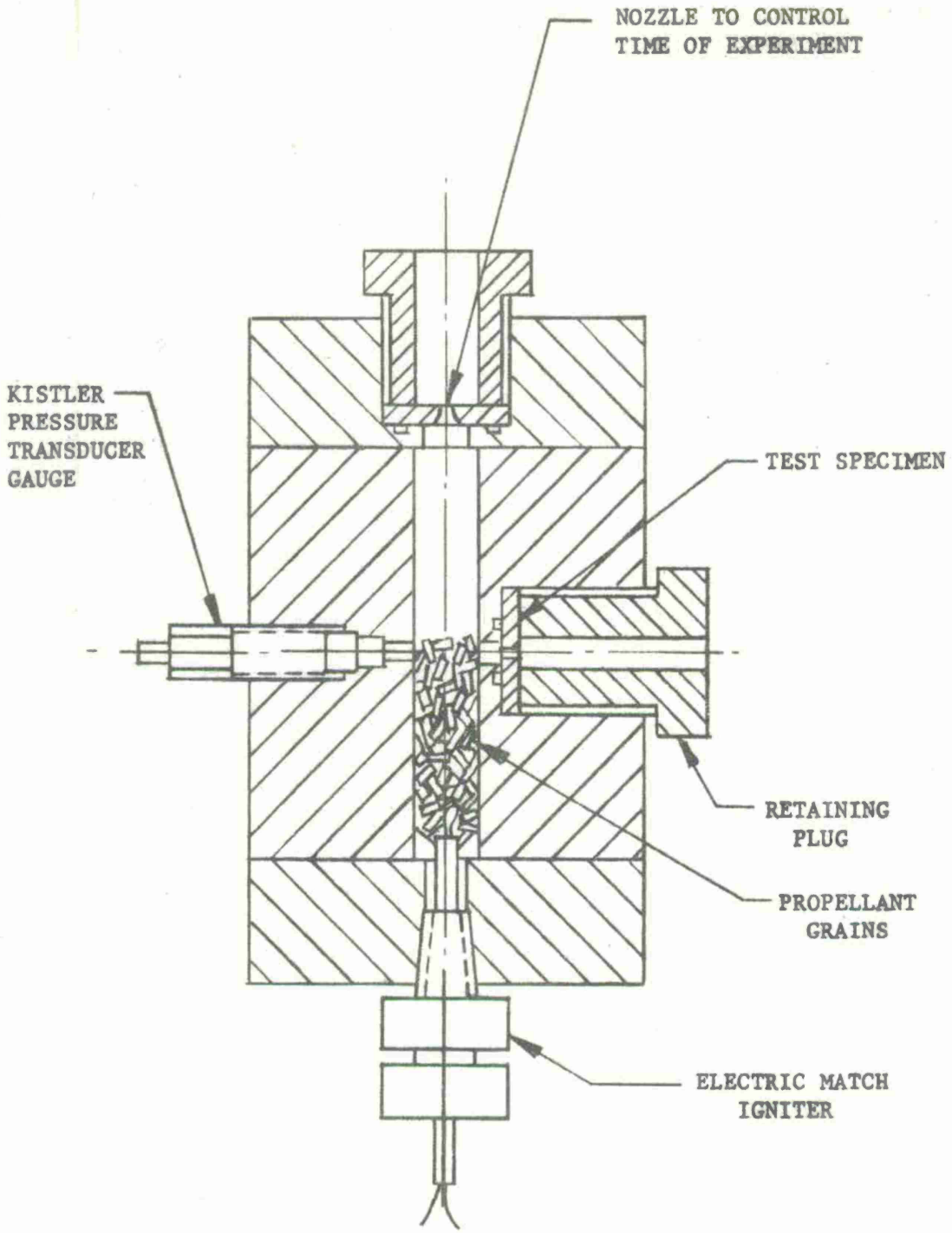

Figure 16. Schematic of Low-Pressure Vessel Used in Erosion Experiments.

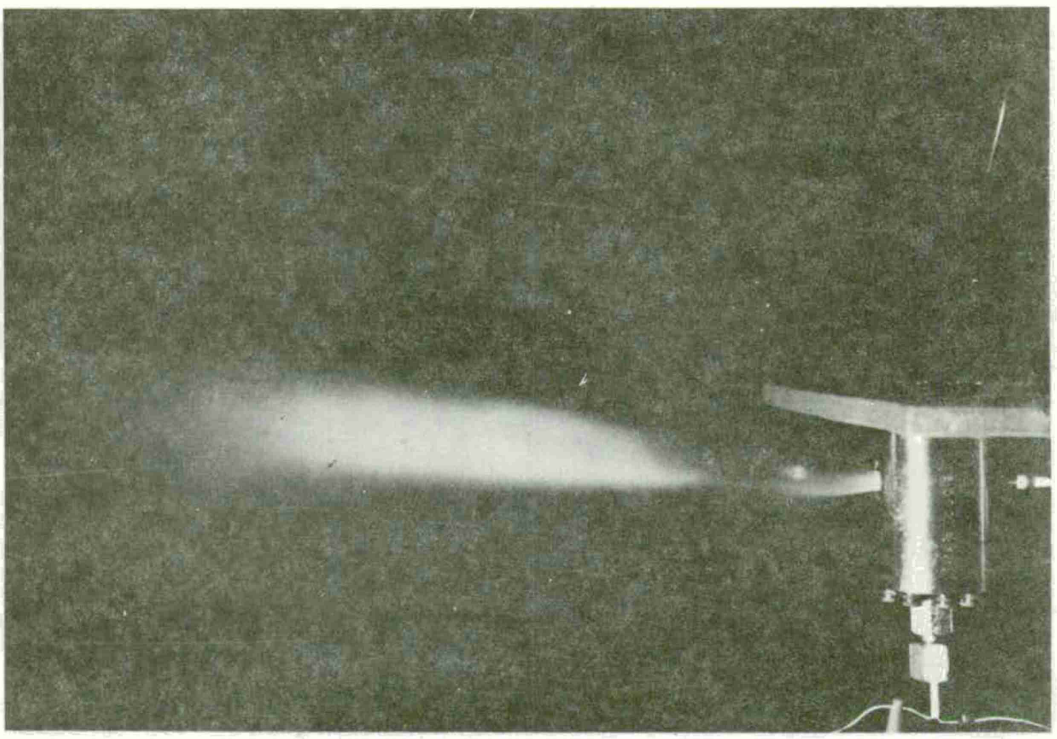

Figure 17. Plume Resulting from Passing Propellant Gases, Generated in a Low Pressure Vessel, through an Aluminum Disc into Air

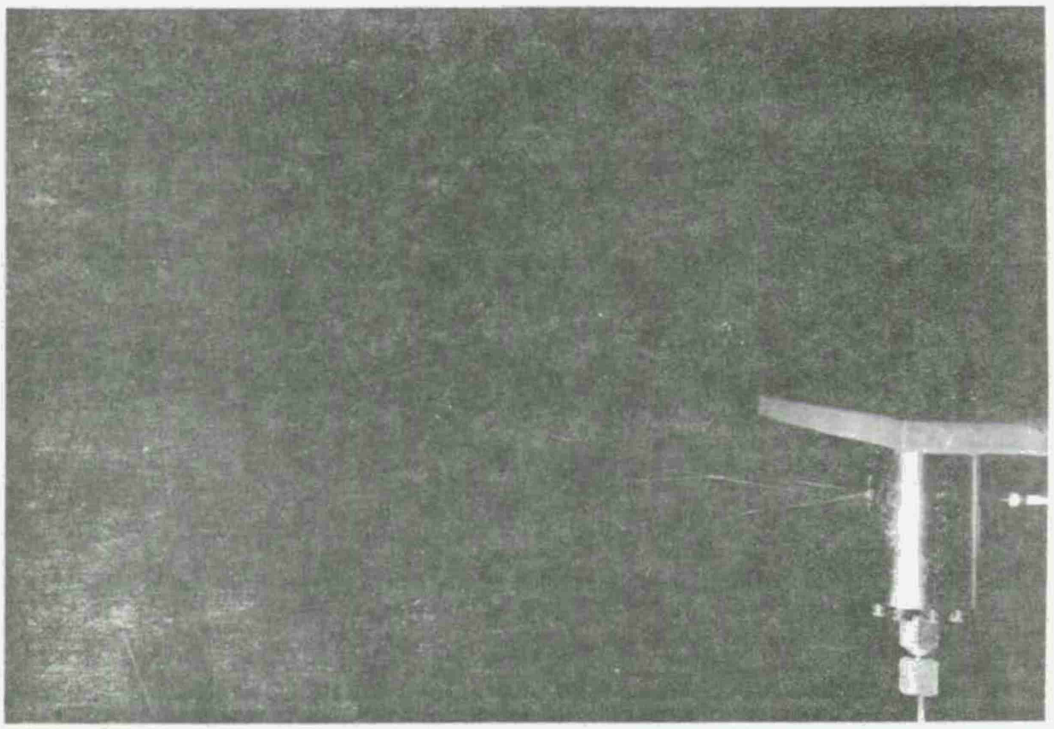

Figure 18. Plume Resulting from Passing Propellant Gases, Generated in a Low Pressure Vessel, through a Brass Disc into Air

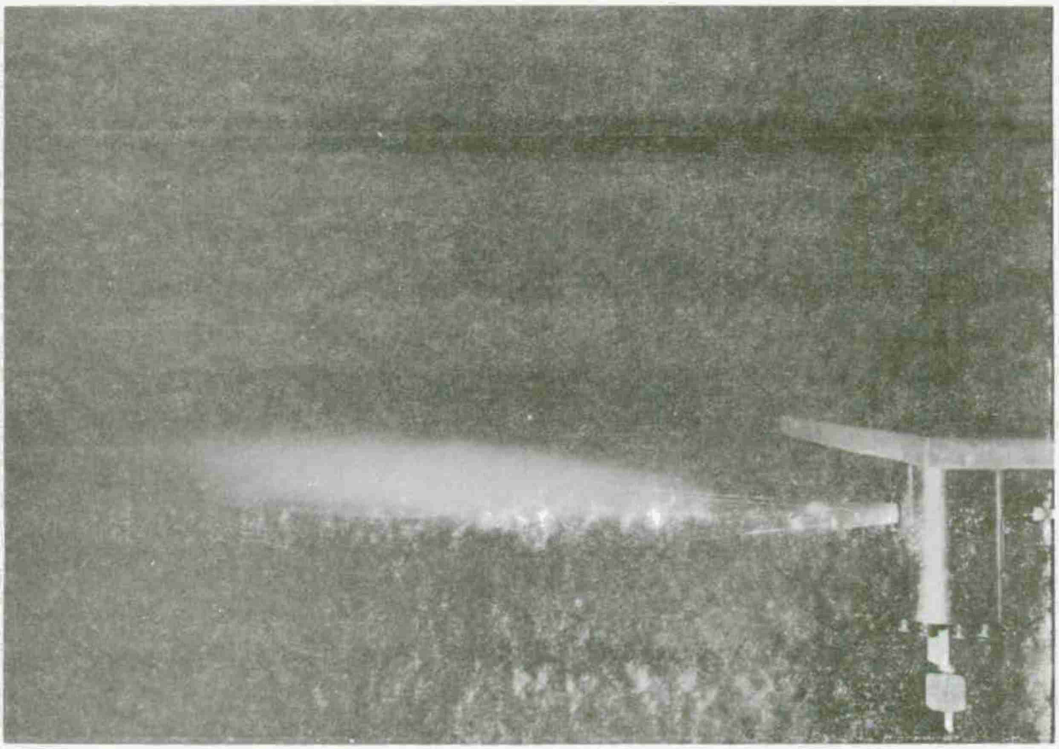

Figure 19. Plume Resulting from Passing Propellant Gases, Generated in a Low Pressure Vessel, through an Aluminum Disc into Air

For the next experiment a plexiglas tube, opened at one end, was attached to the low-pressure vessel so that the "burn-through" plume would be constrained within it. The tube was fitted with a valve to allow flushing of the tube with any gas. After argon is allowed to flow through the tube, the experiment was conducted in the same way as previously described. Figure 20 was obtained by leaving the shutter of the camera open during the experiment. The result is amazingly different. There is no characteristic secondary flash. Instead, the presence of the inert atmosphere of argon reduces the bright flash to a dull orange glow. More important, however, is the fact that the primary reaction zone is still in evidence even though the reaction is occurring in an argon atmosphere. The conclusion can be immediately drawn that the primary reaction zone is the result of an exothermic reaction of the vulnerable aluminum surfaces with the products of the propellant combustion. Figure 20 also demonstrates that by allowing the plume to discharge into an inert atmosphere, it is possible to quench the secondary reaction zone.

A comparison has been made between the erosion resulting from discharging into an air environment and that resulting from discharging into an inert atmosphere. The results of these comparisons show that the amount of erosion (increase in mean diameter of the text specimen) is independent of the existence of the secondary reaction zone. It is therefore concluded that this secondary plume contributes little, if anything, to the erosion sustained by the test specimen. Figure 20 also shows propellant "streaks" exiting the vent nozzle at the top of the test fixture.

Figure 21 is a photograph of a similar experiment. Instead of an argon atmosphere, however, nitrogen was used to flush the plexiglas tube. The effect of the nitrogen was to reduce the glow produced by the secondary reaction plume. However, there is no reduction in the intensity or the size of the primary reaction zone or in the amount of erosion sustained by the test specimen.

Although Figures 20 and 21 show the discharge into argon and nitrogen respectively, it is possible to channel these exhaust products into the plexiglas tube without the presence of an inert atmosphere. When this is done, there is a fine granular grayish-white dust deposited on part of the tube's interior surface. X-ray diffraction analysis of this powder has identified it as aluminum oxide. Hence, the oxidation of aluminum to aluminum oxide is occurring in the secondary plume. This fact is also confirmed by rapid scan emission spectroscopy discussed in Section 5.5.

This series of experiments is conveniently summarized in Figure 22. The top photograph (a) is the expansion of the secondary plume into an air environment; photograph (b) is the same experiment with the plume constrained in a nitrogen atmosphere. As in the previous photographs, the reduction of the secondary plume is clearly evident. Other

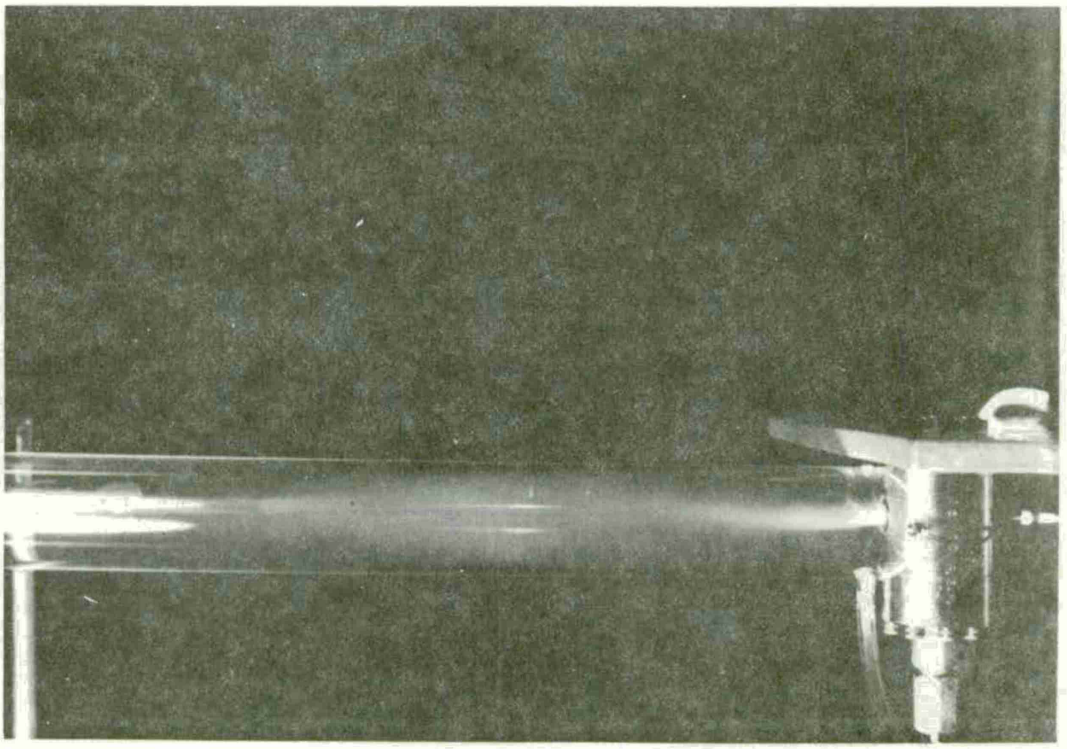

Figure 20. Plume Resulting from Passing Propellant Gases, Generated in a Low Pressure Vessel, through an Aluminum Disc into an Argon Environment

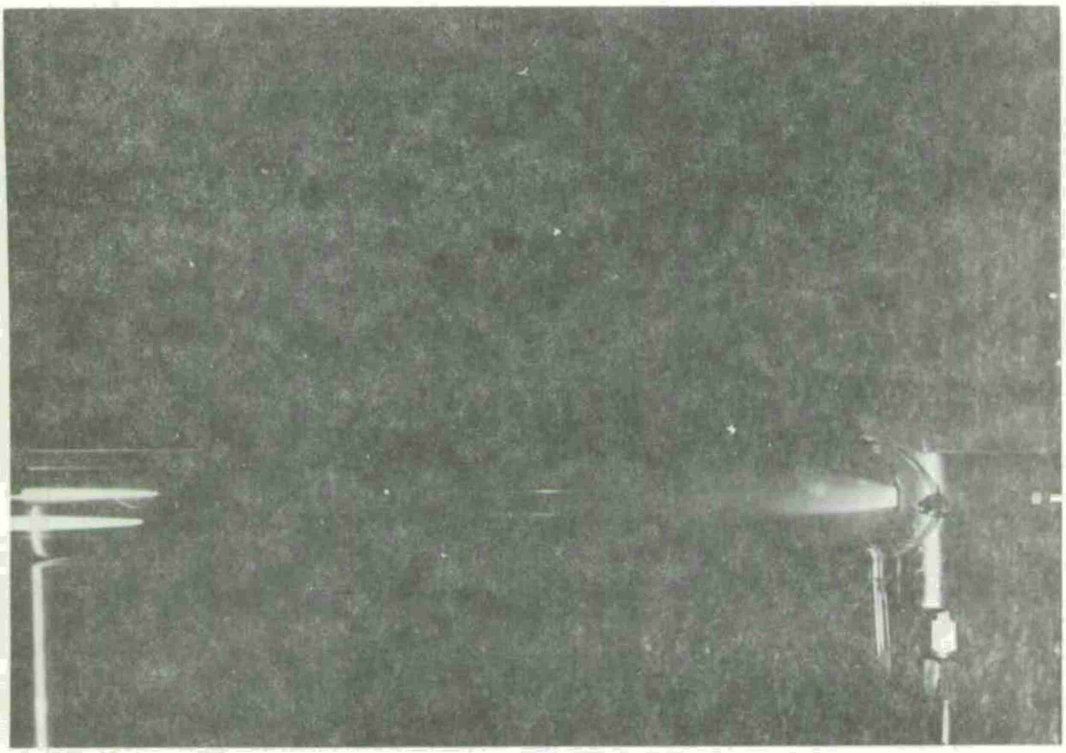

Figure 21. Plume Resulting from Passing Propellant Gases, Generated in a Low Pressure Vessel, through an Aluminum Disc into a Nitrogen Environment

significant results from this series of experiments include:

1. "Burn-through" occurs in two distinct zones -- a primary zone, close to the specimen; and a secondary zone external to the test fixture,

2. The primary zone is the major contributor to the erosion of the specimen,

3. The primary zone is an exothermic reaction between the exposed aluminum and the propellant gases,

4. The secondary zone is principally the oxidation of aluminum to aluminum oxide.

SECTION 5.3. HIGH SPEED MOTION PICTURE STUDY USING AN INERT ATMOSPHERE

A primary objective of the experimental program was the identification of the fundamental processes which occur during "burn-through" and the determination of the relationship of these processes to the interior ballistic cycle. The two reaction zones concept has been observed quite dramatically in the experiment wherein the gaseous plume was discharged into the plexiglas cyclinder which was being flushed with nitrogen (Figures 21 and 22, Section 5.2). Although the bright secondary cloud was extinguished, the localized primary reaction zone was still present. A similar effect has been observed in a high speed motion picture study of "burn-through" as it occurred in a 5.56mm aluminum cartridge case. As in the experiment with the erosion test fixture, there was a large cylindrically shaped discharge occurring external to the weapon/cartridge case and a small localized region near the surface of the case.

To better understand the relationship between "burn-through" and the interior ballistic cycle, a second series of high speed motion pictures were made. In this experiment it would have been ideal to focus the camera on the surface of the hole and observe it grow as a function of time, but the extensiveness and brightness of the secondary plume presented an impenetrable cloud. However, it was possible to discharge the "burn-through" cloud into an inert atmosphere to achieve a quenching of the secondary plume. To accomplish this, a test weapon was placed inside an air tight box as shown in Figure 23. The lens of a Fastex camera was focused through the viewing slot in the universal receiver -- the same as shown in Figure 13 -- on the exit plane of a hole drilled in the head region of the particular cartridge case under investigation. Both aluminum and brass cartridge cases -- with a hole drilled in the head region -- were investigated and are discussed in this section of the report. Since the camera was tilted at approximately a firty-five degree angle with respect to the exit plane of the hole, the induced orifice appears to have an elliptical cross section.

After the lid was put in place and clamped down, as shown in Figure 24, the test gas was allowed to fill the interior of the box. A small orifice in the front of the box allowed expulsion of the air initially present. The gas was allowed to flow continuously throughout the box assuring a one hundred percent atmosphere of the test gas. The most difficult problem was to achieve maximum illumination of the hole. Four flood lights, directed through the window on top of the box, were used to achieve satisfactory lighting. However, it may be possible to use the collimated, high intensity beam of a continuous laser to obtain an optimum illumination of the hole.

Figure 25 shows a series of selected frames from the motion pictures taken during the firing of an aluminum case with an 0.0312

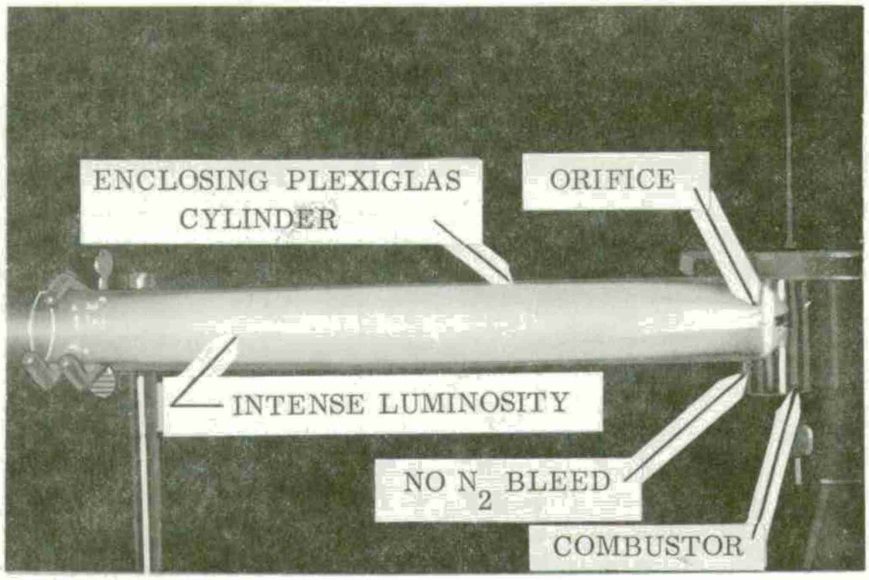

a. Jet Entering Air Environment

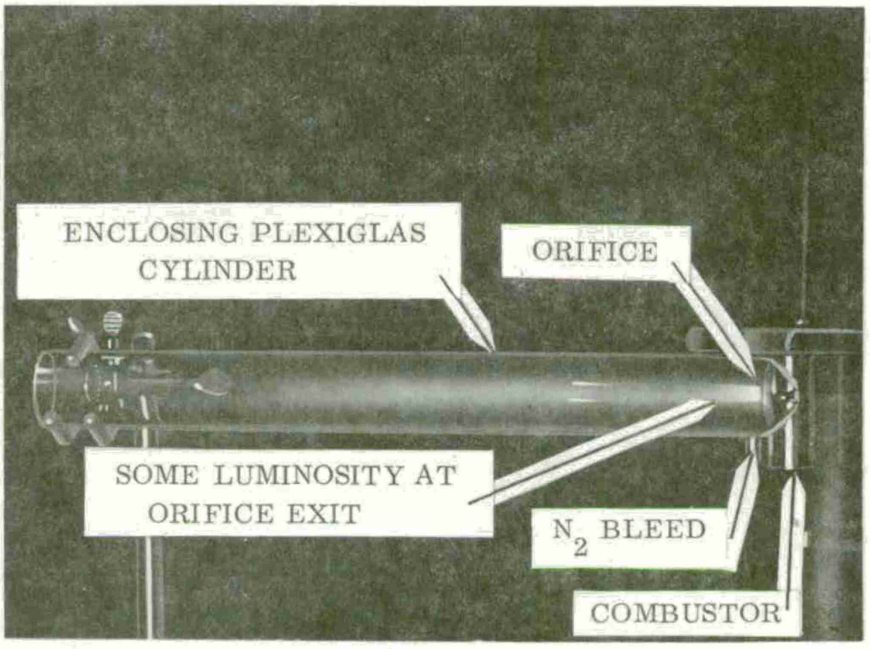

b. Jet Entering Nitrogen Environment

Figure 22. Plume Resulting from Passing Propellant Gases, Generated in a Low Pressure Vessel, through an Aluminum Disc into a. Air and b. Nitrogen Environments

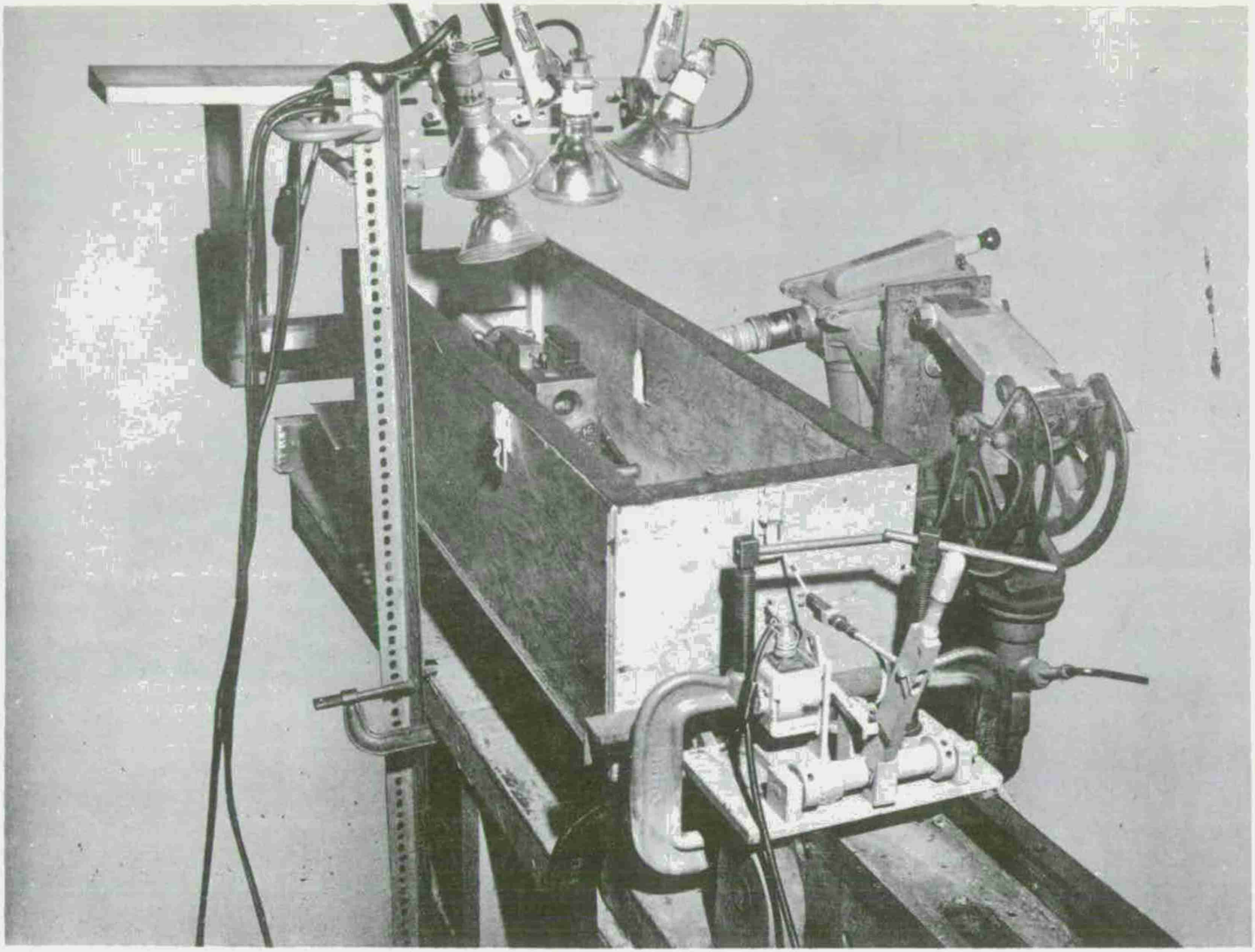

Figure 23. Slotted Universal Receiver in Box (Observe floodlights and Fastex Camera.)

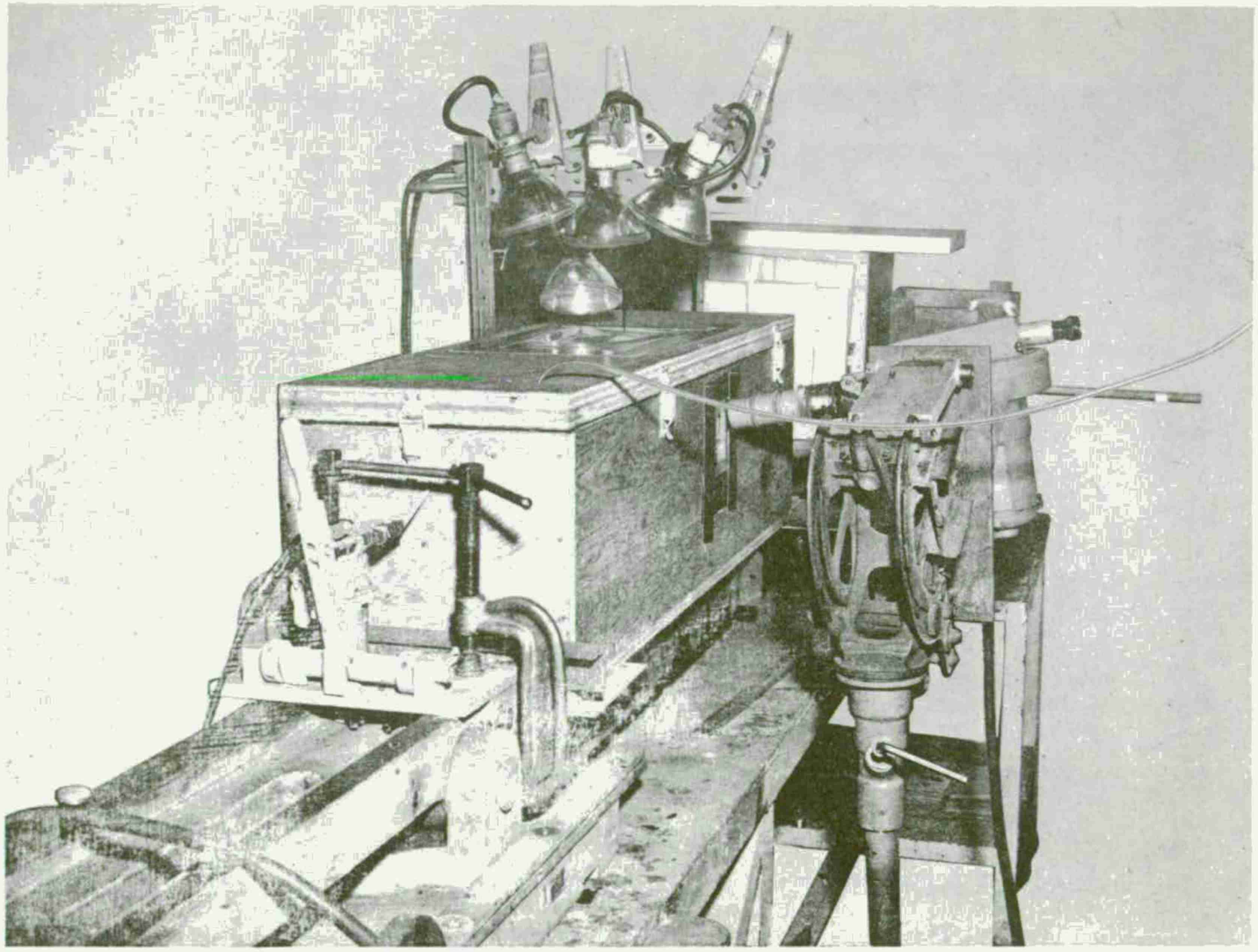

Figure 24. Airtight Box with Lid in Place

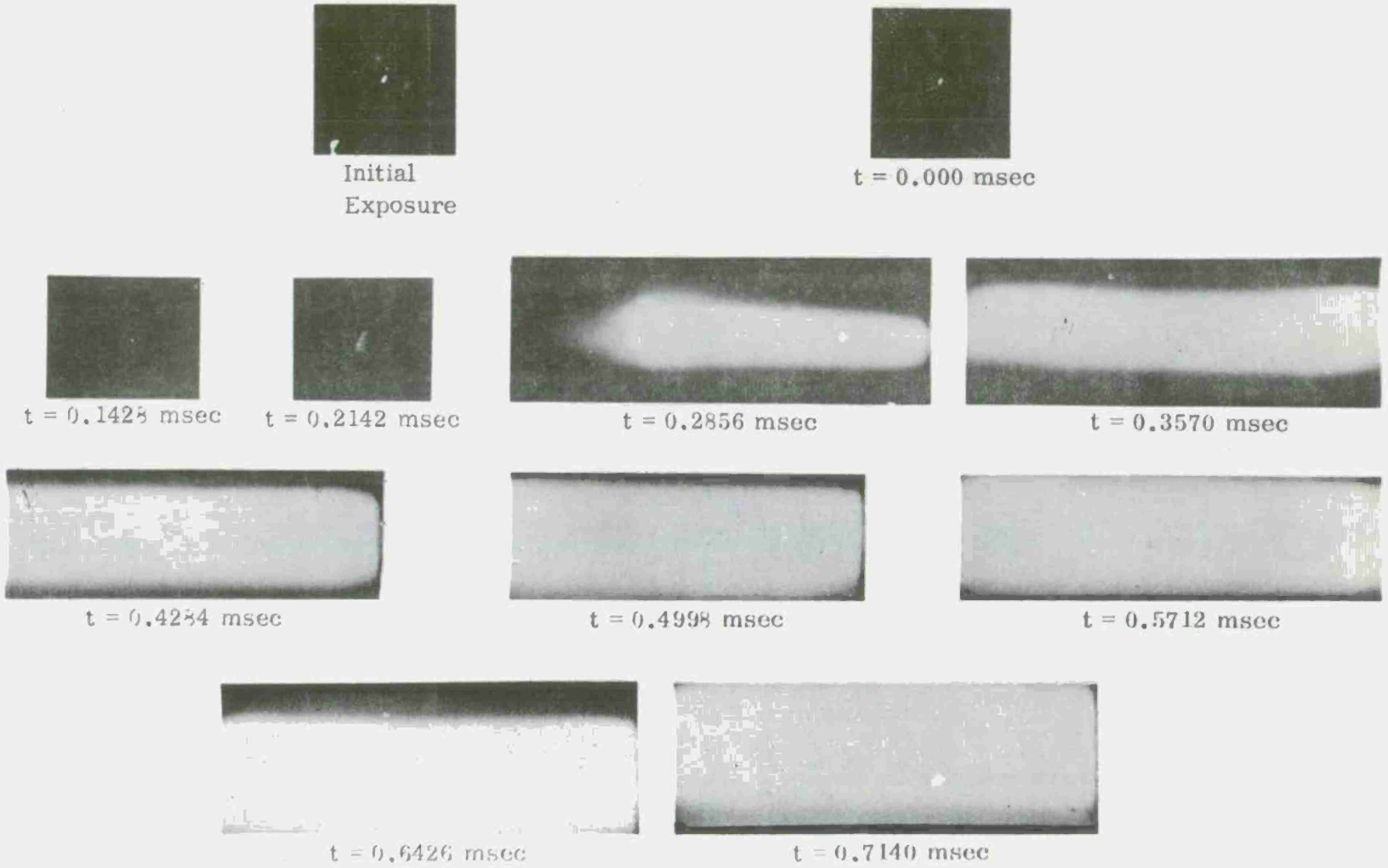

Figure 25. High Speed Motion Picture Study of "Burn-Through" into Air

inch diameter hole in the head region. In this and the next five figures, the induced hole can be observed at the left of the frame, and the discharge can be seen throughout the viewing slot in the universal receiver. Unless a particular frame is completely swamped out by the intensity of the "burn-through", the plume will be constrained by the walls of the viewing slot.

The first frame (Figure 25 -- top left) shows the appearance of the hole initially. As the camera built up speed, the exposure became a small dot -- top right. It must be understood that this dot is only a reflection of the lighting from the edge of the hole and does not represent the actual size of the induced orifice. By using the time marks on the edge of the film, it is possible to identify when, after the initiation of the primer, a particular frame was occurring. There are two frames where the periphery of the hole is defined by an orange hue.

A similar experiment was performed with a brass cartridge case substituted for the aluminum case. An analysis of this motion picture sequence will be discussed in the next paragraph. However, for the time being this orange-colored discharge can be tentatively identified as a combination of primer and propellant gases. At 0.2856 millisecond there was a rather extensive, bright white region of incandescence. This was the first evidence of the localized primary reaction zone. As time progressed, this white region grew in size and intensity until it completely filled the field of view after 0.7140 millisecond. Since the inert atmosphere was not introduced to achieve the quenching of the secondary plume, it is not surprising that the last series of frames are completely dominated by the white flash.

Figure 26 is a similarly prepared photograph taken of the discharge associated with propellant gas flow through a 0.0312 inch diameter hole in a brass cartridge case (loaded with a standard charge of 27.4 grains of ball propellant). The previous supposition that the orange-colored discharge was a combination of primer and propellant gases is confirmed in this firing. It is necessary to examine very closely what is actually happening and in what time frame events are occurring in Figure 26 since this information will serve as a reference or benchmark for the experiments with aluminum cartridge cases. At 0.0714 millisecond the first evidence of gas emanating from the hole is observed. The next three successive frames (at 0.1428, 0.2142, and 0.2856 millisecond) show the orange-colored glow at approximately the same brightness. After 0.3570 millisecond -- third frame, second row -- the initial orange diminished but subsequently at 0.5712 millisecond the intensity of the glow increased. This change in intensity is perplexing until one considers what was going on inside the cartridge case. Undoubtedly, the first two orange flashes represent the primer's output into the cartridge case. Then, there occurred a brief interval during the early stages of

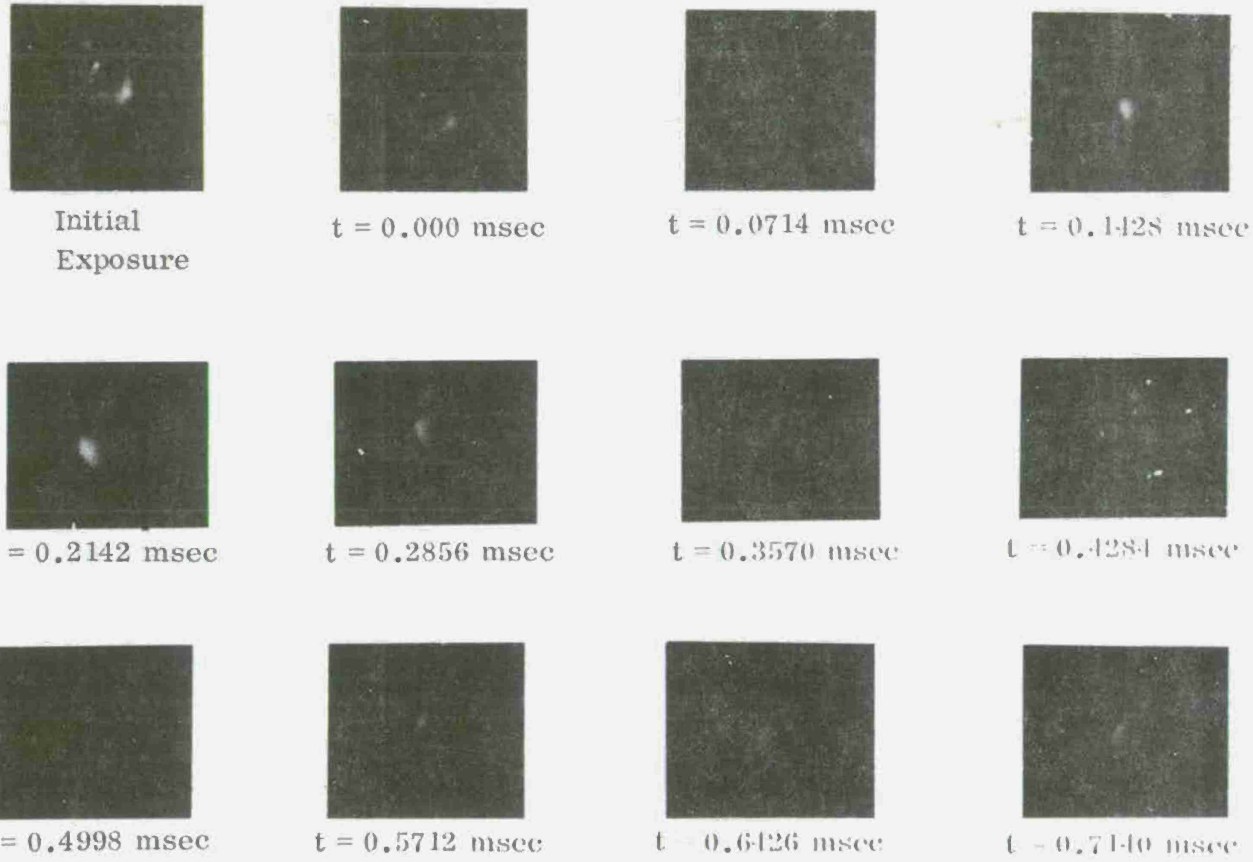

5.56MM BRASS CARTRIDGE CASE

Framing Rate: 14000 Frames/Sec

Propellant Charge: 27.4 Grains

Atmosphere: Helium

Hole Size: 0.0312 in. (dia.)

Figure 26. High Speed Motion Pictures Study of Gaseous Discharge from Brass Cartridge Case into Air

propellant combustion. Once ignition of the propellant grains was well defined, the brightness of the orange glow increased and followed the behavior of the pressure-time curve.

One of the reasons for initiating this high speed motion picture study was to understand the dynamics of the growth of the hole. As noted in the previous discussions, it was necessary to penetrate the bright plume to examine the preiphery of the hole. The orientation of the camera, therefore, was changed to obtain a better view of the hole in the film sequence presented in Figure 27. The information to be conveyed is presented in the first three frames. Unfortunately, the lighting used to take the motion picture from which the frames of Figure 27 were abstracted makes it impossible to show the initial exposure of the hole. If such information were available, it would be a simple matter to measure an effective diameter of the hole as shown in Figure 27. Since such is not the case, the hole's diameter in the first frame -- taken after 0.0714 millisecond -- can be considered representative of the hole's initial size. An effective initial diameter of 0.170 inch is obtained by simply measuring the length of the dark line as it appears on the photograph. The fact that an 0.0135 inch diameter hole appears to be 0.170 inch should not disturb anyone since this photograph has undergone several magnifications in its preparation. As observed in the next two frames -- taken after 0.1428 and 0.2142 millisecond -- the growth of this effective diameter is very small. In fact, in this greatly magnified representation of the actual dynamics, the hole grows only 0.020 inch. What has been gained from these observations is the fact that the hole's initial diameter does not increase until the primary reaction zone has been established. In this film sequence the primary reaction zone appears at 0.2856 millisecond and obscures subsequent frames so that it is impossible to gain any more information about the hole's size. However, during the early portion of the pressure-time curve, even though there were propellant gases exiting the orifice, the growth of the hole was minimal. Therefore, whatever increase in the hole's diameter must occur after the establishment of the primary reaction zone.

Figure 28 shows selected frames from a high speed motion picture study taken of the discharge resulting from the firing of an aluminum cartridge case (with an 0.0625 inch diameter hole in the head region) into a helium atmosphere. The first evidence of propellant gas discharge is at time $t = 0.000^{+}$ millisecond. Although not specifically identified as such in Figure 28, it is possible to obtain some idea of the initial size of the orifice by looking at the size -- in the vertical direction -- of the orange glow. This initial pulse of orange-colored light is undoubtedly the primer's blast as in the third frame, taken after 0.143 millisecond, then there is a reduction in intensity of the orange glow. As in the experiment of a hole drilled in a brass case (Figure 26), the reappearance of the orange glow after $t = 0.214$ millisecond was to be expected. At this time in

Frame 1. t = 0.714 msec.
Diameter* = 0.170 in.

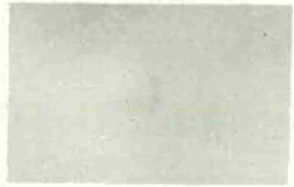

Frame 2. t = 0.2142 msec.
t = 0.1428m Sec
Diameter* = 0.175 inch

Frame 3. t = 0.214 msec.
Diameter* = 0.190 in.

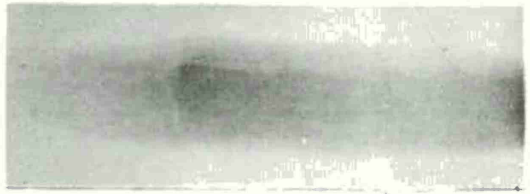

Frame 4. t = 0.2856 msec.

Frame 5. t = 0.3570 msec.

Frame 6. t = 0.4284 msec.

Frame 7. t = 0.4998 msec.

*Effective Diameter: Actual distance measured from negative

5.56MM ALUMINUM CARTRIDGE CASE

Framing Rate: 14,000 Frames/sec.
Atmosphere: Air

Propellant Charge: 27.4 grains
Drilled Hole Diameter: 0.0135 in.

Figure 27. High Speed Motion Picture Study of "Burn-Through" Plume into Air

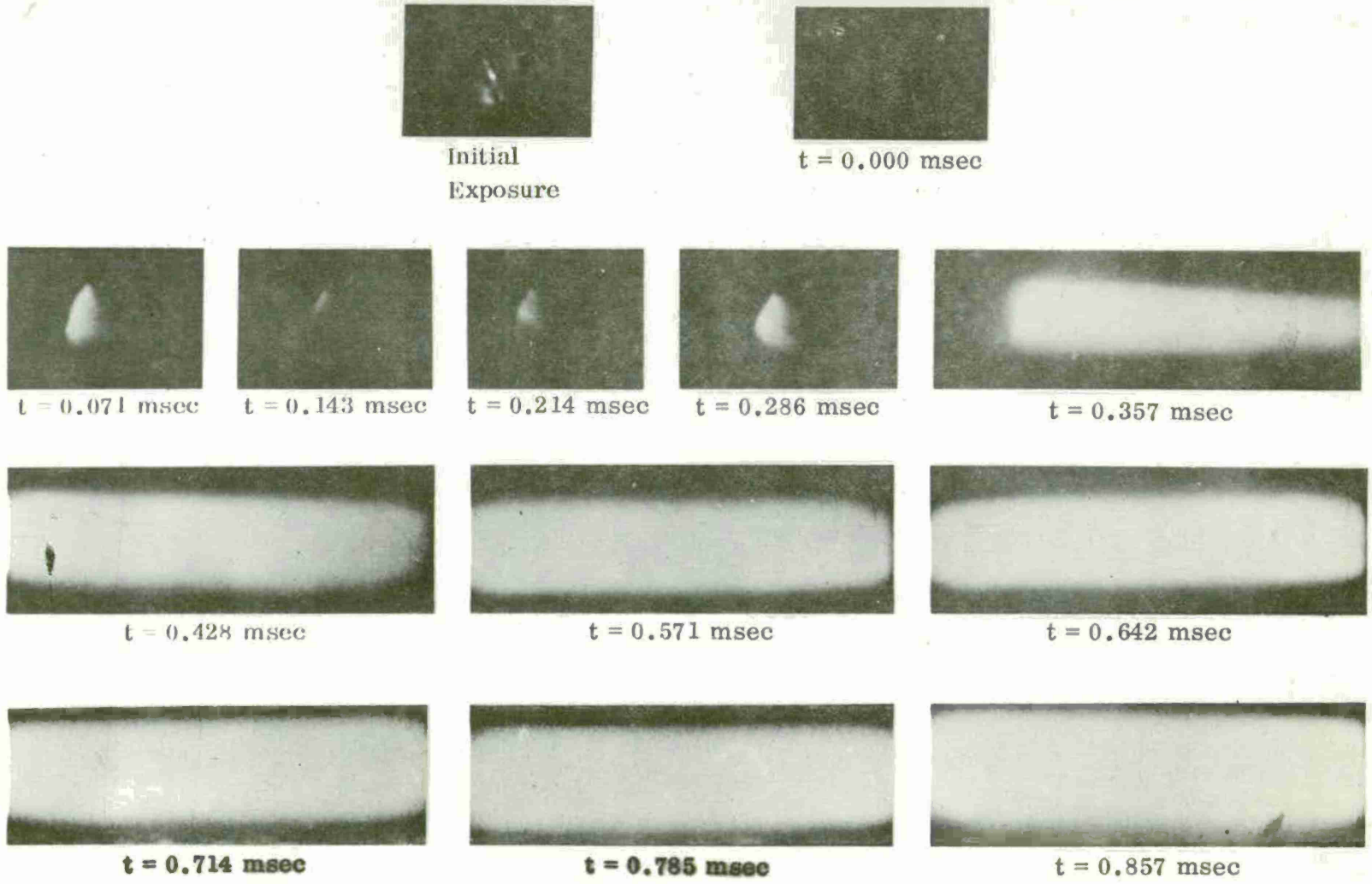

Figure 28. High Speed Motion Picture Study of "Burn-Through" Plume into Helium

the interior ballistic cycle, the combustion wave has been firmly established and the chamber pressure is increasing at a rapid rate. However, in the next frame, t = 0.357 millisecond, the first signs of the primary reaction zone are observed. Even though positive measures were employed to gain a better observation of the hole (through introduction of the inert atmosphere), the primary reaction completely dominated the field of view and precluded obtaining additional information about the growth of the hole. Nevertheless, the fact has been firmly established that the greatest amount of hole growth occurs after the primary reaction zone is initiated. Also, this initiation does not occur instanteously with the primer's blast after a finite delay time. Another interesting by-product of this experiment is that although no air was available, the aluminum, in concert with the combustion products, provided the necessary ingredients for a reaction. Not evident in Figure 28 is the fact that the larger secondary plume has been eliminated. This fact, which sheds light on the chemical reactions occurring within it, will be discussed fully in Section 5.5.

An aluminum cartridge case -- with an 0.0312 inch diameter hole -- loaded with a reduced propellant charge of 23.0 grains was also fired in a helium atmosphere. A more detailed discussion of this firing is provided in Section 6.2.

A typical 5.56mm ball cartridge pressure-time curve is shown in Figure 29. With the initiation of the primer at time 0.000 millisecond, a gaseous discharge is observed through the induced hole. Although the interior ballistic cycle is in the early stage of formation, there is nevertheless a pressure differential between the interior of the cartridge case and the atmosphere -- hence there was gas flow. Characteristically, the initiation of the primary reaction zone is observed at approximately 0.30 to 0.35 millisecond. With the appearance of this zone our ability to discern any additional information of hole growth is thwarted. Nevertheless, there is a minimum of growth up to that point in time. Shortly after the establishment of the localized primary zone, the secondary cloud is formed.

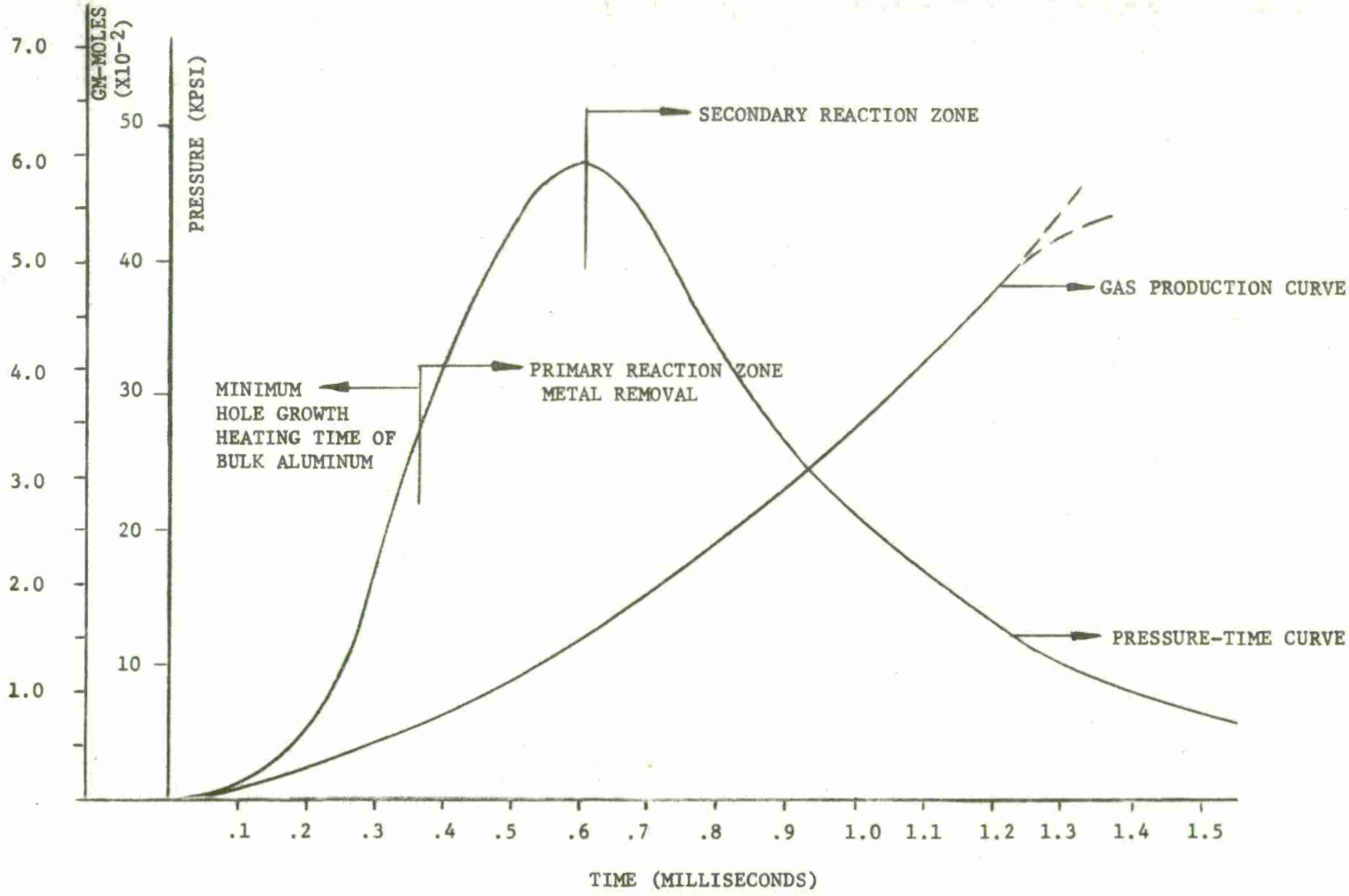

Figure 29. 5.56mm Ball Pressure - Time and Gas Production Curves (Events associated with "burn-through" are identified.)

SECTION 5.4. HOLOGRAPHIC INTERFEROMETRY

Holographic interferometry was used to obtain further insight into the nature of the plume evolving from the aluminum cartridge case "burn-through". From a series of holographic interferograms, it would be possible to determine if the plume is completely gaseous, or if there are solid particulates trapped within it. In addition, techniques are available to analyze holographic interferograms to determine the temperature and density profiles of the plume.

To obtain holographic interferograms of the plume, a 0.0135 inch diameter hole was drilled into the head region of a number of 5.56mm aluminum cartridge cases. The cases were assembled and fired in a standard velocity barrel and universal receiver. This experimental setup presented an undistributed path for the gaseous discharge as it exited the induced orifice in the head of the cartridge case. The M16A1 rifle was not used because it does not allow for the unrestricted flow of the "burn-through" plume; the discharge is reflected and baffled by the weapon's bolt and ejection port. The holocamera, test weapon, and projectile impact tank are shown in Figure 30.

A delay mechanism on the holocamera allowed triggering at different time intervals after initiation of the primer. Each interferogram then depicts the nature of the plume at the instant of time corresponding to the delay setting on the camera. Assuming that the plume exiting a number of identically prepared aluminum cartridge cases -- same hole size, case material, and propellant charge -- will be reasonably uniform, it is possible to view the compilation of the photographs at the time dependent behavior of the plume.

Figure 31 is holographic interferogram before firing the test weapon and shows the surrounding air with no interference patterns. The quiescent air has a uniform brightness. The point of origin for the plume, the hole in the cartridge case, is approximately that indicated by the arrow.

Figure 32 represents the first in a series of holographic interferograms after firing. The plume, in the vicinity of the test weapon and hence the cartridge case, is characterized by the very irregular -- implying turbulence -- closely spaced, fringe pattern. The alternate dark and light bands far from the plume are whole and fractional fringes, which show that weak compression fronts (shock waves) were driven through the quiescent air. This gaseous discharge produced shock fronts in much the same way as a spherical blast wave is initiated by explosion. There is also the formation of Mach cones somewhat distant to the basic fringe pattern. It is possible that solid particulate may be at the apex of these Mach cones.

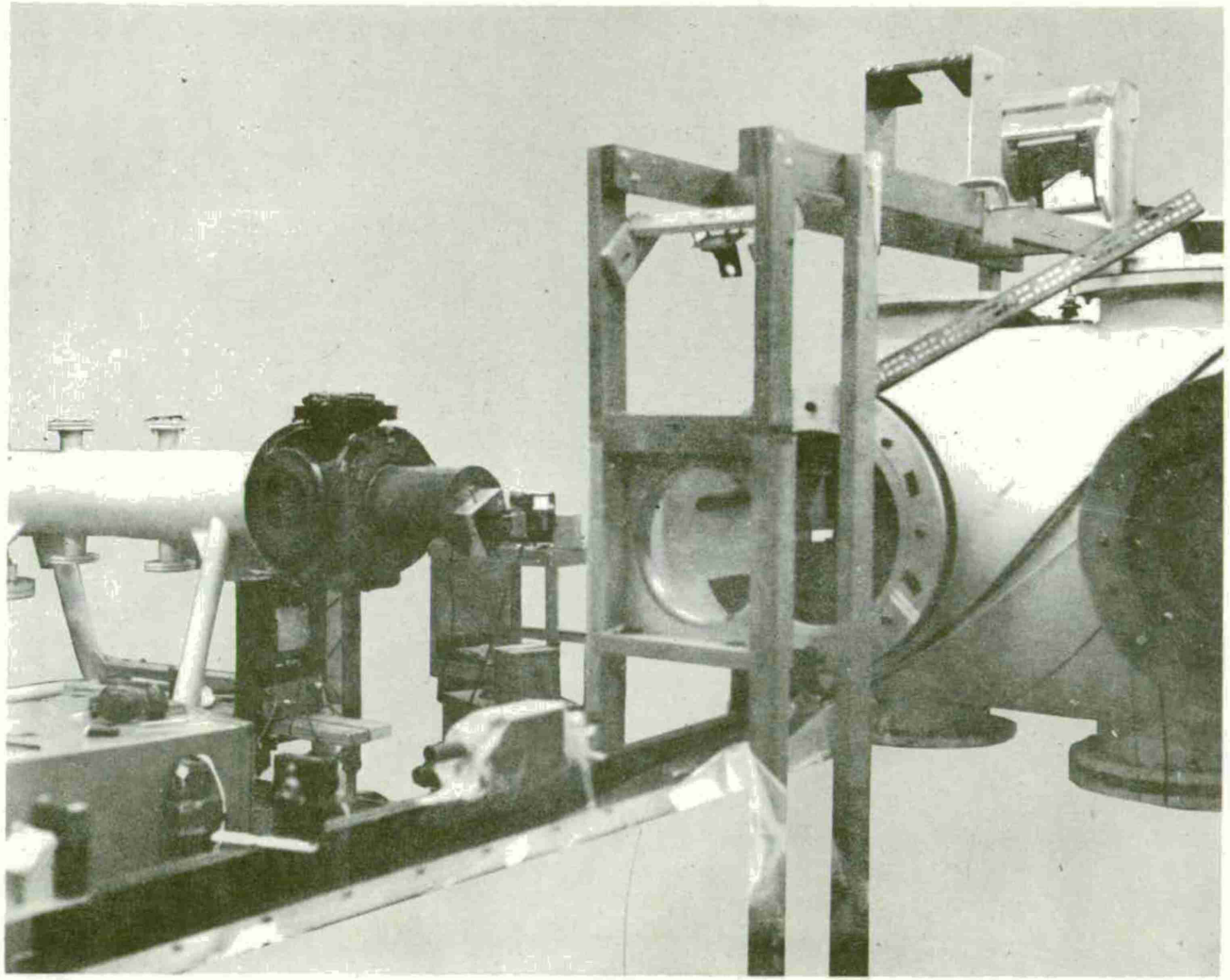

Figure 30. Experimental Setup for Holographic Interferograms Showing Velocity Barrel and Universal Receiver and Holocamera

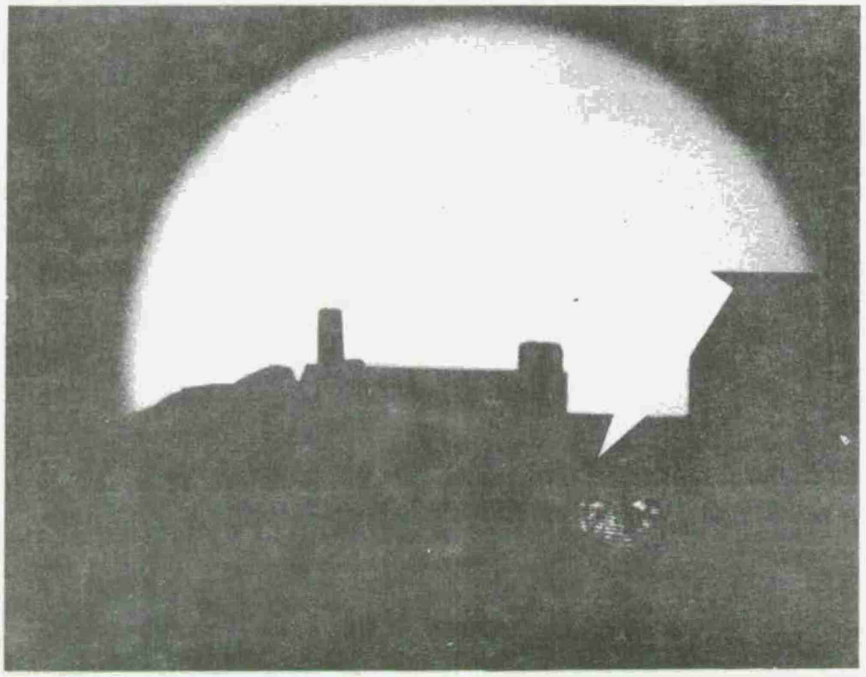

Figure 31. Holographic Interferogram of Test Weapon and Surrounding Air (Note absence of interference patterns.)

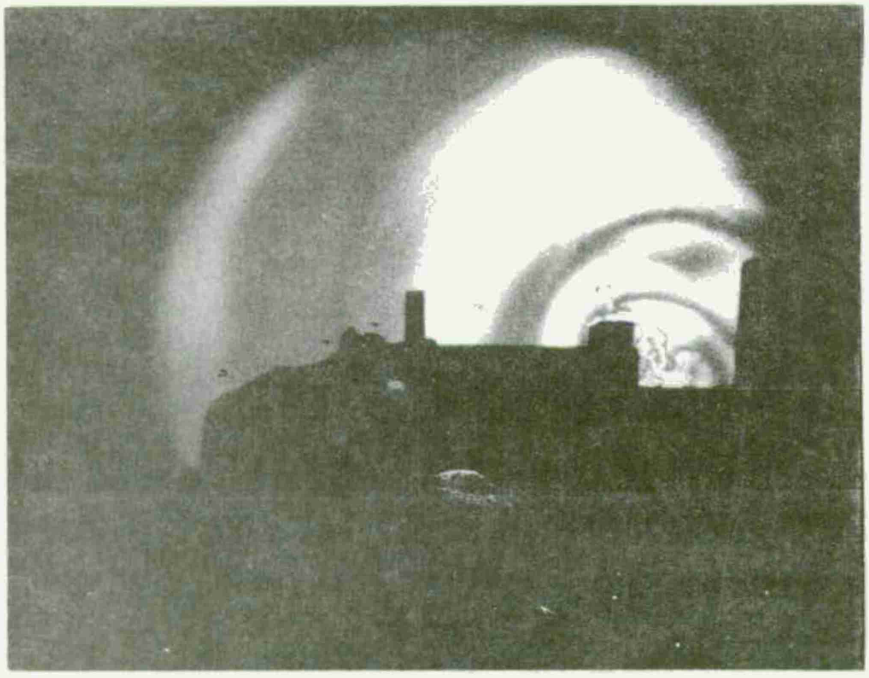

Figure 32. First Holographic Interferograms in Sequence (Taken 0.094 millisecond after the interferogram of Figure 31.)

The next in the sequence of interferograms, Figure 33, is taken 0.015 millisecond after the exposure given in Figure 32. The flow pattern of the gaseous discharge seems to be forming along a line whose origin is at the surface of the cartridge case. As in the previous photograph, two flow regions are evident -- the hot plume shown by the closely spaced fringes and the almost spherical wavelets driven by the plume. The V-shaped wave patterns in the spherical wavelets are more pronounced in this photograph. This interferogram was used to prepare the density, hence the temperature, profiles of the plume.

The third in the series of interferograms, Figure 34, is taken 0.196 millisecond after Figure 33. The central core region with the closely spaced fringe pattern appears to have propagated further from the weapon. Again, there is the appearance of two distinct regions -- the central core region and the spherical shock front. Also clearly visible are the three shock waves resulting from the compression of the gas on the inside surface of the front. The line superimposed on the photograph may be viewed as the axis of the fringe pattern and represents the direction of propagation for the shock front. This line is extrapolated to the origin of the plume -- the hole in the cartridge case.

Figures 35 and 36 are taken 0.098 and 0.490 millisecond, respectively, after the exposure shown in Figure 34. The well-defined shock fronts are no longer visible as the central core now has expanded and includes the entire field of view, due to the highly irregular nature of the fringe pattern. Figures 35 and 36 contribute little to the preparation of the density and temperature profiles, but do give evidence of the extent of the gaseous discharge after 0.490 millisecond.

To show the feasibility of reducing the interferogram to a density field, one radial density profile through the plume was made for Figure 33 at about 3/4 the plume distance from the hole (as is indicated by the arrow). An axisymmetric data reduction procedure was used to calculate density, although the plume is not suspected to be axisymmetric because of the geometry of the wedge-like slot in the universal receiver from which the plume emanates, and the fact that the central core appears to be turbulent. A technique for calculating the density field -- the Abel Inversion Procedure -- is presented below.

Data reduction is comprised of three parts as outlined by White, Fox and Rungaldier:[11] using the desired view of the holographic interferogram to record the fringe pattern with a microdensitometer; interpreting fringe number from the microdensitometer trace; and computing density by means of the standard equation for fringe shift.

---

[11]Witte, A.B., Fox, J., and Rungaldier, H., "Localized Measurements of Wave Density Fluctuations Using Pulsed Laser Holographic Interferometry" AIAA Paper No. 70-727, presented at the AIAA Reacting Turbulent Flows Conference, San Diego, California, 17-18 June 1970.

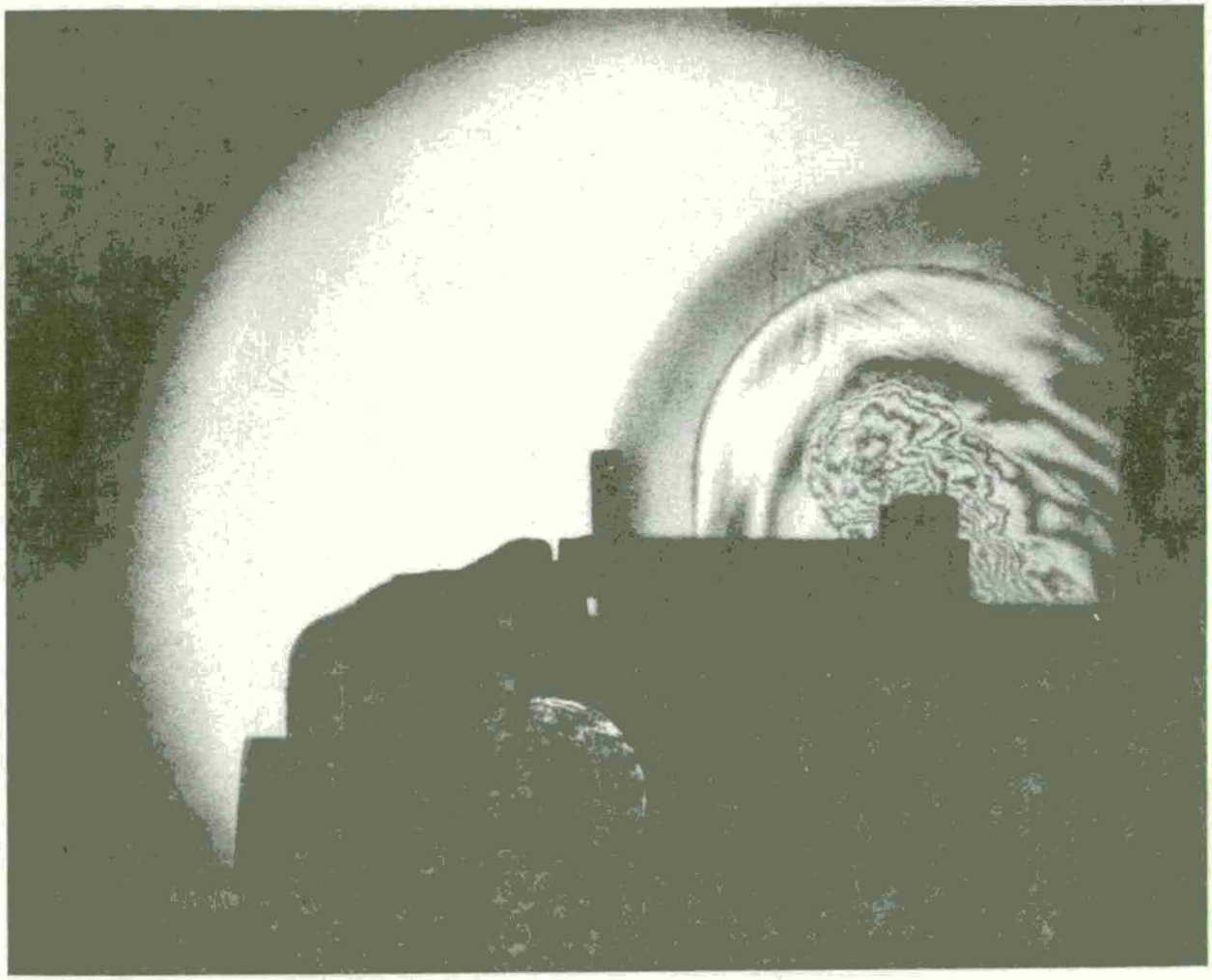

Figure 33. Second Holographic Interferogram in Sequence (Taken 0.015 millisecond after the interferogram of Figure 32.)

Figure 34. Third Holographic Interferogram in Sequence (Taken 0.196 millisecond after the interferogram of Figure 33.)

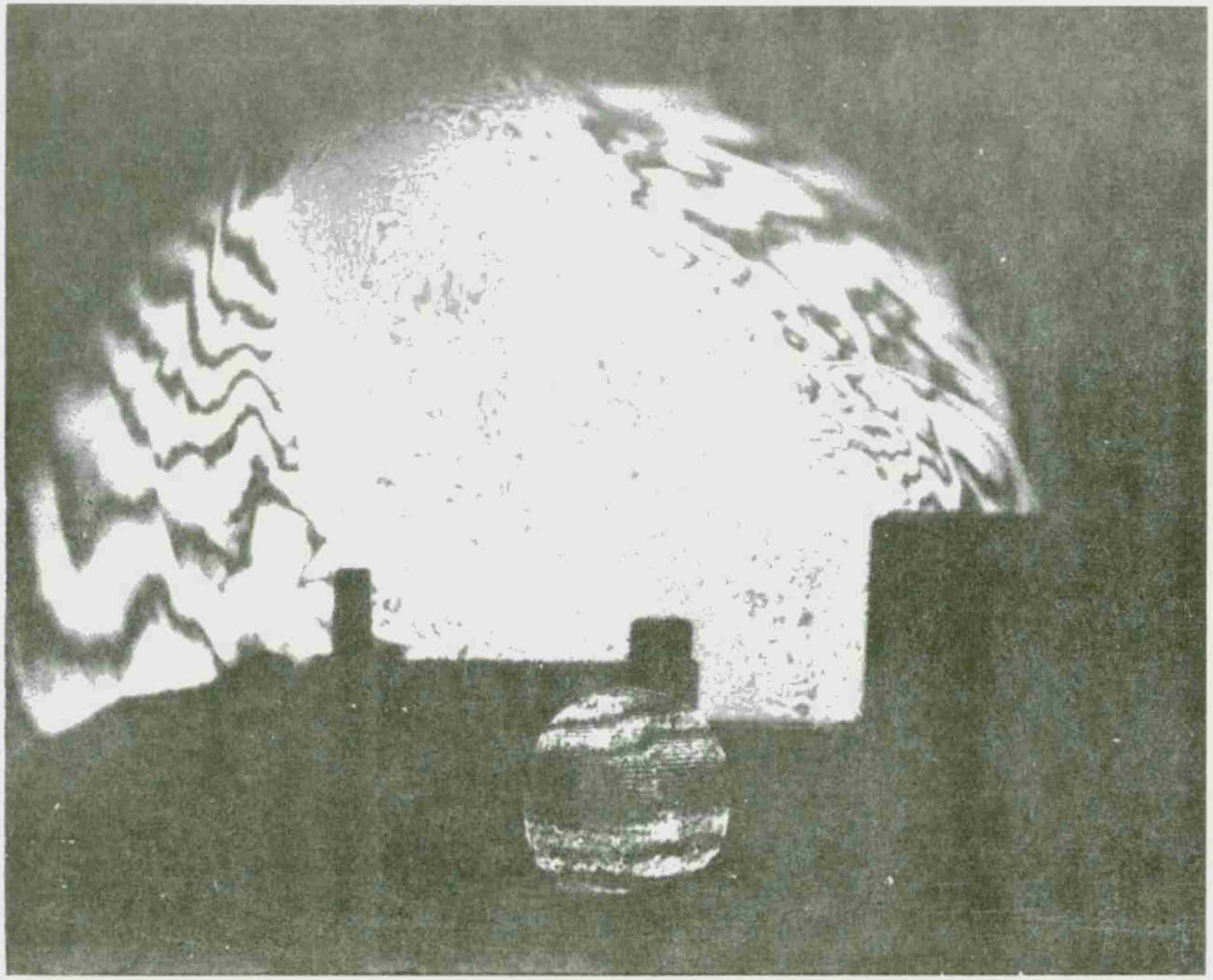

Figure 35. Fourth Holographic Interferogram in Sequence (Taken 0.098 millisecond after the interferogram of Figure 34.)

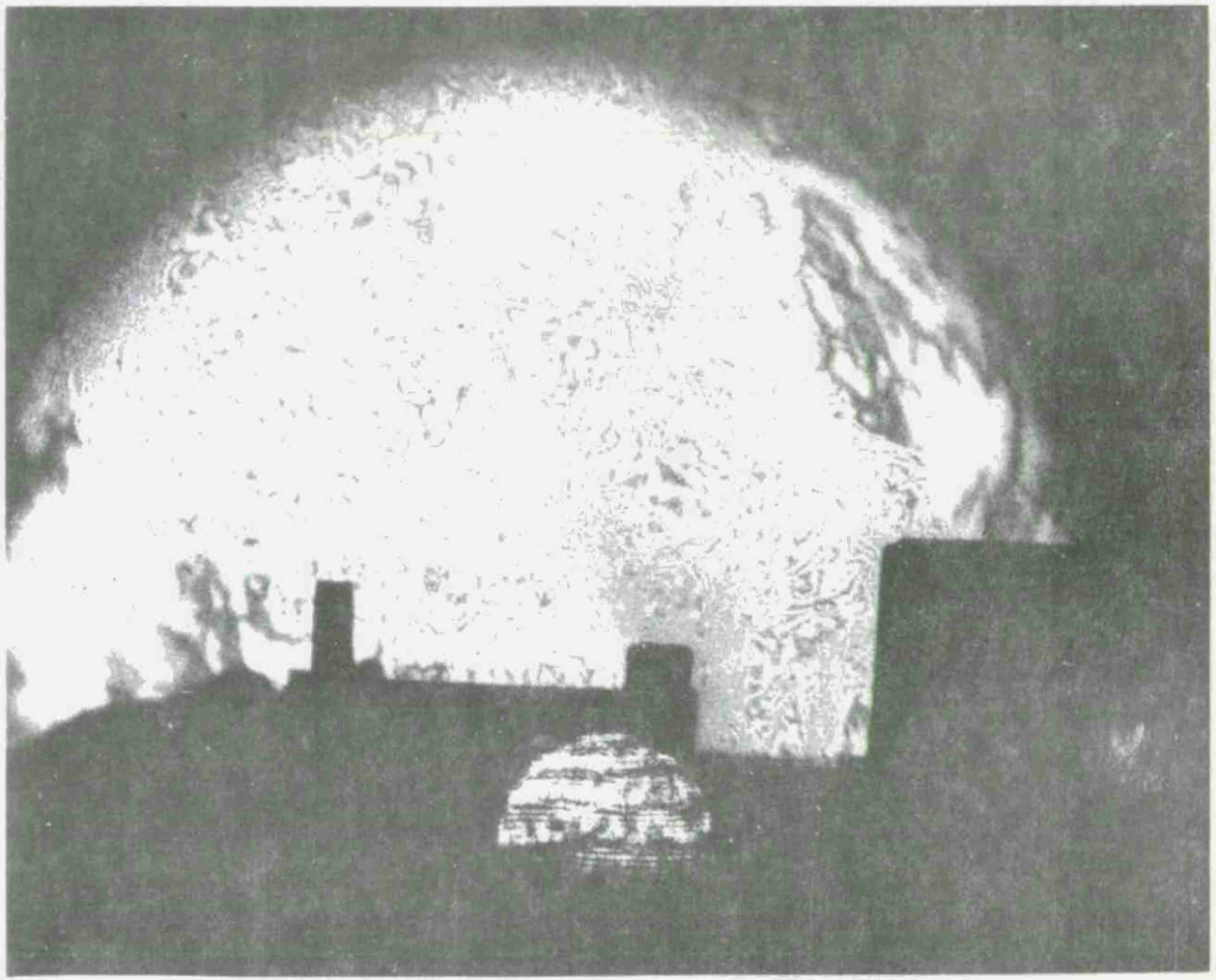

Figure 36. Fifth Holographic Interferogram in Sequence (Taken 0.490 millisecond after the interferogram of Figure 35.)

$$S(x,y) = \frac{K}{\lambda} \int_{o}^{z} \left[\rho(x,y,z) - \rho_{\infty} \right] \, dZ$$

Where K = Gladestone-Dale constant for propellant gases.

λ = characteristic wave length.

ρ (x, y, z) = desired three dimensional density field.

ρ_{∞} = density profile of surrounding air.

S (x, y) = fringe number.

With the assumption of axisymmetric flow, equation (1) can be inverted as the Abel integral to obtain

$$\rho(y) - \rho = \frac{-\lambda}{\pi K} \int_{y^2}^{r^2} s \, \frac{\frac{dS}{dr^2} \, dr^2}{(r^2 - y^2)^{\frac{1}{2}}}$$

where r = generalized radius vector.

Further simplification of equation (2) is possible to yield

$$\rho(y) - \rho = \frac{-2\lambda}{\pi K} \int_{y^2}^{r^2} s \, \frac{dS}{dr^2} \, d(r^2 - y^2)^{\frac{1}{2}}$$

which may be cast into the following finite difference form (the Schardin-Van Voorhis approximation[12]), for which the density is assumed constant in each of N thin annular rings of thickness Δ

$$\rho(y) - \rho \quad \frac{2\lambda}{\pi K \Delta} \sum_{k=1}^{N-1} (S_k - S_{k+1}) \quad \frac{\sqrt{(k+1)^2 + i^2} - \sqrt{k^2 - i^2}}{2k + 1}$$

where the following substitutions have been made $r_s = N\Delta$, $y = i\Delta$ and the indice i takes on the following values: i = 0, 1, 2 . . . . . N-1.

---

[12]Witte, A.B., and Wuerker, R.F., "Laser Holographic Interferometry Study of High Speed Flow Field", AIAA Paper No. 69-347, presented at the AIAA 4th Aerodynamic Testing Conference, Cincinnati, Ohio, 28-30 April 1969.

The following procedure was employed to determine the appropriate fringe number:

1. The shock wave was located.

2. The first fringe is assigned the value $S_1 = \frac{+\lambda}{2}$

3. The location of fringe change is then determined - i.e., where the flow begins as a compression and then finally a rarefaction due to expansion and combustion.

4. The fringes are then numbered in decreasing order from the point identified in 3.

The results of the exercise for the interferogram shown as Figure 37 are conveniently presented in Figure 38.

The actual density field, calculated by the above method, is shown in Figure 38. The gas density, ρ , normalized by the ambient density ρ_o , is plotted as the ordinate, and the position vector, r, normalized by a characteristic hole size, r_o = 0.05 inch (the final hole size) is shown on the abscissa. The extreme density field indicates that a weak shock wave was encountered at about $\frac{r}{r_o} = 27.5$, where $\frac{\rho}{\rho_o} = 1.35$. As expected, $\frac{\rho}{\rho_o}$ drops off in the rarefraction part of the flow field following the shock wave from about $7 < r/r_o < 22$. At about $r/r_o = 7$, the hot core region is encountered and the density decreases quite rapidly for the range $o<r/r_o<7$. The relative minimum of ρ/ρ_o at about $r/r_o = 5$ is caused by the strong irregularity -- the turbulent region of gas -- in the fringe pattern at that point. The fringe pattern is so irregular near $r/r_o = 0$ that the density field calculation becomes unstable there. However, because of the trend in the curve, it is possible that when a value of ρ/ρ_o is determined at $r/r_o = 0$, the gas temperature in the vicinity of the hole is $R \geq / 1500^oK$. This entire calculation is predicated on the fact there is no additional energy

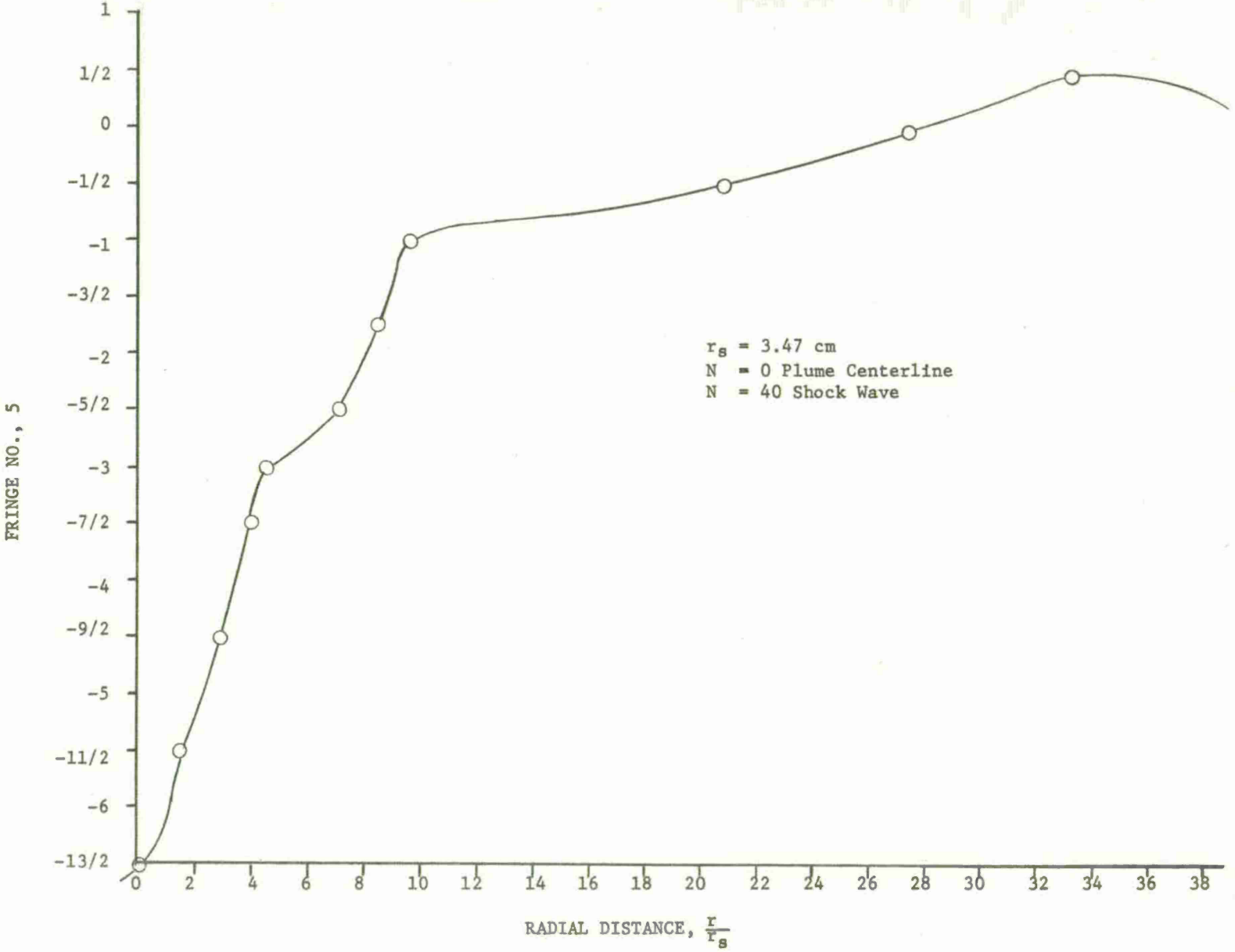

Figure 37. Fringe Number as a Function of Radial Distance for Interferogram of Figure 33.

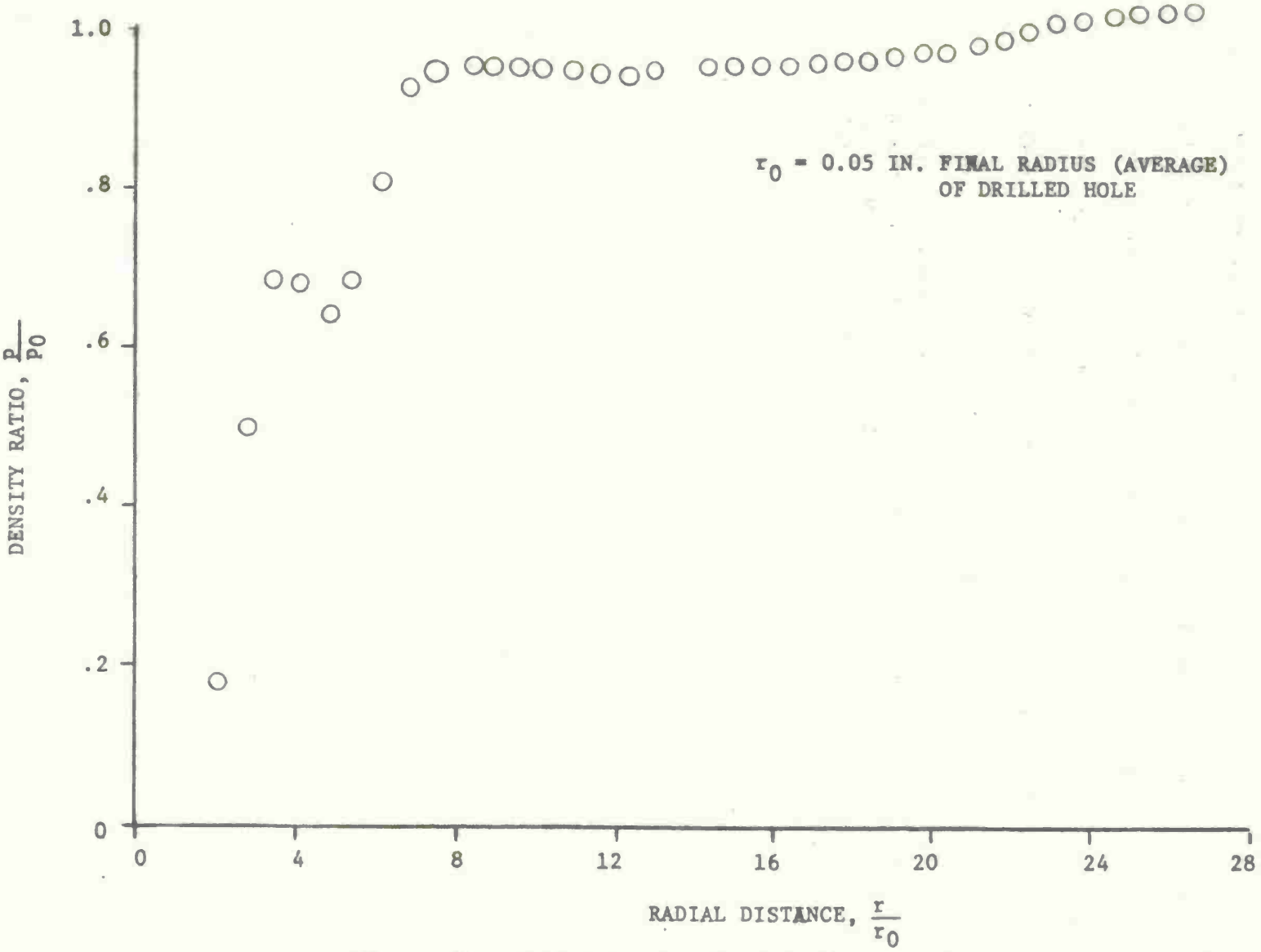

Figure 38. Radial Density Profile for Interferogram of Figure 33.

source at the vicinity of the hole. Some concern is expressed about this fact since the high speed motion picture analysis clearly demonstrated a localized exothermic reaction at the surface of the cartridge case. It is possible, however, to regard the theoretically determined value of 1500°K as a lower bound on the temperature. The presence of a reaction would increase this temperature.

It is possible to comment on the particulate matter effluxing from the plume. The moving particles caused weak shock waves called Mach cones which can be analyzed to estimate particle Mach number. The particles evidenced in Figure 33 are moving at approximately M = 1.4 or about 1500 ft/sec.

SECTION 5.5. EMISSION SPECTROSCOPY

A total emission spectrum of the gaseous discharge would allow identification of the transient species in the plume and possibly give some information concerning the exothermic reactions. To obtain the emission spectra of the gaseous discharge effluxing from an aluminum cartridge case during "burn-through", failures were induced in the head region of a number of cartridge cases. The procedure which was followed is identical to the one outlined to obtain the holographic interferograms. Again, a 5.56mm velocity barrel and a standard universal receiver were assembled and were used as the test weapon. The experimental setup for this investigation is shown in Figure 39; the spectrograph, laser, and test weapon are all clearly identified.

In order to determine the maximum amount of information from the emission spectra, the following experiments were performed. First, an aluminum cartridge case was placed in the focus of a ruby laser. The laser was fired and the induced spark spectrum due to metal vaporization was recorded. This spectrum served as a reference for the spectrum observed in the actual firing since the analysis of the high speed motion pictures leads to the conclusion that the aluminum is reacting in the gaseous discharge. For the actual firing, the spectrograph was placed so that the slit was about 3 feet from the test weapon and the image of the plume was focused through a lens onto the slit. A Jarrell-Ash 0.75 meter Spectrograph equipped with a holder for Polaroid film was used to obtain both spectra -- the metal vaporization spectrum and the spectrum of the discharge during the actual firing. The spectral range of interest was from 250 - 650 nm (nm = nanometer = 10^{-9} meter). A mercury reference spectrum from Pearse and Gaydon[13] was used to identify the various lines.

Due to the limitations of the spectral range covered by any one setting of the grating, it was necessary to make four separate cartridge case firings. Again, the argument is presented that if four cartridges are identical, then the "burn-through" from each identical case may be reasonably uniform. The total emission spectrum of the "burn-through" is shown in Figure 40 and is identified as "b". The mercury-lamp-reference spectrum (a) and the laser-spark spectrum (c) are superimposed over "b" for comparison. The four separate firings are arranged in order of increasing wave-length. Intensity comparison between spectral lines is precluded by the different grating settings. Hence, species identification is possible only by the position of the line and comparison with the mercury-reference spectrum.

---

[13] Pearse, R.W.B., and Gaydon, A.S., The Identification of Molecular Spectra (3rd edition), Chapman and Hall, Ltd., London, 1965.

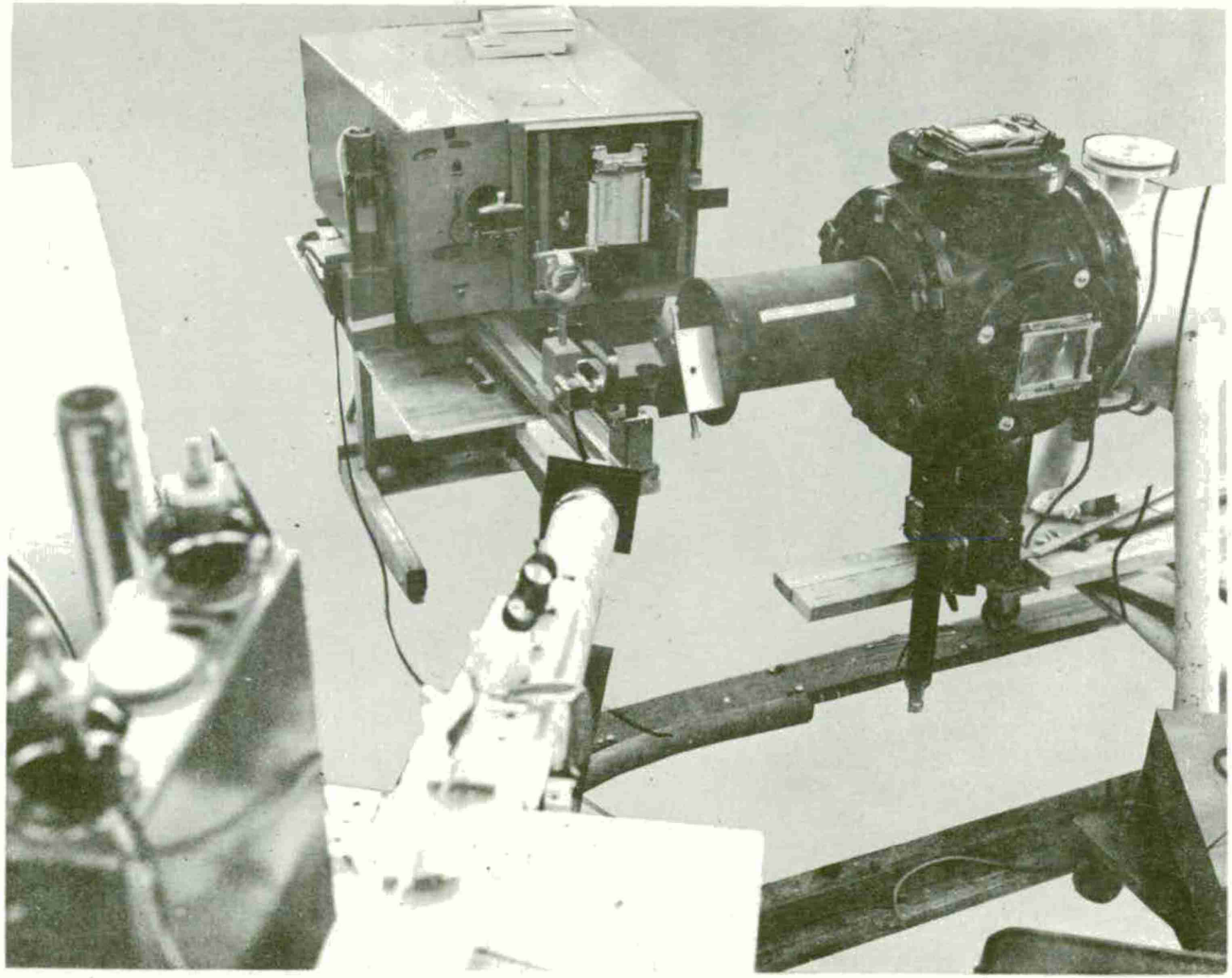

Figure 39. Experimental Setup to Obtain Emission Spectra

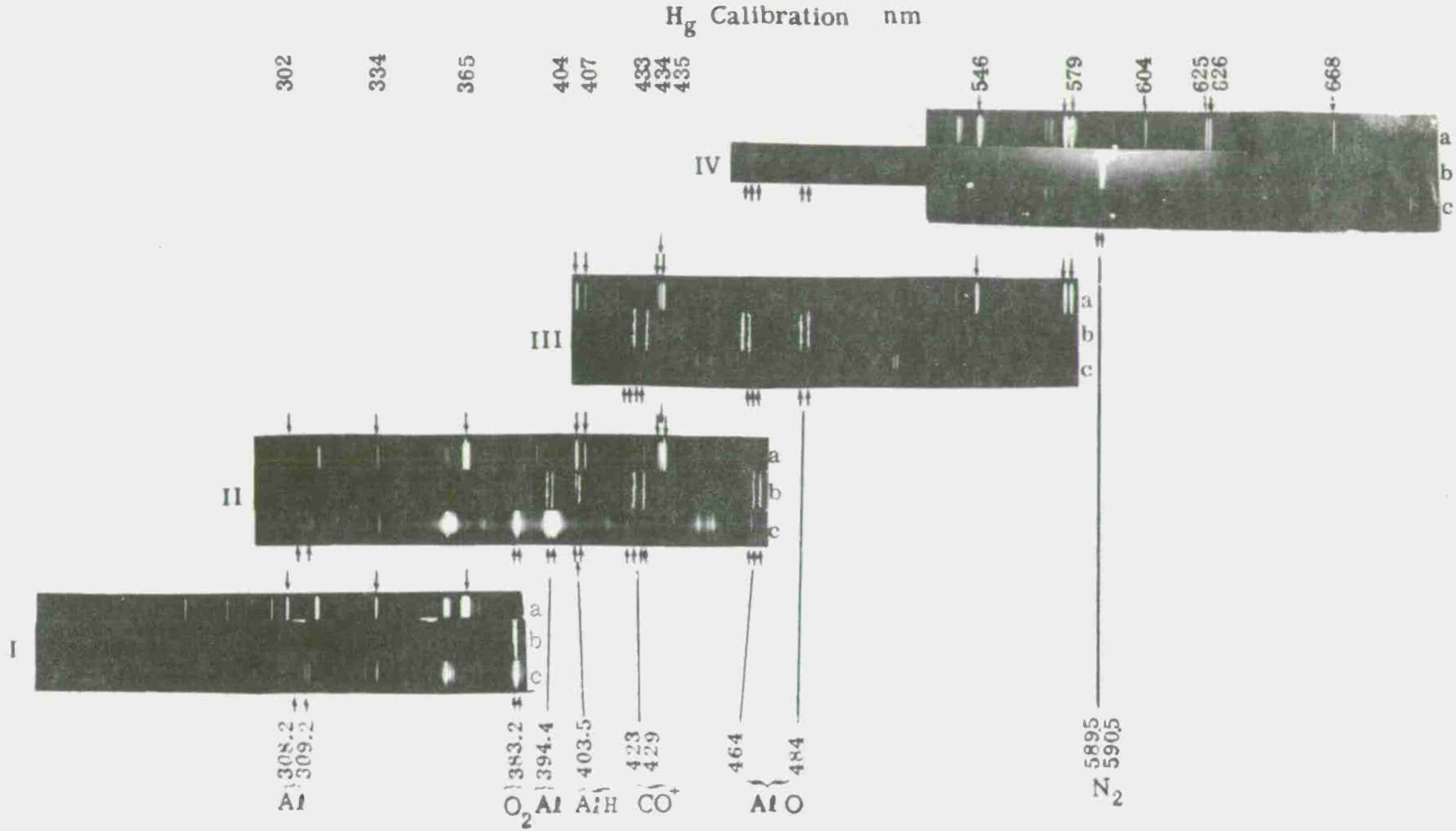

a. Mercury spectrum as reference
b. Emission from fired cartridge
c. Spark emission excited by ruby laser

Figure 40. Emission Spectra of "Burn-Through" Plume

The highest energy emission spectra of the "burn-through" plume is represented by the two sharp lines at 383.2 and 383.4 nm (Plate I (b)). It is tempting to identify a species of aluminum as possessing the highest energy in the spectrum, but Pearse and Gaydon[13] do not report any lines corresponding to Al or molecular Al at these wavelengths. However, lines of O_2 are reported by Pearse and Gaydon at the wavelengths of 382.5, 382.9, and 383.0 nm. Thus, these lines may well be caused by an excited state of O_2 in the plume.

Continuing in order of increasing wavelength -- decreasing energy -- the two lines at 394.4 and 397.2 nm are the next to be encountered. Reference 13 identifies these lines as two of the Al atomic lines and are characterized as the most intense persistent atomic lines. Actually, Pearse and Gaydon list four persistent lines. All four of these lines are observed in the laser spark emission spectra as intense reversals (Plate II, (c)).

The next lines observed occur at 403.5, 405.0, and 406.5 nm. There is an AlH line at 406.6 nm listed by Reference 13. It is interesting to note, however, that these lines are completely absent from the laser-spark spectrum. Therefore, it is concluded that these lines are definitely due to the reaction occurring between liberated aluminum and the propellant product gases. There is another group of sharp lines between 423.0 and 429.0 nm. These lines do not appear at any wavelength corresponding to Al band positions, but may be CO^+ since there is an emission line in this vicinity according to Pearse and Gaydon[13].

There is a series of bands beginning at about 437 nm and extending upward to 488 nm. The most intense of these bands lie around 464 and 484 nm and are clearly identified as an AlO band. No other lines in the plume-emission spectra can be identified as Al or AlO bands. The two sharp lines in the plume-emission spectra can be identified as an N_2 band (Plate IV (b)).

In summary, Al and AlO bands have been clearly identified in the emission spectra taken of the "burn-through" plume. Other aluminum species such as AlH may also be present. In addition, the plume spectrum has a band structure region from 440 to 540 nm. This structure is not observed in the laser-spark spectrum which is characterized by more lines and less intense bands. It is concluded that the AlO bands are formed more readily in the "burn-through" plume than in the laser-spark emission spectra and that the AlO bands arise from a reaction between the hot propellant gases and the aluminum case.

---

[13] Pearse, R.W.B., and Gaydon, A.S., The Identification of Molecular Spectra (3rd Edition), Chapman and Hall, Ltd., London, 1965.

CHAPTER 6. CASE DAMAGE WITH INDUCED CASE FAILURES

In this portion of the study additional insight was sought regarding the nature of "burn-through". Here, attention was fixed on the dynamics of the interaction of propellant gas and the case surface during the internal ballistic cycle. These data were obtained using an erosion test fixture and test weapons to evaluate effects of propellant gas on aluminum alloy discs, and aluminum-cased ball 5.56mm ammunition in which failures were induced to precipate "burn-through".

SECTION 6.1. EROSION TEST FIXTURES

Although the majority of the information presented in the document was obtained by investigating "burn-through" resulting from induced failures in 5.56mm aluminum cartridge cases and firing these cases in M16A1 rifles or test barrels, a series of combustion chambers were also fabricated to stimulate a ballistic environment.

The use of combustion chambers to investigate "burn-through" affords flexibility in studying the erosivity of various alloys (without actually manufacturing the cartridge cases) and investigating concepts which may be employed in the cartridge design to thwart "burn-through". In addition to these two advantages, the combustion chamber can be designed so that the exterior surface of the specimen (test disc) is accessible for photographic and spectroscope observations. Caution must be exercised in assuming that the ballistics of the 5.56mm system are duplicated in the combustion chamber. In particular, peak chamber pressure, time to peak chamber pressure, and duration of the pressure-time curve had to be closely approximated to that which occurs in a 5.56mm ballistic system.

The first erosion text fixture -- combustion chamber -- to study "burn-through" was fabricated at Frankford Arsenal and involved modifications to action time universal receiver/pressure barrel system. A sketch of this device is shown in Figure 41. Two combustion chambers were employed by the Guggenheim Aerospace Propulsion Laboratory of Princeton University to study the "Erosive Effects of Combustion Gases on Metallic Combustion Chambers" (Contract DAAA25-71-C-0109). One combustion chamber was a low-pressure vessel and was used in firings up to 15 kpsi (Figure 16). The other combustion chamber, tested successfully to 60 kpsi (Figure 42), is a modification of the original Frankford Arsenal system. Most of the data reported by Princeton University in their final report Contract DAAA25-71-C-0109[14] was obtained from firings in these bombs. To present a concise and understanding of the "burn-through" phenomenon, some of the important findings given in Reference 14 are presented in this document.

All of the erosion test fixtures operate on the same principle. Test discs (thicknesses up to 0.150 inch were evaluated) with a predrilled hole were exposed to propellant gases generated inside the chamber. The predrilled hole simulated the induced hole in the 5.56mm

---

[14] Plett, E.G., and Summerfield, M., "Erosive Effects of Combustion Gases on Metallic Combustion Chambers", Final Report on Contract DAAA 25-71-C-0109. Department of Aerospace and Mechanical Sciences, Princeton University, August 1971.

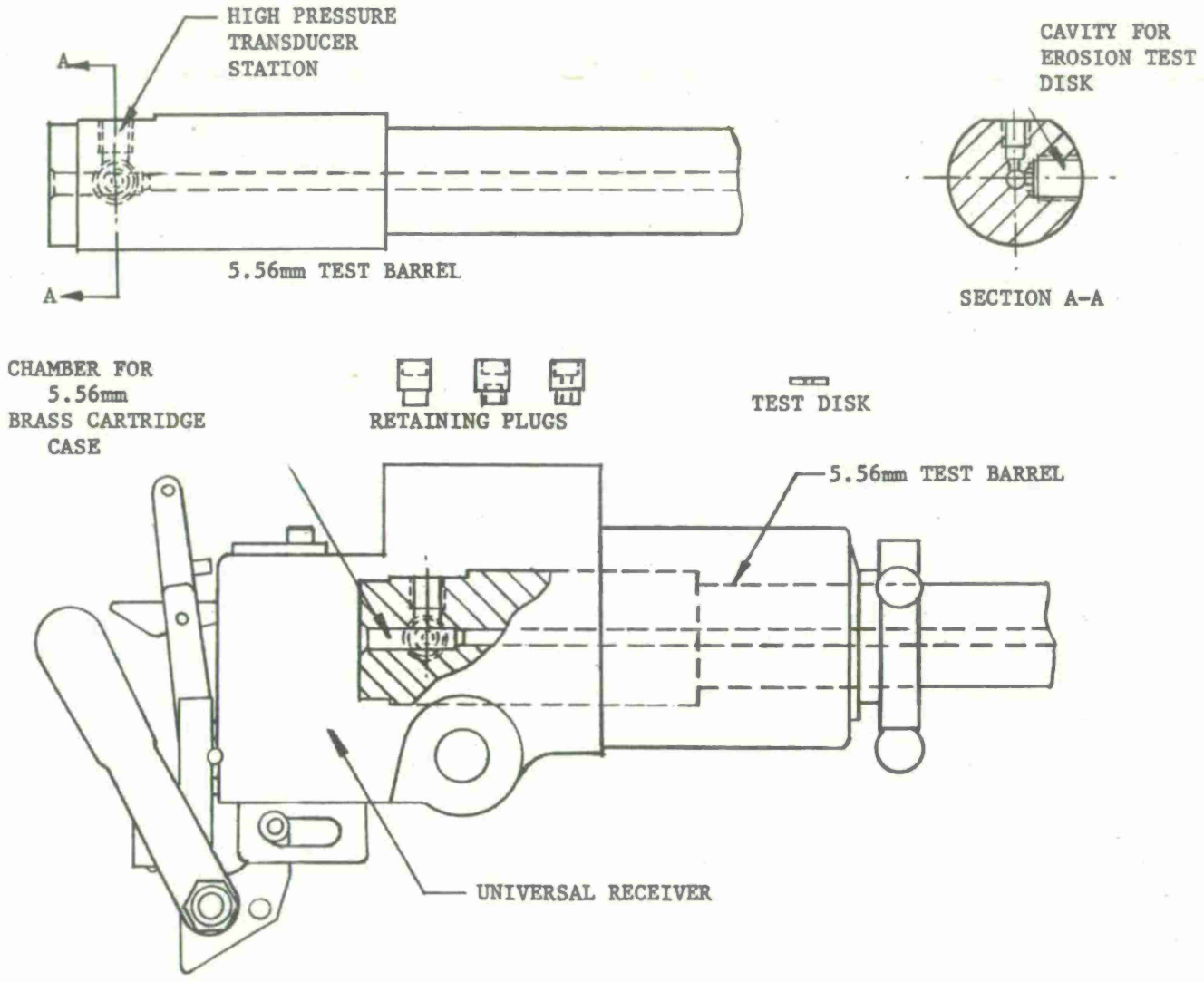

Figure 41. Sketch of High Pressure Erosion Test Fixture

aluminum cartridge case. Diametrically opposite the test disc was a pressure transducer which recorded the pressure-time history of the propellant gases. An adjustable vent nozzle in the Princeton bombs was used to control the experiment time. In the low-pressure vessel, ignition was obtained by an electrical match. A preweighed charge of propellant was placed in a 5.56mm brass cartridge case and used in the high-pressure combustion chamber, shown in Figure 42.

Data reduction on the test discs was accomplished in two ways. First, the mean increase in diameter of the hole was determined by measuring the initial and final diameters of the hole. An accurate measure of the initial and final orifice diameters was obtained by using a comparator to produce a fifty times magnification of the entire orifice. Figure 43 presents a 50 X magnification of a 0.042 inch (diameter) hole in a brass specimen. Unfortunately, the increase in diameter of the eroded hole was not uniform. (Figure 44 shows the irregular circumference in an aluminum test specimen after firing.) Therefore, it was necessary to measure a number of final diameters (including the minimum and maximum) and by averaging obtain a value for the mean increase in diameter. An additional complication arose because it was also possible for one side of the specimen to have sustained more erosion than the other. This is evident in Figures 45 and 46 which show the magnified hole of a brass specimen. Here the final diameter for the inside or combustor side was approximately seven and one-half divisions of the scale superimposed over the disc. However, the final diameter for the eroded hole on the outside or atmosphere side of the test disc was ten units. This substantiates the fact that both sides of the test disc experience different increases in mean diameter -- for each firing -- an average value was calculated and used. As a consequence, the averaging processes involved in this technique masked certain features of the eroded specimen.

In the second data reduction method, the amount (weight) of metal removed as a result of the propellant gas flowing throughout the hole was determined by weighing the disc before and after firing. A correlation between increase in mean diameter and weight loss of the test specimen is presented in Section 8.3. These data resulted from an investigation of the erosivity of a novel propellant and are presented in Figure 94.

Figure 47 is a plot of the mean increase in diameter vs peak chamber pressure for 7475-T6 aluminum, 6061-T6 aluminum, 70-30 brass, and 4130 steel. Each datum point is the average of the increase in diameter of the combustor and atmosphere sides of the test specimens. Variations in peak chamber pressures were obtained by using different charges of IMR 4198 propellant. To assure valid comparison between the erosivity of all the materials under consideration, it was necessary that the initial hole size, specimen thickness, and vent

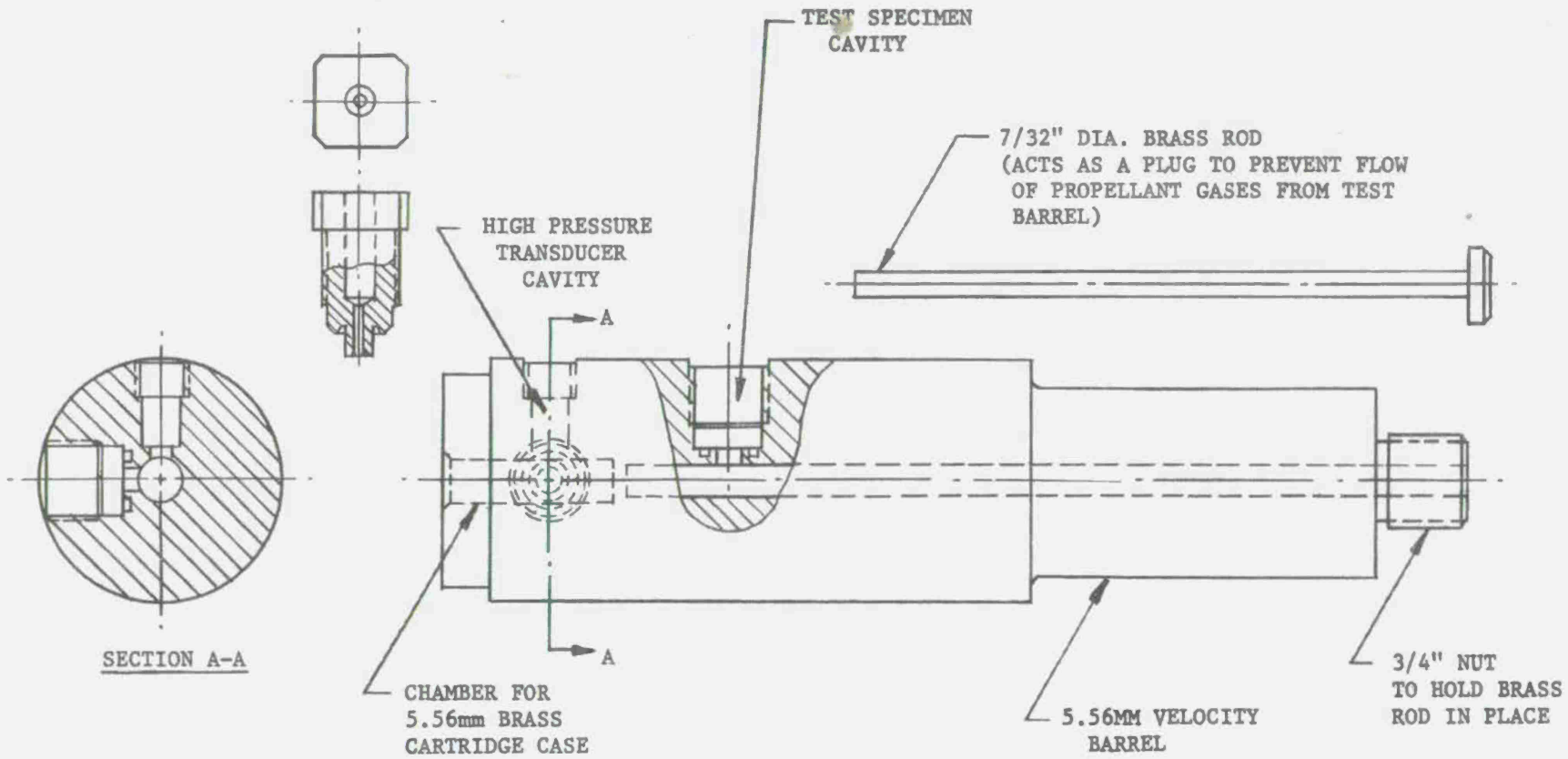

Figure 42. Sketch of High Pressure Bomb Used in Princeton University Studies

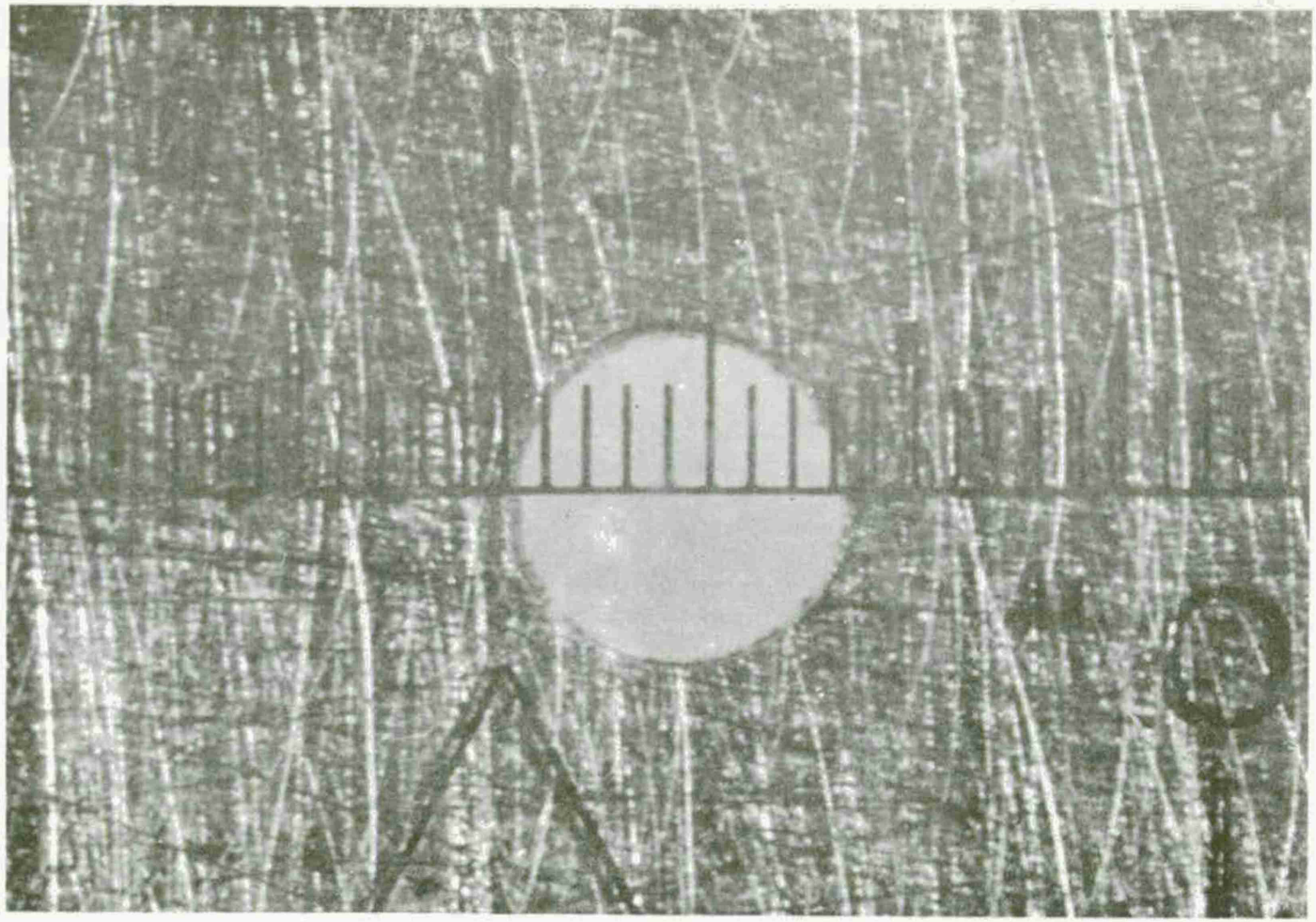

Figure 43. A 50 Times Magnification of an Induced Hole (0.042 inch diameter) in a Brass Test Specimen, Before Firing

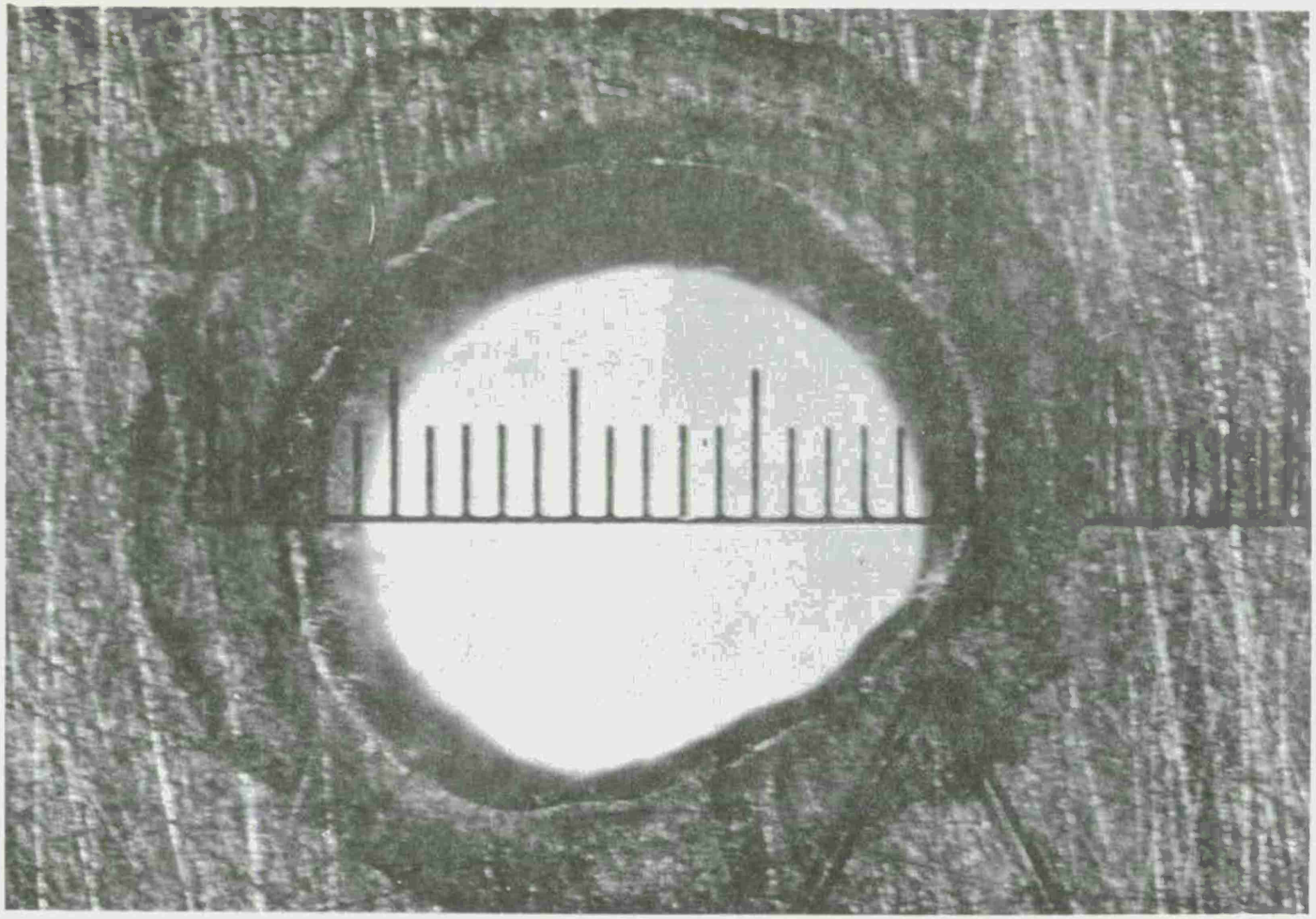

Figure 44. A 50 Times Magnification of an Induced Hole (initially 0.040 inch diameter) in an Aluminum Test Specimen, After Firing (Note the irregularity of the circumference.)

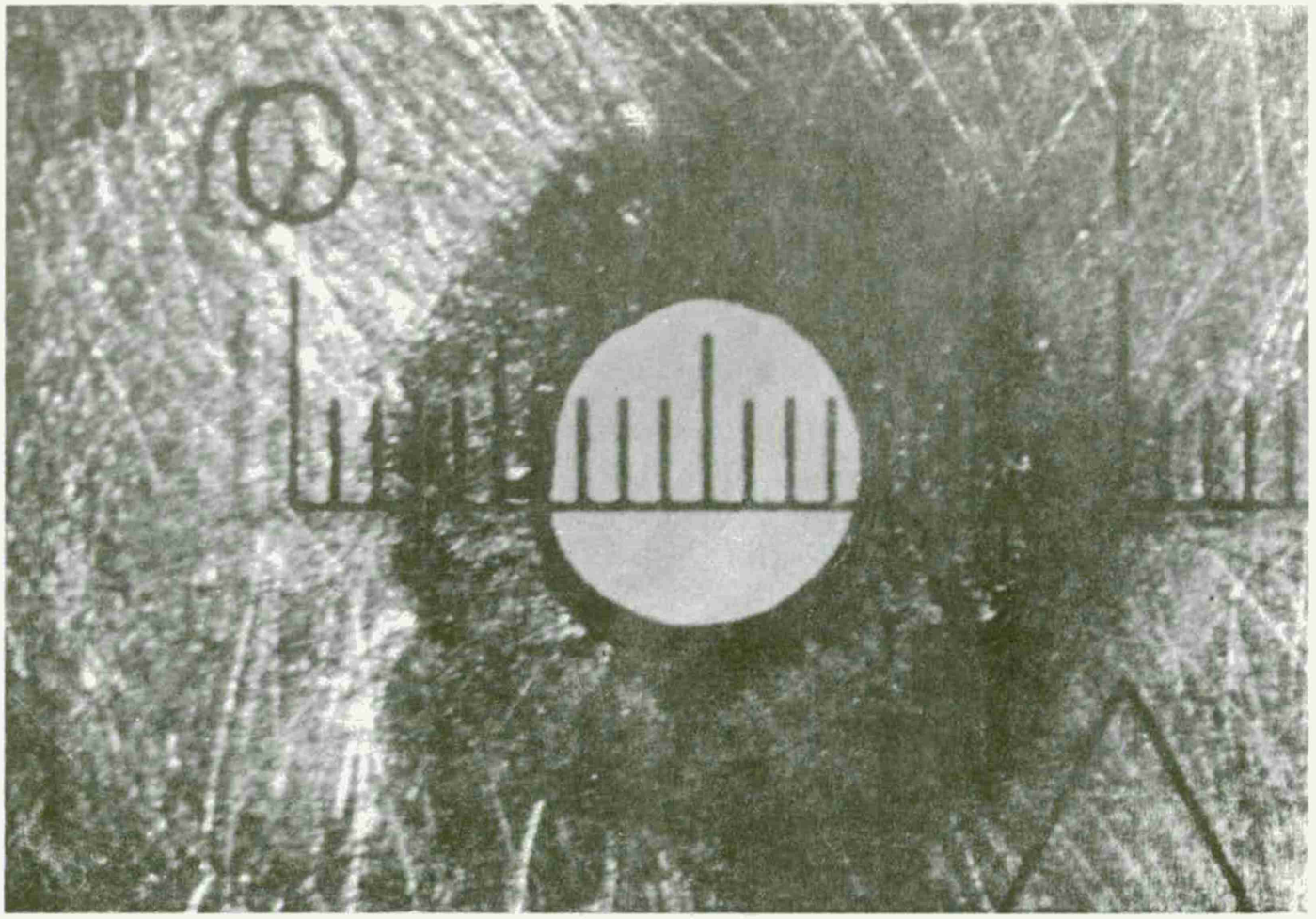

Figure 45. Inside or Combustor Surface of a Brass Test Specimen after Firing
(Note the effecti[illegible]diameter is 7.5 units.)

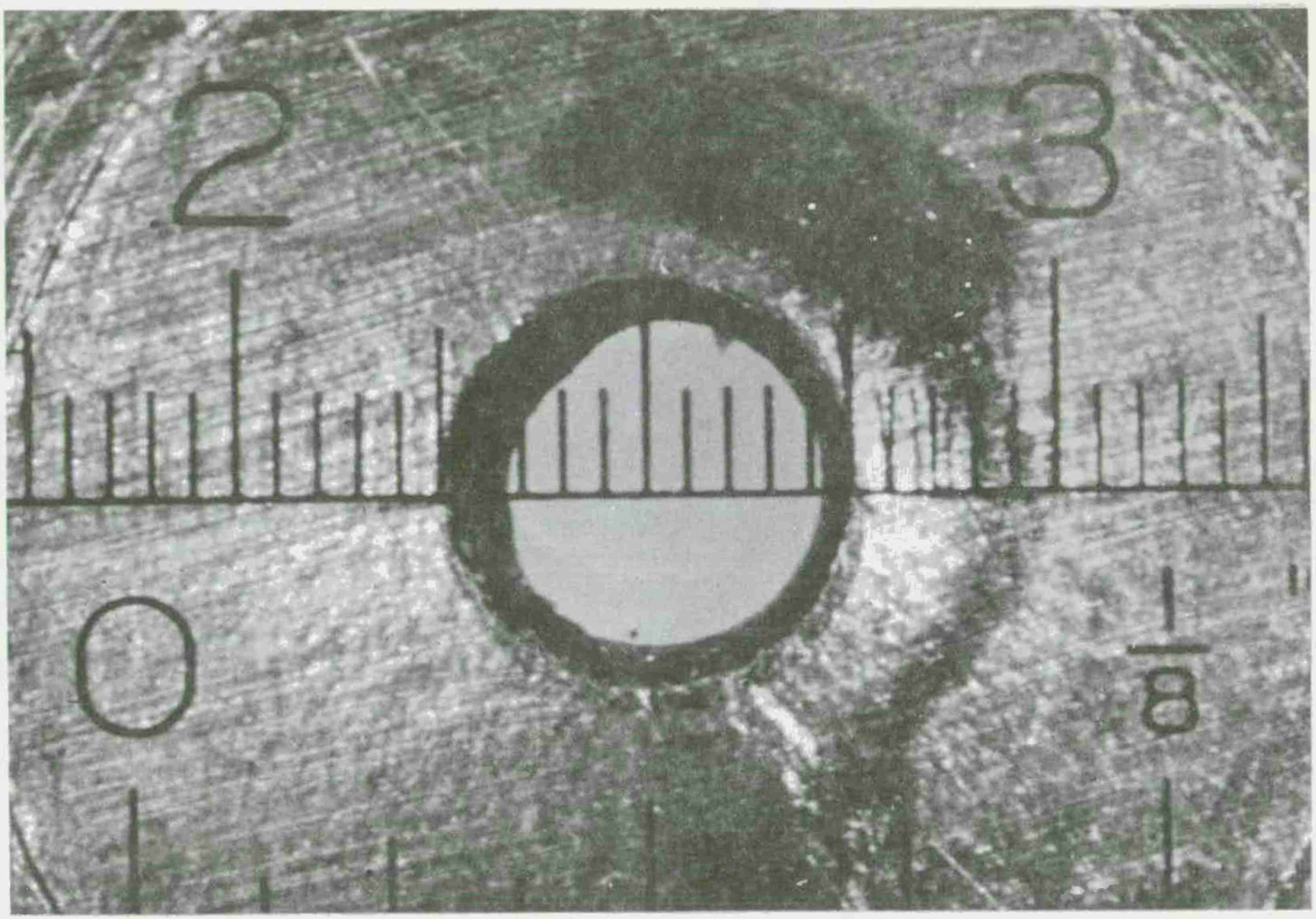

Figure 46. Outside or Atmosphere Surface of a Brass Test Specimen after Firing
(Note the effective diameter is 10 units.)

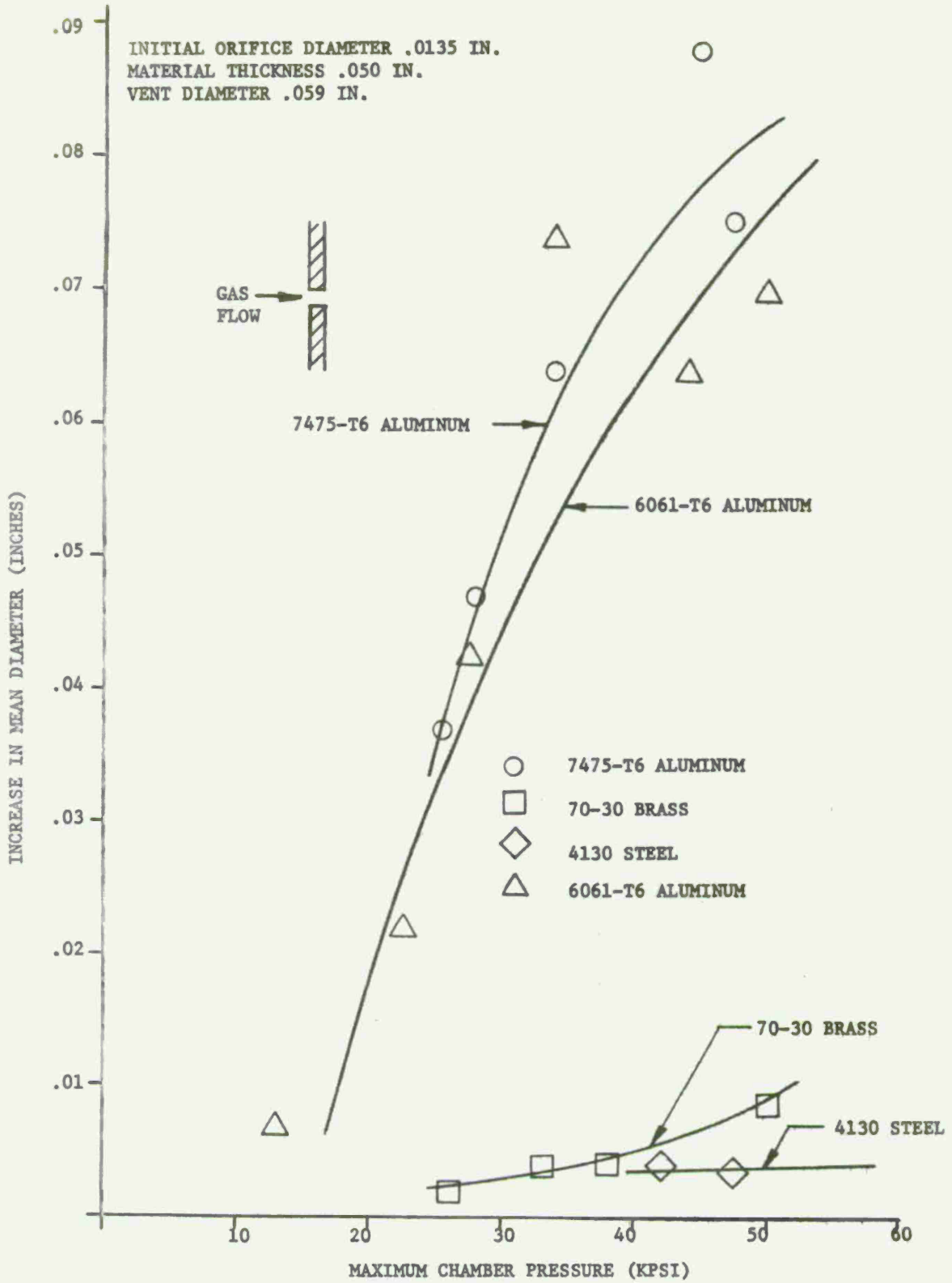

Figure 47. Mean Increase in Diameter VS Peak Chamber Pressure for Test Specimens of Aluminum Alloys 7475-T6 and 6061-T6, 4130 Steel, and 70-30 Brass.

diameter (used to control the experiment time) were the same for each test disc.

A number of facts became easily apparent. For all the materials tested, as the peak chamber pressure increased, the erosivity (as indicated by the increase in mean diameter) also increased. The erosion characteristics of aluminum alloys 7475-T6 and 6061-T6 are defined by the same statistical envelope, and therefore it could be concluded that both materials erode at approximately the same rate. On the other hand, the erosivities of the 70-30 brass and the 4130 steel are drastically different from the erosion characteristics of the two aluminum alloys tested. It has, therefore, been postulated that the lower solidus temperatures and greater chemical reactivities of the aluminum alloys may be responsible for the increased erosion when compared to a brass or steel specimen under similar experimental conditions.

The effect of the peak chamber pressure on erosivity is clearly evidenced in Figure 47. Two other physical characteristics of the test disc should also be considered -- the thickness of the disc and the initial diameter of the predrilled hole. Figure 48 shows the increase in mean diameter as a function of peak chamber pressure for test discs of three different thicknesses. These data indicate that for a particular peak pressure level, the increase in mean diameter (erosion) is increased as the test thickness is correspondingly increased. Of course, all discs were fabricated from the same alloy (7475) and in all firings the experiment time was controlled by the same size vent diameter (0.059 inch).

To account for the increased erosion with increased disc thickness, it is possible to consider that eroded aluminum entrained in the boundary layer or the core flow reacted in its hot gaseous environment thus feeding additional energy to the orifice walls. The theoretical treatments given in References 5 and 15 predict that the highest heat transfer rates, based upon convective heating across a flat plate turbulent boundary layer, occurs at the leading edge, or the inlet of the orifice. With entrainment and chemical reactions in the gas flow, it is possible that more energy is

---

[5] Squire, W.H. and Donnard, R.E., "An Analysis of Local Temperature Profiles Encountered in the Aluminum Cartridge Case Drilled Hole Experiment", Frankford Arsenal Technical Note TN-1163, August 1971.

[15] Squire, W.H. and Donnard, R.E., "An Analysis of 5.56mm Aluminum Cartridge Case 'Burn-Through' Phenomenon", Paper presented at the Army Science Conference, 14-16 June 1972, West Point, New York.

transferred to a point downstream than at the inlet of the orifice. The increase in energy from chemical reactions and gas flow as a function of increased distance from the orifice entrance is a possible explanation for the data in Figure 48.

The initial diameter of the predrilled hole, or differences in curvature, should have an effect on the erosion sustained by the specimen. A smaller diameter hole allows for a greater percentage increase in heat flow per unit of radial distance into the surrounding material than a larger diameter hole under similar experimental conditions. Thus, a smaller diameter hole dissipates heat more rapidly and hence does not heat up as soon as a larger hole. Therefore, the smaller hole will have a later onset of erosion and should erode less than a larger hole.

In a similarly performed experiment, the Princeton group also studied the erosivity of a titanium alloy. As titanium's melting point is approximately 1800° C, one would expect little or no erosion sustained by a titanium disc. Although titanium is characterized by the high melting point, it is also known to be very chemically reactive. From an examination of the erosivity of titanium as a function of peak chamber pressure, presented in Figure 49, it is obvious that titanium erodes as much as, if not more than, the two aluminum alloys tested at comparable pressure levels. The Princeton group has also observed that the outside (atmosphere) surface of the titantium disc was severely scarred and pitted. An additional observation was made that the increase in mean diameter of the induced orifice on the atmosphere side was greater than that on the combustor side. Both of these observations suggest that chemical attack, as opposed to boundary layer convection, is the dominant mode of heat transfer in producing the observed damage.

A two piece cartridge case -- titanium head and lower body, and an aluminum upper body -- was fabricated, assembled, and prepared for the induced failure test by scratching. The head of the fired cartridge case is shown in Figure 50 and displays evidence of severe erosion in the head region. Both experiments -- erosion test fixture and actual cartridge case firings -- indicate the importance of chemical reactions in overall cartridge case degradation.

The basic experiment, using erosion fixtures, was modified to include one series of tests wherein the single disc of the test material was replaced by a double disc arrangement of brass and aluminum. The thickness of each specimen was adjusted so that the total thickness of the combination was approximately that of the single disc. This was necessary so that comparisons could be drawn between the erosion of the double disc arrangement and the erosion of a single disc. The same initial hole size and vent diameter were required to assure valid comparison between the single and double disc experiments.

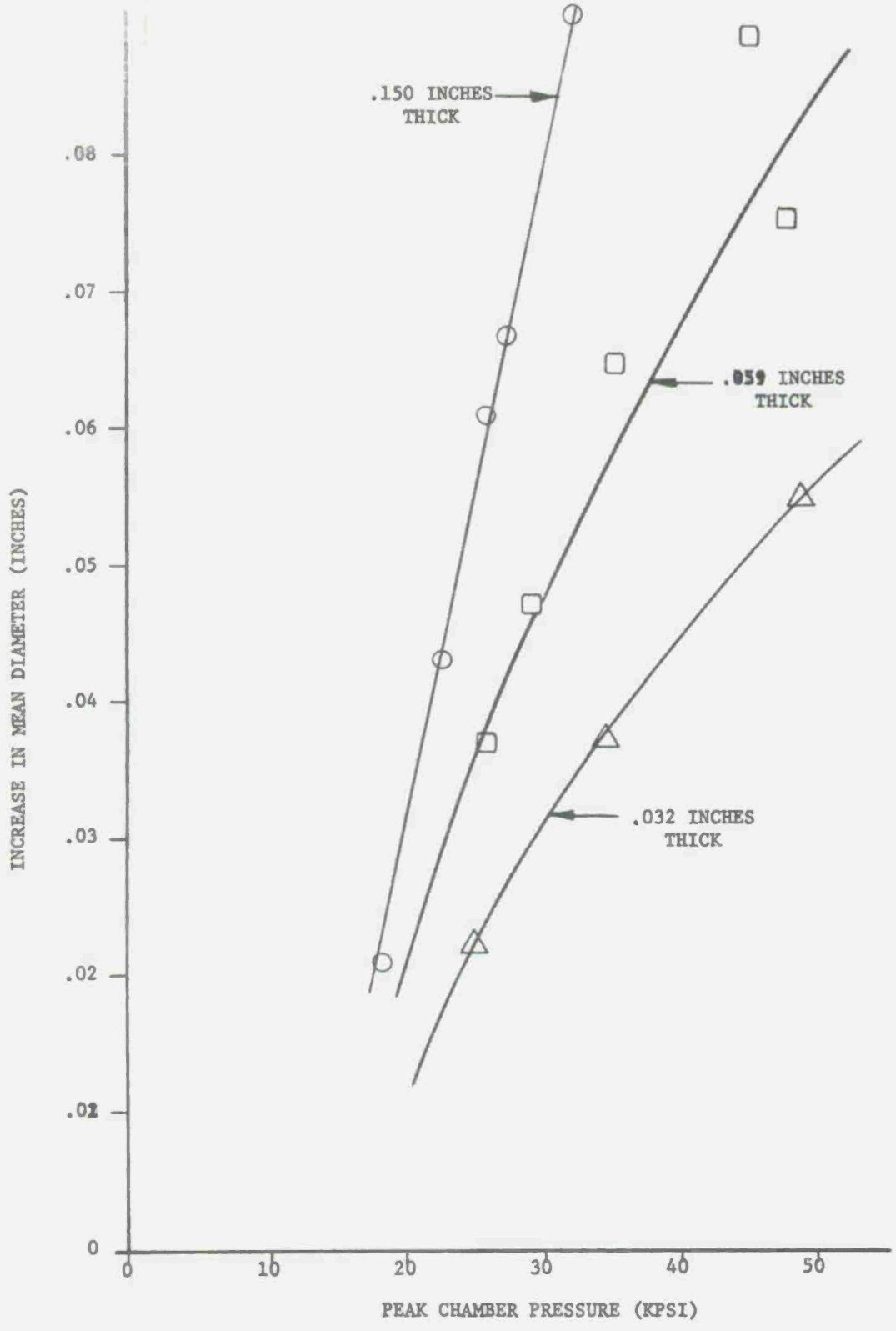

Figure 48. Mean Increase in Diameter VS Peak Chamber Pressure for Various Thicknesses of 6061-T6 Aluminum Test Specimens.

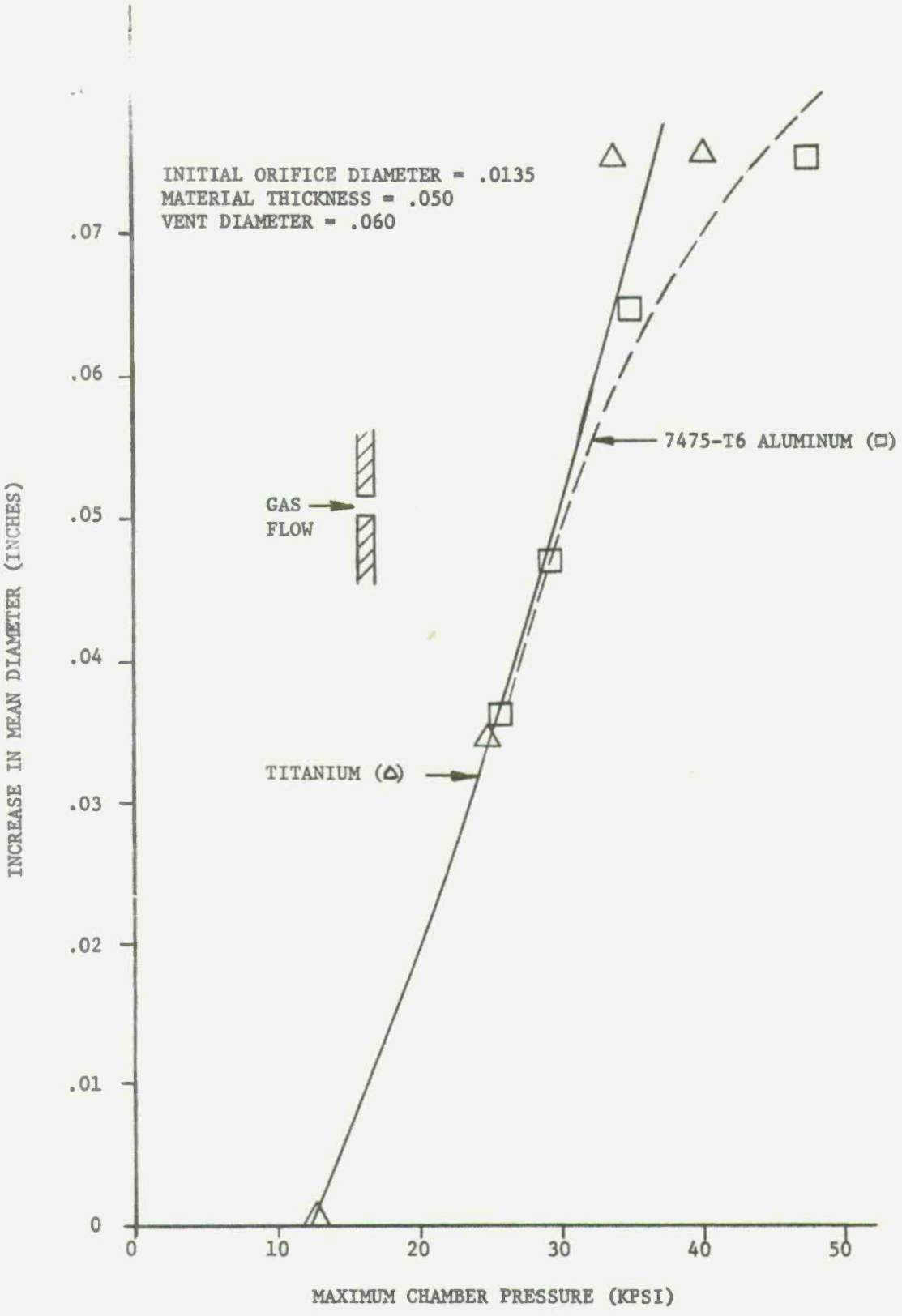

Figure 49. Mean Increase in Diameter VS Peak Chamber Pressure for Test Specimens of Titanium and Aluminum Alloy 7475-T6.

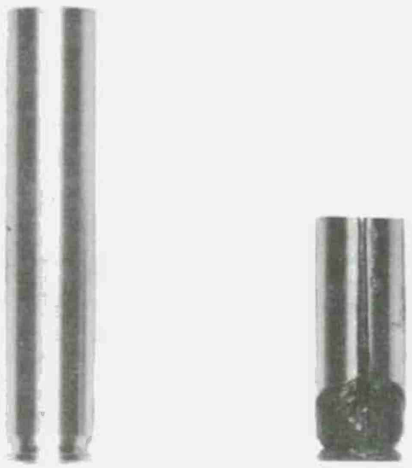

Figure 50. Titanium Portion of a Two-Piece Aluminum-Titanium Cartridge Case Before and After Firing (Note the severe damage in the head region of the case after firing.)

Good alignment of the holes in each specimen was a prerequisite to assure a duplication of a smooth, uninterrupted channel for gas flow.

Figure 51 shows a plot of increase in mean diameter as a function of peak chamber pressure for two variations of the double disc experiment. First, the aluminum was placed closest to the combustor and the brass faced the atmosphere. This arrangement produced the data given by the upper curve. In the second experiment, the orientation of the two test specimens was reversed and produced the data shown in the lower curve. As can be readily seen, the results of the double disc experiment are highly sensitive to the relative orientation of the test discs. As indicated in the plot, the mean increase in diameter for each disc in the composite is shown separately. Thus, for a particular firing or peak chamber pressure, two data points are reported. As expected the erosion of the aluminum disc is greater than that of the brass disc.

By measuring the amount of metal removed from the brass specimen in both cases of the experiment and by using an analytical expression for net heat input, it is possible to calculate the additional energy flux to the brass specimen as a result of the exothermic reaction. This exercise is presented in Section 6.4. The brass specimen, in a sense, is being used as a colorimeter for the primary reaction occurring with the aluminum specimen.

It is possible to view the lower curve -- brass inside, aluminum outside -- as a means to thwart "burn-through". If it is possible to manufacture aluminum cartridge cases with a "protective" layer of brass physically bonded to the interior surface of the case, the results shown in Figure 51 suggest that the erosion will be subsequently reduced.

A clad metal composite system, consisting of different materials bonded together to form a laminate was purchased from Texas Instruments, Inc. The composite in strip form 0.150 inch thick, 1.25 inches wide, and 15 feet long was fabricated from the following metals: 5052 aluminum (60%); 4022 aluminum (9%); 1006 steel (28%); and 85-15 brass (3%) -- the values in parentheses indicates the volumetric percentages of the particular metal in the total laminate.

There were two attempts to assess ballistically the laminate in order to ascertain its insensitivity to erosion. First, erosion test discs were fabricated from the composite and used in the high pressure combustor. The results of firing clad metal erosion discs, shown in Figure 52, duplicated those produced by the double disc experiment. Again, it was readily apparent that the amount of erosion sustained by the clad metal disc was highly dependent on the relative orientation of the specimen. When the aluminum side of the disc faced the combustor and the brass was exposed to the atmosphere, there was

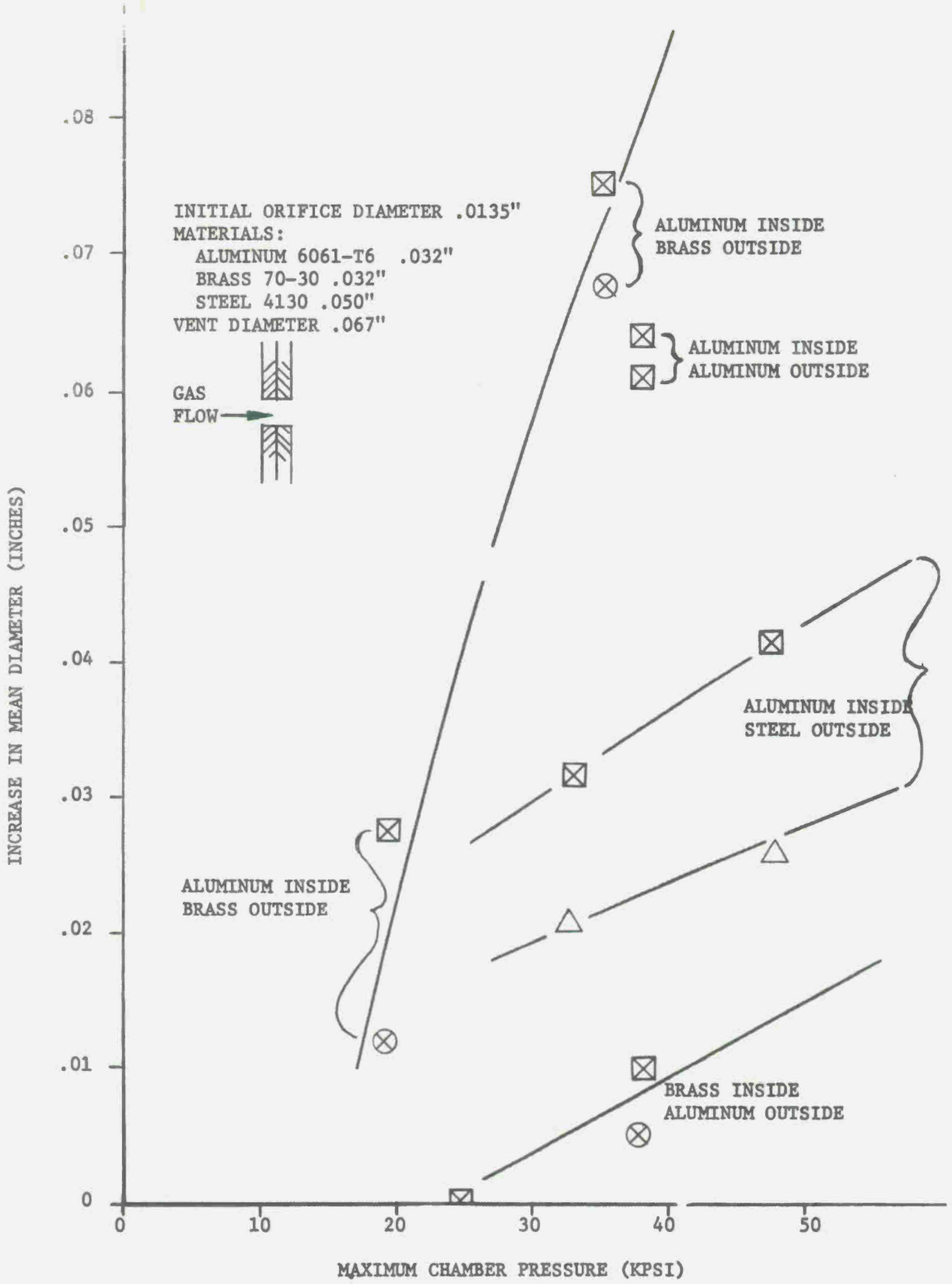

Figure 51. Mean Increase in Diameter VS Peak Chamber Pressure for Double-Disc Test Specimens (Orientation is as indicated.)

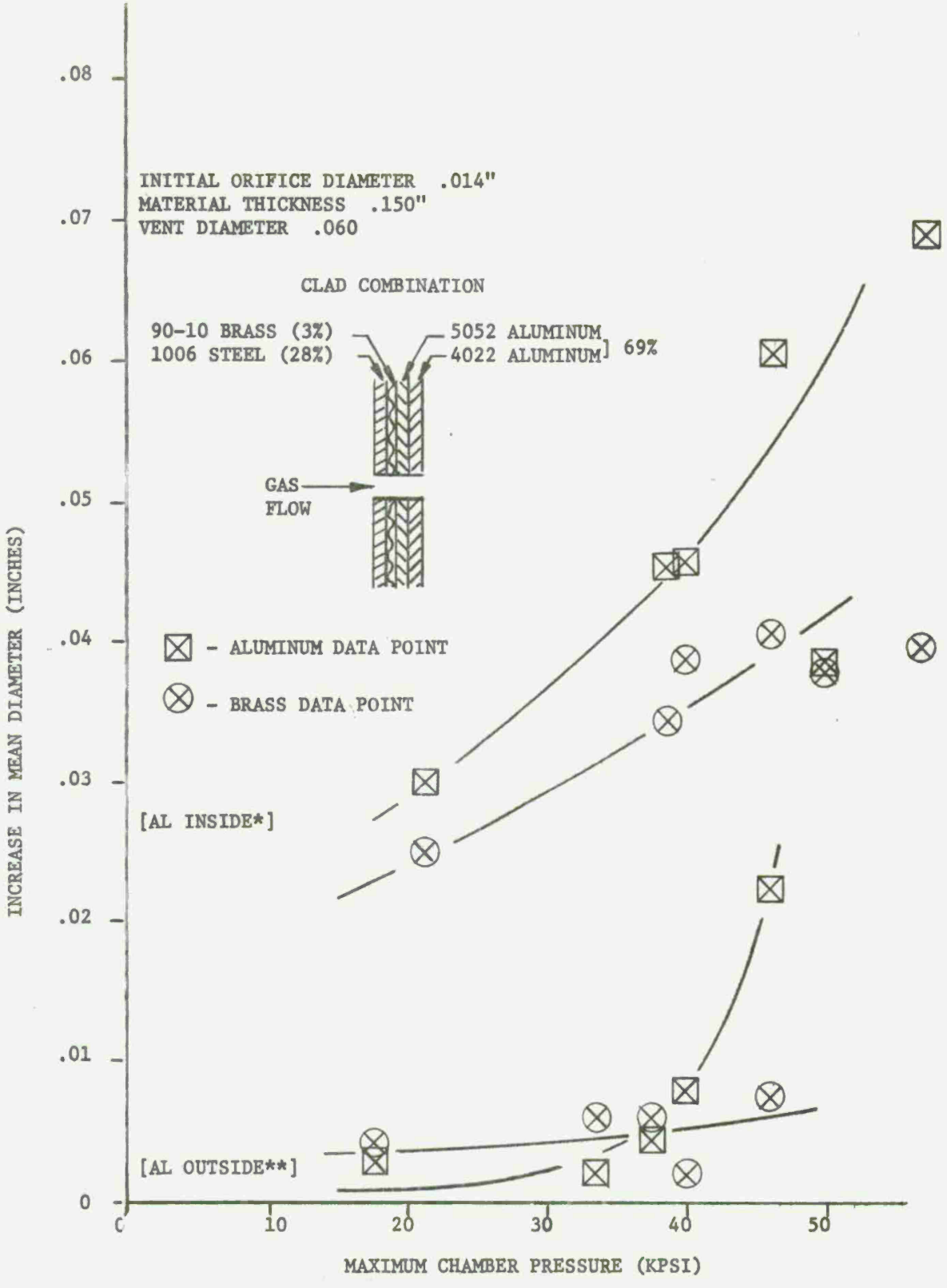

*AL INSIDE -- ALUMINUM SIDE FACED COMBUSTOR
**AL OUTSIDE -- ALUMINUM SIDE FACED ATMOSPHERE

Figure 52. Mean Increase in Diameter VS Peak Chamber Pressure for Clad Metal Test Specimen (Orientation is as indicated.)

no reduction in the amount of erosion -- upper curve. However, when the orientation was reversed -- brass closest to the combustor and aluminum facing the atmosphere -- the amount of erosion was comparable to that sustained by a solid brass specimen of equal thickness, as seen in the lower set of data.

The second effort to determine the performance of clad metal laminates for use in small arms cartridge cases was the attempt to fabricate 5.56mm cartridge cases using conventional blank, cup and draw processing. The laminate used in this portion of the investigation consisted of the following metals: 5052 aluminum (67%); 1010 steel (30%); 90-10 brass (3%). Because the clad materials supplied by Texas Instruments were novel for such intended use, a number of problems arose. These problems were principally due to the lack of adequate heat treatments needed before the various drawing operations and proper strength levels required in the head region. The actual case fabrication activity culminated in a two-piece cartridge case -- clad metal and aluminum. The cases were prepared for the induced failure test by scratching the clad metal portion of the sidewall. Firing of these cases in an M16A1 rifle produced the characteristic bright flash and serious erosion of the head region. The fired cartridge case is shown in Figure 53. It should be noted that the brass side of the laminate faced the interior of the cartridge case as dictated by the results of firing clad metal test specimens in the high-pressure combustor. The inability of a clad metal cartridge case to reduce the effect of "burn-through" is another example in which it is not possible nor meaningful to extrapolate understandings of results gained from closed or venting bomb experiments to a gun environment.

The effect of placing a thin rubber membrane (0.015 inch thick) between the aluminum test specimen and the combustor is shown in Figure 54. The two figures, connected with this orientation, are shown as the data points just off the abscissa and quite dramatically indicate the ability of a thin rubber membrane to thwart erosion. One firing was attempted with the reverse orientation -- the upper datum point -- and produced no reduction in the amount of erosion.

Post mortem examinations of the rubber and aluminum discs yield two possible explanations for the action of the rubber in reducing the erosion. The test conducted at 37 kpsi produced a very small hole in the rubber and minimal increase in diameter of the aluminum disc. The small hole in the rubber was not aligned with the predrilled orifice in the test specimen and the results suggest that the rubber acted as a seal and physically prevented the flow of propellant gas throughout the hole. On the other hand, a firing at 43 kpsi resulted in a large hole in the rubber and again minimal erosion of the aluminum disc. Since some rubber was removed during the firing,

Figure 53. Photograph of Two-Piece Cartridge Case, Upper Portion of Aluminum, Lower Portion of Clad Metal (Note the "burn-through" damage in the head region.)

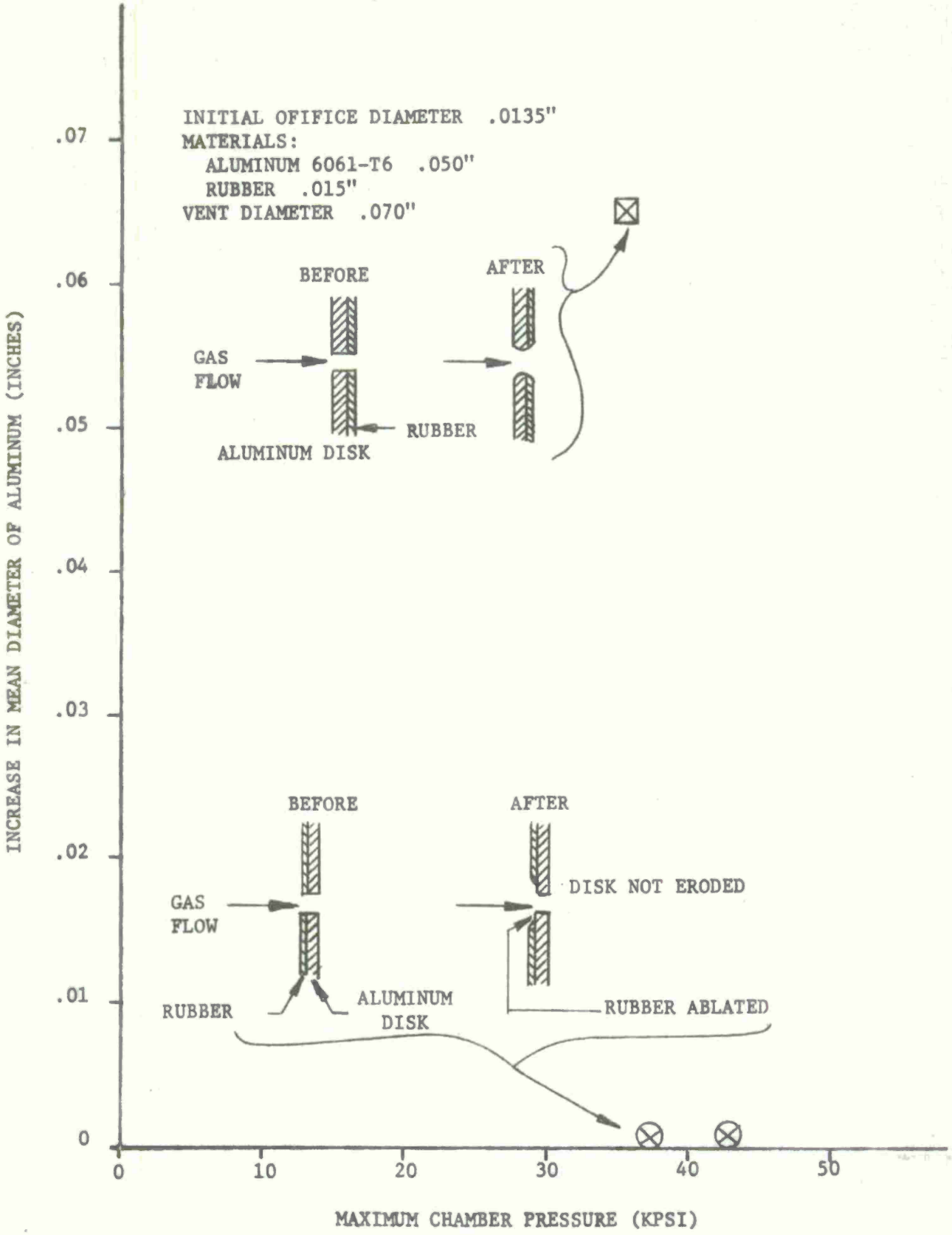

Figure 54. Mean Increase in Diameter VS Peak Chamber Pressure for Aluminum Test Specimens Protected by Rubber Membrane (Orientation is as indicated.)

there exists the possibility that the rubber was ablated by the propellant gas flow. Once the rubber was injected into the boundary layer of the gas stream, it is feasible that it produced a cooling effect, thereby reducing the heat transfer to the hole's surface.

An engineering solution to the "burn-through" phenomenon, wherein a provision has been incorporated in the cartridge design to prevent the catastrophic results given certain types of mechanical case failure, is currently available and is discussed in Reference 6. This solution, called Flexible Internal Element, employs an effect similar to that produced by the rubber membrane in the rubber/aluminum disc experiment.

---

[6] Donnard, R.E., and Squire, W.H., "The Aluminum Cartridge Case Exploratory Development Program - Status Report", Report M72-6-1, April 1972, Frankford Arsenal, Phila., Pa.

SECTION 6.2. DRILLED HOLE EXPERIMENT

The drilled hole test was devised to determine the relationship between the damage sustained by an aluminum cartridge case during "burn-through" and parameters such as the initial area of the induced gas path, peak propellant pressure, propellant flow time and the total amount of gaseous discharge. A total of one hundred and seventy-five aluminum alloy (7575) cartridge cases were prepared for the test by drilling a hole of predetermined size in the head region of each case. In order to provide gas paths which approximate the initial size of the fissure during an actual failure process, the following hole sizes were selected: (1) 0.0135 inch (diameter) hole; (2) 0.0250 inch; (4) 0.0400 inch; and (5) 0.0612 inch. The exact location of this induced orifice is shown in Figure 55.

Various peak propellant pressures were obtained by loading the cases with one of the following charges of WC846 ball propellant (Army Lot 46892): (1) 21.0 grains; (2) 23.0 grains; (3) 25.0 grains; (4) 27.0 grains; and (5) 28.0 grains. Propellant acceptance data indicate that with the charge levels of the aforementioned propellant, peak chamber pressures would range from 30 kpsi (21.0 grains) to 54 kpsi (28.0 grains). This range of pressure levels clearly includes those experienced by a normally functioning cartridge cases; i.e., cases not undergoing "burn-through". Furthermore, in order to obtain an acceptable confidence limit, a sample size of five firings was used to represent each condition of the experiment (peak pressure level and hole size).

Attention is now focused on the ability to relate, in a quantative sense, the amount of damage sustained by an aluminum cartridge case during the failure mode. First, there is the rather obvious way of observing two cartridge cases which have experienced "burn-through" and then determining qualitatively which one of the two cases experienced the more damage. Secondly, it is possible to measure the initial and final orifice diameter and thereby obtain the increased orifice diameter. The last technique involves weighing the cartridge case before and after firing. The difference between the two weights, the amount of aluminum lost as a result of the "burn-through", can be used as an indicator to determine the severity of a "burn-through". Each of the three techniques has certain advantages and disadvantages which makes it more or less desirable for a particular application.

The first technique, observation of the damaged region, is undoubtedly the quickest, but also the most inaccurate. It is, therefore, of use only to identify gross behavior.

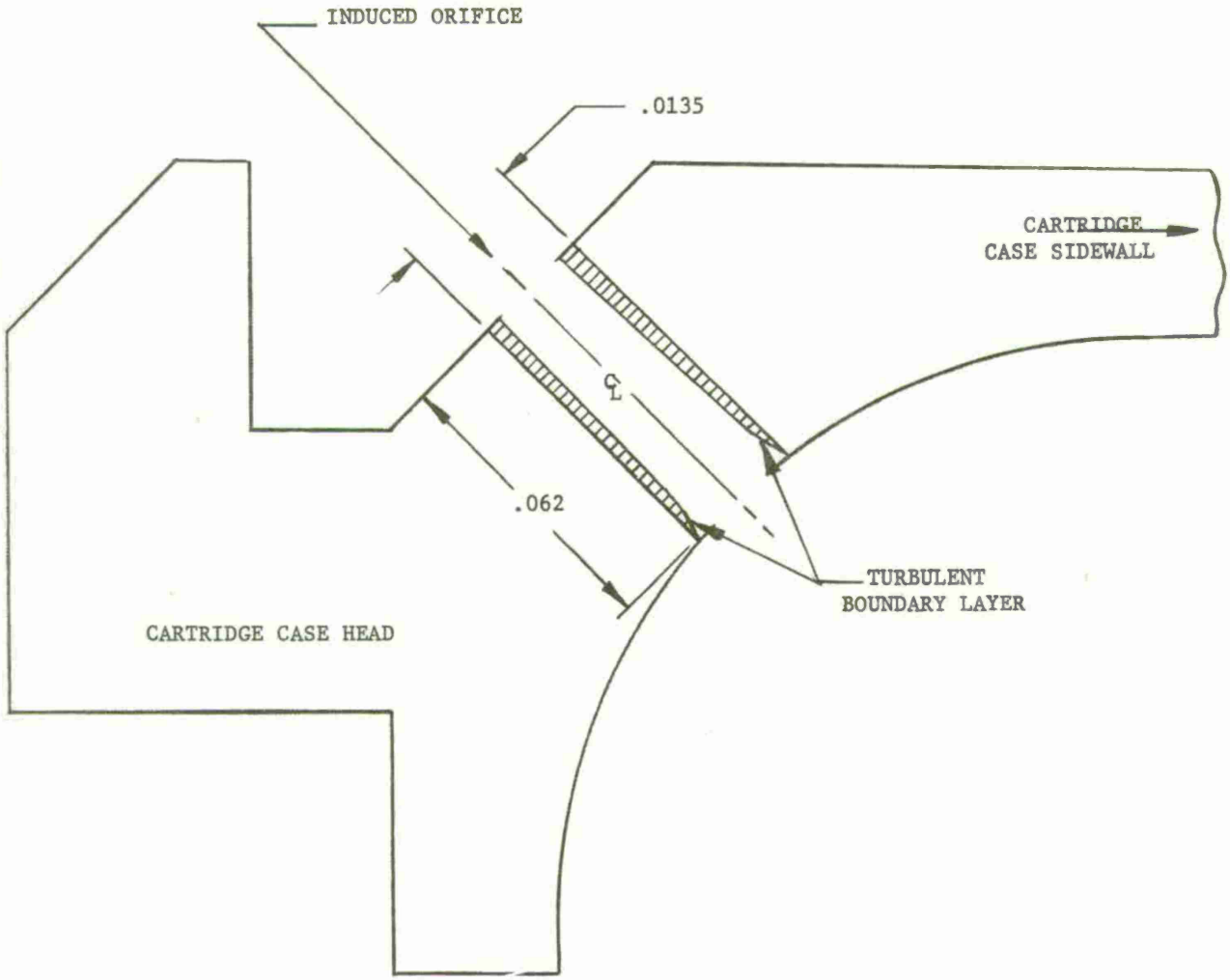

Figure 55. Head Region of 5.56mm Cartridge Case Showing Location of Induced Orifice.

Determination of the increased orifice diameter is a procedure which is particularly amenable to the test specimens used in the erosion test fixture described in the previous section and reported in Reference 14. This procedure can only be used if the geometry of the final hole is reasonably cicular. As is shown in Figure 5, the erosion that is sustained by an aluminum cartridge case does not have a circular geometry. Also, it is only possible to measure the erosion on the inside surface of the cartridge case by first sectioning it. These last two facts preclude using the "increase in mean diameter of the induced orifice" as an indicator for the damage sustained by aluminum cartridge cases during "burn-through".

A more accurate method of determining the effect of "burn-through" in a cartridge case is to weigh the case before and after firing. An analytical chemical balance, which will give weights to four-decimal-place accuracy, is used to determine the two weights in question. Of course, the case is weighed after the hole is drilled in the head region and before the case is primed, loaded and assembled. After firing, the case must be deprimed and cleaned in solvent before the final weight is determined. The difference in the two weights is the amount of metal removed (lost) during "burn-through". This procedure is the most accurate.

The drilled hole experiment was performed by dividing the testing program into two phases. Since a "burn-through" not only produces cartridge case damage and a luminous cloud of reacting gases, but also seriously erodes the chamber of the test weapon, it is necessary to structure the testing program to preclude biasing the test results because of increased (and often irregular) chamber dimensions. The first part of the experiment consisted of firing one hundred and twenty-five predrilled cartridges and, in addition, determining the weight loss of each case, measuring muzzle velocity and action time. This test sample resulted from five firings of each combination of five hole sizes and five propellant charges -- (five firings) X (five hole sizes) X (five propellant charges). For the sake of completeness the data obtained from this part of the experiment are presented both in tabular and graphical form. Each entry in Table I or Figure 56 represents the average of the five firings for each condition of the experiment (hole size and propellant charge). The average weight loss is related to the measurable parameters of muzzle velocity or action time. However, more insight can be gained by using propellant acceptance data to relate peak chamber pressure with propellant charge weight and then presenting weight loss as a function of chamber pressure as was done to prepare Figure 56. The reliance upon propellant acceptance data to identify the peak chamber pressure is necessary since pressures were not taken during this portion of the experiment.

Table I. Data from First Portion of Drilled Hole Experiment
(Each entry is the average of five firings per condition of experiment.)

Hole Size (Diameter Inches)	Propellant Charge (Grains)	Average Weight Loss (Grams)	Average Muzzle Velocity (ft/sec)	Average Action Time (msec)
0.0135	21.0	0.024	2655	1.809
0.0135	23.0	0.035	2837	1.381
0.0135	25.0	0.044	2963	1.332
0.0135	27.0	0.071	3186	1.245
0.0135	28.0	0.098	3311	1.131
0.0250	21.0	0.044	2560	1.944
0.0250	23.0	0.046	2731	1.414
0.0250	25.0	0.048	2844	1.268
0.0250	27.0	0.073	3081	1.217
0.0250	28.0	0.094	3202	1.200
0.0312	21.0	0.038	2508	2.024
0.0312	23.0	0.047	2693	1.465
0.0312	25.0	0.053	2830	1.285
0.0312	27.0	0.101	2975	1.254
0.0312	28.0	0.122	3101	1.236
0.0400	21.0	0.051	2381	1.531
0.0400	23.0	0.061	2567	1.588
0.0400	25.0	0.068	2703	1.335
0.0400	27.0	0.143	2914	1.276
0.0400	28.0	0.187	3035	1.284
0.0625	21.0	0.037	2103	1.880
0.0625	23.0	0.046	2207	1.752
0.0625	25.0	0.063	2416	1.547
0.0625	27.0	0.078	2585	1.483
0.0625	28.0	0.094	2678	1.369

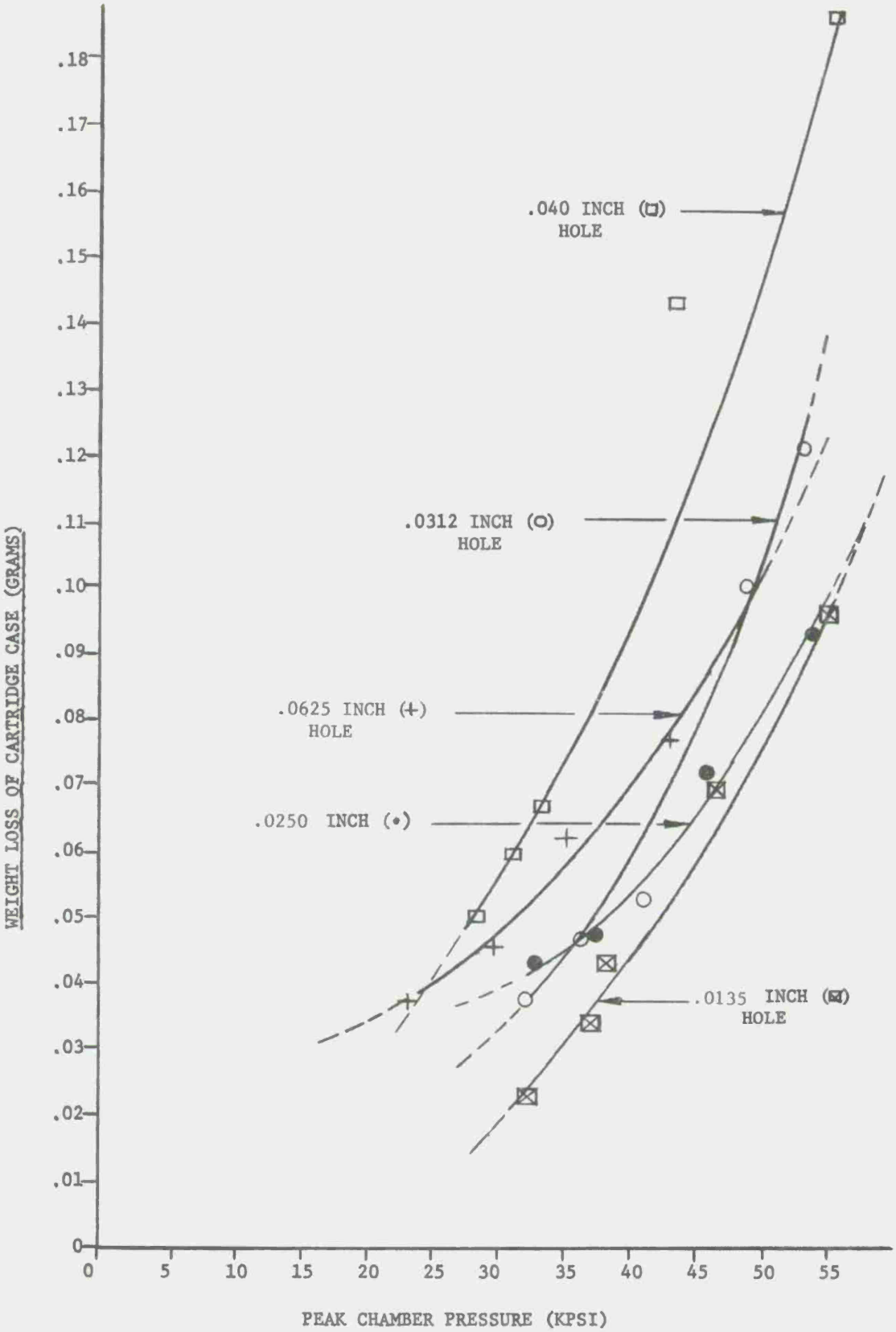

Figure 56. Cartridge Case Weight Loss as a Function of Peak Chamber Pressure from Induced Orifice Experiment (Hole sizes are as indicated.)

Figure 56 shows the dependency of weight loss on peak chamber pressure for a particular initial hole size. It is not surprising that the smallest hole size (0.0135 inch diameter) results in the least amount of damage for a given peak chamber pressure. A trend exists for initial hole sizes of 0.0250 inch, 0.0312 inch, and 0.0400 inch -- as the hole size is increased the corresponding damage (weight loss) is also increased. Since such an effect is true for most peak chamber pressures, a series of curves, connecting the individual data points, are presented in Figure 56 to allow a prediction of the erosion sustained by any initial hole size or peak propellant pressure. Of paramount importance, Figure 56 shows the sensitivity of peak chamber pressure on cartridge case damage. For every reported condition of the experiment, the damage (weight loss) increased as the peak chamber pressure increased.

The fact that the smallest hole size yields minimum damage may be resolved by considering that smaller holes have a greater percentage increase in heat flow area per unit depth into the surrounding material than the larger holes. In other words, the orifice size affects the amount eroded since a small orifice dissipates the heat input to the surface into the surrounding material more readily than does a larger hole. Consequently, it takes a smaller hole longer to begin erosion (assuming a pure heating effect) than a larger hole, given the same conditions of the experiment, since the smaller hole is dissipating the heat input more effectively.

However, the largest hole size, 0.0625 inch (diameter), does not follow the trend established by the smaller hole sizes. Instead of defining a curve for increased pressure levels, the curve for the 0.0625 inch hole falls within the envelope of data defined by the 0.0400 inch hole (upper bound) and the 0.0135 inch hole (lower bound). At first this fact is indeed surprising. By examining the average muzzle velocities resulting from firing cartridges with the 0.0625 inch (diameter) hole, loaded with the propellant charges of interest, values ranging from 2103 ft/sec (21.0 grains) to 2678 ft/sec (28.0 grains) are obtained. These velocities are significantly lower than those recorded for cartridges with a 0.0135 inch hole and the same propellant charges, 2655 ft/sec (21.0 grains) and 3311 ft/sec (28.0 grains). The conclusion is drawn that firing a cartridge with a 0.0625 inch hole does not represent an efficient ballistic system as, with such a large hole, unburnt propellant grains may be ejected from the interior of the cartridge case. Although no information on peak chamber pressure was taken during this portion of the experiment, it is apparent that the anticipated peak chamber pressures were not experienced. Since the observation has been made that the damage sustained by the cartridge case is pressure sensitive, it can be expected that with reduced pressure levels, the resulting damage will also be less.

Since the lifetime of the test barrel in this type of testing is extremely short, and since the preparation of the barrel to obtain the pressure-time curve is time consuming and expensive, for every combination of hole size and propellant charge level only two cartridges were fired. Therefore, the total sample for the second portion of the drilled hole experiment was fifty cartridges (two cartridges for each condition) X (five hole sizes) X (five propellant charge levels).

In addition to the pressure-time history of an aluminum cartridge case undergoing "burn-through", it was also necessary to obtain data on the duration and magnitude of the gaseous discharge. This information was obtained by focusing the sensing element of a RCA 919 photoelectric cell on the exit plane of the induced orifice in the cartridge case. Past work with this particular type of photoelectric cell demonstrated that its response time was short and that it is sensitive to radiation of wavelengths from the infra-red to the visible and hence is desirable for this type of experimentation. A schematic representation of this experiment program is shown in Figure 57.

The gaseous clouds effluxing from a series of brass cartridge cases with similar hole sizes and propellant charge levels have a characteristic orange hue; this type of discharge was discussed in Section 5.3. Since this orange-colored gas flow precedes the "burn-through" plume, it is necessary to filter out the background gaseous discharge. To accomplish this, the gain on the oscilloscope and the bias on the photoelectric cell were adjusted to give a zero D.C. level signal for the cell's output when exposed to the discharge from a brass cartridge case. Figure 58 shows the Polaroid of the oscilloscope's screen. The lower trace is the pressure-time history while the upper (straight line) is the adjusted zero D.C. level. Therefore, any additional signal received by the photoelectric cell was the result of the characteristic "burn-through" plume. The point in time when the photoelectric cell's trace departs the horizontal represents the initiation; the time interval until the curve returns to zero is the duration of the plume. As in the first portion of the experiment, muzzle velocity, action time, and cartridge case weight loss were measured. In a sense, the second part of the experiment provides all the desired data to fulfill the test objectives. However, due to the relatively small test sample resulting from two cartridges per condition of the experiment, it is necessary to rely on the results of the first portion to provide a good statistical sample and determine the relationship between weight loss and peak pressure.

Three pieces of data are presented in Figure 59 (a), (b), and (c). Figure 59 (a) shows the pressure-time and photoelectric cell-time curves resulting from the firing of an aluminum cartridge case with a 0.0400 inch (diameter) hole loaded with 21.0 grains of ball propellant. Figures 59 (b) and (c) are similar data, except that the propellant

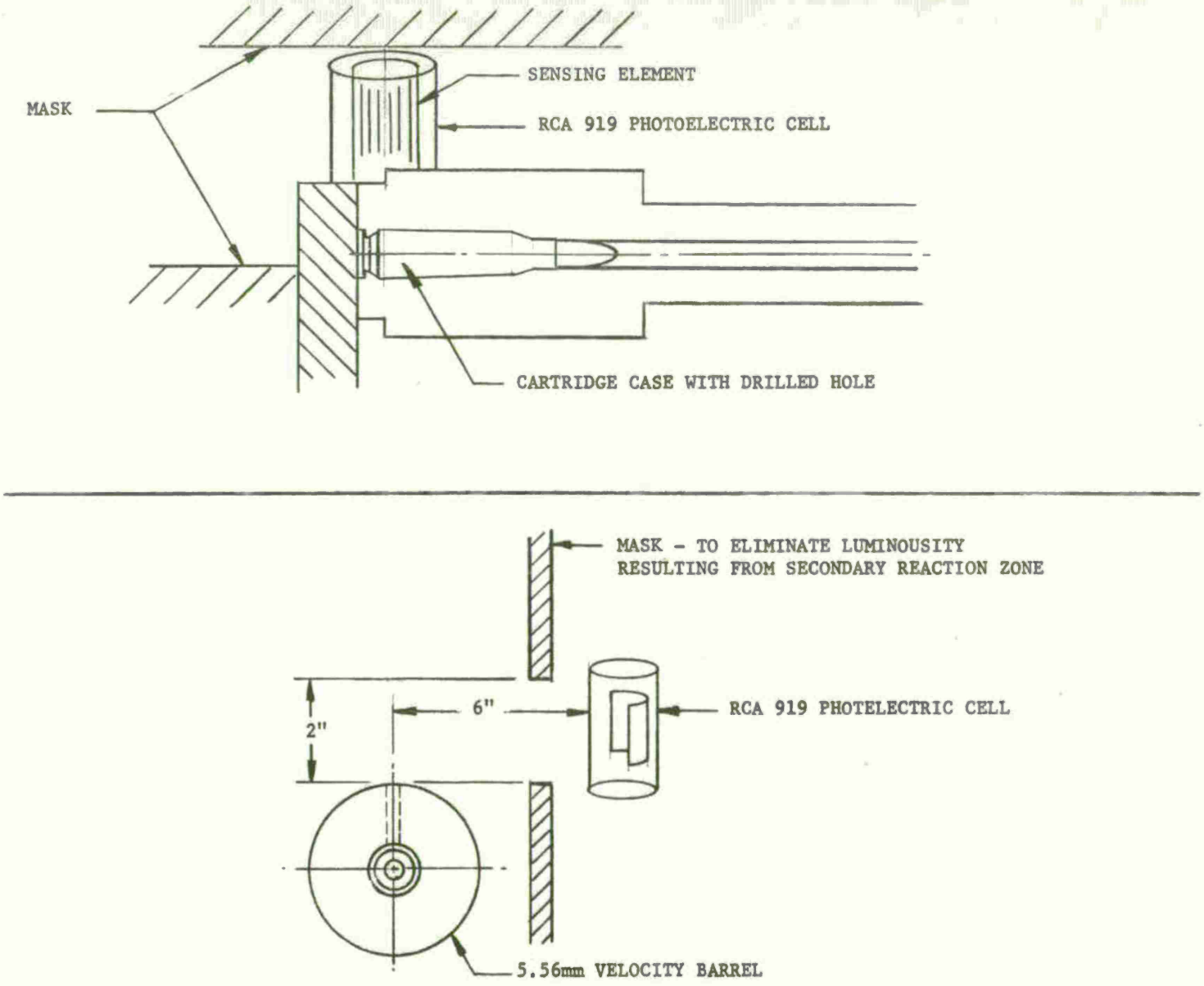

Figure 57. Sketch of Photoelectric Cell's Position for Induced Orifice Experiment.

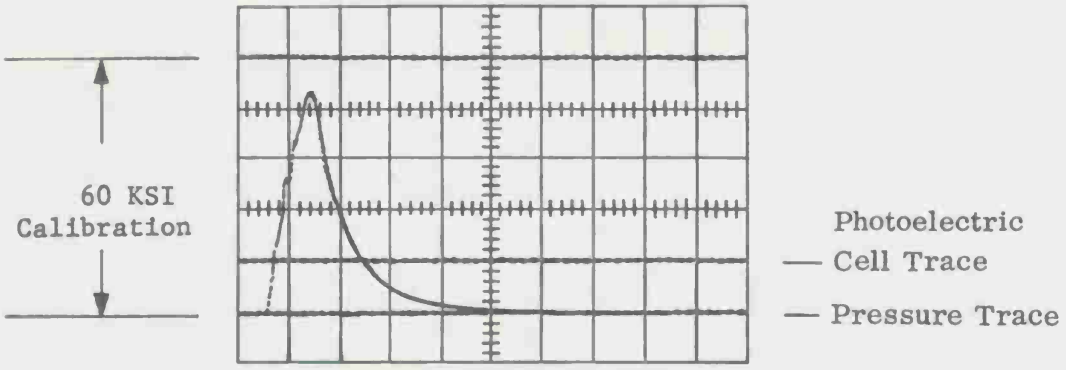

Sweep: 0.5 msec/cm

Brass Cartridge Case, 0.0135" Dia. Drilled Hole, 28.0 Grains of WC 846 Propellant

Figure 58. A 5.56mm Brass Cartridge Case Pressure - Time Curve and Adjusted Photoelectric Cell Trace Showing Zero D.C. Voltage for Propellant Gas Discharge

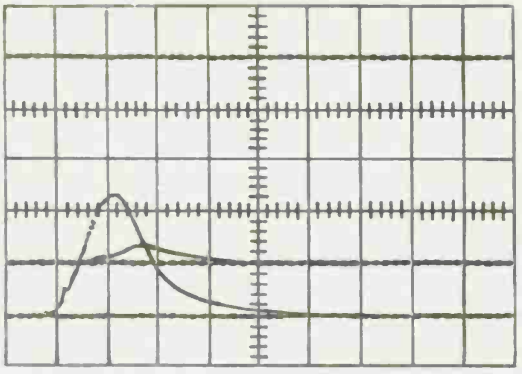

a. Pressure Calibration: 60 kpsi between Lines,
Sweep: 0.5 msec/cm (Both Traces,
Photoelectric Cell Gain: 50 mV/cm,
21.0 Grs. WC 846 Propellant

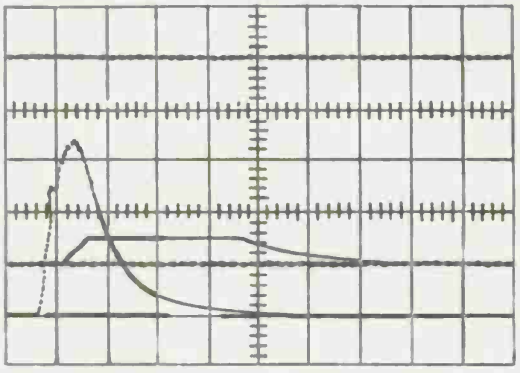

b. 27.0 Grs. WC 846 Propellant

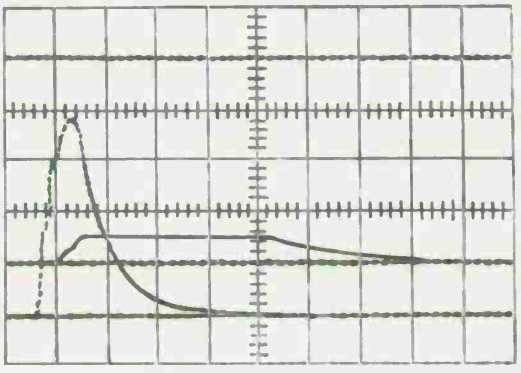

c. 28.0 Grs. WC 846 Propellant

Figure 59. Pressure-Time and Photoelectric Cell Time Curves for 5.56mm Aluminum Cartridge Cases Evidencing "Burn-Through" (Propellant charge weight as indicated.)

charges are 27.0 and 28.0 grains respectively. In all instances, the lower traces are the pressure-time curves and show quite dramatically the effect of charge weight on the shape and magnitude of the curve. More important, however, is the upper trace, the photoelectric cell curve. From such data it is possible to determine the initiation of the flash, the amount of gaseous discharge and the duration of the flash. Since the propellant charge used to obtain Figure 59 (a) was 21.0 grains, it is not surprising that the peak pressure was only 27,600 psi. The photoelectric cell output lags the pressure curve, defines a relatively small area, and returns to a zero level before the pressure curve. When the propellant charge was increased to 27.0 grains, both the pressure and photoelectric cell curves, shown in Figure 59 (b), take on a different appearance. The more apparent differences occur in the shape and magnitude of the photoelectric cell curve lags the pressure curve, but in this instance, very quickly reaches a "level plateau", which lasts for an appreciable period of time, and returns to zero after the pressure curve. The same general characterization is true of Figure 59 (c) (28.0 grains) with the exception that the "level plateau" extends for a longer period of time than the plateau displayed in Figure 59 (b). It should be noted that this plateau does not represent any physical process but corresponds to a saturation (overdriving) of the photoelectric cell. Although it is possible to arrange the photoelectric cell and accompanying electronics to record the entire signal, doing so would preclude an accurate representation of the weaker signals -- those from firings with low prepellant charges. The length of this plateau is, in a sense, a measure of the magnitude of the "burn-through" plume; the greater the effective length of this plateau, the greater the gaseous discharge.

The fifty Polaroids resulting from this portion of drilled hole experiment were measured and the parameters, identified in Figure 60, were determined. From this data reduction, the curves in Figures 61, 62, and 63 were prepared.

The data presented in Figure 61 show the relationship between the peak propellant pressure and the time lag experienced before the "burn-through" was initiated at the surface of the cartridge case. An envelope for all the data points is defined by the smaller (0.0135 inch) and the larger (0.0625 inch) hole sizes. From these data it is concluded that for a given pressure level, the larger hole gives rise to a "burn-through" before the smaller hole. Or, for a given time, it takes a higher pressure for the smaller hole to begin "burn-through" than a larger hole. Generalizing, it is possible to state that the time lag and peak propellant pressure are inversely proportional. An extension of this generalization is presented in Figure 62, wherein duration of the gaseous plume (defined by the time interval between initiation and termination of the photoelectric cell output) is plotted as a function of peak chamber pressure. It is apparent that the "burn-through" plume has greater duration at higher pressure

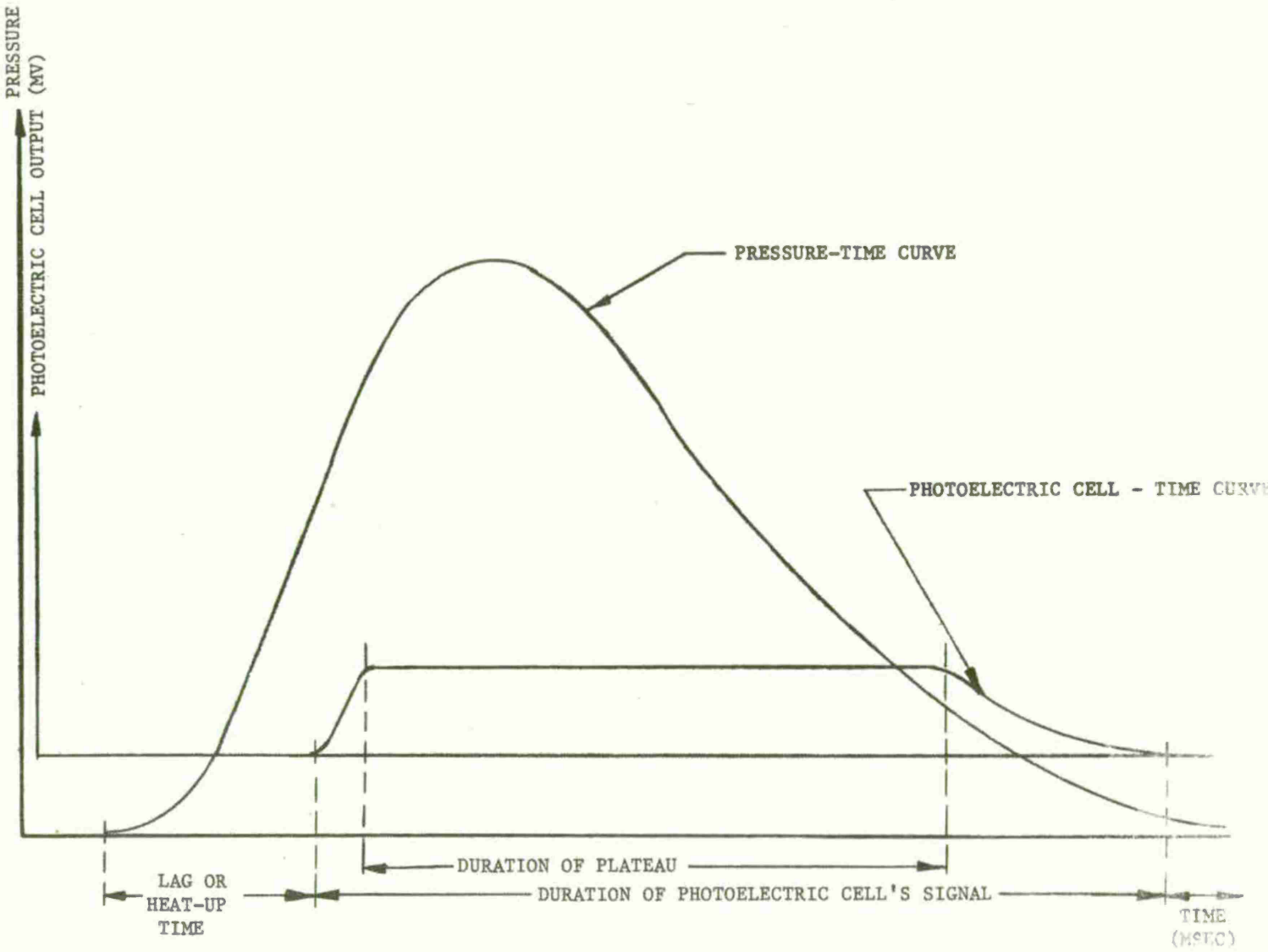

Figure 60. Sketch to Identify Parameters for Discussion in Analysis of Photoelectric Cell Pressure-Time Curves.

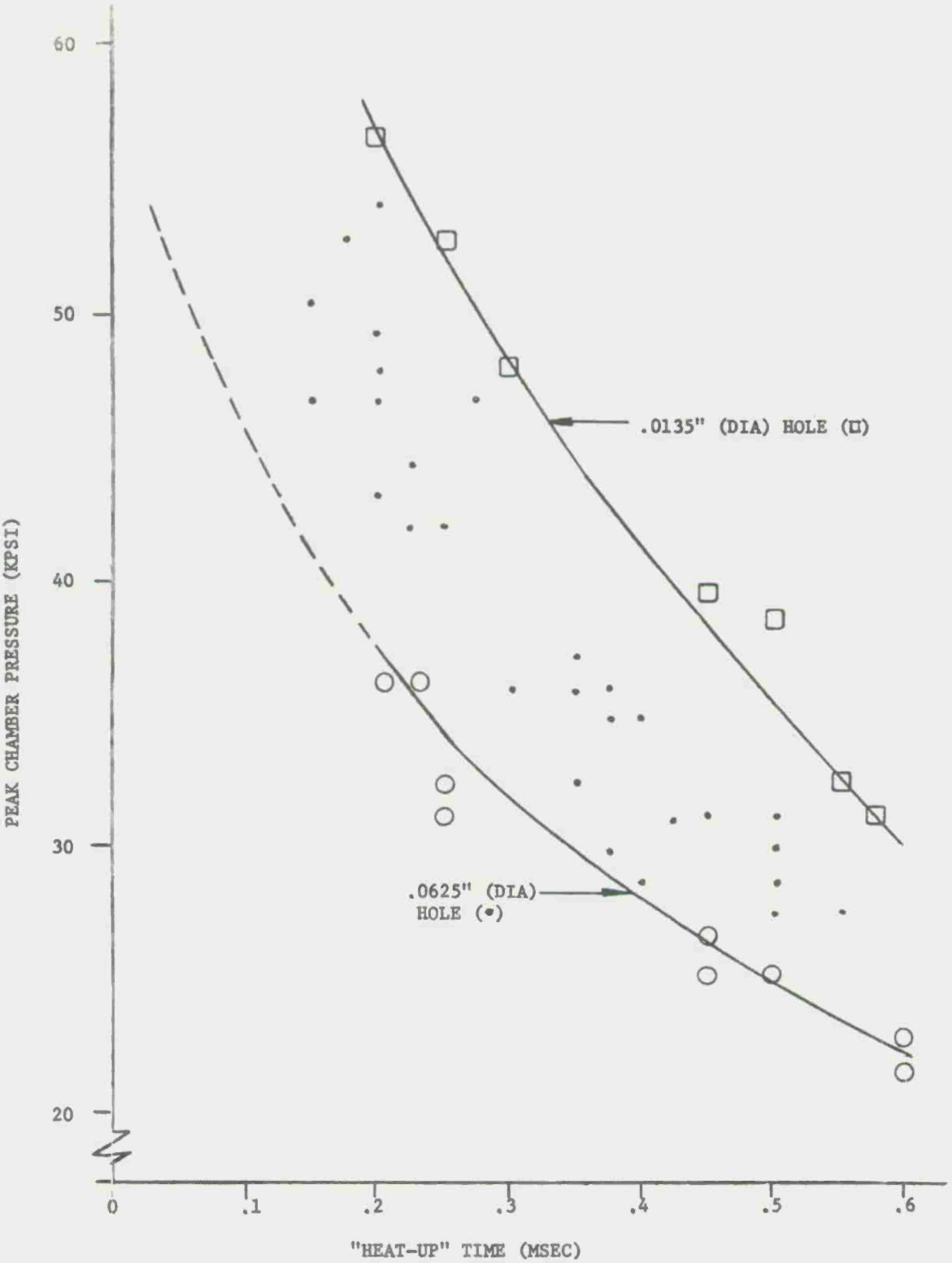

Figure 61. Peak Chamber Pressure VS "Heat-UP" Time (Hole size as indicated)

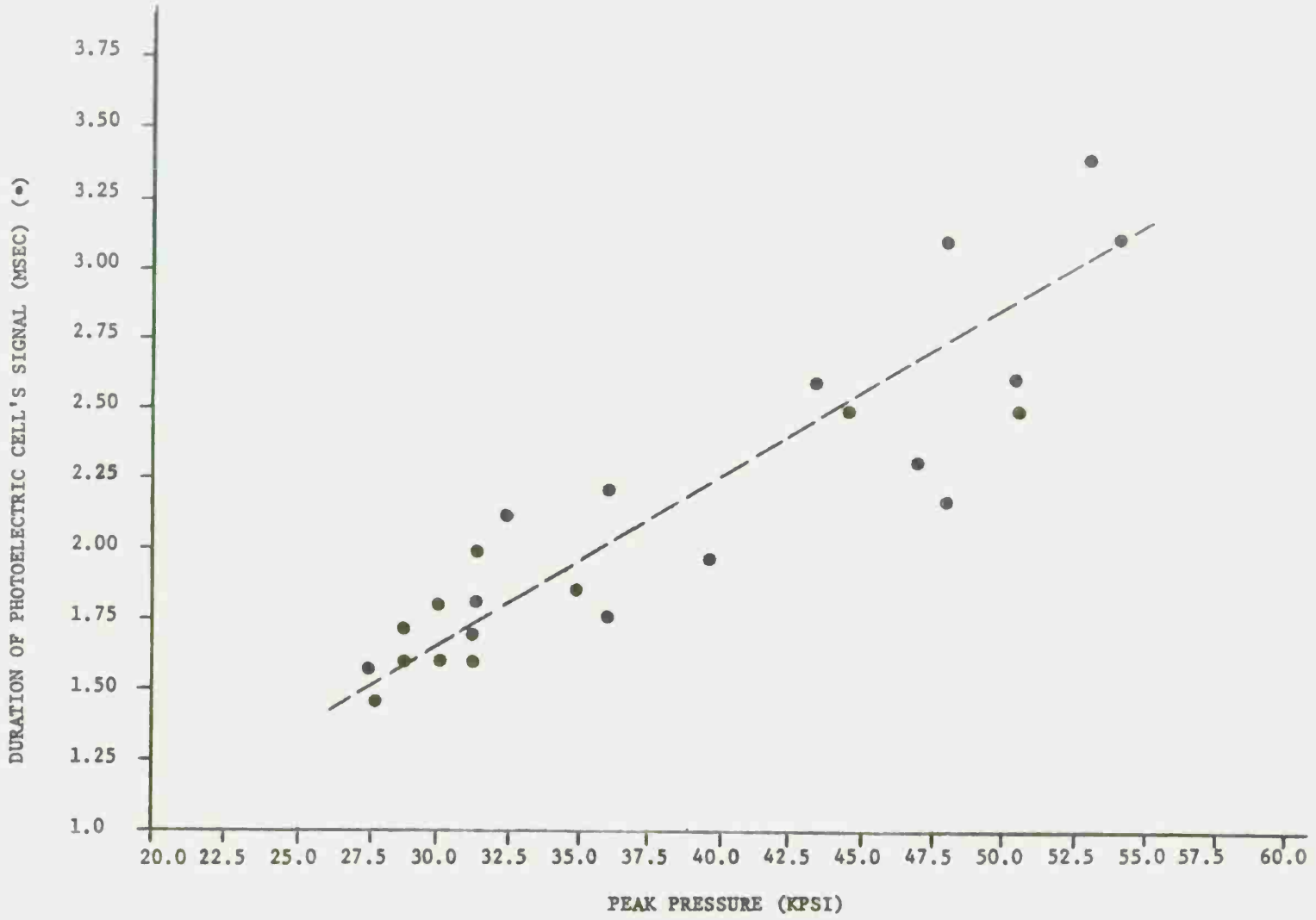

Figure 62. Peak Chamber Pressure VS Duration of Signal Sensed by the Photoelectric Cell (An indication of the duration of the "burn-through"plume.)

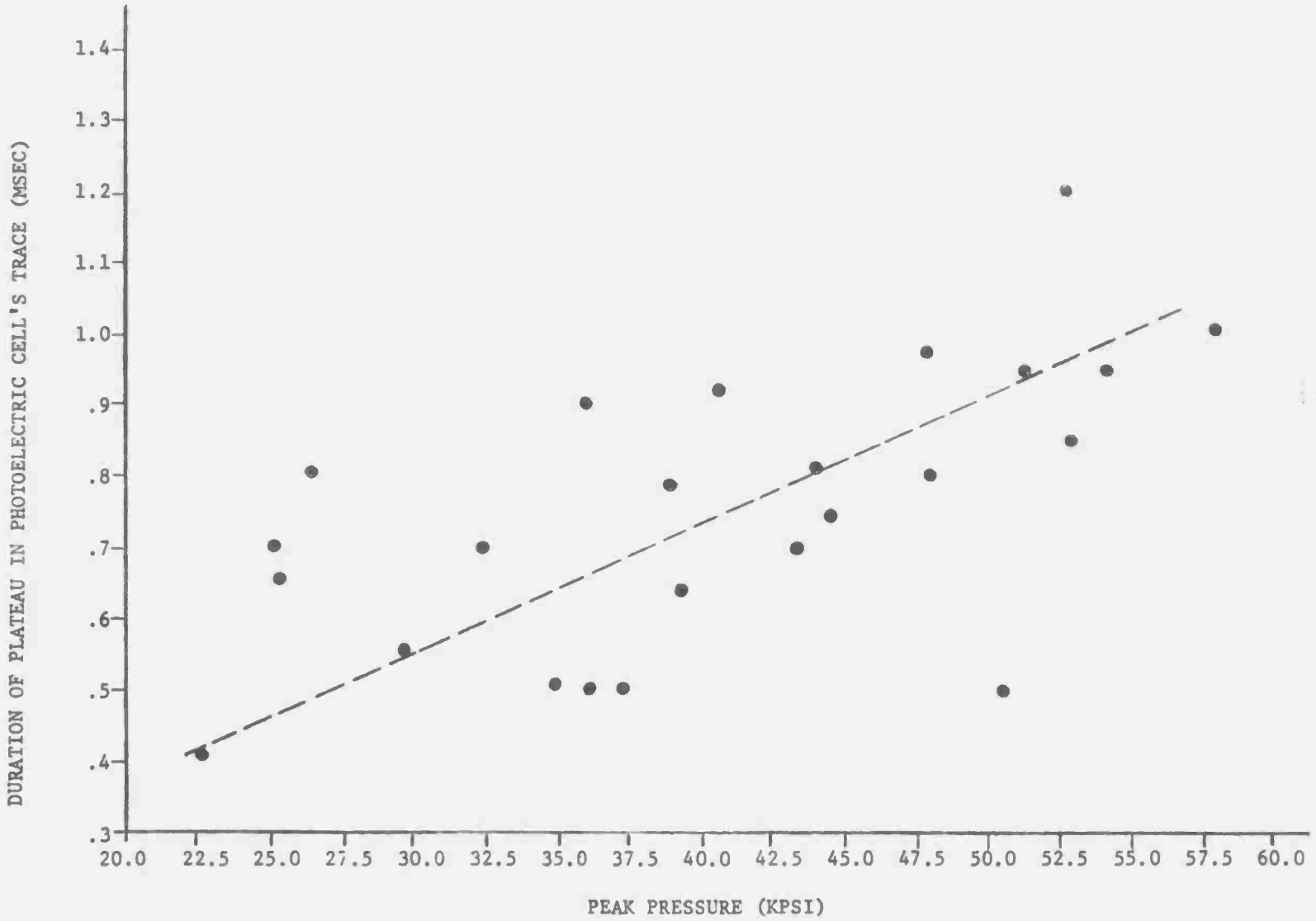

Figure 63. Peak Chamber Pressure VS Duration of the Level Plateau in the Photoelectric Cell's Trace (An indication of the degree of the cell's saturation by the "burn-through" plume.)

levels. Accepting the fact that the length of the plateau is indicative of the amount of gaseous output (Figure 63) it is possible to conclude that the amount of discharge associated with a given "burn-through" and peak pressure are directly related.

The fact that firing a predrilled aluminum cartridge case with a reduced propellant charge yields different "burn-through" characteristics from firing a similar case with a standard charge has been clearly established. In light of this, a high speed motion picture study of the firing of an aluminum cartridge case, with 0.0312 inch diameter hole, loaded with a reduced propellant charge of 23.0 grains is also discussed in this section. The technique, introduced in Section 5.3 which involved the firing into an inert atmosphere, was used to obtain the data shown in Figure 64.

A peak chamber pressure of 36 kpsi can be expected from firing a cartridge loaded with a propellant charge of 23.0 grains. Using the time marks to place events in their proper chronological order, the primary reaction zone was observed at 0.428 millisecond. This delay is in consonance with that reported from the work with the photoelectric cell trained on the hole and fired under similar ballistic conditions; i.e., same hole size and propellant charge. After 0.571 millisecond the intensity of the primary reaction zone decreased. Although the intensity of the reaction has subsided, it is difficult to locate the hole and therefore ascertain any additional information about its size. However, at t equals 0.643 millisecond, the reaction built in intensity and continued until 0.785 millisecond. This firing was unique because the primary reaction zone subsided after 0.996 millisecond .

To conclude this section, a brief summation is presented. The drilled hole experiment was conceived, designed, and conducted to determine the parametric coupling of damage, sustained by an aluminum cartridge case as a result of "burn-through", to the peak chamber pressure, the diameter of the induced orifice, the propellant flow time, and the total amount of gaseous discharge. The relationship between the weight loss of an aluminum cartridge case (an indicator of the damage) and peak chamber pressure is presented graphically in Figure 56. From Figure 56 it is immediately concluded that the severity of the damage is increased as the peak chamber pressure is increased. A similar statement is also applicable for initial hole size. As the diameter of the hole is increased, the cartridge case weight loss is also increased. The exception to this statement is the family of data resulting from the 0.0625 inch (diameter) hole. These data fall within the envelope defined by the 0.040 inch (diameter) hole and the 0.0135 inch (diameter) hole. An explanation for this seemingly anomalous behavior may be the fact that the muzzle velocities (hence peak pressures) are significantly lower than expected. With such reduced pressure levels, it is to be expected

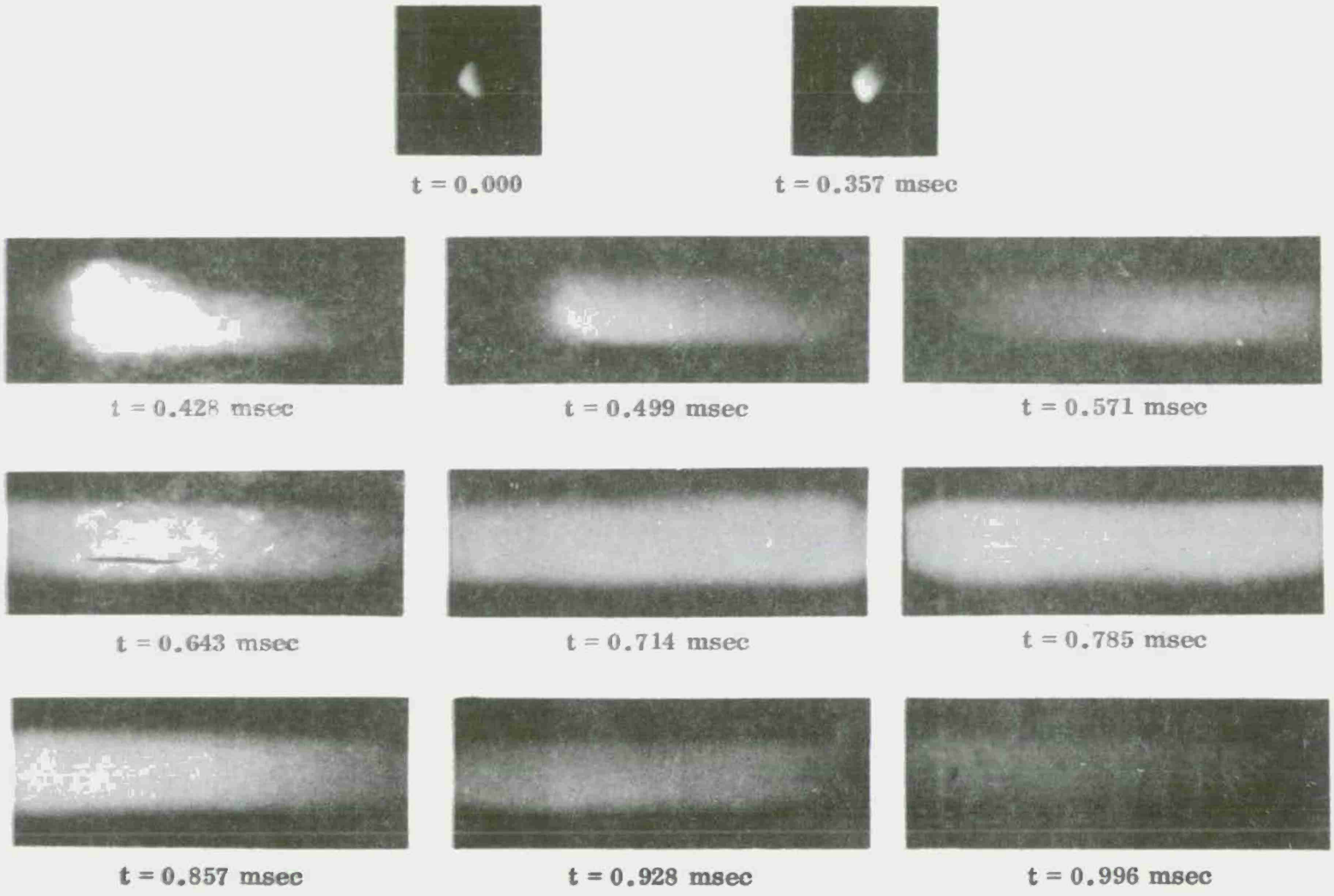

Figure 64. High Speed Motion Picture Study of "Burn-Through" Plume into Helium (Reduced propellant charge used.)

that the weight loss will correspondingly be somewhat lower.

The results of the work with the photoelectric cell, focused at the surface of the cartridge case, provide the information that the weight loss is directly proportional to the propellant flow time and total amount of gaseous discharge. An interesting by-product of this work is the fact that there is a certain delay, or lag time, before the "burn-through" gets underway; this parameter is also correlated with peak chamber pressure.

SECTION 6.3. STANDARD SLIT EXPERIMENT

Reference 9 identifies a technique for simulating a split in the sidewall of an aluminum cartridge case by inducing a scratch of known depth. The need for a technique of this type is a direct consequence of the fact that a large percentage of the "normally occurring" failures (those produced during firing which were not the result of any prior machining or drilling of the cartridge case) result from natural splits. Furthermore, in a comparative sense, it can be established from examining the cases that the appearance of the damage sustained by the cartridge case from a drilled hole and the damage resulting from a "naturally" occurring split are not exactly identical. Therefore, to duplicate the failure mode which occurs the more frequently and approximate the post-damage appearance of the cartridge case, an experiment similar to that described in the previous section, on a somewhat more limited scale, was performed, using slit cartridge cases.

As is shown in Figure 65, the scratch is nominally 0.005 inch deep and extends from a point immediately adjacent to the exterior groove for a distance of 0.75 inch. In this experiment, however, the charge of WC846 ball propellant (Lot 44111) was varied from 21.0 to 28.0 grains in 1.0 grain intervals. Again the quantitive assessment of "burn-through" severity was obtained by weighing the cases before and after firing. Also, a sample size of five cartridges for each propellant charge level was used to provide for an adequate sample evaluation.

The reduced data from firing the "slit" cartridge cases are plotted in Figure 66 with cartridge case weight loss as a function of peak chamber pressure. Also shown for comparative purposes on this same graph is the curve for the 0.0135 inch diameter hole from the drilled hole experiment discussed in Section 6.2. Evaluation of Figure 66 evidences that for any peak chamber pressure, the damage (cartridge case weight loss) is greater when "burn-through" is simulated by slitting the cartridge case than when small holes are drilled in the head region. This is particularly true at the higher pressures where the curve for the erosion of the "slit" cartridge case is significantly greater than that of the "drilled" case. It is possible to account for the apparent increased erosion with slit cartridge cases by considering: (1) upon firing, the scratch is opened thereby presenting a fresh aluminum surface devoid of its protective oxide coating (a more detailed discussion of this fact is presented in Section 6.6); (2) upon slitting, the scratch may have many rough edges or sharp corners where heat transfer occurs at excessive rates (See Reference 5); and (3) the gas path presented by the scratch is appreciably larger (in cross sectional area) than the induced hole.

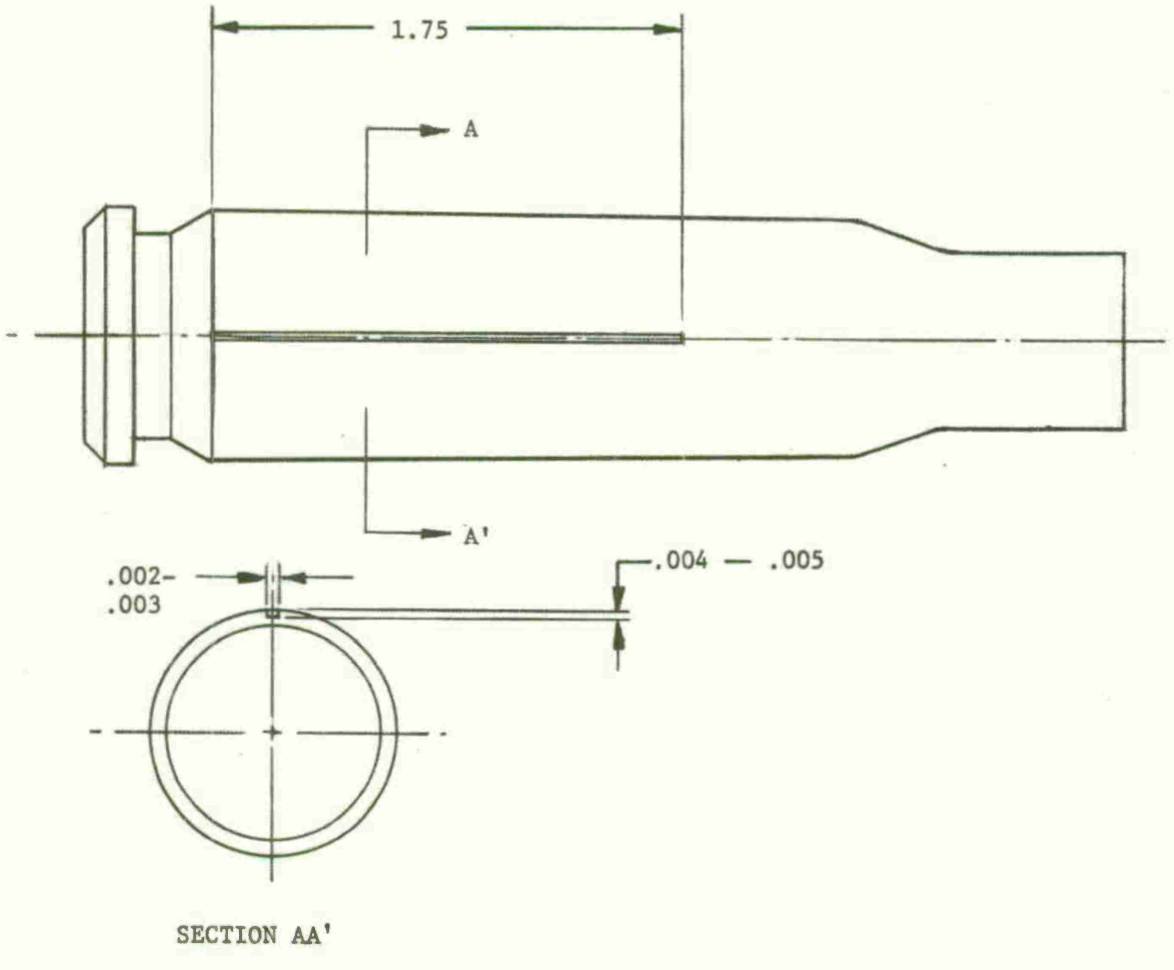

Figure 65. Sketch Showing Location of Standard Slit in 5.56mm Aluminum Cartridge Case (Note that the slit initiates at extractor groove)

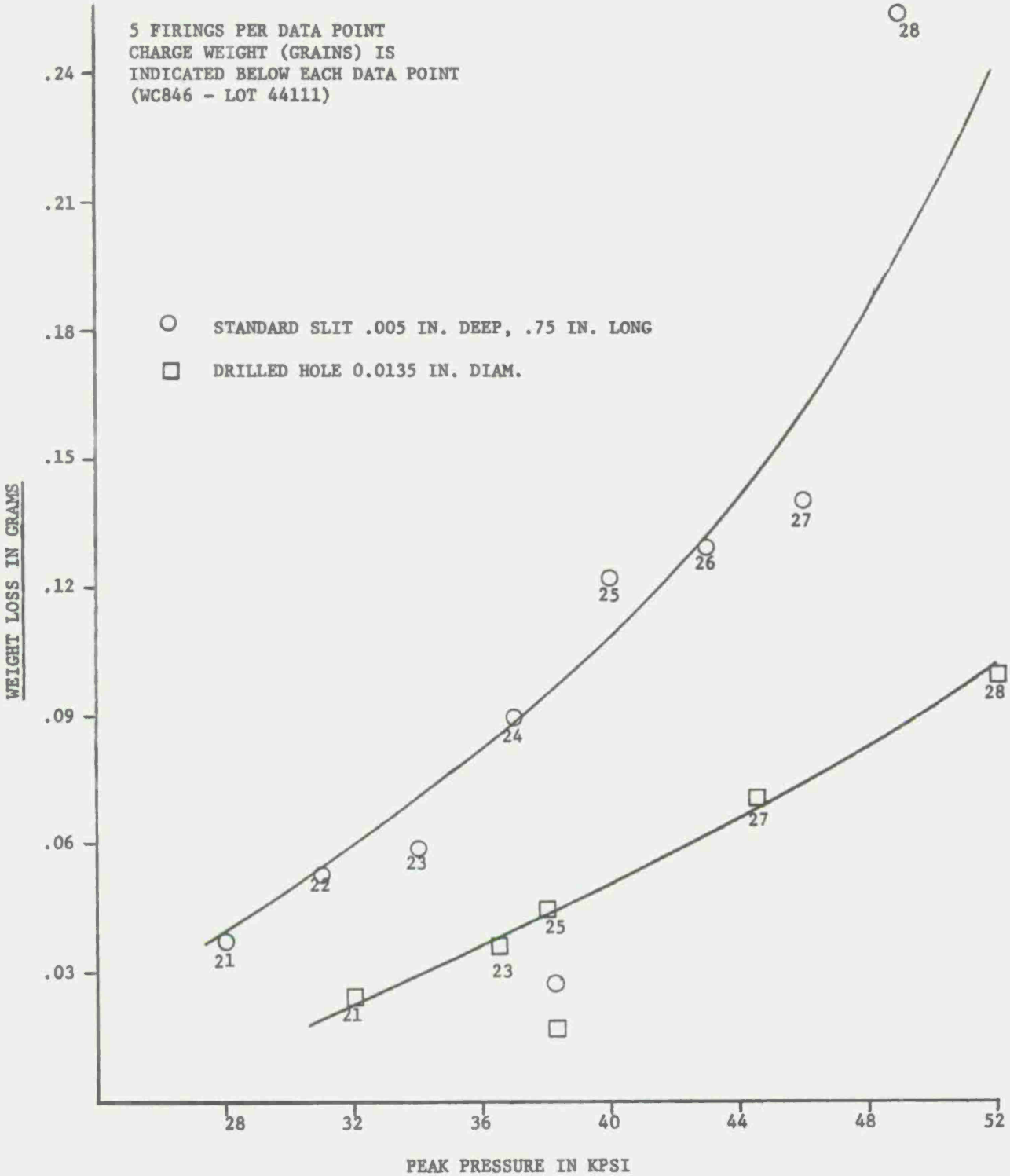

Figure 66. Cartridge Case Weight Loss VS Peak Chamber Pressure for Standard Slit and Drilled Hole Experiments.

A photograph showing the damage to three groups of slit cartridge cases is presented in Figure 67. Each cartridge case in the group was loaded with the charge of ball propellant indicated below the family of fired cases. It is obvious that as the propellant charge is increased, thereby increasing the peak chamber pressure, the degree of erosion is also increased. Comparing the damage of the cartridge cases shown in Figure 67 (scratched prior to firing) and the damage inflicted on the cartridge case shown in Figure 1 (a natural failure), it is apparent that scratching the exterior surface of a cartridge case produces a good approximation of "burn-through".

However, since it is impossible to know with any degree of accuracy the size (effective diameter) of the orifice once the slit produces a path for the propellant gases or the condition of the cracked surface, the analytical modeling of "burn-through" resulting from slitting the case initially is very difficult.

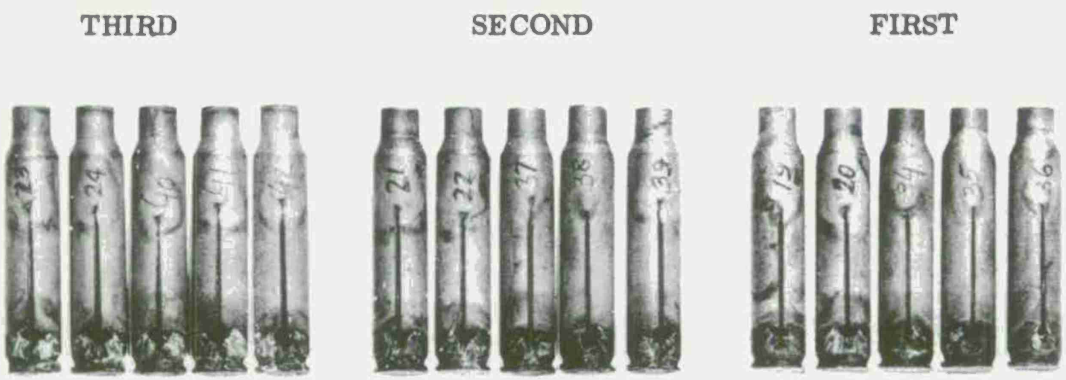

WC846 PROPELLANT

Figure 67. Slit Cartridge Cases after Firing (Propellant charge is as indicated.)

SECTION 6.4. HEAT FLUX FROM LOCALIZED EXOTHERMIC CHEMISTRY

This section addresses the determination of the additional energy flux resulting from an exothermic reaction at the surface of an aluminum specimen. High speed motion pictures taken at the surface of an aluminum cartridge case during "burn-through" show evidence of a localized exothermic reaction. A number of theories (mathematical models, see References 5 and 14) have been developed to account for the degradation of an aluminum cartridge case given propellant gas flow through an orifice. All models constructed to date have been either on a pure thermal approach (convective heat transfer and then conduction within the solid) or on a mechanical erosion process coupled with the thermal approach. These theories admit to the presence of the exothermic reaction, and hence to the role of chemistry in the failure of an aluminum cartridge case. However, the implementation of the theories with the effect of the exothermic reaction has been hindered by the lack of information concerning the magnitude of the exothermic reaction.

It would be ideal to put a sensor in the vicinity of this localized exothermic reaction and record the total amount of thermal energy conveyed to it. The energy flux, of course, would be the scalar sum of that energy resulting from the propellant gas flow and that given off by the exothermic reaction. Unfortunately, the state-of-the-art of instrumentation science precludes using a sensor under "burn-through" conditions to measure exclusively the amount of energy transferred to it.

However, there are sufficient data available to allow a determination of the energy liberation by this reaction. As discussed in Section 6.0, one experiment performed with the "high pressure" erosion test fixture involved passing propellant gases through brass (70-30) and aluminum (alloy 7475) test specimens which were held adjacent to each other so that the induced holes were aligned and thus presented an uninterrupted path for the gases. The thickness of each specimen was adjusted so that the total thickness of the combination was approximately that of the single disc. This is necessary so that comparisons can be drawn between the erosion of the double disc arrangement and the erosion of a single disc. Of course, it is understood that the other parameters affecting erosion were held constant during each experiment.

As previously mentioned, an interesting observation of the double disc experiment is the fact that the amount of erosion is highly sensitive to the relative orientation of the two discs. To explain further, if the propellant gases pass first through the aluminum disc and then through the brass disc (Figure 68, Case I), the amount of erosion, indicated by the increase in hole size, is much greater than if the propellant gases first pass through the brass disc and then through the aluminum disc (Figure 68, Case II).

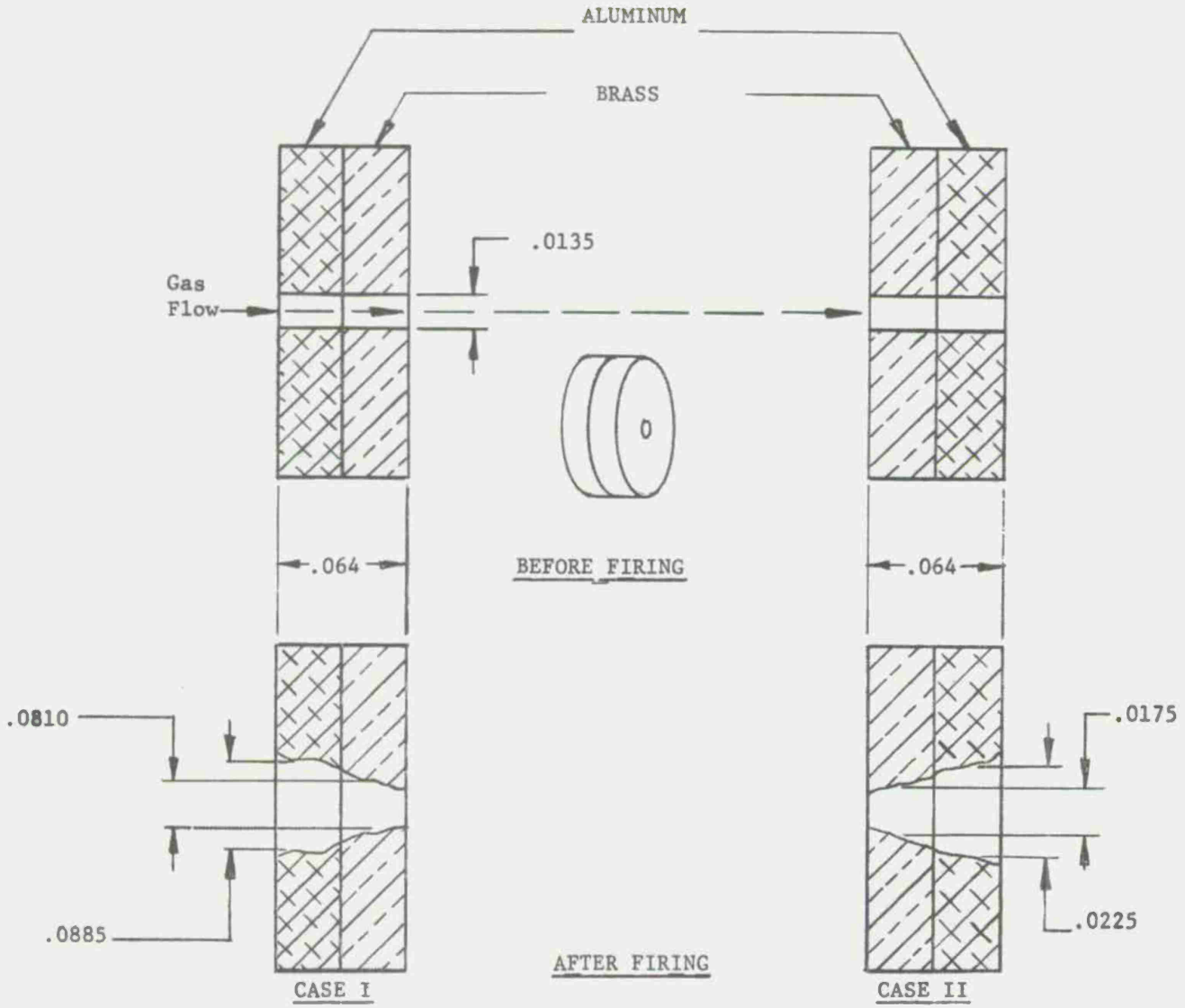

N.B. TEST SPECIMENS IDENTIFIED AS "AFTER FIRING" ARE NOT DRAWN TO SCALE

Figure 68. Cases of Double Disc Experiment: Case I, Aluminum Inside and Brass Outside; Case II Brass Inside and Aluminum Outside

To account for this anomalous behavior, the following hypothesis has been constructed. If the aluminum disc first witnesses flow of propellant gas (Case I), the localized exothermic reaction is exposed to the brass specimen. The final result is that the brass specimen is exposed to much more heat flux than would be expected if the aluminum specimen were not present. If, on the other hand, the propellant gas first passes through the brass specimen and then the aluminum (Case II), the exothermic reaction associated with the aluminum is carried (by) the first moving propellant gas stream) to the atmosphere. There is no material on which the exothermic reaction can act. The additional energy, supplied to the test specimen when the experiment is performed in a manner described by Case I of Figure 68, is the subject of this section.

To begin, it is possible to view the brass specimen in Case I as a calorimeter and calculate the amount of heat transferred to it by the exothermic reaction and propellant gas flow. That is, the amount of energy which causes erosion (metal removal) is calculated by considering the amount of energy required to raise the removed metal to the melting point and an additional amount required to achieve melting (latent heat of fusion). The brass specimen in Case II is investigated in the same way except that its erosion is NOT influenced by a heat flux from the exothermic reaction.

It must be remembered, however, that the heat flux not only produces the erosion but also raises the temperature of the entire specimen to some value above ambient. Therefore, there is a residual amount of heat left in the specimen which does not cause melting. In order to obtain the total heat flux to the brass specimen under examination, an instantaneous temperature as a function of time and position is required. These data are not available since the specimen was not instrumented to obtain the necessary temperature profile.

It can be argued that the residual energy left in the specimen is approximately the same for both cases of the experiment. During the course of the erosion process, the unmelted (solid) portion of the specimen is separated from the source of thermal energy, the gas stream and reaction zone, by a melted region. This melted region, prior to its removal, presents a constant heat flux to the solid portion. Ozisik[16] gives the temperature distribution in a region exterior to a cylindrical hole, extending to infinity, and subject to a constant heat flux. From his analysis it is possible to identify a phenomenological distance $\varepsilon(t)$, called the thermal layer, representing the distance beyond which the initial temperature distribution remains unaffected by the imposed

[16]Ozisik, M.N., Boundary Value Problems of Heat Conduction, International Textbook Company, Scranton, Pa. 1968.

boundary condition. The results of the analysis show that the thickness of the thermal layer is given by

$$\varepsilon(t) = \sqrt{6Kt} \qquad (1)$$

which, when the appropriate values for brass are substituted becomes,

$$\varepsilon(t) = 0.18 \times 10^{-3} \qquad (2)$$

The time used in this equation is 2.0 milliseconds, a representative time for gas flow. Since this distance is small compared to the overall dimensions of the specimen (diameter) it is concluded that the outer portions (periphery) of the test disc cannot differentiate between the net heat flux resulting from propellant gas flow and exothermic reaction or from exclusively propellant gas flow.

The quantity of heat required to remove metal in either Case I or Case II is given by

$$Q_{\text{removed case}} = M_{\text{removed case i}}\, C_p\, \Delta T + M_{\text{removed case i}}\, H_f \qquad (3)$$

where

$Q_{\text{removed case i}}$ is the quantity of heat required to remove metal in either experiment,

$M_{\text{removed case i}}$ is the amount of metal removed in either experiment,

C_p is the specific heat.

ΔT is the difference between the liquidus temperature and ambient,

H_f is the latent heat of fusion.

Continuing, the amount of metal removed in either Case I or Case II will be

$$M_{\text{removed case i}} = \text{density} \times \text{volume}$$

It is therefore necessary to determine the volume of the metal removed. Consider Figure 69, which depicts the outcome of the experiment. The volume will be

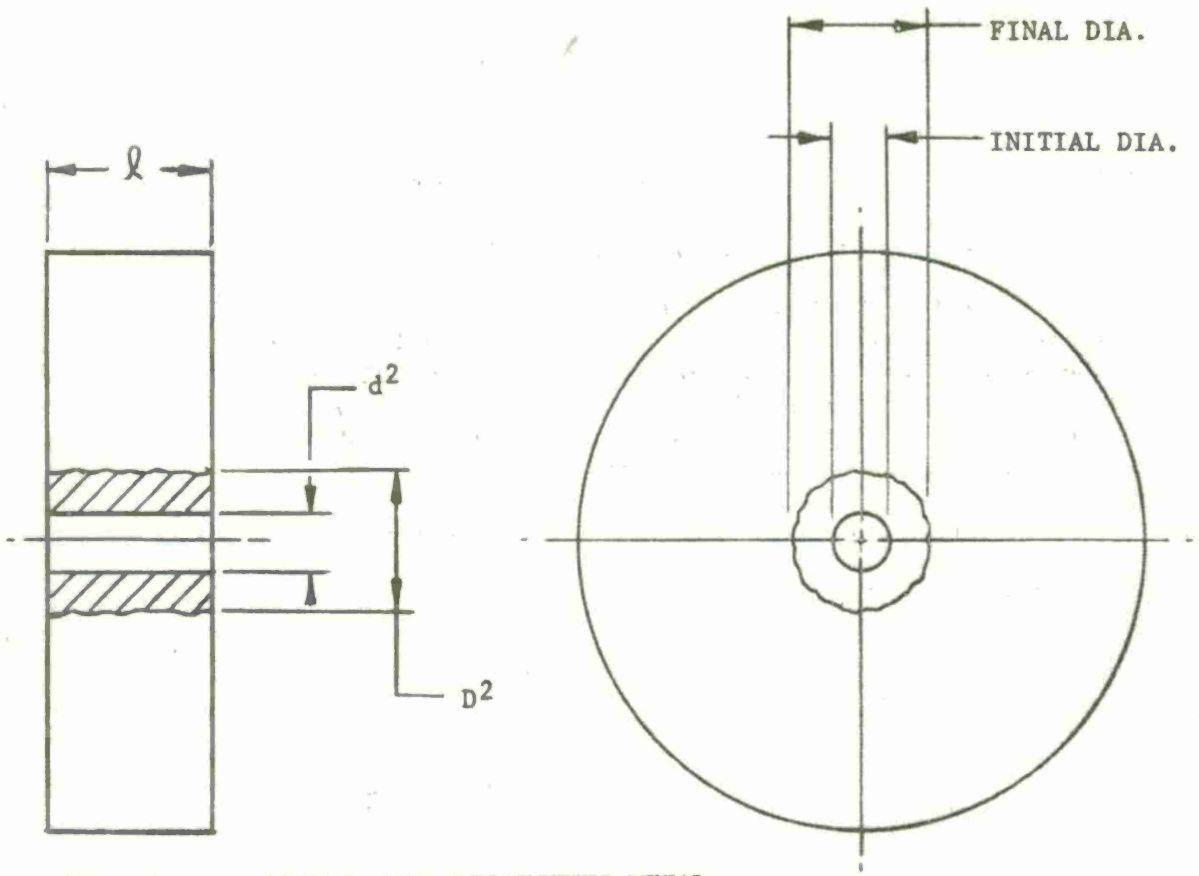

(BRASS) SHADED AREA REPRESENTS METAL WHICH IS REMOVED BY EROSION.

$$VOL = .7854\,\ell\,(D^2 - d^2)$$

Figure 69. Idealized Erosion of Brass Specimen.

$$\text{Volume} = \pi r_2^2 l - \pi r_2^2 l$$

$$\text{Volume} = \pi l \left(r_2^2 - r_1^2 \right)$$

Hence, the amount of metal removed in either experiment will be

$$M_{\text{removed case i}} = \rho \pi l \left(r_2^2 - r_1^2 \right) \tag{4}$$

Substitution of equation (4) into equation (3) yields

$$Q_{\text{removed case i}} = \rho \pi l \left(r_2^2 - r_1^2 \right) C_p \Delta T + \rho \pi l \left(r_2^2 - r_1^2 \right) Hf$$

$$Q_{\text{removed case i}} = \rho \pi l \left(r_2^2 - r_1^2 \right) C_p \Delta T + H_f \tag{5}$$

The properties of 70-30 brass needed to evaluate equation (5) are:

$$\rho = 532.52^{\text{lb}}\ \text{m/ft}^3,\ C_p = 0.092^{\text{BTU/lb}_m\ {}^{\circ}\text{F}},\ \Delta T = T_{\text{liquidus}} - T_{\text{ambient}} = 1680^{\circ}\ \text{F};\ \text{and}\ H_f = 80^{\text{BTU/lb}_m}.$$

From Table II the values necessary to evaluate equation (5) for Case I are $l = 0.032$ inch, $r_1 = 0.00675$ inch and $r_2 = 0.0405$ inch; likewise, for Case II $l = 0.032$ inch, $r_1 = 0.0675$ inch, and $r_2 = 0.00875$ inch. Substituting these values into equation (5), the following values required to cause the observed metal removal are obtained:

$$Q_{\text{Case I}} = 1.158 \times 10^{-2}\ \text{BTU}$$

$$Q_{\text{Case II}} = 2.249 \times 10^{-4}\ \text{BTU}$$

$Q_{\text{Case I}}$ and $Q_{\text{Case II}}$ represent the amount of heat required to remove metal in the respective cases of the experiment. These values do not represent the total amount of heat transferred to the specimen as the residual heat has been discounted. It is difficult to interpret the significance of the heat required to remove the metal in either case of the experiment by examining the magnitude of each value independently. However, considerable insight can be gained by investigating the ratio of $Q_{\text{Case I}} / Q_{\text{Case II}}$. The value obtained from such a procedure can be viewed as that quantity of energy which is transferred to the brass specimen from the exothermic reaction. Therefore,

$$\frac{Q_{\text{Case I}}}{Q_{\text{Case II}}} = \frac{1.158 \times 10^{-2}}{2.249 \times 10^{-4}} = 51.48 \quad .$$

The conclusion is then drawn that, assuming the erosion is the result of a pure heating and melting effect, from gas flow and exothermic chemistry, a factor of 51.48 more energy is transferred to the brass specimen during the exothermic reaction.

A sloughing theory has been postulated which also accounts for the erosion of a brass or aluminum specimen. It differs from the melting theory in that it considers a decrease in yield strength of the material with increase in temperature. Instead of the removal of metal being governed by equation (5), a critical temperature is identified. Once the local temperature in the specimen realizes this temperature it is automatically removed. The critical temperature is lower than the melting temperature and thus there is no need to consider the additional

heat of fusion term. Assuming that the critical temperature will be the same regardless of whether the experiment is performed according to Case I or Case II, equation (5) is rewritten as:

$$Q_{\text{removed case i}} = m_{\text{removed case i}}\ A\ C_p\ \Delta\ T$$

where, as previously defined,

$M_{\text{removed case i}}$ is the total amount (weight) of metal removed in either experiment.

C_p is the specific heat, and

$\Delta\ T$ is the temperature difference.

However, under the sloughing theory,

$\Delta\ T = Tc - T_{\text{ambient}}$ where

Tc =the critical temperature for metal removal

T_{ambient} =the initial temperature of the specimen.

To be more specific;

$$Q_{\text{Case I}} = M_{\text{removed Case I}}\ Cp \left(Tc - T_{\text{ambient}} \right) \qquad (6)$$

and

$$Q_{\text{Case II}} = M_{\text{removed Case II}}\ Cp \left(Tc - T_{\text{ambient}} \right) \qquad (7)$$

Without substituting any values for the parameters in equations (6) and (7), the ratio Q Case I/ Q Case II is constructed as it was for the pure melting concept.

$$\frac{Q_{\text{Case I}}}{Q_{\text{Case II}}} = \frac{M_{\text{removed I}}\ Cp \left(T_c - T_{\text{ambient}} \right)}{M_{\text{removed II}}\ Cp \left(T_c - T_{\text{ambient}} \right)} = \frac{M_{\text{removed Case I}}}{M_{\text{removed Case II}}}$$

It is obvious that the ratio of energy required to cause metal removal (in either case of the experiment), is merely the ratio of metal removed under each case of the experiment. The same result applies to the pure melting theory. With the assumptions that Case I and Case II do not differ as far as the flow dynamics are concerned and that the residual heat in the specimen is approximately the same, a factor of 51.48 times more energy is incident to the brass specimen as a result of the exothermic reaction.

The data to be used in this analysis are shown in Figure 50 and summarized in Table II.

Table II. Summarized Data from Double Disc Experiment

Material	Aluminum	Brass	Brass	Aluminum
Orientation*	Inside	Outside	Inside	Outside
Peak Pressure (kpsi)	35	35	35	35
Thickness (in)	0.032	0.032	0.032	0.032
Initial Diameter (in)	0.0135	0.0135	0.0135	0.0135
Final Diameter (in)	0.0885	0.0810	0.0175	0.0225
Increase in Diameter (in)	0.0750	0.0675	0.0040	0.0090

*Inside: Identifies the specimen closer to the combustor
Outside: Identifies the specimen closer to the atmosphere

Only the increase in diameter of the brass specimen when laminated with aluminum is analyzed since photographic observations show that no exothermic reactions result when propellant gases flow through a hole in a brass test specimen. (See Figures 18 and 26).

Researchers at Princeton University[14] have been able to predict successfully the amount of erosion witnessed by the brass specimen on the basis of a pure melting theory. Hence, the mathematics which follow are based on the assumption that the erosion of a brass specimen is due to a pure heating and melting effect. Later, this assumption will be relaxed.

[14] Plett, E.G., and Summerfield, M., "Erosive Effects of Combustion Gases on Metalic Combustion Chambers", Final Report on Contract DAAA 25-71-C-0109, Department of Aerospace and Mechanical Sciences, Princeton University, August 1971.

SECTION 6.5 POST-MORTEM EXAMINATION

A number of 5.56mm aluminum alloy cartridge cases, which had undergone "burn-through", and a number of aluminum test specimens, which were studied in the erosion test fixture, were forwarded to the Metallurgical Research Division of the Reynolds Metals Company (RMC). A post-mortem metallurgical examination was conducted on the aluminum cartridge cases and test specimens. In addition to this study, the Physical Metallurgy Division of the Aluminum Company of America (ALCOA) examined a 7.62mm aluminum alloy cartridge case (alloy 7475) which failed during burst fire in the 7.62mm minigun and resulted in "burn-through". Since this failure also caused damage to one of the bolt faces and an extractor, these components were also sent to ALCOA for metallurgical examination. Although the results of both of these studies have been informally documented,[17,18] some consideration of these examinations are given here since the results bear heavily on understanding the aluminum cartridge case "burn-through" phenomenon.

Figure 70 (a) shows a 4X magnification of one of the 5.56mm cartridge cases evidencing two distinct regions of erosion. The large, circular region at the top of the photomacrograph is a pressure hole; the cartridge case did not obturate around the metering hole as there is evidence of gas flow over the exterior surface toward the rear of the case. The second region of interest is the area of erosion resulting from gas flow through the induced orifice at the head of the cartridge case. As the interior ballistic cycle developed, the hot propellant gases flowed through the pressure-metering hole and the induced orifice causing melting and subsequent ablation of the melted zone. In areas not directly exposed to the flow of hot gases, a residual layer of crystalline-appearing material is observed. Similar layers of crystalline material are also observed to coat the damaged areas near the base of the case. Figure 70 (b) and (c) shows the location of this layer. RMC's report notes that the surface of the damaged area appears to have been molten near the orifice and becomes transformed to cleanly eroded pathways as one proceeds in the direction of gas flow. RMC generalize that there was little apparent damage at the interior origin of the hole, but considerable ablation and erosion on the exterior surface of the case. The same generalization accounts for the damage on the erosion test specimen.

---

[17] Barkman, E.F., "Letter to Mr. Henry George", 7 January 1971, Reynolds Metal Company, Richmond, Va.

[18] Rogers, R.W., "Letter to Mr. Marvin Rosenbaum", 7 December 1970, Aluminum Company of America, New Kensington, Pa.

a. Magnified 4X

b. Magnified 4X

c. Magnified 12X

Figure 70. Photomacrographs of "Burn-Through" Areas in 5.56mm Aluminum Cartridge Cases

Microscopic examination of the metallographically prepared cross-section revealed a layer of gross melting in backwash areas and in areas apparently not directly exposed to the flow of hot gases. The melted zones were characterized by a change in microstructure from a wrought to a cast-appearing structure. In addition to the layer of gross melting observed in "burn-through" areas, a small degree of incipient solid solution and eutectic melting was observed immediately adjacent to the "burn-through" surface. This was illustrated by the presence of rosettes and grain boundary melting. The layers of crystalline-appearing material observed on the "burn-through" surfaces appeared to vary widely in structure and composition. Figure 71 (a) and (b) are photomicrographs -- magnification 100X and 250X respectively -- taken of the "burn-through" region in a 5.56mm aluminum cartridge case. Note that Figure 71 (a) clearly shows the existence of a melted layer sandwiched between the crystalline layer and the matrix aluminum. Figure 72 is another photomicrograph taken at 250X magnification of an aluminum specimen used in the erosion test fixture. Again, the region of gross melting is found between an external layer of non-metallic compounds and the solid aluminum matrix. Also observable in this photograph is the intergranular crack extending through the region of gross surface melting into the matrix.

As previously stated, the molten layer observed in "burn-through" areas appears to consist of numerous phases. In order to identify the various phases, Electron Microprobe X-ray analyses were run on two selected areas. The nonmetallic region (identified by the arrows) in Figure 73 (shown previously as Figure 71 (b)) and the melted zone shown in Figure 74 were both examined by Electron Microprobe X-ray Analysis. From this analysis, it was apparent that the areas consist of mixtures of metallic aluminum, oxides, and carbon-bearing compounds of the elements present. These layers, in general, are characterized by areas high in aluminum, iron, magnesium, calcium, oxygen, zinc and carbon. In addition to the probe analysis of the grossly melted area, an area illustrating what appears to be aluminum melted structure was analyzed. Microscopic examination and electron probe analysis of this area revealed that it consists of a layer rich in solute alloying elements, typical for this alloy, along with finely dispersed oxides.

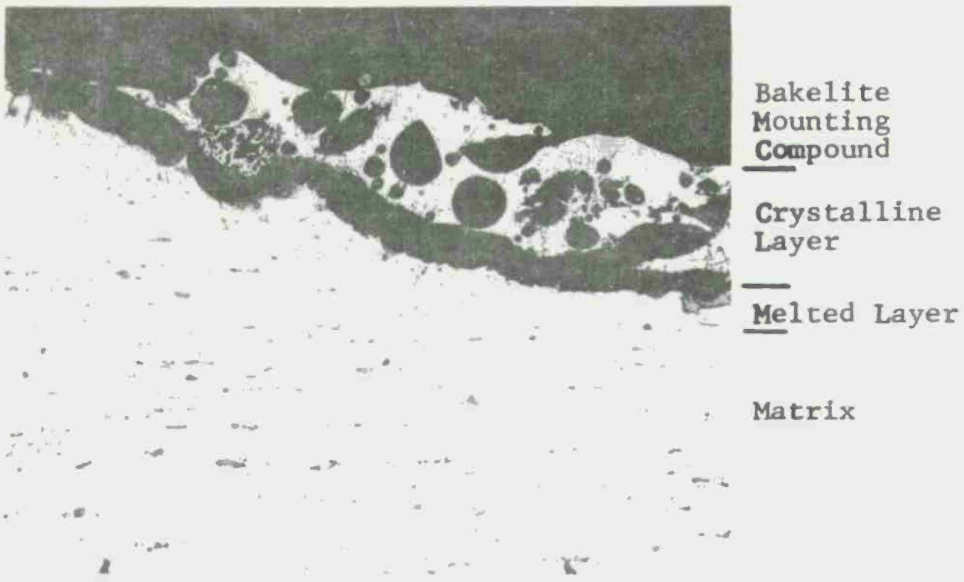

a. Magnified 100X

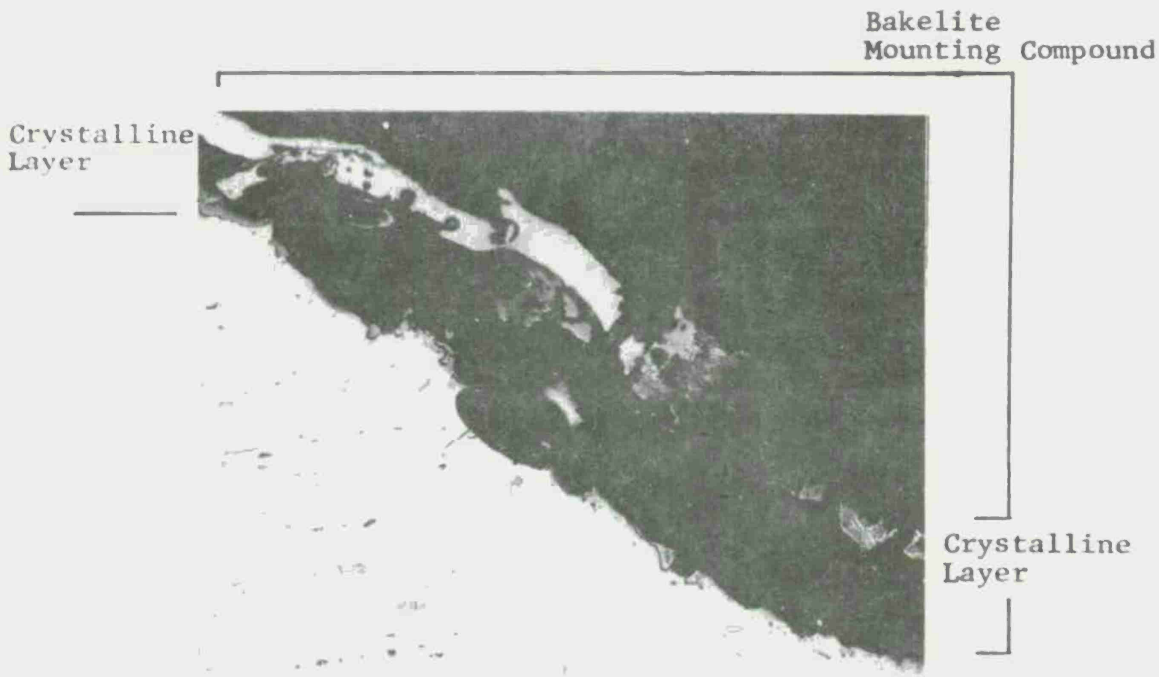

b. Magnified 250X

Figure 71. Photomicrographs of Cross Sections of "Burn-Through" Regions in 5.56mm Aluminum Cartridge Cases

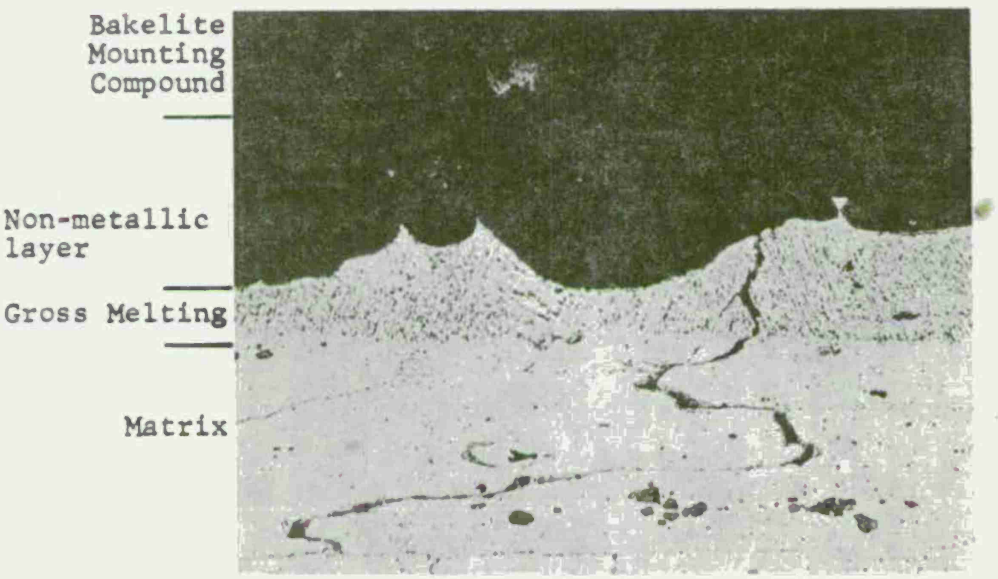

b. Magnified 250X

Figure 72. Photomicrograph of "Burn-Through" Region of Aluminum Specimen Fired in Erosion Test Fixture

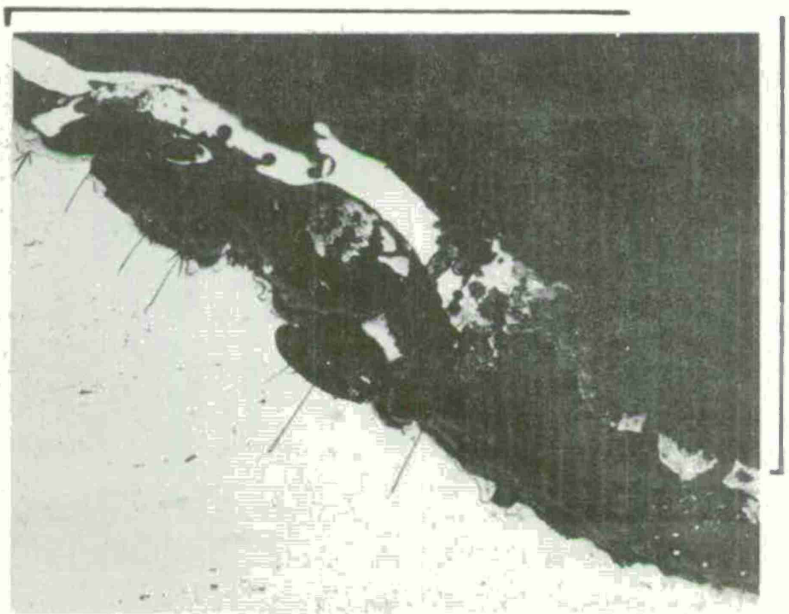

Magnified 250X

Figure 73. Photomicrograph Identifying Region of Fired Cartridge Case Investigated by Electron Microprobe X-ray Analysis

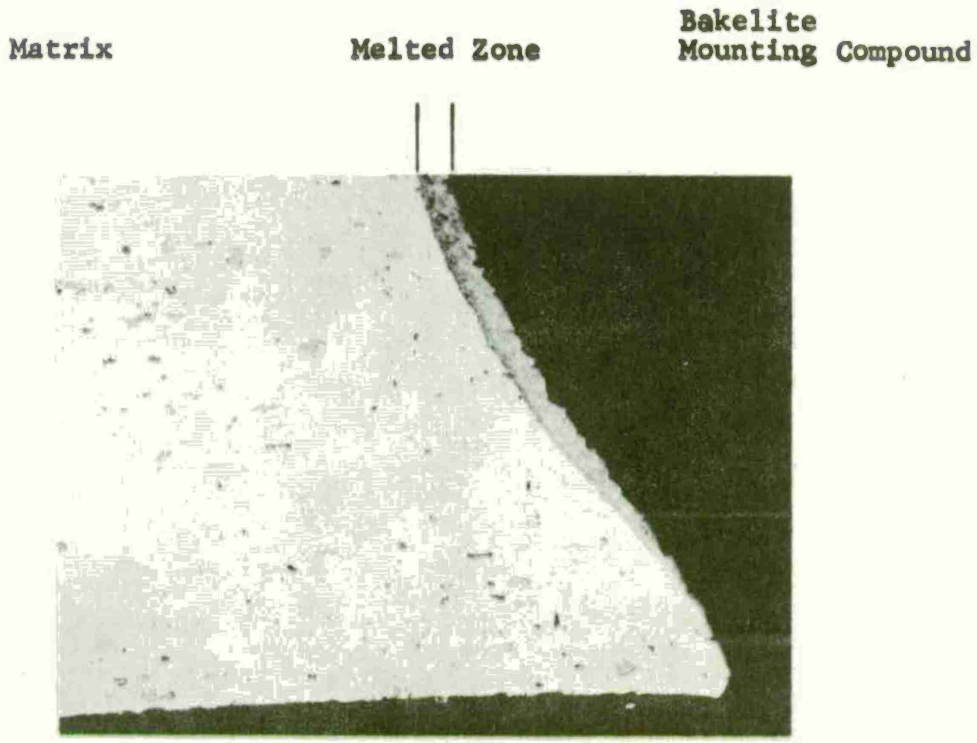

Figure 74. Photomicrograph Identifying Region of Test Disc Investigated by Electron Microprobe X-ray Analysis

SECTION 6.6 ALUMINUM SURFACE DURING LOCALIZED EXOTHERMIC CHEMISTRY

The localized primary reaction has been shown to be instrumented in producing the observed damage (metal removal) sustained by an aluminum cartridge case or test disk as the result of "burn-through". The physics and chemistry of the aluminum surface during the localized primary zone -- first reported in the high speed motion picture study discussed in Section 5.1 and shown isolated in Figure 22 of Section 5.2 -- will now be discussed.

It is well known that aluminum chemically is a very active metal. In fact, aluminum is ranked immediately behind magnesium in the activity series and will liberate hydrogen from steam. Although the literature is rich in work devoted to the ignition and combustion of aluminum, it is not immediately apparent that the available information is able to describe or account for the localized primary reaction zone which occurs during "burn-through" in 5.56mm aluminum cartridge cases. One reason for our caution is the physical nature of the metal which is involved in the "burn-through" process. "Burn-through" involves the bulk or solid aluminum in the head of an aluminum cartridge case. Previous work on the ignition and combustion of aluminum has studied aluminum powder[19 thru 23], or aluminum wire[24,25].

There has been some work by A.V. Grosse and J.B. Conway of the Research Institute, Temple University, Philadelphia, Pa. on the

---

[19] Friedman, R. and Maucek, A., Ninth Symposium (International) on Combustion, pp. 703-712 Academic Press, New York, 1963.

[20] Fassell, W.M., Jr., Papp, C.A., Hilldenbrand, D.L., and Sernka, R.P. Solid Propellant Rocket Research, M. Summerfield, ed., pp. 259-269, Academic Press, New York, 1960.

[21] Davis, A. Combustion and Flame, 7, pp. 359-367, 1963.

[22] Drew, C.M., Gordon, A.S., and Knipe, R.H., Heterogeneous Combustion, Wolfhard, H.G., Glassman, I., and Green, L., Jr. eds., pp. 17-39, Academic Press, New York, 1964.

[23] Prentice, J.L., Drew, C.M., and Christensen, H.C., Pyrodynamics, 3, pp. 81-90, 1965.

[24] Brzustowski, T.A., Vapor-Phase Diffusion Flames in the Combustion of Magnesium and Aluminum, Ph.D. Thesis, Princeton University, Dept. of Aeronautical Engineering, 1963.

[25] Kirschfeld, L., Metal, 15, pp. 873-878, 1961.

ignition and combustion of bulk aluminum[26,27]. Much of the prior ignition and combustion studies of aluminum were devoted to aluminum powder because of its use as an additive in rocket engines and other ballistic systems to increase thrust, stability, mass impetus, and overall system performance. To extrapolate these data, taken of aluminum powder, approximate size 50 to 300 microns, at relatively low pressures (500 to 5,000 psi) for application to an aluminum cartridge case is unjustifiable.

Most experimenters in the field of aluminum combustion believe that a particle's history, its surface condition, the presence or absence of specific impurities, oxidizer species and concentrations, other constituents in the reacting atmosphere, pressure of the reacting atmosphere, the geometry and size of the metal, the nature and rate of heating, and thermal and fluid dynamic environment -- all play a role in establishing the observed "ignition temperature", combustion mode, and reaction rate in any experimental situation[28]. Because of this complex nature of metal combustion, it is felt that investigations using aluminum wire (such as those performed at Princeton University during the direction of Dr. I. Glassman) would lead to a more fundamental understanding of the basic processes. Studying metal combustion by means of burning wires allows a stabilization of the reaction in time and space. In wire studies localized preignition phenomena can be observed over a range of temperatures at sufficiently low reaction rates to enable a better and slower observation of the mechanisms and kinetics. Another advantage of burning wire studies is that reactions can be quenched prior to ignition for detailed study of partially reacted specimens. Droplet and fragment formation on the burning specimen can be continuously observed. Finally, precise measurement of the wire temperature, up to and including ignition, can be determined as a function of time. Ignition and combustion can be influenced by heating rate, gaseous concentrations, pressures, surface conditions, and the nature of the metal itself.

The foregoing narrative more or less substantiates the advantages of studying burning wires as opposed to small particles for understanding metal combustion. The important question is now raised

---

[26] Grosse, A.V., and Conway, J.B., Industrial Engineering Chemistry, 50,pp. 663-672, 1958.

[27] Conway, J.B., and Grosse, A.V., Temple University Research Institute Final Technical Report on Contract N9-ONR-87301, July 1954.

[28] Kuehl, D.K., AIAA Journal, 3, No. 12, pp. 2239-2247, 1965.

concerning whether or not any understandings gained from powder or wire combustion are applicable to the aluminum cartridge case "burn-through" phenomenon. As the frequency of a natural "burn-through" is incredibly small, resulting from advances in super strength alloys and better processing techniques, it is necessary to simulate "burn-through" in aluminum cartridge cases to allow for systematic investigation. Therefore, most of this document is concerned with "induced" failures. Figure 55 shows the location of a small hole (sizes ranging from 0.0135 to 0.0625 inch in diameter have been investigated in this study) in the head region of an aluminum cartridge case. Drilling a hole at this location allows for the unrestricted flow of propellant gases -- generated during the interior ballistic cycle -- to exit the cartridge case. As the flow processes develop along the axis of the small bore, energy transport to the bore's sidewalls occurs by convective heating across a well-defined boundary layer. An analytical treatment of the flow and subsequent heating is given in Reference (5).

In a comparison between "burn-through" resulting from passage of propellant gases through a predrilled hole in an aluminum cartridge case and an electrically heated wire, major differences exist. The heatup of the bulk aluminum is transient as opposed to the well-defined, steady state heating of the wire specimen. As the flow ensues throughout the bore, the surface condition is constantly changing. It is difficult to determine experimentally the constituency of the propellant gas products. Although the flow throughout the bore has been assumed to be choked, it is impossible to measure directly the pressure in the core flow. These facts are mentioned only to show the significant differences between the ignition and combustion experienced by the aluminum in a cartridge case and that in a wire experiment.

The determination of the composition of the gaseous products given off from the combustion of a double base propellant, such as WC846, is a difficult and costly experiment. However, recent advances in chemical equilibrium and kinetics have led to the generation of a series of computer programs to predict combustion products. Stiefel and Hody[29] have modified one such program and report that the major combustion products of WC846 ball propellant are: CO (0.4419); H_2O (0.1968); H_2 (0.1531); N_2 (0.1078); and CO_2 (0.09861) (the values in the parenthesis represent the respective concentrations in mole fractions). It is possible to use atmospheres of these gases and

---

[5] Squire, W.H., and Donnard, R.E., "An Analysis of Local Temperature Profiles Encountered in the Aluminum Cartridge Case Drilled Hole Experiment", Technical Note TN 1163, Frankford Arsenal, Phila., Pa., August 1971.

[29] Stiefel, L., and Hody, G.L., "The Composition of the Exhaust Products of Military Weapons", Technical Report R-1948, Frankford Arsenal, Phila., Pa., March 1970.

investigate the ignition and combustion of various aluminum alloys in their presence.

One such experiment was performed by the Guggenheim Laboratories of Princeton University.[30] The apparatus used for their tests is shown schematically in Figure 75. It was originally used by Brzustowski to study the ignition and combustion of electrically heated aluminum and magnesium wires. A complete discussion of the device is given in Reference 24.

The material under consideration is inserted into the pressure chamber, equipped with viewing ports, and held in place between two electrodes. The pressure vessel is first evacuated and then filled to the desired pressure level with the test atmosphere. Ignition and combustion of the test specimen, aluminum wire 0.035 inch (diameter), is achieved through electrically heating the wire by means of a motor driven variac. The heating is continued until the wire breaks. Combustion should be self-sustaining after the wire breaks. Ohmic heating is an ideal method in such an experiment as it is possible to monitor very closely the applied voltage and current. A photograph of an aluminum wire burning in a pure oxygen atmosphere is shown in Figure 76. This photograph, supplied by the Guggenheim Laboratories, is taken at sub-atmospheric pressure to expand the flame zone, thereby allowing spectroscopic examination of that region.

During this investigation pure oxygen simulated a highly reactive gaseous atmosphere and argon represented an inert atmosphere. In addition to these gases, carbon dioxide, carbon monoxide, and nitrogen were also used as test atmospheres. These gases were thought to be representative of the propellant combustion products as reported by Stiefel and Hody[29].

Although the metallurgical structure of the aluminum alloys used to manufacture small arms cartridge cases is complicated, aluminum can be viewed as consisting of two regions. There is the bulk material whose physical and metallurgical properties are listed in Table III. There is also another important region in the structural make-up

---

[30] Plett, E.G., and Summerfield, M., "Second and Third Bimonthly Progress Reports for the Period December 1970-March 1971, Contract DAAA25-71-C0109", Princeton University, April 1971.

[24] Brzustowski, T.A., "Vapor-Phase Diffusion Flames in the Combustion of Magnesium and Aluminum", Ph.D. Thesis, Princeton University, Dept. of Aeronautical Engineering, 1963.

[29] Stiefel, L., and Hody, G.L., "The Composition of the Exhaust Products of Military Weapons", Technical Report R-1948, Frankford Arsenal, Phila., Pa., March 1970.

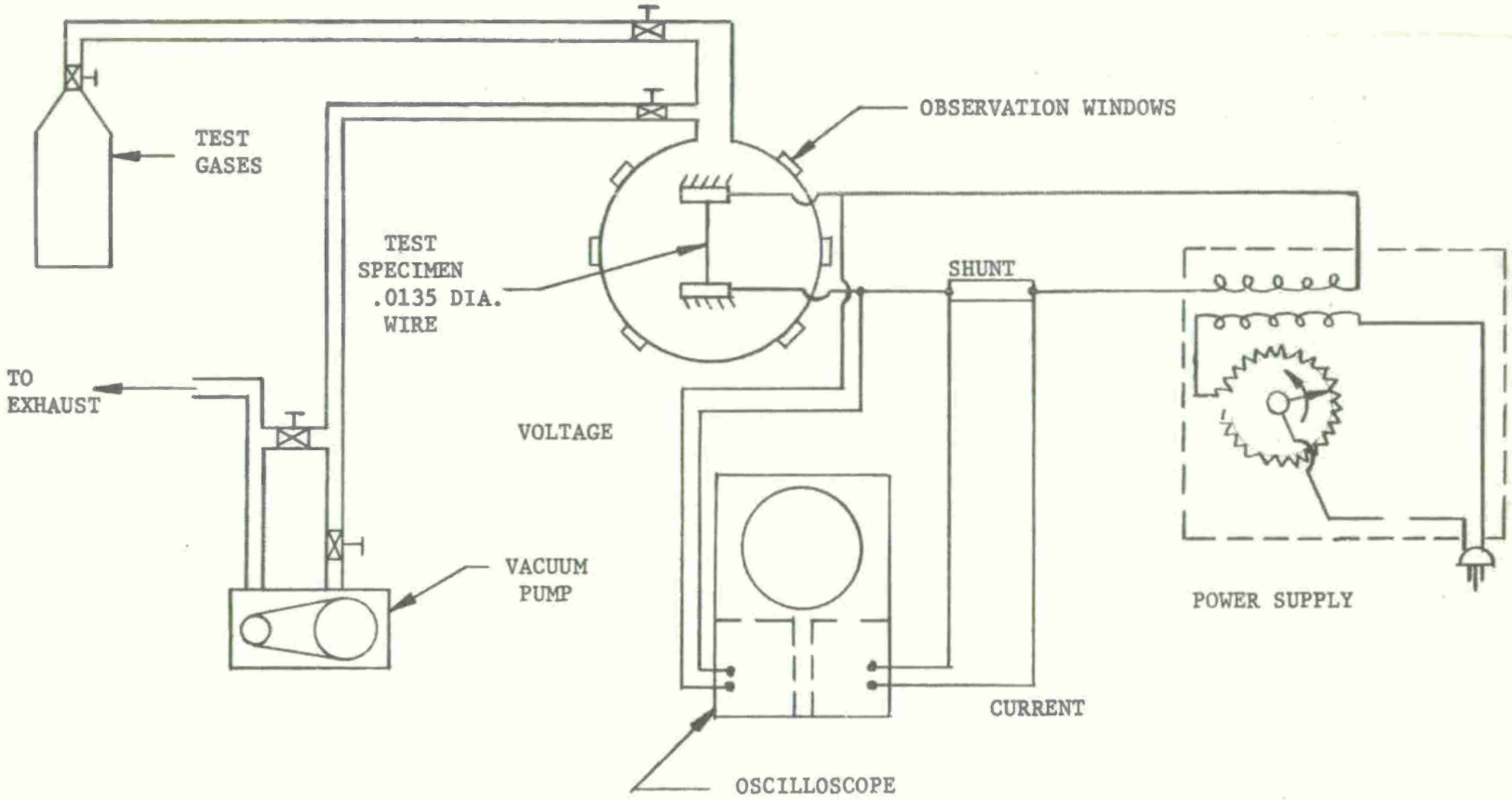

Figure 75. Schematic of Test Apparatus for Studies of Metal Reactivity in the Presence of Stagnant Test Gases.

Figure 76. Pure Aluminum Wire Electrically Heated and Burning in Test Apparatus of Figure 75

of aluminum. In the presence of air or any oxygen atmosphere, an oxide coating is quickly formed. Characteristically, this oxide coating is only a few microns thick and forms a protective type of coating. Its physical and metallurgical properties are drastically different from those of the bulk aluminum. One major difference between the oxide layer and bulk aluminum is the melting point. Christensen, et al.[31] report that the melting point of the oxide is approximately 3680°F, whereas the usually quoted value for the melting point of bulk aluminum (alloy 7075) is between 890 and 1180°F. Bulk aluminum is also known to have a finite reaction rate which builds up the oxide thickness at elevated temperatures in an oxidizing atmosphere. It is therefore reasonable to assume that in the stagnant atmosphere of the wire burning device, as the temperature of the specimen is increased, the thickness of this oxide shell is also increasing.

Table III. Properties of 70-30 Brass and 7075 Aluminum

Property	70-30 Brass	7075 Aluminum
Density (lb_m/ft^3)	532.52	174.80
Thermal Conductivity (BTU - ft/ft^2 hr °F)	70.00	70.15
Specific Heat (BTU/lb_m °F)	0.09	0.23
Thermal Diffusivity (ft^2/hr)	1.46	1.74
Solidus Temperature (°F)	1680	890
Liquidus Temperature (°F)	1750	1180

Kuehl[28] states "...it has been commonly supposed that metals forming protective oxides, including both aluminum and beryllium, will ignite only after the protective oxide becomes molten, or after the metal is broken in such a way as to expose an unprotected surface to a hot oxidizing atmosphere". This is also confirmed by Brzustowski[24]

---

[24] Brzustowski, T.A., "Vapor-Phase Diffusion Flames in the Combustion of Magnesium and Aluminum", Ph.D. Thesis, Princeton University, Dept. of Aeronautical Engineering, 1963.

[28] Kuehl, D.K., AIAA Journal, 3, No. 12, pp. 2239-2247, 1965.

[31] Christensen, H.C., Knipe, R.H., and Gordon, A.S., Pyrodynamics, 3, pp. 91-119, 1965.

who found that it was necessary to melt the aluminum oxide on the surface before the aluminum could react rapidly with the oxygen and burn. Both of these conclusions were drawn from studies performed in the stagnant oxidizing atmosphere of a wire bruning chamber.

It is difficult to conceive that the aluminum wire will remain intact until the oxide has melted at 2300°K when the bulk aluminum, which comprises most of the specimen, has a solidus temperature of 890°F. One would expect that when the wire temperature reached the solidus temperature of the bulk material, the wire would collapse. However, Brzustowski[24] has observed that as the temperature of the wire is raised, thereby accelerating the rate process, the specimen in an oxygen atmosphere will continue to oxidize. In fact, the thin oxide coating, which increases as the temperature is increased, will physically support the core of the specimen which had earlier melted. If the heating current was applied too rapidly in Brzustowski's experiment, the wire melted and ruptured before it was hot enough to ignite. Furthermore, Brzustowski found that reproducible ignition could only be obtained when the current was increased gradually. This permitted formation of a coating of oxide strong enough to contain the molten metal. Ignition occurred when the oxide coating failed in the middle portion of the wire.

A convenient representation of the data from this experiment performed at Princeton University is shown in Figure 77. After the initial resistance of the wire is obtained with an ohmmeter, it is easy to determine the resistance at any other time by dividing the applied voltage at any time by the instanteous current. Figure 77 is a plot of normalized wire resistance as a function of time abstracted from the Princeton University Progress Report[30].

In Figure 77, internal melting is evidenced by a sharp increase in wire resistivity as shown at 13.0 seconds. As previously mentioned five test gases were used in separate investigations. The resistance history of the wire in the presence of each test gas is very much the same at the point of internal melting (13.0 seconds). Once internal

---

[24] Brzustowski, T.A., "Vapor-Phase Diffusion Flames in the Combustion of Magnesium and Aluminum", Ph.D. Thesis, Princeton University, Dept. of Aeronautical Engineering, 1963.

[30] Plett, E.G., and Summerfield, M., "Second and Third Bimonthly Progress Reports for the Period December 1970-March 1971, Contract DAAA25-71-C0109", Princeton University, April 1971.

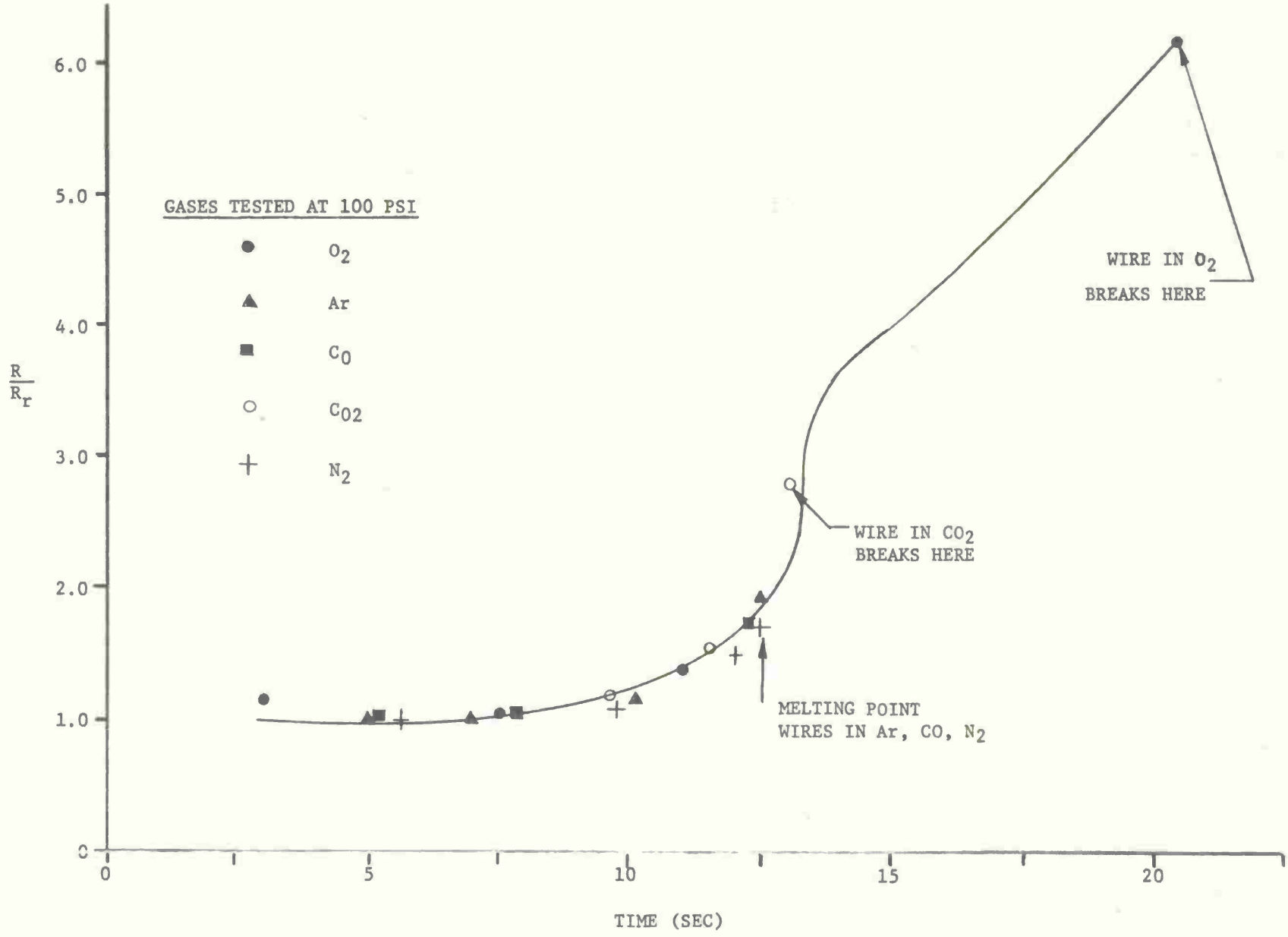

Figure 77. Normalized Resistance VS Time (Wires were in stagnant gaseous environment in test apparatus of Figure 75.)

melting of the wire specimen begins, the oxide coating must be strong enough to support the molten core to allow for additional thermal input. In the pure oxygen and carbon dioxide atmospheres, the oxide coating (possibly becuase of increased thicknesses) is strong enough to keep the wire intact beyond the early melting stage. The wires in argon, carbon monoxide, and nitrogen break as soon as internal melting occurs at a point in the wire, since no strong shell has formed on the surface (even though persumably there was no oxide coating on the specimen initially). The wire tested in the carbon dioxide atmosphere broke soon after a short length of wire melted internally. The wires in pure oxygen survived the internal melting stage; the interior molten core is probably realizing an increase in temperature to the point where the aluminum oxide coating breaks. Breakage of the aluminum oxide occurs simultaneously with a bright flash of bruning aluminum and a shower of glowing particles that are scattered throughout the chamber. Visually, one observes the wire beginning to glow at the point where internal melting begins. This glowing becomes brighter as the temperature rises and reaches its maximum and the wire breaks and produces the characteristic bright flash.

It is concluded from these observations of aluminum wires, electrically heated in a 100 psi atmosphere of various gases, and from inspection of the aluminum wires after the testing that: (1) argon does not react with aluminum; (2) carbon monoxide reacts too slowly to be of a consequence in the experiment time; (3) nitrogen shows no apparent reaction; (4) carbon monoxide is somewhat reactive, but this is also a slow reaction; and (5) pure oxygen is very reactive. However, it must be remembered that the test atmospheres are stagnant, not heated to ballistic temperatures, and at relatively low pressure. The wire burning exercise does demonstrate that for the aluminum wire to be ignited it must realize an amount of heat greater than that required to cause melting. This is evidenced by the requirement that the oxide coating supports the specimen until it melts. During the period between melting of the core and melting of the protective oxide coating, an appreciable amount of energy is transferred to the already molten aluminum.

Before any attempt is made to identify which constituent in the propellant combustion product is most instrumental in causing "burn-through", it is essential that the test gases be ballistically heated and pressurized to a level normally experienced in a small arms cartridge case. One possible way to ballistically heat and pressurize the test gases is to use a bomb similar to the device shown in Figure 78. This bomb, a modification of a currently working bomb, is reuseable and easy to load and disassemble. The teflon piston is driven forward by the pressure released from combustion of a propellant charge in the

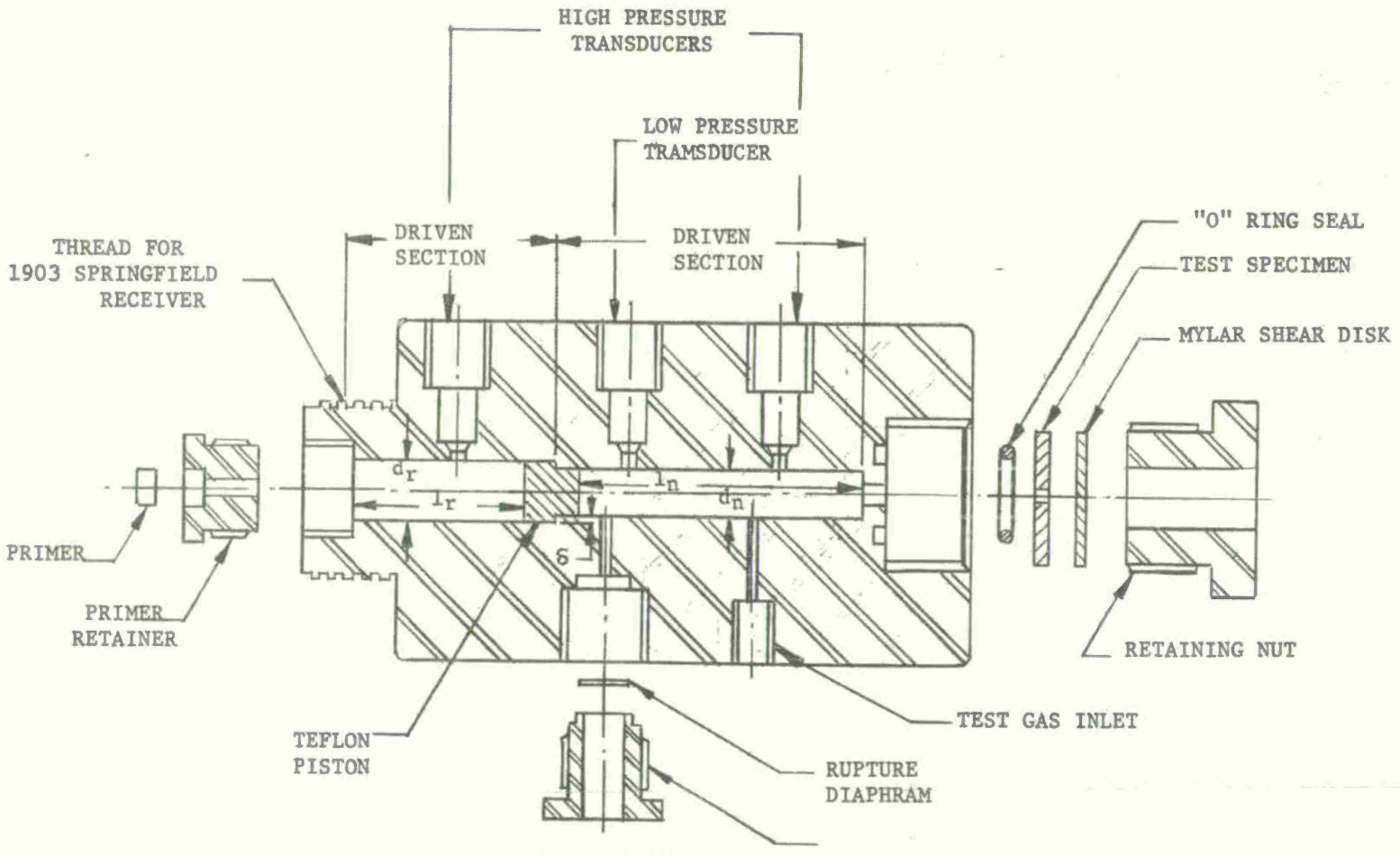

Figure 78. Device to Investigate Relationship between "Burn-Through" and Selected Test Discs

"driver" section of the bomb. As the piston is accelerated toward the disc at the far end of the bomb, the test gas, inserted in the "driven" section, is compressed. With the proper design/selection of the correct length and diameter of the "driven" section, and initial pressure of the test gas, it should be possible to heat and pressurize the test gas to the desired levels.

The test disc is held in place with a retaining nut which is designed to allow observation of the external surface of the test specimen. The design of the retaining nut also serves in a functional capacity to permit depressurization of the "driven" section and removal of the piston. Pressure transducers record the propellant gas pressure in the "driven" section, initial pressure of the test gas, and the pressure obtained by compressing the test gas. The design of the piston and the step-like nature at the interface of the "driver" and "driven" sections affords good sealing properties and precludes contamination of the test gas by the propellant gases. As the pressure in the "driver" section is increased, the piston is deformed to conform with the diameter of the "driven" section. Such a piston, made of teflon or another deformable plastic, is inexpensive and easily replaced. Ignition of the "driver" section is obtained by a conventional small arms primer. The "driver" section is threaded to be accepted by a 1903 Springfield Receiver which is used to initiate the primer.

CHAPTER 7. WEAPON DAMAGE RESULTING FROM "BURN-THROUGH"

Once "burn-through" is initiated, the hot gaseous conglomerate is exposed to the exterior surface of the cartridge case and to any weapon parts in its path. The presence of exothermic chemical reactions in the gaseous plume is readily substantiated by the fact that the discharge deeply scars and erodes the gun steel, even though the melting point of the steel is in excess of 2500°F. Figure 3 clearly shows the after-effects of "burn-through". Without the large amount of energy inherent in the plume, it is highly improbable that the expansion of the discharge -- a cooling effect -- could cause the extensive damage. Not only does the "burn-through" plume damage the chamber, bolt, and other vulnerable parts of the M16A1, but as shown in Figure 10, the magazine is ejected and destroyed. It is possible to generalize that the large release of energy may be classified as a deflagration.

Induced "burn-through" experiments performed in an universal receiver and test barrel also cause severe erosion of the chamber. The face plate on the breech block and the firing pin are also damaged. An eroded face plate is shown in Figure 79.

Figure 80 (a) and (b) are photomicrographs -- taken at 500X -- of the bolt face and extraction finger from an M16A1 which experienced a "burn-through". Apparent in these photomicrographs is the visible erosion and deposit of aluminous material. An Electron Microprobe Analysis, performed by ALCOA[18], of the dark-gray deposit and the underlying steel surface revealed the following percentages of the elements indicated in Table IV.

Table IV. Results of Electron Microprobe Analysis

Element	Al	Fe	O	Mg	Ni	C, Si, Cr, Cu, Zn
Gray Deposit	69	4	24	1-2	0	< 1
Sub-Surface	28	68	0	< 1	1-2	< 1

The material deposited on the surface is then aluminum oxide. Further, it is possible to conclude that the sub-surface steel contained close to the maximum solubility limit of aluminum in iron. From this conclusion and the visual evidence of erosion, it is evident that the hot gases permitted the surface layer of the steel gun parts to alloy with the aluminum present in the "burn-through" plume.

---

[18] Rogers, R.W., "Letter to Mr. Marvin Rosenbaum", 7 December 1970, Aluminum Company of America, New Kensington, Pa.

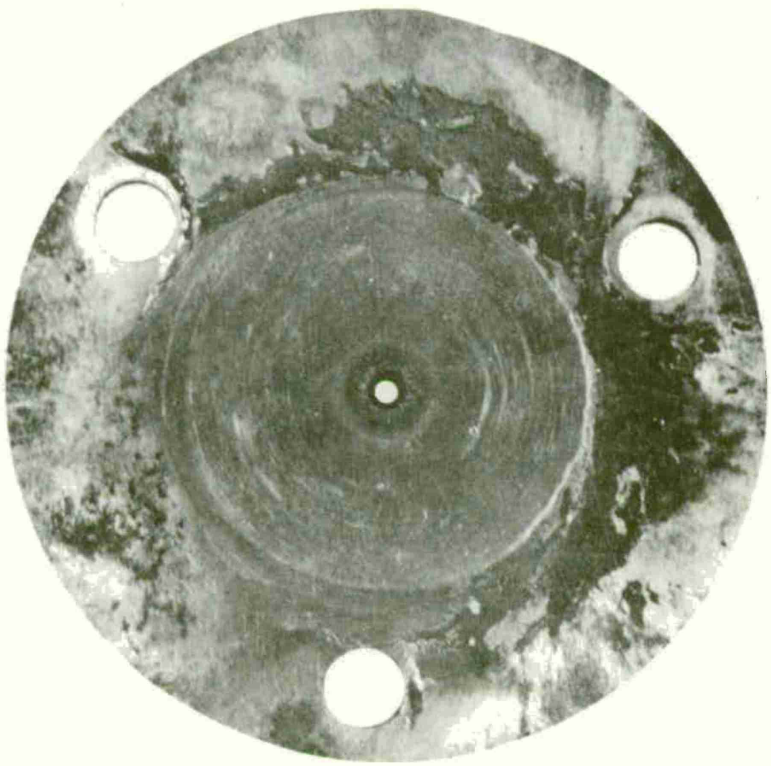

Figure 79. Eroded Face Plate

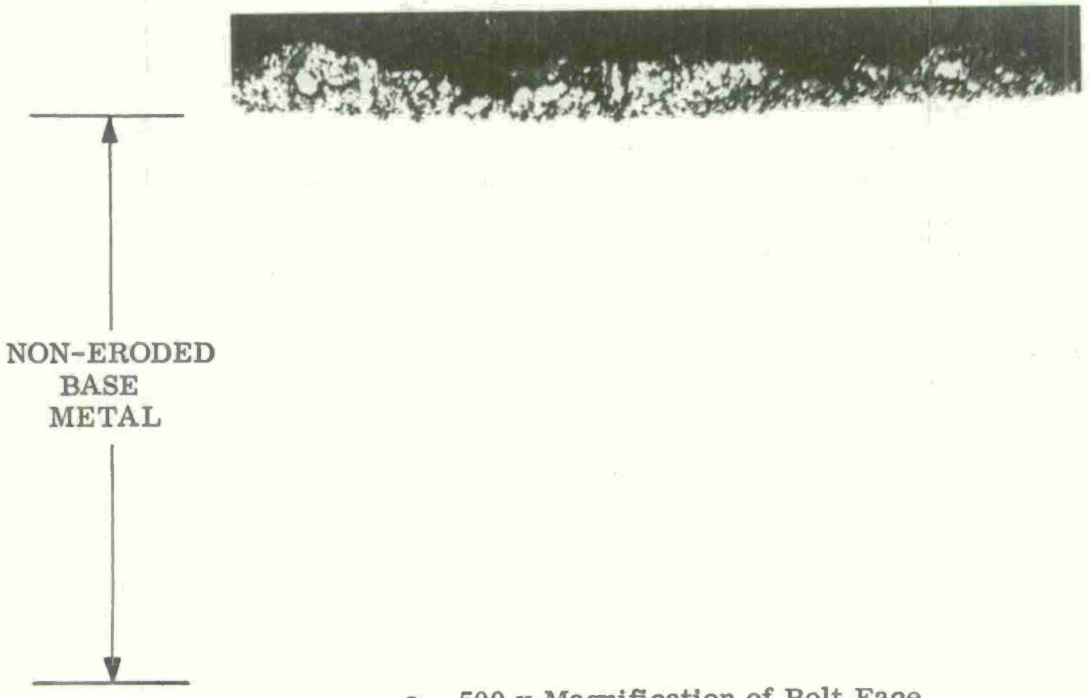

a. 500 x Magnification of Bolt Face

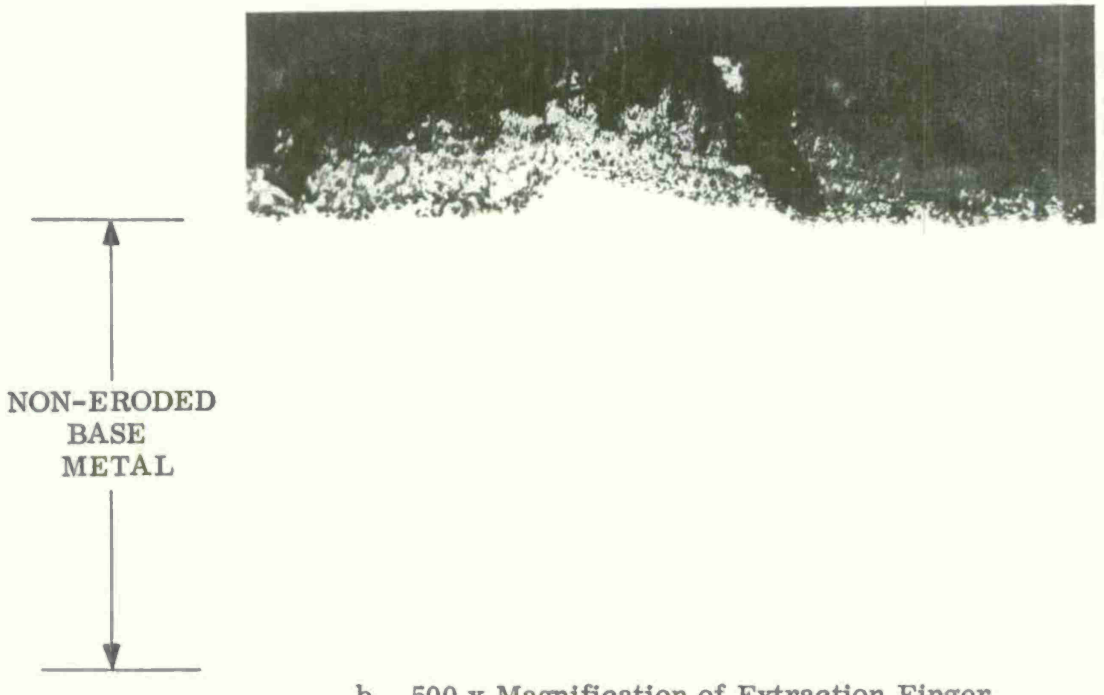

b. 500 x Magnification of Extraction Finger

Figure 80. Photomicrographs of M16A1 Parts Exposed to "Burn-Through"

CHAPTER 8. OTHER CONSIDERATIONS

In this final section, related aspects of "burn-through", not covered earlier in this report, are discussed. These aspects deal with vapor-phase reaction of aluminum and hot energetic propellant gas products, with some effects of gas path geometry in conjunction with the heat flux and resulting case damage, and with a preliminary assessment of the effects produced by use of HMX propellants characterized by both a low adiabatic flame temperature and low oxidizing potential of combustion products.

SECTION 8.1. DISCUSSION OF VAPOR-PHASE REACTION

The presence of the localized primary reaction zone and secondary plume have been verified through photographic observation of "burn-through". A rigorous discussion of aluminum's combustion dynamics is presented by Brzustowski in his dissertation of the vapor-phase reaction associated with an electrically heated aluminum wire. In Reference 24 Brzustowski cautions against extrapolating his understanding as to regimes (especially pressure levels) much above those considered in his investigation.

However, there are a few salient characteristics of a vapor-phase reaction which may have a direct application to our understanding of an aluminum cartridge case "burn-through". A prequisite for a vapor-phase reaction is that the aluminum must be in the gaseous state. The aluminum fuel, having been evaporated from the surface, then diffuses outward toward the flame zone where it reacts with the oxygen diffusing inward from the ambient air. Another more stringent requirement for a vapor-phase reaction to occur is that the flame temperature must exceed the metal's surface temperature. Actually, the flame temperature is constrained by the boiling point of the oxide -- the surface temperature must be below the boiling point of the metal. These required temperature differences exist only for those metals for which the boiling point of the oxide is greater than the boiling point of the metal[24]. Glassman[32] has predicted that lithium, sodium, magnesium, aluminum, calcium, potassium, beryllium, and silicon could burn in the vapor phase. A characteristic of the atmosphere resulting from Brzustowski's wire burning experiment, which has direct carryover to the aluminum cartridge case "burn-through", is the intense visible radiation occurring away from the metal surface. The analogous visible radiation occurring during "burn-through" has been identified as the secondary reaction zone.

From an analysis of flame spectrograms, Brzustowski[24] concluded that there were many different forms of Al_2O_3 compromising the white smoke which surrounded the electrically heated test specimens. Aluminum oxide lines were identified in the emission spectra taken of the secondary plume during an aluminum cartridge case "burn-through".

---

24 Brzustowski, T.A., "Vapor-Phase Diffusion Flames in the Combustion of Magnesium and Aluminum", Ph.D. Thesis, Princeton University, Dept. of Aeronautical Engineering, 1963.

32 Glassman, I. "Metal Combustion Processes", A.R.S. Preprint 938-59, November 1959, (bibliography).

As far as the localized primary reaction zone is concerned, Brzustowski[24] has also observed that there are intense reactions occurring at very small distances from the surface of the burning solid. Actually, the primary reaction zone may be regarded as a "boot-strapping" reaction which is only terminated by the removal of the fuel. Since the fuel for this reaction results from evaporization of aluminum from the exposed surface by rapid convective heating of the propellant gas flow, the reaction is terminated only when the propellant gas flow subsides.

Figure 28 presents a series of selected frames abstracted from a high speed motion picture study of the firing of an aluminum cartridge case (with a 0.0625 inch diameter hole in the head region) in a helium atmosphere. In the frames identified $t = 0.000^{+}$ to $t = 0.286$ millisecond, propellant gases, as indicated by their orange glow, are observed exiting the orifice. This is the heat-up period. The frames identified $t = 0.357$ millisecond shows the first evidence of the localized primary reaction zone. This region of exothermic reaction continues for the remainder of the experiment time shown. However, the presence of this zone in a gun environment experimentally confirms one of Brzustowski's[24] postulates; namely, that in order to initiate the vapor-phase reaction, the aluminum must undergo melting. Figure 81, taken from Reference 5, shows the interior surface temperature of a hole drilled in the head of an aluminum cartridge case as a function of the interior ballistic cycle. As is seen in this figure, the interior surface reaches the solidus temperature -- and hence the initial stages of melting -- at approximately 0.35 millisecond. The time of 0.357 millisecond, from the high speed motion picture study, compares quite favorably with the graph's prediction of 0.35 millisecond.

It is therefore concluded that as the propellant gas flows throughout the induced hole, the bulk aluminum situated below the protective oxide coating, which lines the surface of the hole, is melting. Due to the continuing efflux of propellant gases, the protective oxide coating can no longer maintain its structural integrity and is washed away because the bulk aluminum immediately below has melted. Once fresh aluminum is exposed to the propellant gases, the protective oxide layer is unable to form and a vapor-phase reaction is initiated.

---

[24] Brzustowski, T.A. "Vapor-Phase Diffusion Flames in the Combustion of Magnesium and Aluminum", Ph.D. Thesis, Princeton University, Dept. of Aeronautical Engineering, 1963.

[5] Squire, W.H., and Donnard, R.E., "An Analysis of Local Temperature Profiles Encountered in the Aluminum Cartridge Case Drilled Hole Experiment", Technical Note TN-1163, August 1971, Frankford Arsenal, Phila., Pa.

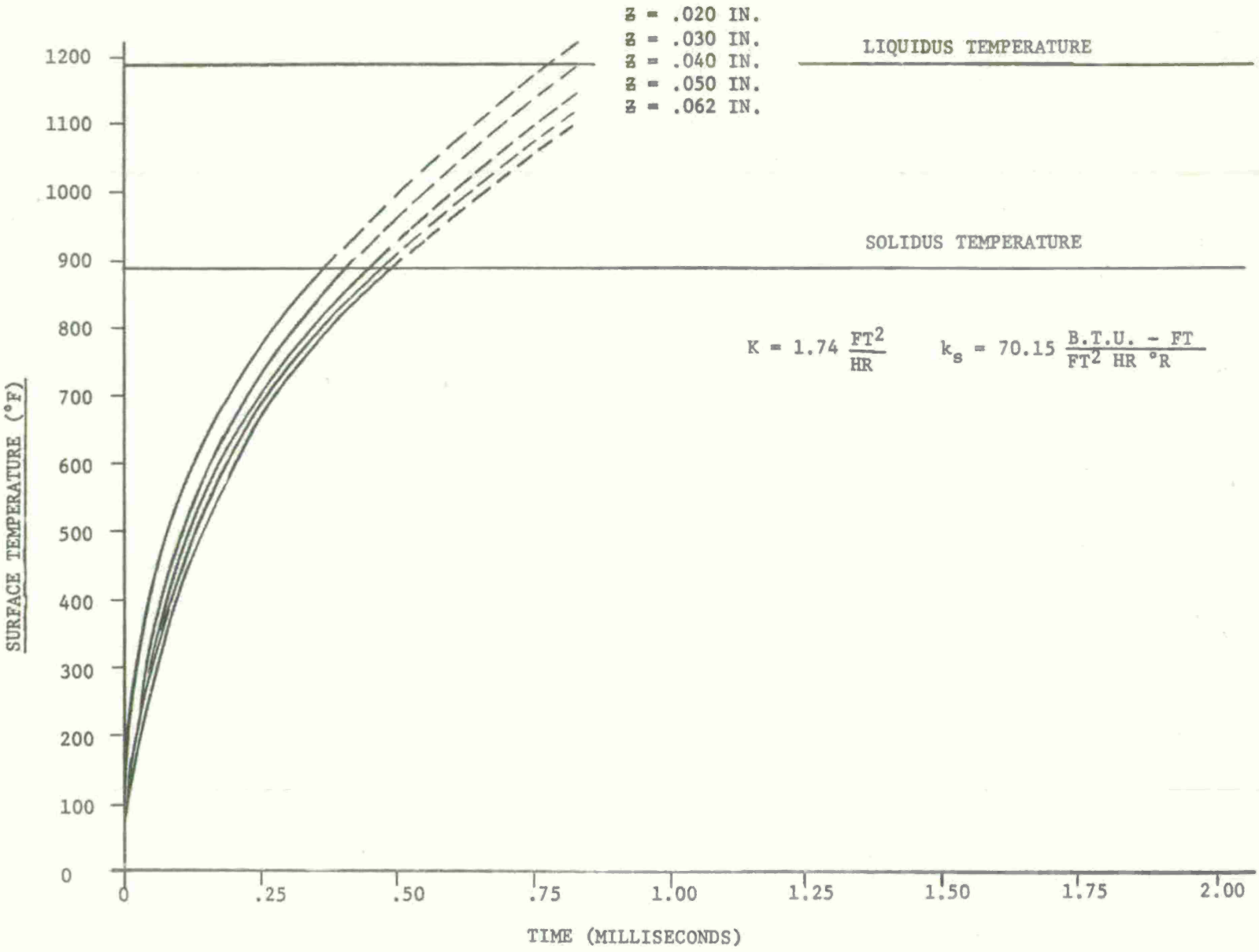

Figure 81. Surface Temperature of an Aluminum Bore VS Time (Position as indicated.)

SECTION 8.2. THE AXIAL DEPENDENCE OF THE APPLIED HEAT FLUX AND THE EFFECT OF LEADING EDGES

Reference 5 provides an analytical investigation of the gas dynamics and heat transfer occurring when propellant gases exit an aluminum cartridge case through a 0.0135 inch diameter hole in the head region. Although this analysis is structured for the simulation of "burn-through" in an aluminum cartridge case, it is sufficiently general to allow application to the passage of propellant gases through small holes in aluminum test specimen Figure 82 (a) shows a conceptual representation of the heat flux incident to the aluminum as predicted by the analytical model of Reference 5. The fluid mechanics of this analytical model are based on channel flow with friction and do not consider any leading edge or corner flow effect.

Shapiro[33] points out that the region of greatest heat transfer under such flow conditions occurs at the leading edge. Unfortunately, the mathematical manipulation of the governing equations and the numerics required to obtain a stable, converging solution precludes consideration of this effect in Reference 5. The high rates of heat transfer at the leading edge, however, may be confirmed through use of the correct governing differential equations and the use of an adequate numerical scheme. These high rates at the inlet of the bore are difficult to accept in light of the fact that the greatest erosion occurs at the exit of the bore (outside) as depicted in Figure 82 (b). However, there is considerable discussion in Section 6.1 which suggests that a possible cause for this anomalous behavior is the entrainment of vaporized aluminum in the boundary layer. Once vaporized and entrained in the boundary, the aluminum reacts exothermically as described in Section 6.4.

It seems from an intuitive standpoint that the longer the distance the vaporized and entrained congolmerate must traverse, the more substantial will be the erosive effect. This fact may be used to explain the phenomenon shown in Figure 48 wherein the mean increase in diameter, for several thicknesses of aluminum test specimens, is plotted as a function of peak chamber pressure. As is observed in Figure 48, when the specimen thickness is increased for a given peak chamber pressure, the mean increase in diameter is also increased.

---

[5] Squire, W.H., and Donnard, R.E., "An Analysis of Local Temperature Profiles Encountered in the Aluminum Cartridge Case Drilled Hole Experiment", Technical Note TN-1163, August 1971, Frankford Arsenal, Phila., Pa.

[33] Shapiro, A.H., The Dynamics and Thermodynamics of Compressible Fluid Flow, Vol. 1, Ronald Press, New York, 1953.

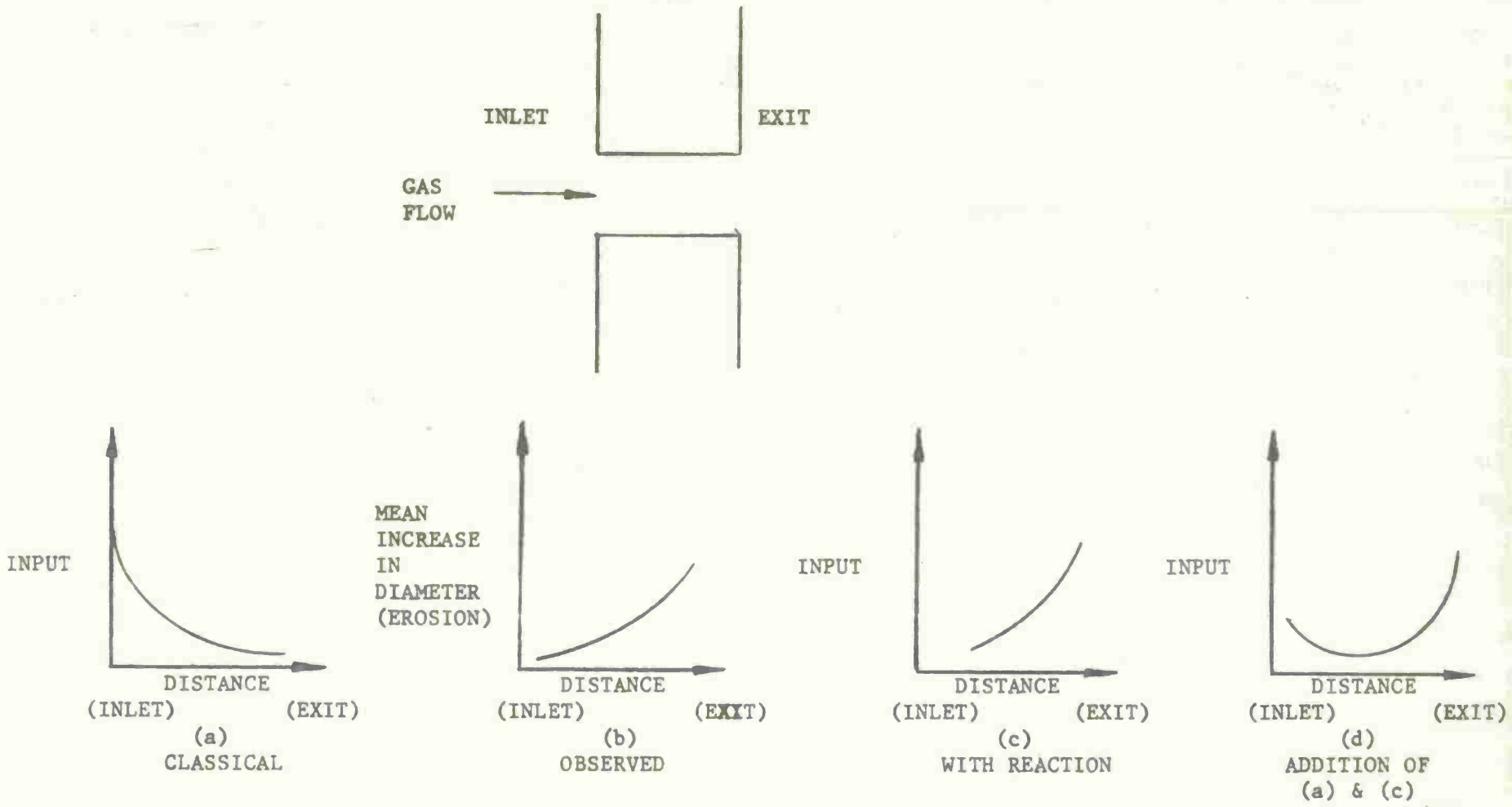

Figure 82. A Conceptual Representation of the Effects of Distance and Reaction on the Erosion of Test Specimens.

Since the analysis in Section 6.4 indicates that the heat flux from the chemical reactions is much greater than that resulting from the gas dynamics, the total heat flux incident to the bore's surface is the addition seen in Figures 82 (a) and 82 (c). The results of this "conceptual" addition is seen in Figure 82 (d).

The fact that the leading edge of the test specimenm or the inlet of the hole drilled in the head of an aluminum cartridge case, receives a high rate of transfer deserves additional consideration. If the feasibility of aluminum cartridge cases is to be demonstrated, and if the results of the "burn-through" investigation are to be beneficial, then of paramount importance is the development of systems to be incorporated in the cartridge design to protect the vulnerable aluminum surfaces. To date, two solutions have been demonstrated in erosion test fixtures. (Actually only one has been effectively demonstrated in cartridge case test firings). One is the placement of a thin rubber membrane between the test fixture and the vulnerable aluminum. This technique has been modified and applied to aluminum cartridge cases and shown to be a successful and feasible solution to the "burn-through" phenomenon[6,34].

The other solution, shown to be feasible during firings in an erosion test fixture, was the use of a clad metal composite with the additional stipluation that the brass surface be closest to the combustor. The commonality of both of these "potential" solutions is that they offer protection to the highly vulnerable leading edge. In fact, the results shown in Figure 54 may be explained by considering that the rubber membrane actually gets extruded into the induced orifice. The physical presence of a "protecting" material affects the net heat transfer to the aluminum and thus alters or eliminates the erosion patterns.

---

[6] Donnard, R.E., and Squire, W.H., "The Aluminum Cartridge Case Exploratory Development Program - Status Report", Report M 72-6-1, April 1972, Frankford Arsenal, Phila., Pa.

[34] U.S. Patent Applied for "Noneroding Lightweight Cartridge Cases", Disclosure Number AMSMU2188, February 1973, Skochko, Leonard W. and Donnard, Reed E.

SECTION 8.3. HMX Propellant Study

Novel HMX propellant types, characterized by relatively low adiabatic flame temperatures, were developed for application to a caseless system. Activity involving the mathematical modeling of the aluminum cartridge case "burn-through" phenomenon[5,14] indicates that the onset of "burn-through" is sensitive to the adiabatic flame temperature of the propellant gas. Since the adiabatic flame temperature of typical small arms propellants (WC 846: 2800-2900°K and IMR 8208M: 2900-3000°K) is constrained to a narrow range, it is diffcult, using these standard propellants, to ascertain the effect of the adiabatic flame temperature of the propellant gases on "burn-through". Thus, the availability of these HMX propellants affords an opportunity to assess the dependency of "burn-through" on the adiabatic flame temperature.

One half pound quantities of four HMX propellant samples -- the adiabatic flame temperatures of which are 1800°K, 2100°K, 2300°K, and 2500°K -- were purchased from the Thiokol Chemical Corporation (TCC), Wasatch Division, Brigham City, Utah, on purchase order DAAA-25-72-M1743. It was planned at the time of the procurement to evaluate erosivity of the HMX propellants both in a combustor (using aluminum test specimens) and in a 5.56mm gun environment (using aluminum cartridge cases). However, the HMX propellants that were provided were not designed to be fired in a 5.56mm weapon as the grain size was exceedingly large and nonuniform and the process by which the propellant was fabricated produced HMX propellants of inferior quality[35]. Technical personnel at TCC expressed serious reservations about using the samples for gun tests but had no objection to using the propellants in a combustor[35]. However, due to high priority assigned to this evaluation, Frankford Arsenal assumed responsibility for the propellants' performance and took measures to alter the HMX propellants so that peak chamber

---

[5] Squire, W.H., and Donnard, R.E., "An Analysis of Local Temperature Profiles Encountered in the Aluminum Cartridge Case Drilled Hole Experiment", Technical Note TN-1163, August 1971, Frankford Arsenal, Phila., Pa.

[14] Plett, Edelbert G. and Summerfield, Martin, "Erosive Effects of Combustion Gases on Metallic Combustion Chambers, Final Report on Contract DAAA25-71-C0109", Dept. of Aerospace and Mechanical Sciences, Princeton University.

[35] Bernstein, C.N., "Thiokol HMX Propellant for Aluminum Case Erosion Tests," Memorandum for Record, SASA, 31 March 1972.

pressures typical of a 5.56mm system could be obtained.

Preliminary gun firings with these propellants, using standard brass cartridge cases and conventional M193 ball projectiles, are presented in Table V. The data are average velocities and action times for the four HMX propellants in four different granulations. The granulations are: (a) as received, (b) test sample ground and 100% of the sample passed through a 20 mesh screen, (c) test sample ground and 100% of the sample passed through a 30 mesh screen, and (d) test sample ground and 100% of the sample passed through a 40 mesh screen. Although chamber pressures were not taken during this portion of the experimental program, it was concluded from the low velocities and long action times that the chamber pressures were not in the 40 to 55 kpsi range. It was apparent from the data that the granulation resulting from grinding the propellant and passing 100% of the test sample through a 20 mesh sieve provided the best ballistics -- highest velocities and shortest action times. For this reason, portions of the four HMX propellant samples were ground and 100% of each test sample passed through a 20 mesh screen; these samples were used in a combustor to assess the erosivity of the aluminum test specimens.

The aluminum discs used in this experiment, performed at Princeton University, were fabricated from alloy 6061 in the T6 temper, 0.100 inch thick, and had a 0.0135 inch diameter hole pre-drilled through the center of the disc. Two indicators of erosivity were used to assess the degree of erosion under a particular set of experimental conditions, specimen weight loss and mean increase in diameter of the test disc. A total of fourteen firings were made with various charges of the four HMX propellants under investigation. Although the peak chamber pressures in these firings included the range experienced in a gun environment (40 to 50 kpsi), the experiment times, the duration of the pressure-time curve, were exceedingly long. The long experiment times are characteristic of the firings in the venting bomb. The reduced data from which this exercise are presented in Table VI and in Figure 83.

Figure 83 shows the erosion characteristics of the four HMX propellant samples together with IMR 4198 (used as a standard propellant) and a reduced flame temperature propellant identified as X propellant (composition of X propellant, by weight, 80% nitrocellulose, 19% oxamide, and 1% diphenylamine). As expected, the erosivity of X propellant is less than the standard IMR propellant due to its approximately 800°K lower flame temperature. However, the shape and slope of the erosivity of X propellant curve is similar to that of the IMR propellant. On the other hand, the erosion characteristics of all four HMX propellants are noticably different from those of IMR 4198 and X propellant.

Table V. Preliminary HMX Firings

Propellant HMX 1800				
Granulation	As received	100% - 20 mesh	100% - 30 mesh	100% - 40 mesh
Charge* (Grains)	20.97	21.75	19.60	18.79
Average Velocity (Ft/Sec)	441	1240	994	899
Average Action Time (m Sec)	Missed	4.795	5.357	5.912
Propellant HMX 2100				
Granulation	As received	100% - 20 mesh	100% - 30 mesh	100% - 40 mesh
Charge* (Grains)	21.72	23.35	22.40	21.97
Average Velocity (Ft/Sec)	1035	1886	1119	962
Average Action Time (m Sec)	4.238	2.628	4.453	3.666
Propellant HMX 2300				
Granulation	As received	100% - 20 mesh	100% - 30 mesh	100% - 40 mesh
Charge* (Grains)	22.60	26.14	23.42	23.00
Average Velocity (Ft/Sec)	1637	2329	1726	1106
Average Action Time (m Sec)	2.158	1.495	2.517	3.645
Propellant HMX 2500				
Granulation	As received	100% - 20 mesh	100% - 30 mesh	100% - 40 mesh
Charge* (Grains)	22.47	26.00	24.12	23.41
Average Velocity (Ft/Sec)	1816	2525	2223	1269
Average Action Time (m Sec)	2.284	1.967	2.321	3.354

*In all firings the charge indicated represents the maximum amount of propellant required to fill completely the cartridge case and yet permit seating of the projectile (zero air space).

TABLE VI. HMX FIRINGS IN VENTING BOMB

Specimen Number	13	15	19*	20*	9*	21*	17	18	22	24	12	14	16	23
Propellant	1800	1800**	1800/2500	1800/2500	1800/2500	1800/2500	2100	2100	2100	2300	2500	2500	2500	2500
Charge (Grams)	1.3	1.3	1.1 0.2	1.1 0.2	1.3 0.2	1.3 0.2	1.3	1.3	1.3	1.3	1.0	1.3	1.3	1.15
Peak Chamber Pressure (kpsi)	38.0	Missed	26.0	25.5	27.5	58.5	33.0	41.25	34.25	50.5	28.5	59.5	58.25	27.0
Time to Peak Pressure (mSec)	9.8	Missed	3.8	3.2	3.5	2.8	6.6	7.2	4.4	4.0	4.3	3.2	2.6	3.8
Mean Increase in Diameter - Combustor Side (in)	0.0179	0.1057	0.0133	0.0137	0.0265	0.0796	0.0598	0.0680	0.0451	0.0855	0.0503	0.1152	0.1080	0.0722
Mean Increase in Diameter - Atmosphere Side (in)	0.0034	0.0645	0.0	0.0015	0.0080	0.0404	0.0257	0.0292	0.0238	0.0538	0.0213	0.0625	0.0615	0.0390
Specimen Weight Loss (Grams X 10^{-3})	0.6	21.9	0.4	0.3	1.6	11.9	7.1	8.9	5.3	15.5	5.0	28.7	22.1	10.5

*Problems were encountered in igniting HMX 1800 with a conventional 5.56mm primer. To circumvent this, a small amount of HMX 2500 (weight as indicated) was placed adjscent to the primer's vent; the remainder of the charge was HMX 1800 (weight as indicated).

**Two other firings were attempted with HMX 1800 - both resulted in misfires - primer discharge - no propellant ignition.

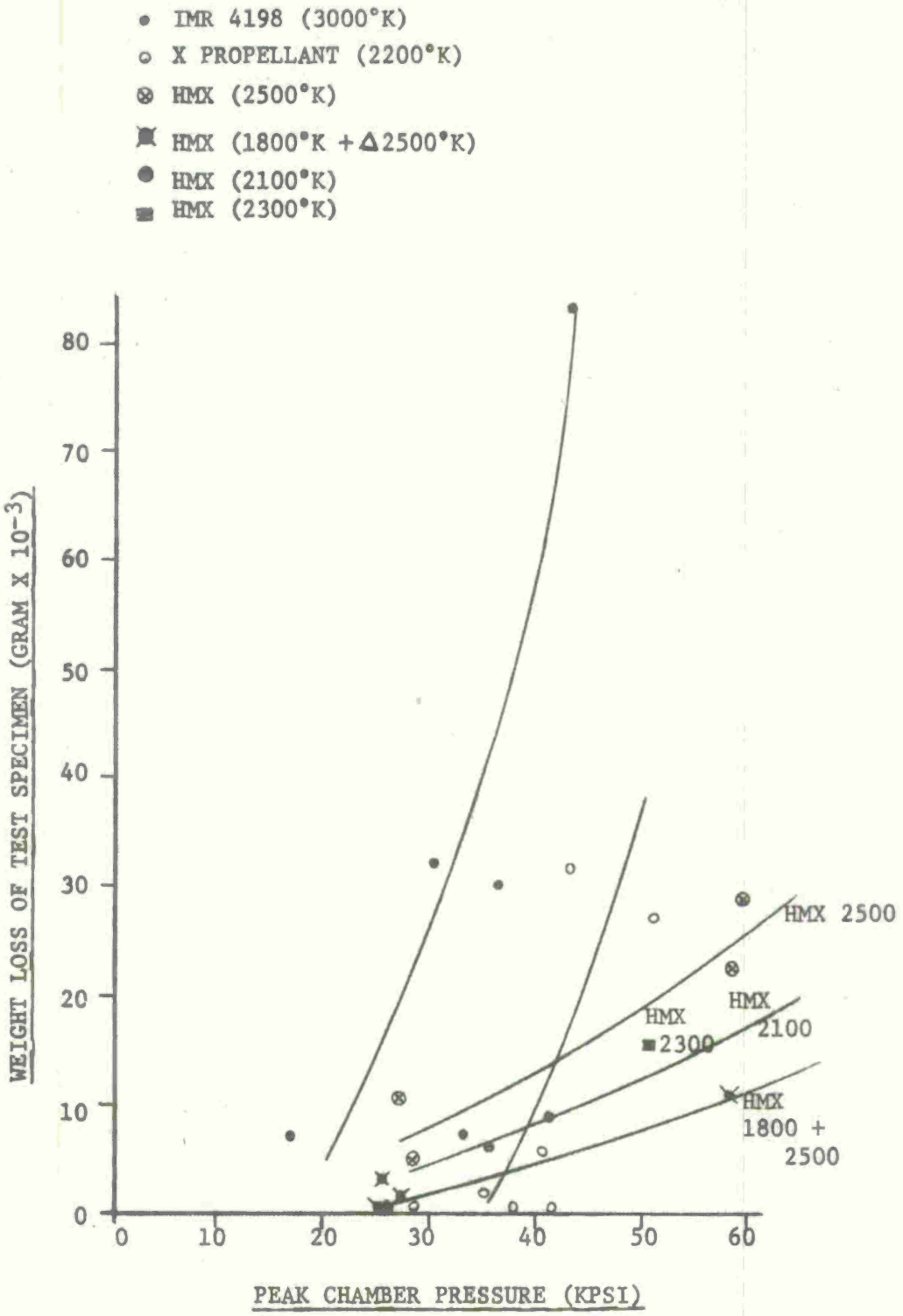

Figure 83. Weight Loss of Test Specimens VS Peak Chamber Pressure for Propellant Types as Indicated.

Not only do the curves show that the HMX propellants yield less specimen weight loss (at a particular pressure level) than IMR 4198 and X propellant, but the HMX curves have a significantly different slope. Of course, the trend of reduced flame temperature yielding lower specimen weight loss is also true with the HMX propellants as, for a particular peak chamber pressure, specimen weight loss is decreased as the HMX propellant flame temperature is correspondingly decreased from 2500°K to 1800°K.

The test discs also provide valuable insight into the erosion behavior of HMX propellants. Visual observation of the discs reveals that there is little apparent burning on the atmosphere (numbered) side of the test specimen. This observation can be coupled with the fact that the mean increase in diameter of the combustor (unnumbered) side is greater than the mean increase in diameter of the atmosphere side so as to conclude that the HMX propellants behave differently in a venting bomb or combustor than conventional single or double-base propellants. Past firings at Princeton University[14] with conventional propellants have shown that the mean increase in diameter of the predrilled hole is greater on the atmosphere side than on the combustor side; this has been attributed to the localized primary reaction zone occurring at or near the test disc. Figures 84 through 88 are photographs showing the atmosphere side of test specimens exposed to gas flow from the indicated HMX propellant types. Also shown in the photographs are the peak pressures experienced during firing, the mean increase in diameter of the specimen side shown, the weight loss of the specimen, and the specimen number. Figures 89 through 93 are similar photographs of the combustor side. A correlation between weight loss of the specimens and the increase in mean diameters of both the combustor and atmosphere sides of the specimens is presented in Figure 94. As can be readily seen, there is a strong correlation between weight loss and increase in mean diameter.

The results from firing in an erosion test accelerated activity to investigate erosivity of HMX propellants in a gun environment at 40-55 kpsi peak chamber pressures. To attain these peak chamber pressures, heavier 5.56mm projectiles were used. (The conventional M193 projectile weighs 54 grains; two "heavier" projectiles used in this study were a 97 grain projectile identified "heavy" and a 66 grain projectile identified "light"). In addition to the change to "heavier" projectiles, the test samples of HMX propellants were sieved twice. After grinding, 100% of the sample was passed through a 20 mesh screen; then, the portion which would not pass through a 35 mesh screen was retained (0% of the test sample passed through the

---

[14] Plett, Edelbert G. and Summerfield, Martin, "Erosive Effects of Combustion Gases on Metallic Combustion Chambers, Final Report on Contract DAAA25-71-C0109", Department of Aerospace and Mechanical Sciences, Princeton University.

HMX PROPELLANT -- 1800°K

100% 20 MESH
0.0135 INCH (DIA) HOLE
0.100 INCH THICK
6061 T-6 ALUMINUM
NUMBERED SIDE - ATMOSPHERE

PEAK PRESSURE (Kpsi)	38.0	Missed
CHARGE (grams)	1.3	1.3
WEIGHT LOSS (grams x 10^{-3})	0.6×10^{-3}	21.9×10^{-3}
INCREASE IN DIAMETER (inch)	0.0034	0.06445
SPECIMEN NUMBER	13	15

Figure 84. Erosion Characteristics of HMX Propellant 1800°K - Test Discs, Numbered Side

HMX PROPELLANT 1800°K AND 2500°K

100% 20 MESH
0.0135 INCH (DIA) HOLE
0.100 INCH THICK
6061 T-6 ALUMINUM
NUMBERED SIDE - ATMOSPHERE

PEAK PRESSURE (Kpsi)	25.5	26.0	27.5	58.5
CHARGE (grams 1800)	1.10	1.10	1.30	1.30
(grams 2500)	0.200	0.20	0.20	0.20
WEIGHT LOSS (grams x 10^{-3})	0.3×10^{-3}	0.4×10^{-3}	1.6×10^{-3}	11.9×10^{-3}
INCREASE IN DIAMETER (inch)	0.0015	0.000	0.00795	0.0404
SPECIMEN NUMBER	20	19	9	21

Figure 85. Erosion Characteristics of HMX Propellants 1800°K and 2500°K - Test Discs, Numbered Side

HMX PROPELLANT -- 2100°K

100% 20 MESH
0.0135 INCH (DIA) HOLE
0.100 INCH THICK
6161 T-6 ALUMINUM
NUMBERED SIDE - ATMOSPHERE

PEAK PRESSURE (Kpsi)	33.0	34.25	41.25
CHARGE (grams)	1.30	1.30	1.30
WEIGHT LOSS (grams $x10^{-3}$)	$7.1x10^{-3}$	$5.3x10^{-3}$	$8.9x10^{-3}$
INCREASE IN DIAMETER (inch)	0.0257	0.0238	0.0292
SPECIMEN NUMBER	17	22	18

Figure 86. Erosion Characteristics of HMX Propellant 2100°K - Test Discs, Numbered Side

HMX PROPELLANT -- 2300°K

100% 20 MESH
0.0135 INCH (DIA) HOLE
0.100 INCH THICK
6061 T-6 ALUMINUM
NUMBERED SIDE - ATMOSPHERE

PEAK PRESSURE (Kpsi)	50.5
CHARGE (grams)	1.30
WEIGHT LOSS (grams x 10^{-3})	15.5×10^{-3}
INCREASE IN DIAMETER (inch)	0.05375
SPECIMEN NUMBER	24

Figure 87. Erosion Characteristics of HMX Propellant 2300°K - Test Discs, Numbered Side

HMX PROPELLANT -- 2500°K

100% 20 MESH
0.0135 INCH (DIA) HOLE
0.100 INCH THICK
6061 T-6 ALUMINUM
NUMBERED SIDE - ATMOSPHERE

PEAK PRESSURE (Kpsi)	27	28.5	58.25	59.5
CHARGE (grams)	1.15	1.00	1.30	1.30
WEIGHT LOSS (grams x 10^{-3})	10.5×10^{-3}	5×10^{-3}	22.1×10^{-3}	28.7×10^{-3}
INCREASE IN DIAMETER (inch)	0.0390	0.02125	0.0615	0.06245
SPECIMEN NUMBER	23	12	16	14

Figure 88. Erosion Characteristics of HMX Propellant 2500°K - Test Discs, Numbered Side

HMX PROPELLANT -- 1800°K

100% 20 MESH
0.0135 INCH (DIA) HOLE
0.100 INCH THICK
6061 T-6 ALUMINUM
UNNUMBERED SIDE - COMBUSTOR

PEAK PRESSURE (Kpsi)	38.0	Missed
CHARGE (grams)	1.3	1.3
WEIGHT LOSS (grams x 10^{-3})	0.6×10^{-3}	21.9×10^{-3}
INCREASE IN DIAMETER (inch)	0.0179	0.10565
SPECIMEN NUMBER	13	15

Figure 89. Erosion Characteristic of HMX Propellant 1800°K - Test Discs, Unnumbered Side

HMX PROPELLANT 1800°K AND 2500°K

100% 20 MESH
0.0135 INCH (DIA) HOLE
0.100 INCH THICK
6061 T-6 ALUMINUM
UNNUMBERED SIDE - COMBUSTOR

PEAK PRESSURE (Kpsi)	25.5	26.0	27.5	58.5
CHARGE (grams 1800)	1.10	1.10	1.30	1.30
(grams 2500)	0.200	0.20	0.20	0.20
WEIGHT LOSS (grams x 10^{-3})	0.3×10^{-3}	0.4×10^{-3}	1.6×10^{-3}	11.9×10^{-3}
INCREASE IN DIAMETER (inch)	0.01370	0.01325	0.0265	0.0796
SPECIMEN NUMBER	20	19	9	21

Figure 90. Erosion Characteristics of HMX Propellants 1800°K and 2500°K - Test Discs, Unnumbered Side

HMX PROPELLANT -- 2100°K

100% 20 MESH
0.0135 INCH (DIA) HOLE
0.100 INCH THICK
6061 T-6 ALUMINUM
UNNUMBERED SIDE - COMBUSTOR

PEAK PRESSURE (Kpsi)	33.0	34.25	41.25
CHARGE (grams)	1.30	1.30	1.30
WEIGHT LOSS (grams x 10^{-3})	7.1×10^{-3}	5.3×10^{-3}	8.9×10^{-3}
INCREASE IN DIAMETER (inch)	0.05975	0.04505	0.06795
SPECIMEN NUMBER	17	22	18

Figure 91. Erosion Characteristics of HMX Propellant 2100°K - Test Discs, Unnumbered Side

HMX PROPELLANT -- 2300°K

100% 20 MESH
0.0135 INCH (DIA) HOLE
0.100 INCH THICK
6061 T-6 ALUMINUM
UNNUMBERED SIDE - COMBUSTOR

PEAK PRESSURE (Kpsi)	50.5
CHARGE (grams)	1.30
WEIGHT LOSS (grams x 10^{-3})	15.5 x 10^{-3}
INCREASE IN DIAMETER (inch)	0.08545
SPECIMEN NUMBER	24

Figure 92. Erosion Characteristics of HMX Propellant 2300°K - Test Discs, Unnumbered Side

HMX PROPELLANT -- 2500°K

100% 20 MESH
0.0135 INCH (DIA) HOLE
0.100 INCH THICK
6061 T-6 ALUMINUM
UNNUMBERED SIDE - COMBUSTOR

PEAK PRESSURE (Kpsi)	27	28.5	58.25	59.5
CHARGE (grams)	1.15	1.00	1.30	1.30
WEIGHT LOSS (grams x 10^{-3})	10.5×10^{-3}	5×10^{-3}	22.1×10^{-3}	28.7×10^{-3}
INCREASE IN DIAMETER (inch)	0.0722	0.0503	0.10795	0.11515
SPECIMEN NUMBER	23	12	16	14

Figure 93. Erosion Characteristics of HMX Propellant 2500°K - Test Discs, Unnumbered Side

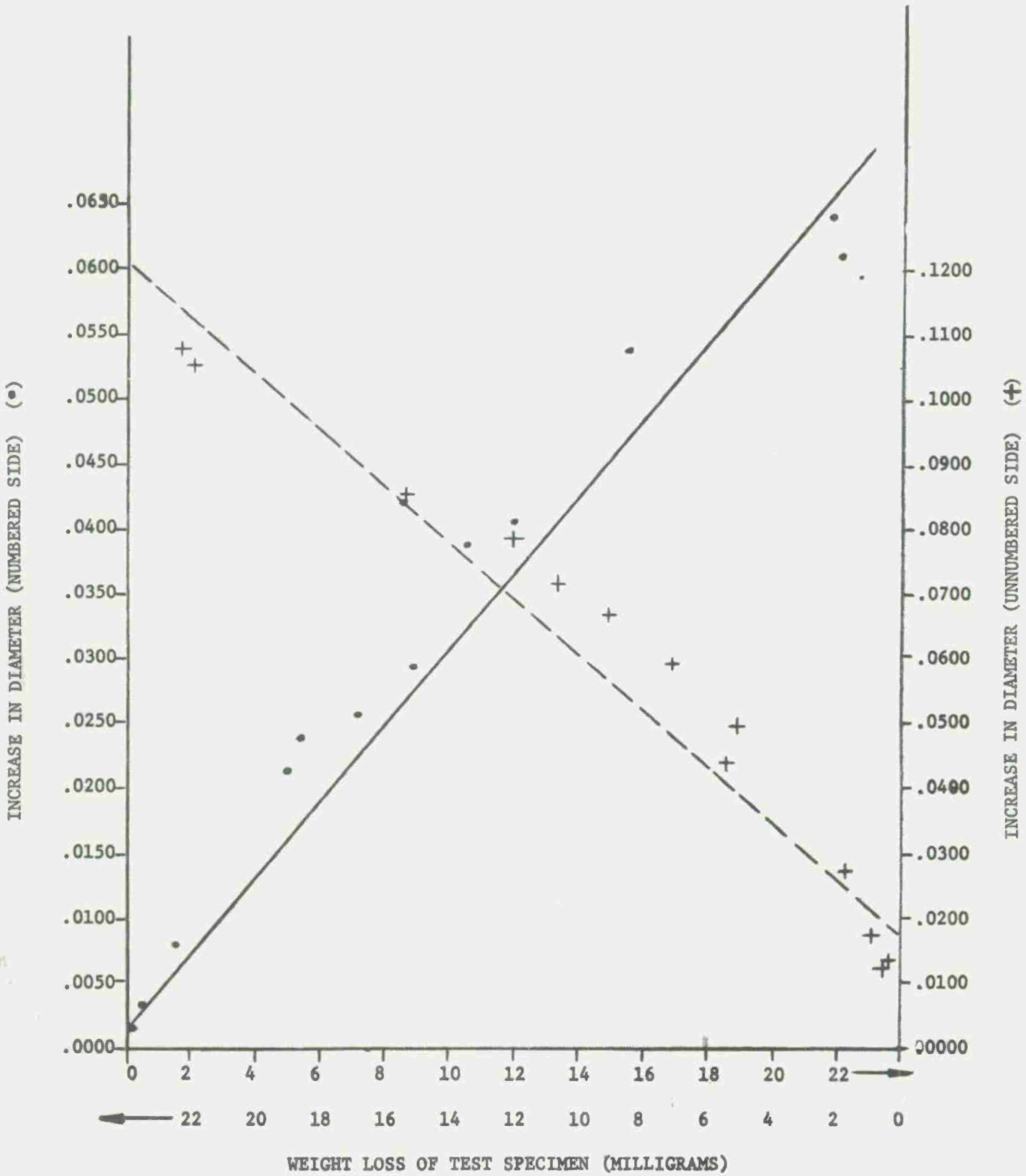

Figure 94. Correlation Between Increase in Diameter (Numbered and Unnumbered Sides) VS Weight Loss of Test Specimen.

35 mesh screen). The second sieving was performed to remove "fines" from the test samples.

Figure 95 shows four pressure-time curves of HMX propellant firings. A brass cartridge case was filled to its maximum capacity (zero air space) for each firing. As indicated in the photograph, the peak pressures (using the 97 grain projectile) were 36,500 psi (HMX 1800), 51,000 psi (HMX 2100), 60,000 psi (HMX 2300), and off scale at 63,000 psi (HMX 2500).

Aluminum cartridge cases which were scratched (0.004 - 0.005 inch deep, 0.75 inch long) or which had a 0.0312 inch diameter hole drilled in the head region were used to test the erosivity of the HMX propellants. The results of firing the aluminum cartridge cases are presented in Figures 96 through 98. Two attempts were made to fire HMX 1800 in aluminum cartridge cases which were scratched; both firings resulted in bullet-in-bores, and hence no HMX 1800 firings are reported. Although both scratched cases and cases with predrilled holes were used to test the erosivity of the HMX propellants, the emphasis was placed on scratched cases as they are more representatives of actual failures. The results indicate that in gun firings there is serious erosion sustained by aluminum cartridge cases using HMX propellants. This fact is particularly true with those cases which had been scratched; the cartridge cases with holes do not seem to be eroded as seriously as those which had been scratched. It is possible to account for the apparent increased erosion with slit cartridge cases by considering: (a) upon firing, the scratch is opened thereby presenting a fresh aluminum surface devoid of its protective oxide coating, (b) upon splitting, the scratch may have many rough edges or sharp corners where heat transfer occurs at excessive rates, and (c) the gas path presented by the scratch is appreciably larger (in cross sectional area) than the induced hole.

Since the aluminum cartridge cases were not weighed before and after firing, a quantitative assessment of erosion severity is not available. There are two by-products of the experimental program which should be noted. First, in a quanlitative sense, there was flash associated with each HMX firing. The flash was sufficient to illuminate completely a darkened range area. The second important by-product of the HMX firings in a gun environment is gained through an observation of the chamber of the test barrel. In firings with conventional single or double-based propellants in aluminum cartridge cases, which were prepared with induced failure sites, the chamber becomes severely eroded after firing several rounds and must be replaced frequently. Figure 99 shows the chamber of the test barrel used in the HMX investigation. There was little barrel (chamber) erosion in this weapon which sustained twelve aluminum cartridge case "burn-throughs".

PRESSURE-TIME CURVES OF HMX PROPELLANT FIRINGS
Brass Cartridge Cases
F.A. #41 Primers
97 Grain Projectiles

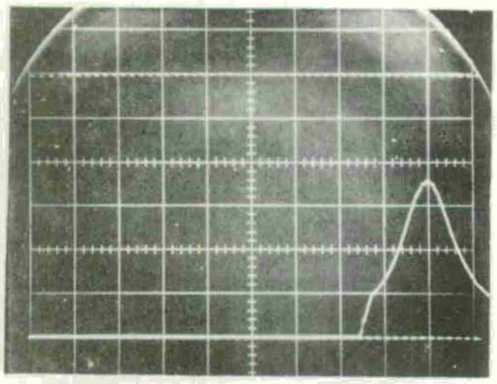

HMX 1800°K
Granulation:
100% - 20 mesh
0% - 35 mesh
Charge 20.15 grains
Peak Chamber Pressure: 36.5 kpsi

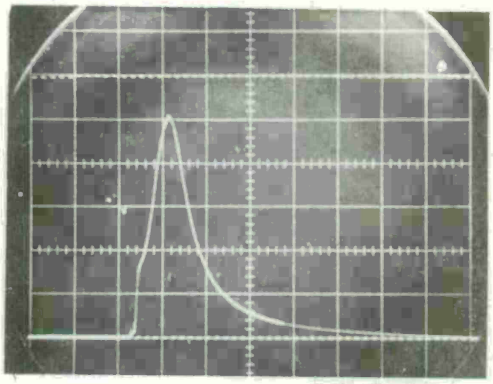

HMX 2100°K
Granulation:
100% - 20 mesh
0% - 35 mesh
Charge 22.09 grains
Peak Chamber Pressure: 51 kpsi

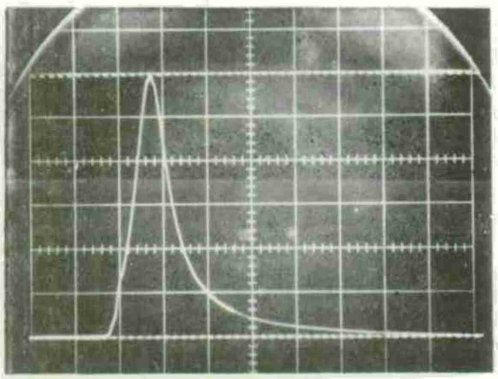

HMX 2300°K
Granulation:
100% - 20 mesh
0% - 35 mesh
Charge: 23.48 grains
Peak Chamber Pressure: 60 kpsi

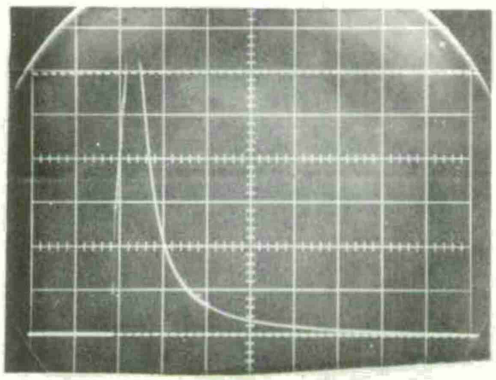

HMX 2500°K
Granulation:
100% - 20 mesh
0% - 35 mesh
Charge: 23.00 grains
Peak Chamber Pressure: off-scale at 63 kpsi

Calibration:

60 kpsi between calibration lines
(10 kpsi/major division)

Time:

5 milliseconds full sweep
(0.5 milliseconds/major division)

Figure 95. Pressure-Time Curves Obtained from Gun Firings with Conditions and Propellants as Indicated

HMX PROPELLANT -- 2100°K

100% 20 MESH
0% 35 MESH
CHARGE 22.09 GRAINS

CARTRIDGE CASE	Slit	Slit	0.0312 in (dia) hole	Slit
PEAK CHAMBER PRESSURE	26,500 psi	33,500 psi	36,500 psi	43,000 psi
PROJECTILE	Light	Heavy	Heavy	Heavy
SPECIMEN	1	2	3	4

Figure 96. Erosion Characteristics of HMX Propellant 2100°K - Cartridge Cases

HMX PROPELLANT -- 2300°K

100% 20 MESH
0% 35 MESH
CHARGE 23.25 GRAINS

CARTRIDGE CASE	Slit	Slit	Slit
PEAK CHAMBER PRESSURE	28,000 psi	42,500 psi	47,000 psi
PROJECTILE	Light	Heavy	Heavy
SPECIMEN	1	2	3

Figure 97. Erosion Characteristics of HMX Propellant 2300°K - Cartridge Cases

HMX PROPELLANT -- 2500°K

100% 20 MESH
0% 35 MESH
CHARGE 23.00 GRAINS

CARTRIDGE CASE	Slit	Slit	Slit	0.031 in (dia) hole	Slit
PEAK CHAMBER PRESSURE	27,500 psi	41,500 psi	43,500 psi	48,000 psi	52,000 psi
PROJECTILE	Light	Heavy	Heavy	Heavy	Heavy
SPECIMEN	1	2	3	4	5

Figure 98. Erosion Characteristics of HMX Propellant 2500°K - Cartridge Cases

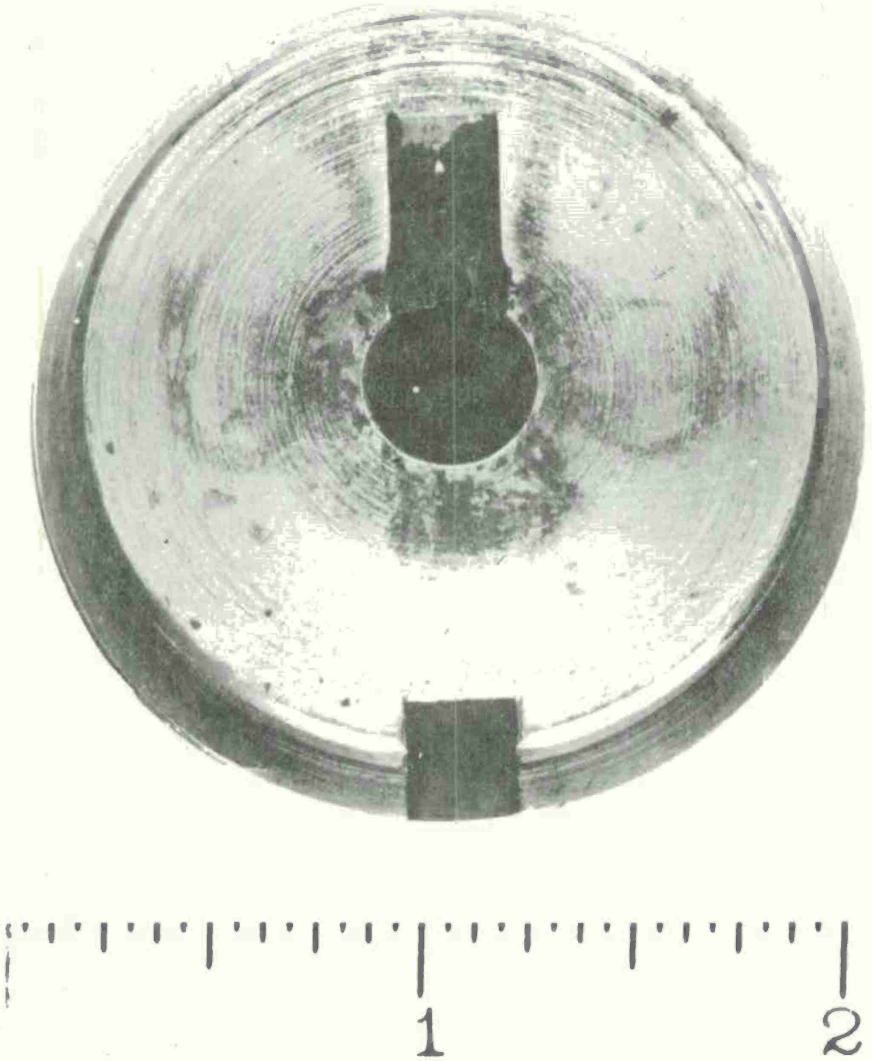

Figure 99. 5.56mm Test Barrel Used for HMX Firings (Observe the minimal chamber erosion.)

CHAPTER 9. CONCLUSIONS

It is concluded that:

1. The catastrophic failure of an aluminum cartridge case does not result from any part of the cartridge case's interior surface "burning-through".
2. The term "burn-through" is a misnomer.
3. Aluminum cartridge case "burn-through" is observed to result in case erosion, weapon damage and the existence of a bright flash surrounding the weapon's chamber.
4. Aluminum case "burn-through" results from the occurrence of a gas path through the cartridge case wall during the early portion of the interior ballistic cycle. The gas path may result from a mechanical defect; i.e., insufficient strength or ductility, or a structural flaw.
5. An aluminum cartridge case "burn-through" can be simulated by drilling a small hole in the head region (e.g. 0.0135 or 0.0625 inch diameter) or by slitting the cartridge's sidewall to a depth of 0.005 inch or greater.
6. "Burn-through" does not occur simultaneously with the primer's blast, but initiates after a finite heat-up time.
7. The "burn-through" plume occurs in two separate and distinct zones. One zone occurs close to the aluminum surface and has been identified as a vapor-phase reaction involving melted/vaporized aluminum and the combustion products. The other, which occurs external to the test weapon/fixture, is principally the oxidation of molten aluminum to aluminum oxide.
8. The primary reaction zone lasts approximately until depressurization of the cartridge case; the secondary cloud typically lasts 4 to 5 milliseconds and extends for at least 36 inches from the point of origin.
9. It is possible to quench the secondary cloud by discharging it into an inert atmosphere.
10. The primary reaction zone is responsible for the damage sustained by the cartridge case of the test specimen.
11. There is a minimum growth of the induced orifice until the primary reaction zone has been established.
12. The predominant line in an emission spectrum of a "burn-through" plume is an aluminum oxide line.
13. The amount of erosion (damage) sustained by a cartridge case or test specimen is directly proportional to the peak chamber pressure, propellant gas flow time, amount of propellant gas discharge, and initial, effective diameter of the induced orifice.
14. There is no appreciable difference in the erosion characteristics of 7475-T6 and 6061-T6 aluminum.

15. Titanium alloys erode more seriously (have greater erosion rates) than do aluminum alloys.

16. Findings, data, and understandings obtained from venting bomb firings do not extrapolate to a gun environment.

17. More damage (erosion) results from firing a slit cartridge case than one with a preplaced hole, given the same ballistic conditions.

18. Clad metal laminates, HMX propellants, and rubber liners all demonstrated an insensitivity to erosion in venting bomb firings.

19. An engineering application of the rubber liner has been successfully demonstrated to thwart "burn-through". Both the use of HMX propellants and clad metal laminates as cartridge case material were unsuccessful in preventing the catastrophic effects of "burn-through".

20. As the thickness of the test specimen is increased, the damage -- as indicated by mean thickness in diameter or weight loss -- is correspondingly increased.

21. HMX propellants provide different erosion characteristics (in a venting bomb) than do conventional ball or IMR propellants.

22. The leading edge of the induced orifice in a test specimen or cartridge case is particularly vulnerable to propellant gas flow.

23. The hot gaseous content of the plume causes the surface layer of steel weapon parts to alloy with the aluminum present in the "burn-through" plume.

24. The surface of an aluminum cartridge case or test specimen shows evidence of a layer of gross melting in backwash areas and in areas apparently not directly exposed to the flow of the propellant gas.

25. A double disk arrangement of brass and aluminum test specimens realizes differing amounts of erosion depending on the relative orientation of the discs.

26. From a mechanistic point of view, the aluminum cartridge case "burn-through" may be considered the result of:

a. Propellant gas flow through an otherwise restricted gas path,

b. Forced convective heating of exposed aluminum surfaces to the point where melting and/or vaporization occurs.

c. Entrainment of this conglomerate in the boundary later,

d. Initiation of a vapor-phase reaction (primary reaction zone),

e. Augmented heat flux to regions downstream in the flow field,

f. Extensive removal of aluminum in the molten state, and

g. Generation of the secondary plume resulting from an exothermic reaction of molten and/or vaporized aluminum with available oxygen.

h. The primary vapor-phase reaction is caused principally by the oxidation of aluminum vapor by both carbon dioxide (CO_2) and water vapor (H_2O) which are present as the result of propellant combustion.

CHAPTER 10. RECOMMENDATIONS

It is recommended that:

1. A bomb be designed, fabricated, and ballistically tested to allow an investigation of the effect on different atmospheres at ballistic temperatures and pressures on the erosivity of aluminum test specimens.
2. An experiment be conducted to devise novel propellants having reduced adiabatic flame temperatures and lower oxidizing potential of the combustion products than is now available in standard propellants.
3. A fundamental study be conducted to identify the basic processes occurring in the primary reaction zone.
4. A more detailed metallographical examination be performed of aluminum surfaces which have witnessed "burn-through".

REFERENCES

1. Donnard, R.E. and Mc Caughey, J.M., "Proposal to Improve Combat Load Effectiveness of Weapon/Ammunition Systems by Demonstrating Feasibility of Lightweight Aluminum Alloy Cartridge Cases in the 5.56mm Weapon", Frankford Arsenal Proposal, December 1969.

2. Lewis, L.D., "Calibre .30 Cartridge Cases Made from Aluminum Alloys", Technical Report Report No. R-16, 25 February 1926, Frankford Arsenal, Phila., Pa.

3. Proceedings of Symposium on Aluminum Cartridge Case Development, 17 January 1956, Frankford Arsenal, Phila., Pa.

4. Miller, S., "Design, Development and Fabrication of 100,000 Cartridges, Ball, Caliber .50, M33 Type Assembled with Case, Cartridge Aluminum, Caliber .50, FAT 39", Technical Report R-1265, June 1956, Frankford Arsenal, Phila., Pa.

5. Squire, W.H., and Donnard, R.E., "An Analysis of Local Temperature Profiles Encountered in the Aluminum Cartridge Case Drilled Hole Experiment," Technical Note TN-1163, August 1971, Frankford Arsenal, Phila., Pa.

6. Donnard, R.E., and Squire, W.H., "The Aluminum Cartridge Case Exploratory Development Program - Status Report", Report M72-6-1, April 1972, Frankford Arsenal, Phila., Pa.

7. Summerfield, M., "Letter to Reed E. Donnard; Subject, 'Cartridge Burn-Through Problems'", September 1969, Princeton University, Guggenheim Aerospace Propulsion Laboratory, Princeton, N. J.

8. Rosenbaum, M., Hennessy, T.J., Marziano, S.J., and Donnard, R.E., "Design and Development of a 7.62mm Aluminum Alloy Cartridge Case", Technical Report R-2062, January 1973, Frankford Arsenal, Phila., Pa.

9. Donnard, R.E., and Skochko, L.W., "Induced-Failure Test Procedure for Aluminum Alloy Cartridge Cases", Report #6019, June 1971, Frankford Arsenal, Phila., Pa.

10. Unpublished data, "The Aluminum Cartridge Case 'Burn-Through' Problem - Characteristics, Isolation, and Method of Elimination", Frankford Arsenal, Phila., Pa.

11. Witte, A.B., Fox, J., and Rungaldier, H., "Localized Measurements of Wake Density Fluctuations Using Pulsed Laser Holographic Interferometry", AISS Paper No. 70-727, presented at the AIAA Reacting Turbulent Flows Conference, San Diego, Calif., 17-18 June 1970.

12. Witte, A.B., and Wuerker, R.F., "Laser Holographic Interferometry Study of High Speed Flow Fields", AIAA Paper No. 69-347, presented at the AIAA 4th Aerodynamic Testing Conference, Cincinnati, Ohio, 28-30 April 1969.

13. Pearse, R.W.B., and Gaydon, A.S., The Identification of Molecular Spectra, (3rd edition), Chapman and Hall Ltd., London, 1965.

14. Plett, Edelbert G. and Summerfield, Martin, "Erosive Effects of Combustion Gases on Metallic Combustion Chambers, Final Report on Contract DAAA25-F1-C0109", Department of Aerospace and Mechanical Sciences, Princeton University.

15. Squire, W.H., and Donnard, R.E., "An Analysis of 5.56mm Aluminum Cartridge Case 'Burn-Through' Phenomenon", Paper presented at the Army Science Conference, 14-16 June 1972, West Point, New York.

16. Ozisik, M.N., Boundary Value Problems of Heat Conduction, International Textbook Company, Scranton, Pa., 1968.

17. Barkman, E.F., "Letter to Mr. Henry George", 7 January 1971, Reynolds Metals Company, Richmond, Va.

18. Rogers, R.W., "Letter to Mr. Marvin Rosenbaum", 7 December 1970, Aluminum Company of America, New Kensington, Pa.

19. Friedman, R., and Maucek, A., "Ninth Symposium (International) on Combustion", pp. 703-712, Academic Press, New York, 1963.

20. Fassell, W.M., Jr., Papp, C.A., Hildenbrand, D.L., and Sernka, R.P., "Solid Propellant Rocket Research", M. Summerfield, ed., pp. 259-269, Academic Press, New York, 1960.

21. Davis, A., "Combustion and Flame", 7, pp. 359-367, 1963.

22. Drew, C.M., Gordon, A.S., and Knipe, R.H., "Heterogeneous Combustion", H.G. Wolfhard, I. Glasman, and L. Green, Jr., eds. pp. 17-39, Academic Press, New York 1964.

23. Prentice, J.L., Drew, C.M., and Christensen, H.C., "Pyrodynamics", 3, pp. 81-90, 1965.

24. Brzustowski, T.A., "Vapor-Phase Diffusion Plames in the Combustion of Magnesium and Aluminum", Ph.D. Thesis, Princeton University, Dept. of Aeronautical Engineering, 1963.

25. Kirschfeld, L., Metal, 15, pp. 873-878, 1961.

26. Grosse, A.V., and Conway, J.B., Industrial Engineering Chemistry, 50, pp. 663-672, 1958.

27. Conway, J.B., and Grosse, A.V., "Temple University Research Institute Final Technical Report on Contract N9-ONR-87301", July 1954.

28. Kuehl, D.K., AIAA Journal, 3, No. 12, pp. 2239-2247, 1965.

29. Stiefel, L., and Hody, G.L., "The Composition of the Exhaust Products of Military Weapons", Technical Report R-1948, Frankford Arsenal, Phila., Pa., March 1970.

30. Plett, E.G., and Summerfield, M. "Second and Third Bimonthly Progress Reports for the Period December 1970-March 1971, Contract DAAA25-71-C0109", Princeton University, April 1971.

31. Christensen, H.C., Knipe, R.H., and Gordon, A.S., Pyrodynamics, 3, pp. 91-119, 1965.

32. Glassman, J., "Metal Combustion Processes". A.R.S. Preprint 938-59, November 1959, bibliography.

33. Shapiro, A.H., The Dynamics and Thermodynamics of Compressible Fluid Flow, Vol. 1, Ronald Press, New York, 1953.

34. U.S. Patent applied for "Noneroding Lightweight Cartridge Cases", Disclosure Number AMSMU2188, February 1973, Skochko, Leonard W., and Donnard, R.E.

35. Bernstein, C.N., "Thiokol HMX Propellant for Aluminum Case Erosion Tests", Memorandum for Record, SASA, 31 March 1972.

36. Donnard, R.E. and Hennessy, T.J., "Aluminum Cartridge Case Feasibility Study using the M16A1 Rifle with the 5.56mm Ball Ammunition as the Test Vehicle", Technical Report R-2065, November 1972, Frankford Arsenal, Phila., PA

DISTRIBUTION

Department of Defense
Director of Defense Research and
Engineering, Dr. M. Currie
Pentagon (Room 3E1006)
Washington, DC 20301

Department of Defense Air
Munitions Requirements and
Development Committee
Washington, DC 20301

1 Attn: COL Poole

1 Attn: COL J. Burress

1 Attn: COL W. Gearan

1 Attn: CDR S. Mikitarin

Department of the Army
Office of the Assistant Secretary
(I&L)
Attn: SAAS-IL
Washington, DC 20310

Department of the Army
Office of the Assistant Secretary
(I&L)
Attn: SAAS-IL-MO (Mr. J. Merit)
Washington, DC 20310

Department of the Army
Office of the Assistant Secretary
(R&D)
Attn: SAAS-RD
Washington, DC 20310

Department of the Army
Deputy Chief of Staff for Mil Op
Attn: DAMO-RQD
Washington, DC 20310

Office of the Deputy Chief of Staff
for Research, Development and
Acquisition HQDA
Washington, DC 20310

1 Attn: DAMA-ZA (LTG H. Cooksey)

1 Attn: DAMA-ZB (MG P. Olenchuk)

1 Attn: DAMA-AR (Dr. M. Lasser)

1 Attn: DAMA-CS (MG L. Van Buskirk)

1 Attn: DAMA-WS (BG D. Keith)

1 Attn: DAMA-WS (BG R. Wing)

1 Attn: DAMA-CSM (COL T. Brain)

1 Attn: DAMA-WSM (COL R. Cook)

1 Attn: DAMA-WSA (COL W. Crouch)

1 Attn: DAMA-WSW (COL L. Baermann)

Office of the Secretary
The Pentagon
Attn: Mr. R. Thorkildsen
Room 3-D 1089
Washington, DC 20301

Commander
US Army Materiel Command
RD&E Directorate
Attn: Dr. Richard Halex
5001 Eisenhower Ave.
Alexandria, VA 22304

Commander
US Army Test and Eval Command
Aberdeen Proving Ground, MD 21005

1 Attn: AMSTE-BC, Mr. Crider

1 Attn: AMSTE-BA

1 Attn: AMSTE-BG

Commander
US Army Materiel Command
5001 Eisenhower Ave.
Alexandria, VA 22333

1 Attn: AMCCG (GEN J. R. Deane, Jr)

1 Attn: AMCDMA (MG G. Sammet, Jr)

1 Attn: AMCSC (Dr. R. Dillaway)

1 Attn: AMCRD (BG H. Griffith)

1 Attn: AMCRP (Mr. G. Dansmann)

1 Attn: AMCRD-F (COL H. Beasley)

1 Attn: AMCRD-W (COL W. Phillips)

1 Attn: AMCRD-DW (Mr. T. Cosgrove)

Commander
US Army Armaments Command
Rock Island, IL 61201

1 Attn: AMSAR-CG (MG B. Lewis)

1 Attn: AMSAR-RDS
(Mr. L. Ambrosini)

1 Attn: AMSAR-SC (Dr. C. Hudson)

1 Attn: AMSAR-RD (COL L. Sherman)

1 Attn: AMSAR-RDT (Dr. E. Haug)

1 Attn: AMSAR-RDG (Mr. J. Blick)

1 Attn: AMSAR-RDF (Mr. W. Benson)

1 Attn: AMSAR-RDS (Mr. R. Milne)

1 Attn: AMSAR-RDT (Dr. Fischer)

1 Attn: AMSAR-RDT (Mr. Beckmann)

1 Attn: AMSAR-RDG (Mr. Artioli)

1 Attn: AMSAR-RDG (Mr. K. Williams)

1 Attn: AMSAR-RDF (Mr. B. Kmech)

Commander
Rock Island Arsenal
Attn: SARRI-LS-C (Mr. R. Swegler)
Rock Island, IL 61201

Commander
Picatinny Arsenal
Dover, NJ 07801

1 Attn: SARPA-AD (Mr. R. Heinemann)

1 Attn: SARPA-AD-D-W (Mr. S. Lerner)

1 Attn: SARPA-AD-D-W (Mr. J. Spicer)

1 Attn: Scientific and Technical
Information Branch

Commander
US Army Materiel System Analysis
Agency
Attn: Dr. Sperraza
Aberdeen Proving Ground, MD 21005

Director
US Army Ballistic Research Lab
Attn: Dr. Eichelberger
Aberdeen Proving Ground, MD 21005

Commander
Foreign Science Technology Center
Attn: AMXST-MCI
Charlottesville, VA 22901

Commander
TRADOC
Ft. Monroe, VA 23651

1 Attn: LTC Fitch

1 Attn: LTC Clowe

Commander
Harry Diamond Labs
Attn: AMXDO-TIB
Washington, DC 20438

Commander
US Army Materials & Mechanics
Research Center
Watertown, MA 02172

1 Attn: Tech Info Division

1 Attn: AMXMR-E
(Mr. E. S. Wright)

1 Attn: AMXMR-TX
(Mr. E. Hegge)

1 Attn: AMXMR-EC
(Mr. P. Riffin)

1 Attn: Dr. Homer Priest

1 Attn: Dr. J. W. Johnson

Commander
US Army Ballistic Research Labs
Aberdeen Proving Ground, MD 21005

1 Attn: R. Cower

1 Attn: L. Watermeir

1 Attn: A. Barrows

1 Attn: AMXRD-BIL
(B. Grollman)

US Army Chem Research & Dev Labs
Edgewood Arsenal
Aberdeen Proving Ground, MD 21010

1 Attn: Dr. E. Metcalfe

1 Attn: Dr. David J. Katsanis

1 Attn: Mr. C. Ferrert

1 Attn: Mr. F. Grunner

Commander
US Army Mobility Eng Research &
Dev Lab
Attn: J. Roysdon, Ch Dml & Ftn Br
Fort Belvoir, VA 22060

Commander
US Army Human Engr Labs
Attn: AMSHE-ENG
Aberdeen Proving Ground, MD 21005

Office of the Director
US Army Special Warfare Lab
Attn: ODCSOPS, H. Cotner
Washington, DC 20315

Commander
US Army Research Office-Durham
Durham, NC 27706

1 Attn: J. Dawson

1 Attn: H. Davis

1 Attn: J. Magor

Defense Materials Info Center
Battelle Memorial Institute
505 King Avenue
Columbus, OH 43201

Commander
Lake City Army Ammunition Plant
Independence, MO 64056

1 Attn: SMULC-ATD-E (Mr. O. Noell)

1 Attn: SMULC-ATD-E (Mr. D. Stonger)

1 Attn: SMULC-ATD
(Mr. J. Piskorski)

Advanced Research Projects Agency
Department of Defense
Washington, DC 20301

1 Attn: Director

1 Attn: Dr. Huggins, Research &
Tech Division

Defense Documentation Center (12)
Cameron Station
Alexandria, VA 22314

Federal Aviation Admin
Attn: Admin Standard Div (MS-110)
800 Independence Ave, SW
Washington, DC 20590

Commander
Hdqs, US Air Force
Attn: ACRDQ-RM, LTC R. G. Dilger
Washington, DC 20330

Commander
Hill Air Force Base
Attn: R. Hamilton
Ogden, UT

Commander
US Air Force Armament Lab
Eglin Air Force Base, FL 32542

1 Attn: ATWH

1 Attn: AFATL (ATRO)
(E. Wintermoyer)

1 Attn: DLOS-AFATL

1 Attn: DLDG, AFATL,
(LTC, J. T. Lindsay)

1 Attn: DLDG, AFATL (D. Uhrig)

1 Attn: DLDG (D. Davis)

Air Force Materials Lab
Air Force Systems Command
Wright Patterson Air Force Base
Dayton, OH 45433

1 Attn: MATF (Mr. H. Johnson)

1 Attn: MATF (Mr. L. Kennard)

National Aeronautics & Space Agcy
Attn: B. Achhammer, Matl Div
1540 H Street, NW
Washington, DC 20546

National Aerospace & Space Agcy
Ames Research Center
Attn: CPT Paul E. Bovenkerk,
Chem Rsch Projects Office
Moffett Field, CA 94035

Bureau of Naval Weapons
Department of the Navy
Attn: RUME
Washington, DC 20360

Chief, Office of Naval Research
Department of the Navy
Washington, DC 20360

Commander
US Naval Explosive Ordnance
Disposal Facility
Indian Head, MD 20640

Commander
US Naval Ordnance Station
Indian Head, MD 20640

1 Attn: ES43 (S. Mitchell)

1 Attn: ES43C1 (R. Montoya)

Commander
Naval Weapons Center
Attn: Mr. J. Prentice, Code 6082
China Lake, CA 93555

AAI Corp
York Road
Cockeysville, MD 21030

Aluminum Company of America
Aerospace & Military Dept
Application Engineering Div
P. O. Box 1012
Attn: Mr. E. W. Johnson
New Kensington, PA 15068

Aluminum Company of America
Alcoa Research Labs
Physical Metallurgy Div
New Kensington, PA 15068

1 Attn: R. W. Rogers, Jr.

1 Attn: H. Y. Hunsicker

Amron Corp
525 Progress Avenue
Waukesna, WI 53186

Mr. R. H. Brown
1411 Pacific Avenue
Natrona Heights, PA 15065

Columbia University
Attn: Dr. J. Weiner
New York, NY 10027

Dow Chemical Company
Attn: Dr. R. S. Busk
Midland, MI 48640

Dr. LaVerne W. Eastwood
Route 2
Woodsfield, OH 43793

The Franklin Institute
Research Buildings
20th and Race Streets
Phila., PA 19103

1 Attn: Dr. Z. Zudans

1 Attn: Dr. M. Reddi

1 Attn: Mr. H. Fishman

Guggenheim Aerospace Propulsion
Laboratories, Princeton Univ
James Forestal Campus
Princeton, NJ 08540

1 Attn: Dr. M. Summerfield

1 Attn: Dr. E. G. Plett

Martin-Marietta, Inc.
19200 So. Western Avenue
Attn: Mr. G. A. Moudry
Torrence, CA 90509

University of Illinois
College of Engineering
Box 4348
Attn: Dr. W. Rostoker
Chicago, IL 60680

Director
Institute for Defense Analysis
400 Army-Navy Drive
Attn: P. Mitchell
Arlington, VA 22202

International Lead Zinc Inst
292 Madison Ave
Attn: Dr. S. Radtke
New York, NY 14305

Kaiser Aluminum and Chem Corp
Dept of Metallurgical Research
Attn: Mr. J. B. Hess
Spokane, WA 99215

Lehigh University
Attn: Dr. G. Irwin
Bethlehem, PA 18018

Les Industries Valcartier, Inc
C.P. 790 Courcelette
Attn: Mr. A. Simard, Director
Rsch Prod Div Ammo
Co. Portneuf, Quebec, Canada

Massachusetts Inst of Tech
Attn: Prof M. Flemings
Room 35-316
Cambridge, MA

Materials Research Lab, Inc
1 Science Road
Attn: Dr. E. J. Ripling
Glenwood, IL 60425

The General Electric Company
Space Technology Center
Attn: Mr. Wilfred Connell
Room U-7026
Valley Forge, PA

Metals and Ceramics Info Center
505 King Avenue
Attn: Mr. Dan Maran
Columbus, OH 43201

New York University
University Heights
Attn: Dr. I. Cadoff
Bronx, NY 10452

Olin Metals Division
Metals Research Lab
Attn: Dr. J. Winter
91 Shelton Avenue
New Haven, CT 06504

R & D Associates
525 Wilshire Blvd
P. O. Box 3580
Santa Monica, CA

1 Attn: Mr. M. Shaefer

1 Attn: Mr. R. Helmbold

Remington Arms Company, Inc
939 Barnum Avenue
Attn: Mr. Jack Scanlon
Bridgeport, CT 06602

Reynolds Metal Company
Metallurgical Research Division
4th and Canal Streets
Richmond, VA 23218

1 Attn: Mr. S. A. Levy

1 Attn: Mr. H. J. Coates

1 Attn: Mr. Erik Barkman

Texas Instruments, Inc
Metallurgical Materials Division
Technical Center
34 Forest Street
Attn: Dr. R. V. Barone
Attleboro, MA 07203

Hercules, Inc.
P.O. Box 98
Attn: Dr. Leon Scott
Magna, UT 84044

Villanova University
Attn: Mr. S. Spadafora
Chemistry Department
Villanova, PA 19085

Teledyne McCormick/Selph
Attn: Charles Garrison
3601 Union Road
Hollister, CA 95023

Frankford Arsenal:

1 Attn: CO's Reading File, B4110/107B

1 Attn: Technical Director, TD/107-1

1 Attn: J. McCaughey, CO/107-1

1 Attn: Director, PD/64-4

1 Attn: G. White, PD/64-4

1 Attn: Chief, PDM/64-4

1 Attn: Chief, PDM-E/64-4

1 Attn: J. Rinnovatore, PDM-E/127-1

1 Attn: S. Cytron, PDM-E/127-1

1 Attn: Chief, PDR-M/513-1

1 Attn: Chief, PDR/64-4

1 Attn: Plans Office, PA/107-2

1 Attn: Chief, PAC/107-2

1 Attn: Patents Br, GC/40-1

1 Attn: Director, QA/235-3

1 Attn: Reliability Br, QAA-R/119-2

Frankford Arsenal - Cont'd

1 Attn: Director, AT/228-1

1 Attn: H. Lipinski/ATE/228-3

1 Attn: C. Mroz, MTM/211-2

1 Attn: Director, MD/220-1

1 Attn: Chief, MDC/219-2

1 Attn: Chief, MDC-A/219-2

1 Attn: A. Cianciosi, MDE/220-1

1 Attn: W. Gadomski, MDC-A/219-2

1 Attn: Chief, MDS/220-2

1 Attn: Chief, MDS-D/220-2

1 Attn: Chief, MDS-B/220-2

1 Attn: S. Kucsan, MDS-B/220-2

20 Attn: Chief, MDS-S/220-2

30 Attn: W. Squire, MDC-A/219-2

1 Attn: T. Hennessy, MDS-S/220-2

1 Attn: L. Skochko, MDS-S/220-2

1 Attn: M. Rosenbaum, MDS-S/220-2

1 Attn: J. Harris, MDS-S/220-2

1 Attn: Chief, MDS-E/220-2

1 Attn: L. Stiefel, MDP-R/64-3

1 Attn: D. Jacobs, MDE/220-1

2 Attn: Library, TSP-L/51-2
(1 - Reference copy)
(1 - Circulation copy)
(1 - Record copy)

Printing & Reproduction Division
Frankford Arsenal
Date Printed: 12 July 1976

DEPARTMENT OF THE ARMY
FRANKFORD ARSENAL
PHILADELPHIA, PA. 19137

OFFICIAL BUSINESS
PENALTY FOR PRIVATE USE $300

SARFA-TSP/T

POSTAGE AND FEES PAID
DEPARTMENT OF THE ARMY
DoD-314